Vol. 119 No. 1, September 1, 1980

ISSN 0003-2670

ANALYTICA CHIMICA ACTA

International journal devoted to all branches of analytical chemistry

ELSEVIER SCIENTIFIC PUBLISHING COMPANY

ANALYTICA CHIMICA ACTA

International journal devoted to all branches of analytical chemistry
Revue internationale consacrée à tous les domaines de la chimie analytique
Internationale Zeitschrift für alle Gebiete der analytischen Chemie

PUBLICATION SCHEDULE FOR 1980 (incorporating the section on Computer Techniques and Optimization).

	J	F	M	A	M	J	J	A	S	O	N	D
Analytica Chimica Acta	113/1 113/2	114	115	116/1	116/2	117	118/1	118/2	119/1	119/2	120	121
Section on Computer Techniques and Optimization			122/1			122/2			122/3			122/4

Scope. *Analytica Chimica Acta* publishes original papers, short communications, and reviews dealing with every aspect of modern chemical analysis, both fundamental and applied. The section on *Computer Techniques and Optimization* is devoted to new developments in chemical analysis by the application of computer techniques and by interdisciplinary approaches, including statistics, systems theory and operation research. The section deals with the following topics: Computerized acquisition, processing and evaluation of data. Computerized methods for the interpretation of analytical data including chemometrics, cluster analysis, and pattern recognition. Storage and retrieval systems. Optimization procedures and their application. Automated analysis for industrial processes and quality control. Organizational problems.

Submission of Papers. Manuscripts (three copies) should be submitted as designated below for rapid and efficient handling:

Papers from the Americas to: Professor Harry L. Pardue, Department of Chemistry, Purdue University, West Lafayette, IN 47090, U.S.A.

Papers from all other countries to: Dr. A. M. G. Macdonald, Department of Chemistry, The University, P.O. Box 363, Birmingham B15 2TT, England.

For the section on *Computer Techniques and Optimization:* Dr. J. T. Clerc, Universität Bern, Pharmazeutisches Institut, Sahlistrasse 10, CH-3012 Bern, Switzerland.

American authors are recommended to send manuscripts and proofs by INTERNATIONAL AIRMAIL.

Information for Authors. Papers in English, French and German are published. There are no page charges. Manuscripts should conform in layout and style to the papers published in this Volume. Authors should consult Vol. 111, p. 343 for detailed information. Reprints of this information are available from the Editors or from: Elsevier Editorial Services Ltd., Mayfield House, 256 Banbury Road, Oxford OX2 7DE (Great Britain).

Reprints. Fifty reprints will be supplied free of charge. Additional reprints (minimum 100) can be ordered. An order form containing price quotations will be sent to the authors together with the proofs of their article.

Advertisements. Advertisement rates are available from the publisher.

Subscriptions. Subscriptions should be sent to: Elsevier Scientific Publishing Company, P.O. Box 211, 1000 AE Amsterdam, The Netherlands. The section on *Computer Techniques and Optimization* can be subscribed to separately.

Publication. *Analytica Chimica Acta* (including the section on *Computer Techniques and Optimization*) appears in 10 volumes in 1980. The subscription for 1980 (Vols. 113—122) is Dfl. 1390.00 plus Dfl. 160.00 (postage) (total approx. U.S. $795.00). The subscription for the *Computer Techniques and Optimization* section only (Vol. 122) is Dfl. 139.00 plus Dfl. 16.00 (postage) (total approx. U.S. $79.50). Journals are sent automatically by airmail to the U.S.A. and Canada at no extra cost and to Japan, Australia and New Zealand for a small additional postal charge. All earlier volumes (Vols. 1—112) except Vols. 23 and 28 are available at Dfl. 153.00 (U.S. $78.50), plus Dfl. 11.00 (U.S. $5.50) postage and handling, per volume.

Claims for issues not received should be made within three months of publication of the issue, otherwise they cannot be honoured free of charge.

Customers in the U.S.A. and Canada who wish to obtain additional bibliographic information on this and other Elsevier journals should contact Elsevier/North Holland Inc., Journal Information Center, 52 Vanderbilt Avenue, New York, NY 10017. Tel: (212) 867-9040.

PARIS
8~13 DECEMBER 1980
PORTE DE VERSAILLES

INTERNATIONAL LABORATORY SHOW 1980

in 1980, the most important international event in Europe concerning the Laboratory

On 25.000 M², 825 firms from 21 countries will make a presentation of techniques, methods and equipment relating to the laboratory

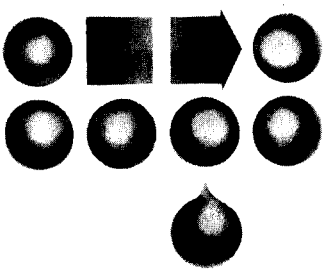

For details and entry-cards, please apply to:

SEPIC S.A.
40, Rue du Colisée
75381 PARIS CEDEX 08, France
Tel.: (1) 225.3776
Telex: 640450

STICHTING BEVORDERING FRANSE VAKBEURZEN
Prins Hendrikkade 20-21
1012 TL AMSTERDAM, The Netherlands
Tel. (020) 24 86 70 / 23 92 04
Telex: 12644 PROSA

The Handbook of Environmental Chemistry

Editor: O. Hutzinger

This handbook is the first advanced level compendium of environmental chemistry to appear to date. It covers the chemistry and physical behavior of compounds in the environment. Under the editorship of Prof. O. Hutzinger, director of the Laboratory of Environmental and Toxicological Chemistry at the University of Amsterdam, 37 international specialists have contributed to the first three volumes.
For a rapid publication of the material each volume will be divided into two parts. Part A of the first three volumes is scheduled to appear by July, 1980, Part B will follow in the Spring of 1981. Each volume contains a subject index.

The Handbook of Environmental Chemistry is a critical and complete outline of our present knowledge in this field and will prove invaluable to environmental scientists, biologists, chemists (biochemists, agricultural and analytical chemists), medical scientists, occupational and environmental hygienists, research geologists, and meteorologists, and industry and administrative bodies.

Volume 1 (in 2 parts)
Part A

The Natural Environment and the Biogeochemical Cycles

With contributions by numerous experts
1980. 54 figures. Approx. 280 pages
Cloth DM 98,–; approx. US $57.90
ISBN 3-540-09688-4

Contents: The Atmosphere.– The Hydrosphere.– Chemical Oceanography.– Chemical Aspects of Soil.– Oxygen Cycle.– Sulfur Cycle.– Phosphorus Cycle.– Metal Cycles and Biological Methylation.– Natural Organohalogen Compounds.

Volume 2 (in 2 parts)
Part A

Reactions and Processes

With contributions by numerous experts
1980. 66 figures. Approx. 310 pages
Cloth DM 126,–; approx. US $74.40
ISBN 3-540-09689-2

Contents: Transport and Transformation of Chemicals: A Perspective.– Transport Processes in Air.– Solubility, Partition Coefficients, Volatility and Evaporation Rates.– Adsorption Processes in Soil.– Sedimentation Processes in the Sea.– Chemical and Photo Oxidations.– Atmospheric Photochemistry.– Photochemistry at Surfaces and Interphases.– Microbial Metabolism.– Plant Metabolism and Distribution.– Metabolism and Distribution by Aquatic Animals.– Laboratory Microecosystems.– Reaction Types in the Environment.

Volume 3 (in 2 parts)
Part A

Anthropogenic Compounds

With contributions by numerous experts
1980. 61 figures. Approx. 290 pages
Cloth DM 98,–; approx. US $57.90
ISBN 3-540-09690-6

Contents: Mercury.– Cadmium.– Polycyclic Aromatic and Heteroaromatic Hydrocarbons.– Fluorocarbons.– Chlorinated Paraffins.– Chloroaromatic Compound Containing Oxygen.– Organic Dyes and Colors.– Inorganic Dyes and Colors.– Radioactive Substances.

5637/5/1a

SPRINGER-VERLG BERLIN HEIDELBERG NEWYORK

Volume 10: Organometallic Chemistry Reviews; Annual Surveys: Silicon - Germanium - Tin - Lead.

edited by D. SEYFERTH, *Massachusetts Institute of Technology, Cambridge, MA, U.S.A. and* R. B. KING, *University of Georgia, Athens, GA, U.S.A.*

CONTENTS: Silicon - Synthesis and reactivity; Annual Survey covering the year 1978 *(J. Y. Corey)*. Organosilicon reaction mechanisms; Annual Survey for the year 1978 *(F. K. Cartledge)*. Silicon: Bonding and Structure; Annual Survey covering the year 1978 *(C. H. Yoder)*. Silicon - Application to organic synthesis; Annual Survey covering the year 1978 *(G. M. Rubottom)*. Germanium; Annual Survey covering the year 1978 *(D. Quane)*. Tin; Annual Survey covering the year 1978 *(P. G. Harrison)*. Lead; Annual Survey covering the year 1978 *(J. Wolters)*. Author Index.

1980 vi + 615 pages
US $ 119.50 / Dfl. 245.00
ISBN 0-444-41848-7

Volume 9: Organometallic Chemistry Reviews.

coordinating editor:
D. SEYFERTH
editors:
A. G. DAVIES, *University College, London, U.K.*
E. O. FISCHER, *Technische Universität München, B.R.D.*
J. F. NORMANT, *Université de Paris IV, France.*
O. A. REUTOV, *University of Moscow, U.S.S.R.*

CONTENTS: Applications of organomagnesium compounds in polymerization *(D. B. Malpass)*. Formation and reactivity of the complexes of carbonyl compounds with orgaoaluminium compounds and aluminium chloride *(A. Sprozynski and K. B. Starowieyski)*. Organofluorosilanes *(R. M. Pike and K. A. Koziski)*. Structural evidence of coordination interactions in organic derivatives of mercury, tin and lead *(N. G. Furmanova , L. G. Kuz'mina and Yu. T. Struchkov)*. The preparation of organotin compounds by the direct reaction *(J. Murphy and R. C. Poller)*. Recent advances in the chemistry of arsonium ylides *(R. K. Bansal and S. K. Sharma)*.

Selected plenary lectures from the Fifth International Symposium on Organosilicon Chemistry held in Karlsruhe, August 14-18, 1978: The environmental chemistry of liquid polydimethylsiloxanes, an overview *(C. L. Frye)*. Cyclic silanes *(E. F. Hengge)*. Silicon as a substituent and a link of heterocyclic rings *(L. Birkofer)*. Recent developments in silyl-transition metal chemistry *(B. J. Aylett)*. Mechanism of nucleophilic substitution at silicon. The nature of the driving force of stereochemistry *(R. Corriu)*. Silicon-containing derivatives of carbonic acid *(V. F. Mironov)*. Novel aspects of silicone chemistry *(W. Buechner)*.

1980 viii + 432 pages
US $ 105.00 / Dfl. 215.00
ISBN: 0-444-41840-7

Volume 8: Organometallic Chemistry Reviews; Annual Surveys: Silicon - Germanium - Tin - Lead.

CONTENTS: Silicon - Synthesis and reactivity; Annual Survey covering the year 1977 *(J. Y. Corey)*. Organosilicon reaction mechanisms; Annual Survey for the year 1977 *(F. K. Cartledge)*. Silicon: Bonding and Structure; Annual Survey covering the year 1977 *(P. R. Jones)*. Silicon - Application to organic synthesis; Annual Survey covering the year 1977 *(G. M. Rubottom)*. Germanium; Annual Survey covering the year 1977 *(D. Quane)*. Tin; Annual Survey covering the year 1977 *(P. G. Harrison)*. Lead; Literature Survey covering the year 1977 *(J. Wolters)*.

1979 viii + 608 pages
US $ 109.75 / Dfl. 225.00
ISBN: 0-444-41789-3

JOURNAL OF ORGANO-METALLIC CHEMISTRY LIBRARY

A series of books presenting reviews of recent developments and techniques in the expanding field of organometallic chemistry

ELSEVIER

P.O. Box 211,
1000 AE Amsterdam,
The Netherlands,

52 Vanderbilt Ave,
New York, N.Y. 10017.

The Dutch guilder price is definitive. US $ prices are subject to exchange rate fluctuations.

7178

ANALYTICA CHIMICA ACTA
VOL. 119 (1980)

ANALYTICA CHIMICA ACTA

International journal devoted to all branches of analytical chemistry

ELSEVIER SCIENTIFIC PUBLISHING COMPANY

Anal. Chim. Acta, Vol. 119 (1980)

Printed in The Netherlands.

Analytica Chimica Acta, 119(1980) 1—24

Review

GLASSY CARBON AS ELECTRODE MATERIAL IN ELECTRO-ANALYTICAL CHEMISTRY

W. E. VAN DER LINDEN* and J. W. DIEKER

Laboratory for Analytical Chemistry, University of Amsterdam, Nieuwe Achtergracht 166, 1018 WV Amsterdam (The Netherlands)

(Received 27th March 1980)

SUMMARY

The review is based on a literature search through Chemical Abstracts and the Science Citation Index. The topics covered are: chemical and electrochemical aspects of the glassy carbon/electrolyte interface for both aqueous solutions and non-aqueous electrolytes; analytical applications of glassy carbon electrodes, including voltammetry, stripping voltammetry, amperometry coulometry, potentiometry and chronopotentiometry; flow-through detectors; chemically modified glassy carbon electrodes; electrosynthesis; and pretreatment techniques.

In 1962, starting from phenolic resins, Yamada and Sato [1] prepared a gas-impermeable carbon which they called glassy carbon. This glassy carbon has interesting physical properties in comparison with other carbons such as, for instance, impregnated carbon (Table 1).

An important feature of their method of formation is that artefacts of various shapes can be produced. Furthermore, glassy carbon exhibits a much lower oxidation rate at elevated temperatures, suggesting a greater inertness to chemical attack than other types of carbons such as various graphites (Table 2). This property, together with the very small pore-size (Table 3) makes glassy carbon an attractive material for the preparation of inert electrodes.

Glassy carbon artefacts are, in general, formed by means of a carefully controlled heating programme of a premodelled polymeric (phenol—formaldehyde) resin body in an inert atmosphere [2]. At temperatures above 300°C, a carbonization process starts. Care must be taken that the polymeric substance does not pass into a liquid or tarry state immediately prior to carbonization because a product quite different from glassy carbon would then be obtained. The carbonization process in which oxygen, nitrogen, etc. are removed (300—500°C) must proceed very slowly to ensure that the gaseous products can diffuse to the surface. Fast heating will lead to high pressures inside the material resulting in cracks, blisters and distortion. For this reason the thickness of the walls of the artefacts is restricted to about 5 mm. In the

TABLE 1

Some properties of glassy carbon in comparison with impregnated carbon [1]

	Glassy carbon		Impregnated carbon
Heat-proof to (°C)	1300	3000	1300
Apparent density (g cm^{-3})	1.46—1.50	1.43—1.48	1.75 — 1.92
Hardness	4—5 (Mohs)	—	45 — 55 (Shore)
Tensile strength (kg cm^{-2})	500—1000	—	400 — 500
Electrical resistivity (10^{-4} ohm cm)	35—50	30—35	9 — 11
Ash content (%)	0.1	0.05	0.2
Gas permeability (cm^2 s^{-1})	10^{-11}—10^{-12}	10^{-9}	10^{-4}—10^{-6}
Thermal conductivity (kcal m^{-1} h^{-1} K^{-1})	3—4	13—15	100—120
Coefficient of thermal expansion (10^{-6} K)	1.8—2.2	—	2.0—2.5

TABLE 2

Oxidation rate at 800 ± 5°C in N_2:O_2 = 81:19 by volume [1]

Type	Reaction time (min) for weight loss (%) of			
	70	80	90	100
Normal graphite	68	95	110	140
Pyro graphite	120	138	175	250
High-density graphite	160	185	225	275
Glassy carbon	205	255	270	365

TABLE 3

Pore-size distribution by mercury method [1]

	Total pore volume (%)	Pore-size distribution (%)			Max. pore-size (nm)
		7×10^2—7×10^3 nm	10^2—7×10^2 nm	10^1—10^2 nm	
Normal	32	27	4	3	7×10^3
High-density graphite	11	3.5	1.5	6	7×10^3
Impregnated graphite	5	—	2.5	2.5	7×10^2
Glassy carbon	0.35	—	—	0.35	1×10^2

temperature range between 500°C and 1200°C, hydrogen is gradually eliminated and only carbon will be left. The carbonization process is accompanied by a shrinkage of the volume of about 50%. The formation of the final structure of glassy carbon has been extensively studied by Jenkins and Kawamura [3] by means of x-ray diffraction, infrared spectroscopy, and the determination of the hardness, Young's modulus and the tensile strength. They concluded from their studies that glassy carbon is made up from aromatic ribbon molecules which are oriented randomly and are tangled in a complicated manner. Annealing at temperatures above 1200°C leads to a

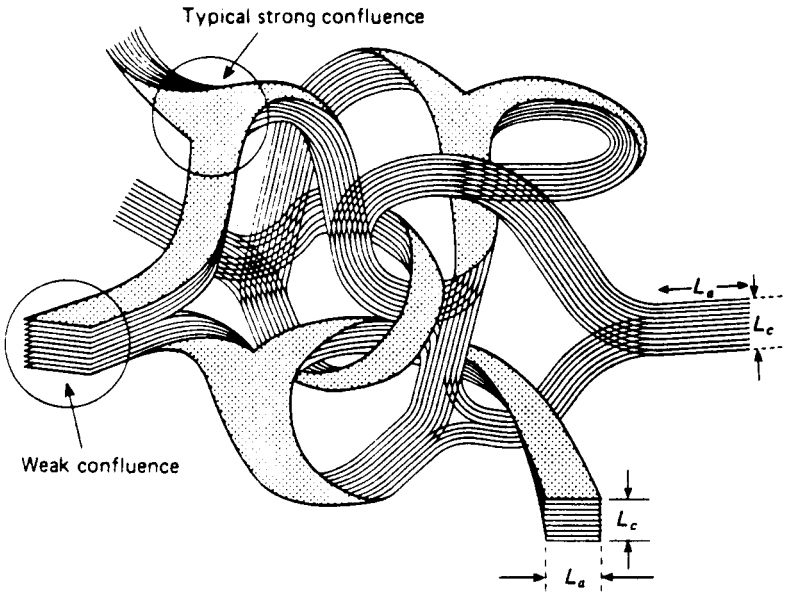

Fig. 1. Schematic structural model for glassy carbon [3]. (Reproduced by kind permission of Cambridge University Press.)

gradual elimination of local defects. The perfectly smooth ribbons thus obtained can stack above each other forming microfibrils. These microfibrils, as can be seen in Fig. 1, twist, bend and intertwine, yielding a glassy carbon end-product.

Several carbonaceous materials are available which look like glassy carbon but which have quite different properties [2], such as LTI pyrolytic graphite (LTI stands for low-temperature isotropic). Also the terminology is often very confusing. Most graphite fibres, for instance, are not graphitic at all but rather a form of glassy carbon. Glassy carbon is synonymous with vitreous carbon.

This review is restricted mainly to the use of glassy carbon as an electrode material.

CHEMICAL AND ELECTROCHEMICAL ASPECTS OF THE GLASSY CARBON/ELECTROLYTE INTERFACE

Information about the physical and chemical state of the glassy carbon surface and the glassy carbon/electrolyte interface is indispensable for a proper understanding of the electrochemical processes that can proceed at glassy carbon electrodes (GCEs). Most of the research on this subject has been done for aqueous solutions as the electrolyte, but organic solutions, other non-aqueous solutions, melts and even solid electrolytes have been used as well.

Glassy carbon electrodes in contact with aqueous solutions

Randin and Yeager [4] have measured differential electrode capacitances of GCEs in concentrated aqueous solutions, using a.c.-impedance measurements. The similarities between the complex potential dependence of the electrical capacity of glassy carbon and pyrolytic graphite, on the plane perpendicular to the basal plane, indicate a similarity of the surface groups present. However, the particular groups cannot be identified from their measurements. The existence of surface groups is confirmed by the work of Laser and Ariel [5] who studied the behaviour of glassy carbon on anodic polarization and subsequent reduction in acidic medium. From current–voltage and reflectance—voltage curves they concluded that the overall process on anodic polarization is the result of three processes: formation of a redox couple caused by chemical adsorption of oxygen, irreversible redox reactions of existing surface groups and, at sufficiently positive potentials, the evolution of oxygen. Possible surface groups formed on oxidation are, for instance, carbonyl groups that subsequently can be reduced to hydroxyl groups at more negative electrode potentials. Also the possibility of the formation of a quinone/hydroquinone couple, as found on oxidized/reduced pyrolytic graphite [6], cannot be excluded.

These results are supported by the pulse voltammetric experiments at GCEs by Dieker et al. [7]. They demonstrate that the large residual currents observed on scanning in either the positive or negative direction at GCEs from various manufacturers cannot be attributed to the presence of electroactive impurities in the solution or to the charging of the electrical double layer. Therefore, they suggested that oxidation as well as reduction of the glassy carbon surface might occur. Dunsch and Naumann [8] have also furnished evidence for the existence of oxygen-containing groups and chemisorbed oxygen at the glassy carbon surface. Majer et al. [9] earlier obtained results that are somewhat at variance with the aforementioned conclusions. They studied the acid—base sensitivity of several unimpregnated and impregnated carbonaceous electrodes by means of potentiometric and voltammetric methods as well as i.r. spectroscopy and scanning electron microscopy. Their conclusion was that GCEs most closely resemble ideal inert redox electrodes and that the H^+ sensitivity is due to oxygen adsorption and/or to oxygen dissolved in the solution. The concentration of surface groups was found to be negligible in contrast to the situation with other carbonaceous electrodes such as graphite and graphite oxide. For these latter electrodes, the presence of oxygen-containing groups was proved although an unambiguous identification was not possible. The presence of carbonyl or even carboxyl groups and hydroxyl groups was suggested.

For the applicability of the GCE in aqueous solutions, the reduction of oxygen and hydrogen ions on the one hand and the anodic evolution of oxygen on the other hand is of interest. To our knowledge no detailed studies of the evolution of oxygen at glassy carbon are available, but several papers have been published on the electrochemical reduction of oxygen at GCEs [10—12]. As far as the electrode material is concerned, it was found

that the history of the GCE exerts a great influence on the voltammetric wave of the oxygen reduction. This can be explained, at least partially, by a process in which the glassy carbon structure gradually passes to the graphitic form [10]. The polishing and/or the electrochemical pretreatment of the electrodes is also very important. Taylor and Humffray [11] observed a difference between polished, cathodically treated and anodically treated GCEs. The reduction to hydroxide rather than to peroxide was enhanced at all potentials by the anodization procedure. Similar results were obtained with chemically oxidized electrodes using chromic acid.

Vasil'ev et al. [13] have studied the influence of the temperature at which the glassy carbon is heated during its preparation. They found that the glassy carbon heated to 3000°C, which is partially graphitized, exhibits the lowest hydrogen overvoltage. The overvoltage increases when the temperature during the production procedure is kept lower. The lowest temperature used by them was 900°C. In that case the carbonization process is not yet completed and the carbon still contains a substantial amount of oxygen.

The interaction between metal ions and GCEs is of particular interest for the analytical chemist and several papers deal with this subject. Štulíková and Vydra [14] have investigated the reduction of iron(III) at glassy carbon in different acid media. Glassy carbon was proven to be very suitable as a material for the manufacture of rotating disc electrodes. The rate of reduction of iron(III) was found to be at least as fast as on platinum and much faster than on carbon paste. The same authors have studied the behaviour of the reduction of copper(II) and subsequent anodic stripping by means of cyclic voltammetry [15]. They concluded that the formation of monolayers or adsorbed atoms of copper, frequently noted on platinum and other metallic electrodes, does not appear to play an important role. The character of the voltammetric wave rather seems to depend to a great extent on whether the monovalent copper ions, produced during the electrochemical reaction, remain adsorbed on the electrode surface sufficiently long to undergo further electrochemical reaction. This degree of adsorption depends on the complexing strength of the medium, but competitive adsorption of other electrolyte species cannot be excluded. Extensive studies have been made on the cathodic deposition of mercury because of the formation of mercury thin film electrodes for anodic stripping voltammetry. Štulíková [16] has found that the nature of the deposit depends in a marked way on the deposition potential. At low overvoltages, mercury is deposited on a few active centres on the glassy carbon surface and large droplets are formed relatively far apart. Deposition potentials more negative than −0.5 V further the formation of more, finer droplets. Apparently, the number of active centres where nucleation can start increases with the applied overvoltage.

Laser and Ariel [17] were able to show by means of current–voltage curves and reflectance–voltage curves that the growth of the mercury drops is coupled with discontinuities in the electrode surface coverage. The growth of fine droplets will eventually lead to overlap and coalescence of neighbouring droplets. Since $(\Sigma r_i^3)^{1/3} < \Sigma r_i$, the surface covered by mercury will

decrease on coalescence and additional sites will become available for further nucleation. These studies might suggest that no closed film formation can take place but Dunsch [18] has shown that the nature of the deposit also depends on the chemical condition of the glassy carbon surface. At oxidized surfaces monolayers are not formed, whereas on surfaces that are carefully cleaned and virtually free from oxygen-containing groups a monolayer is formed, as can be seen from the appearance of a second oxidative desorption peak during the potential scan in the positive direction. The difference in peak potential between the peak related to bulk dissolution and the peak related to monolayer dissolution has a good correlation with the difference in bond energy between the Hg—Hg bond and the Hg—C bond. This bond energy, in turn, depends on the difference in electronegativity or work function of the materials involved. The existence of such a correlation was observed for the first time by Kolb et al. [19] in their study of the so-called "underpotential deposition", a phenomenon which involves the monolayer being deposited at less negative potentials than the bulk phase. According to Dunsch, the formation of mercury—carbon bonds, necessary for the formation of the monolayer, is blocked by the presence of oxygen-containing groups at the surface.

Two peaks were also observed on the anodic stripping of mercury from glassy carbon by Pnev et al. [20] at pH < 1.8. Higher pH values caused the appearance of even a third peak that was attributed to the formation of sparingly soluble mercury salts. The possibility of the formation of two-dimensional nuclei or monolayers of mercury on deposition from very dilute mercury(II) solutions ($<7.5 \times 10^{-7}$ M) was studied by Yoshida and Kihara [21] by means of atomic absorption spectrometry. They found that on reduction from such dilute solutions no atomic mercury is deposited on the surface and all the Hg^0 formed has diffused back into the solution. Apparently, the individual mercury atoms are formed so far apart from each other that no real nucleation could occur. Recently, Daneshwar and Kulkarni [22] have mentioned that on glassy carbon electrodes, completely free of any mercury deposit from previous experiments, the reduction is a first-order reaction involving two electrons. When, however, the GCE is partially covered with mercury droplets, the reduction occurs in two steps according to the following e.c.e. mechanism:

$$Hg^{2+} + 2e \rightleftharpoons Hg^0; Hg^{2+} + Hg^0 \rightleftharpoons Hg_2^{2+}; Hg_2^{2+} + 2e \rightleftharpoons 2Hg^0$$

Nucleation phenomena involved in the electrodeposition of lead and antimony onto glassy carbon have been studied by Palmisano et al. [23] and Lyungrin et al. [24], respectively.

For several electron-transfer reactions at a glassy carbon surface, rate data have been determined. Taylor and Humffray [25] have examined redox systems such as Fe(III)/Fe(II), Cr(III)/Cr(II), Ce(IV)/Ce(III) and $Fe(CN)_6^{3-}$/$Fe(CN)_6^{4-}$ as well as the reduction of iodate. Comparison of the reaction rates with those at platinum, carbon paste (CP) and wax-impregnated

graphite (WIG) reveals a general sequence: $k_{sh}(Pt) > k_{sh}(GC) > k_{sh}(WIG) > k_{sh}(CP)$. All rate constants showed a time dependence that was greater on glassy carbon than on carbon paste or wax-impregnated graphite electrodes. With the exception of iodate a significant increase (about 100-fold) in the rate constants was found after the electrode had been dipped in a $K_2Cr_2O_7$—H_2SO_4 solution for at least 5 min followed by thorough rinsing with water. This chromic acid pretreatment was attended by a 10-fold increase in the double layer capacity (from 25 μF cm^{-2} to about 250 μF cm^{-2}). Also the reproducibility was markedly improved by this procedure. A more detailed study of the hexacyanoferrate couple was carried out by Blaedel and Schieffer [26]. They found that, unlike platinum, gold or boron carbide electrodes, glassy carbon electrodes did not show any hysteresis when the potential was scanned in opposite directions.

Although most attention has been paid to the applicability of glassy carbon in the more positive potential range, it should be noted that also rather negative potentials can be obtained even in water-containing electrolytes. So, Weber and Volke [27] could reduce carbonyl-containing compounds in 50% (v/v) acetone—water mixtures at potentials as low as −2.0 V vs. SCE. The half-wave potentials were found to be only slightly more negative than those obtained on a dropping mercury electrode.

Glassy carbon electrodes in contact with non-aqueous electrolytes

So far, several examples have been given in which it was shown that glassy carbon plays an active role in many electrochemical reactions when in contact with aqueous solutions. Similar observations have been made in organic solvents. Salzberg [28] has examined the electrochemical oxidation of nitrite in acetonitrile. He was able to show by means of Tafel slopes and a.c. voltammetry that the electron transfer is reversible and that the NO_2 radical-molecule formed on oxidation is subsequently desorbed in a unimolecular step. This mechanism differs from that observed at gold electrodes where the nitrogen dioxide leaves the surface as the dimer N_2O_4. The fact that glassy carbon behaves differently from other carbonaceous electrodes is also illustrated by the work of Brennan and Brown [29]. They furnished evidence that the anodic oxidation of n-propylamine on glassy carbon proceeds according to a mechanism similar to that observed on platinum but different from that found at pyrolytic graphite.

Brown and Clarke [30] have investigated the oxidation of thallium(I) to thallium(III) on glassy carbon in liquid ammonia at −30°C. In this case glassy carbon was chosen in view of its high overvoltage with respect to nitrogen evolution which permits a large range of positive potentials to be studied. A decrease in the transfer coefficient, α, for the anodic process at more positive potentials was attributed to deactivation of the surface, probably by oxidation.

Although perhaps of no immediate interest for the analytical chemist, the application of GCEs in melts should be mentioned. The anodic evolution of

chlorine at glassy carbon in an NaCl—$FeCl_3$ melt at 178°C was studied by Abraham et al. [31]. Glassy carbon seems to play an essential role in the mechanism because of the intermediate formation of —C—Cl bonds. Tilak and Conway [32] have presented evidence that a similar mechanism might be operative in aqueous 5 M NaCl solutions at about pH 3.5 at low current densities. An NaCl—$AlCl_3$ melt at 175°C was used by Hussey et al. [33] to study the reduction of Cr(III) at a glassy carbon disc electrode. The reduction proceeds in two steps: in the first step Cr(II) is formed which is consecutively reduced to Cr(0) in a way similar to that observed for nucleation rate-controlled depositions. On re-oxidation, probably to Cr(II), the oxidation product remains adsorbed. Reversible reductions of Ni(II), Co(II), Cd(II) and Pb(II) at GCEs have been observed by Behl [34] in a molten LiCl—KCl eutectic mixture at 450°C.

Carbon anodes are used for alumina production in industrial processes. Thonstad [35] has investigated the mechanism of the anode reaction on carbon in cryolite—alumina melts. He found that on non-porous materials, i.e. pyrolytic graphite and glassy carbon, the double-layer capacitance is approximately 60 μF cm^{-2} in contrast to the porous electrodes which yield values of about 400 μF cm^{-2}. The formation of CO_2 at the anode is mainly controlled by the primary reaction. Glassy carbon and pyrolytic graphite electrodes maintained their smooth surface whereas the porous qualities became quite unevenly worn coupled with a further increase of the double-layer capacitance.

Armstrong et al. [36, 37] have made an extensive study of the electrochemical reactions proceeding at the carbon—sodium polysulphide (liquid) interface, which is of interest in connection with the operation of the sodium—sulphur rechargeable battery. They performed voltammetric studies at a rotating disc electrode of glassy carbon at 305°C and 350°C. Glassy carbon seems to play no specific role in the redox processes involved.

The use of electrodes in molten salts at elevated temperatures makes special demands on the sealing. Presumably because of difficulties of this kind no rotating ring-disc electrodes had been used in molten salts until Phillips et al. [38] described the fabrication of a glassy carbon rotating ring-disc electrode. An elegant procedure to obtain a good seal between glassy carbon and glass has been proposed by Levy and Farina [39]. They deposited a thin film of silicon on a heated glassy carbon rod by passing a stream of silane (SiH_4) over the surface. Subsequently a GSC-4 glass tube was slipped over the rod and sealed to it by evenly heating to the softening point of the glass. Use of this electrode significantly reduced the residual current in a molten LiCl—KCl eutectic mixture at 500°C and practically eliminated the hysteresis effect.

Glassy carbon has also been used in contact with a solid electrolyte. Armstrong et al. [40] have studied the GC/Ag_4RbI_5 interface and compared it with the Pt/Ag_4RbI_5 interface. From impedance measurements they came to the conclusion that the oxidation of iodide to iodine proceeds much more slowly at the GCE than at the platinum electrode.

ANALYTICAL APPLICATIONS OF GLASSY CARBON ELECTRODES

Glassy carbon electrodes were applied for the first time in electroanalytical chemistry by Zittel and Miller [41]. They showed that the usable potential range extends to positive values comparable to those for platinum. The range depends to some extent on the composition of the solution (Fig. 2). In contrast to platinum, the GCE can also be used in the cathodic range even in acidic solutions. In comparison to other carbonaceous electrodes such as wax-impregnated graphite, wax-impregnated carbon and carbon paste electrodes, pyrolytic graphite and glassy carbon electrodes have the largest available potential span (Fig. 3) [42]. In an investigation on the possible anodic potential range, Alder et al. [43] came to the same conclusion in their evaluation of a large number of electrode materials, ranging from metals to semiconductor materials. For the anodic limit, defined as the potential at which the current becomes equal to one-half of the value of the peak-current for the oxidation of 10^{-3} M $Fe(CN)_6^{4-}$ (scan rate 300 mV s^{-1}), they found the following values for glassy carbon: pH 1.0, + 1.3 V vs. SCE; pH 4.2, + 1.4 V vs. SCE; pH 10.0, + 0.95 V vs. SCE. However, it has to be emphasized that all these observations are based on voltammetric experiments in which the potential is changed relatively slowly. It has been shown by Dieker et al. [7] that with the application of normal pulse and differential pulse voltammetry much larger residual currents are observed because of chemical transformations of the surface. In this respect the carbon paste electrode was found to be preferable to the GCE or the platinum electrode.

In the following sections the use of GCEs in the various electroanalytical techniques will be summarized.

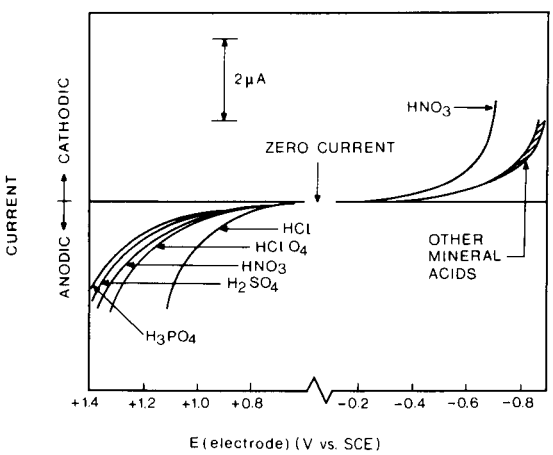

Fig. 2. Usable potential range for GCE in various mineral acids [41]. Test conditions: acid concentrations 0.1 M for HCl, HNO_3 and $HClO_4$, 0.05 M for H_2SO_4 and 0.033 M for H_3PO_4. Scan rate: 0.1 V min^{-1}. (Reproduced by kind permission of the American Chemical Society.)

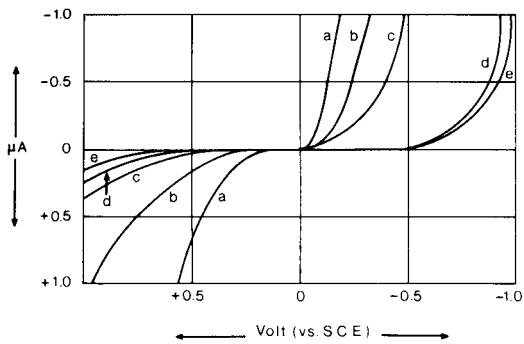

Fig. 3. Current—voltage curves in 0.2 M KNO_3 [42]. (a) Wax-impregnated graphite; (b) wax-impregnated carbon; (c) carbon paste; (d) pyrolytic graphite; (e) glassy carbon. (Reproduced by kind permission of Fresenius Z. Anal. Chem.)

Voltammetry

Zittel and Miller [41] have studied the voltammetric behaviour of Ce(III), Ce(IV), Cr(VI), Fe(II), Hg(I), $Fe(CN)_6^{4-}$, Ag(I), Cu(II) and UO_2^{2+}. For all these ions except Cr(VI), the waves are well defined and reproducible. In the millimolar range the peak current was found to be linearly dependent on the concentration. The voltammetric behaviour of neptunium(VI) in glutamic acid, glutaric acid, malonic acid and propionic acid at a rotating GCE has been described by Plock [44—47]. The reversible one-electron reduction wave was used to study the nature of the respective neptunium(VI) complexes.

The reduction wave of iron(III) at a GCE can be used for quantitative analyses. The reduction is reversible in perchloric acid and slightly irreversible in hydrochloric, nitric and acetic acids, as was shown by Štulíková and Vydra [14]. Presumably this irreversibility is due to a decreased tendency for the iron(III) ion to be adsorbed, because of complexation. The irreversibility is even more pronounced in sulphuric acid medium. It is assumed that the sulphate ion is preferentially adsorbed, displacing the iron from the surface. The calibration curves are linear in perchloric and nitric acid solutions and slightly curved in hydrochloric acid solutions. The practical lower limit of detection is at least 10^{-5} M. Štulíková and Vydra have also shown that at lower pH in complexing media, e.g. EDTA, citric acid and oxalic acid, the limiting current is diffusion-controlled and well suited to form the basis of an analytical method [48]. At higher pH values the quality of the wave deteriorates.

EDTA and related compounds such as EGTA, DCTA, DTPA and TTHA are voltammetrically active at glassy carbon in a wide pH interval [49]. At the rotating GCE, well developed waves are obtained as long as no oxygen is adsorbed on the surface. A slightly curved calibration curve was observed at pH 2.3 in the range 10^{-4}—2×10^{-3} M EDTA. The number of electrons involved in the oxidation is 4.

Thiocyanate can be oxidized irreversibly at a GCE in aqueous solutions,

the oxidation products being mainly cyanide and sulphate. The peak currents measured in linear sweep voltammetry (sweep rate 0.02 V s^{-1}) show a linear dependence on concentration in the millimolar range, as has been shown by Holtzen and Allen [50].

The good resistance of glassy carbon against chemical attack makes it possible to apply the electrode in very corrosive media such as concentrated hydrofluoric acid. Bond et al. [51] studied the electrodeposition of Ag(I), Hg(II), Cd(II), Tl(I), Sn(II) and Pb(II) in this medium. A comparison of a large number of electroanalytical techniques including d.c., a.c. and pulse voltammetry indicates that the pulse techniques offer substantial advantages over linear sweep methods. For Ag(I) and Hg(II) in 49% hydrofluoric acid, detection limits of about 10^{-6}—10^{-5} M are reported.

A rotating glassy carbon disc electrode in combination with a.c. voltammetry can be used for quantitative work. Vydra et al. [52] have shown that the a.c. peak height for the reversible cyanoferrate couple is linearly dependent on the depolarizer concentration in the range 10^{-4}—2×10^{-3} M. However, since the reversibility of a redox system, and thus the peak height, is very sensitive to electrode pretreatment, the method should be applied to reversible systems only.

Recently, Fleet and Fouzder [53] have used a GCE for the reduction of organolead compounds. In the case of differential pulse voltammetry the linear range of the calibration curve extends from 2.5×10^{-4} to 10^{-7} M. This organo-metallic example forms a good transition to the discussion of the use of GCEs in the examination of organic compounds. GCEs have been used in many cases for the elucidation of electron transfer mechanisms of organic compounds. Here, the discussion will be confined to those papers which explicitly mention analytical applications. Jennings et al. [54] have used linear sweep voltammetry for the determination of 2-ethylanthraquinone with a GCE; the reduction of millimolar amounts in methanol, ethanol or propan-2-ol proceeds with a precision better than 2%. The anodic voltammetric characteristics of 11 polynuclear aromatic hydrocarbons have been measured at stationary and rotated glassy carbon disc electrodes in sulpholane, and some of them in acetonitrile as well. The limit of detection with differential pulse voltammetry is about 5×10^{-7} M in sulpholane and 2×10^{-8} in acetonitrile [55].

Weber and Volke [27] mention the possibility of using the reduction of aromatic carbonyl-containing substances at the rotated GCE for determining low concentrations, but no quantitative information is provided. Phenolic analgesics have been determined by linear sweep voltammetry at a GCE by Chan and Fogg [56]. Although no cathodic or anodic waves were observed in aqueous media, a suitable anodic wave appeared in ethanol. The calibration curves were found to be linear down to 10 μg ml^{-1}.

A differential pulse voltammetric determination of adrenaline at glassy carbon has been reported by Ballantine and Woolfson [57]. Other substances of biochemical interest have been investigated by several Japanese

authors. Yao et al. [58] have studied the anodic oxidation of deoxyribonucleic acid at a GCE as well as the simultaneous determination of purine bases and their nucleosides [59]. At appropriate pH values the peak height versus concentration curves are linear.

Because the low rate at which surface functional groups at glassy carbon come to redox equilibrium, Blaedel and Jenkins [60] have proposed that the currents at each potential should be allowed to reach a steady state. By doing so, current transients can be eliminated and very low background currents may be achieved, permitting the determination of micromolar amounts of nicotinamide adenine dinucleotide (NADH).

Stripping voltammetry

Stripping voltammetry is a very attractive technique because of the very low limits of determination that can be attained. Under appropriate conditions several metals can be deposited directly onto the GCE and subsequently stripped by scanning to positive potentials.

Determinations of trace amounts of silver (10^{-6}—10^{-9} M) and copper (10^{-6}—10^{-8} M) are possible in acidic, neutral or alkaline media with an error that does not exceed 5% [61]. Hircq and Lafontan [62] determined 1 ppb silver in uranium and plutonium, whereas Temmerman and Verbeek [63] reached the same limit of detection in the determination of silver in cadmium, provided that the electrode was polished daily and prepolarized at +0.65 V vs. SCE between each run. The importance of the pretreatment in the determination of silver was also mentioned by Monien et al. [42].

Vydra et al. [52] have studied the feasibility of using an a.c. voltammetric technique with rotating glassy carbon electrodes. They report that the sensitivity is not markedly greater than that for d.c. stripping, but the selectivity seems to be considerably improved, allowing the determination of copper and silver in the same solution without the necessity of changing solutions.

Determinations of 10^{-8} M lead have proven to be possible even when cadmium is present in a 10-fold excess. A 10-fold excess of copper completely suppresses the anodic peak of lead [64]. Beniaminova and Kabanova [65] determined as little as 5×10^{-8} M cadmium without interference from lead. They applied the method for the determination of cadmium in high-purity zinc sulphate (Cd content ca. 2.5×10^{-5}%). Dian et al. [66] have used the stripping technique together with pulse voltammetry for the determination of lead.

Several authors have dealt with the determination of mercury by means of anodic stripping voltammetry at GCEs. Luong and Vydra [67] have described the determination in the concentration range 10^{-6}—5×10^{-8} M by using a.s.v. at a rotated glassy carbon disc electrode; 10-fold amounts of Cu, Pb, Zn, Ni, Co and Cd can be tolerated. A decrease in the limit of determination to 5×10^{-10} M has been found attainable by using the second-harmonic a.c. technique [68]. Taddia [69] has described a procedure for

the determination of mercury in air employing a.s.v. Small samples can be analyzed by means of a micro cell constructed by Štulík and Štulíková [70]. The cell volume is about 5 μl, which allows the determination of 100 pg of mercury and 10 pg of lead.

One of the major disadvantages of direct electrodeposition onto the surface of a solid electrode, e.g. a glassy carbon electrode, is the formation of monolayers which on stripping lead to double peaks. This problem can be avoided by coating the electrode with a thin mercury film. The problems associated with the electrodeposition of mercury on glassy carbon have been discussed above. A very attractive procedure has been proposed by Florence [71] who added mercury(II) nitrate to the sample solution and deposited mercury and trace metals simultaneously. The trace metals are then anodically stripped from the mercury film and after the analysis the mercury film can be completely removed from the electrode simply by wiping with a tissue. This technique is highly sensitive and gives excellent resolution of neighbouring peaks.

The discussion of mercury thin film electrodes is, strictly speaking, beyond the scope of this review in as far as the problems at the mercury/solution interface are concerned, but since the pretreatment of the surface of the base electrode is of essential importance, several references [51, 72—77] should be consulted for those cases where glassy carbon has been used as the base electrode.

The stripping technique is not restricted to species that can be electrodeposited on reduction. Cox and Cheng [78] have described the cathodic stripping of phosphate which is formed on the anodic oxidation of iron(II) in the presence of phosphate resulting in a film of sparingly soluble iron(III) phosphate. The calibration curve is linear down to 0.1 ppm.

Amperometry

Although amperometry, and more particularly the amperometric titration technique, forms a logical consequence of the voltammetric techniques, relatively few papers have been published on the use of GCEs in amperometry. Coenegracht et al. [79] have reported on the automatic amperometric microtitration of barbiturates with mercury(II) at a glassy carbon indicator electrode. They were able to titrate 50 μg of barbiturate with an accuracy and a precision of about 2% when the mercury complex formed was extracted into an organic phase (two-phase titration). Biamperometric titrations with glassy carbon electrodes have also been described. Vydra and Peták [80] have demonstrated the applicability of two GCEs for biamperometric EDTA titrations in acidic solution. The iron(III)—EDTA system was studied in some detail. Since the overvoltage for the oxygen reduction at a GCE is rather large, dissolved oxygen does not interfere in the titration of iron(III). The applicability of a pair of GCEs for the indication of aqueous acid—base titrations has been studied by Samcová et al. [81]. They employed biamperometry, bipotentiometry and a.c. polarization. These titrations are

sufficiently accurate and precise even for the determination of very weak acids or bases. An advantage over equilibrium potentiometric titrations is that the measured value is almost instantaneously stable and that low concentrations can be titrated (down to 10^{-5} M using a.c. polarization for the end-point detection).

Coulometry

Glassy carbon has been examined extensively for its suitability as a working electrode by Jennings, Dodson and co-workers [82—87]. Bromine can be generated with a theoretical current efficiency greater than 99.9%, but an additional overpotential of 0.1 V is required to oxidize bromide at a GCE compared with a platinum electrode [82]. The theoretical value has been confirmed by the titration of 100 μeq of arsenic(III) with an accuracy and precision each of 0.1%. The coulometric generation of hydroxide ions at a GCE was tested in the titration of potassium hydrogenphthalate [83]. Under appropriate conditions, 10 mg of phthalate could be determined with a relative standard deviation of 0.4% and a mean error of —0.2%, which shows that glassy carbon behaves satisfactorily as a working cathode for the coulometric titration of acids. The procedure was used for the determination of $1—0.2 \times 10^{-4}$ moles of hydrofluoric acid with adequate precision [84]. In acetic acid—acetic anhydride medium, potassium hydrogenphthalate behaves as a base. Since preliminary work had shown that a glassy carbon anode yielded protons with a current efficiency of 85% only when sodium perchlorate was used as the supporting electrolyte, hydrogen ion generation via the electrochemical oxidation of quinol was used [85]. Milligram samples could be titrated with a relative standard deviation of 0.1—0.2%.

The potentiometric titration of arsenic(III) with coulometrically generated iodine was also examined [86]. In this case, carbon fibre was also considered as a potential electrode material; carbon fibre is manufactured similarly and has the same properties as glassy carbon. It is available as a tow containing up to 10,000 parallel filaments each of about 8 μm in diameter, so that very high limiting currents are observed, which is favourable for high current efficiency. Both glassy carbon and carbon fibre electrodes could be used to generate iodine for the titration of arsenic(III) or thiosulphate but there is some indication that small positive errors occur because of the specific adsorption of iodine at the electrodes. Finally, a small-scale coulometric titration cell with a glassy carbon rod anode has been described [87]. This cell with a volume of about 3 ml was used for the titration of microgram amounts of arsenic(III) and isonicotinylhydrazide (isoniazid) with bromine; the precision was about 2%. It is rather curious that in all the procedures presented by Jennings, Dodson and co-workers no reference is made to pretreatment of the electrode surface, the more so as the coulometric techniques demand a very high current efficiency. The results presented by Jennings, Dodson and co-workers are somewhat at variance with the

statement by Plock and Vasquez [88] that mercury and platinum electrodes yield better precision.

Kabanova and Zalogina [89] have described a coulometric determination of mercury by means of a glassy carbon electrode, based on a preliminary electrochemical preconcentration. Essentially, the method is the same as that used in anodic stripping voltammetry.

Potentiometry

It is well known that platinum electrodes can be used to indicate end-points in acid—base titrations. Doležal and Štulík [90] have compared glassy carbon and platinum electrodes in this respect and have also found acid—base-indicating properties for the GCE. The indication seems to proceed by an irreversible redox system consisting of cathodic reduction of dissolved atmospheric oxygen and anodic oxidation of water, the latter process being dependent on the pH of the solution. Both electrodes can be used with good results and especially for titrations of hydrofluoric acid where the glass electrode would be attacked. The electrode response is 50 mV/pH for platinum and 20 mV/pH for the GCE. No explanation is given for this discrepancy. Dodson and Jennings [91] have demonstrated that the oxidized surface of glassy carbon is no longer inert and that its behaviour resembles that of graphitic oxide. The oxidation was performed by passing a current of 5 mA for 200 s through the cell filled with 1 M H_2SO_4, the GCE being the anode (exposed area 7.1 mm^2) with a platinum cathode. The behaviour is similar to a metal/metal oxide electrode in acidic solution and the electrode was found to be suitable for indication of acid—base end-points. The electrode response was 55 mV/pH in the concentration range 10^{-5}—1 M hydrochloric acid. Glassy carbon combination electrodes have also been described [92]. In this case two GCEs are pretreated by using them in the electrolysis cell in such a way that oxygen is produced at the anode and hydrogen at the cathode. During the acid—base titration the potential difference between the two electrodes is measured and the end-point appears as a peak in the graph of potential against added amount of alkali.

Chronopotentiometry

Chronopotentiometry has been used by Zittel and Miller [93] to study the oxidation of iodide at glassy carbon and pyrolytic graphite electrodes. Apart from the formation of iodine, the reaction $\frac{1}{2} I_2 + H_2O \rightarrow IO^- + 2H^+ + e^-$ seems to proceed to some extent. Since this reaction has not been reported by other investigators who used either metal or boron carbide electrodes, this reaction appears to be peculiar to the carbon electrodes. Vydra and Luong [94—96] have examined the chronopotentiometric method for electrochemical stripping analysis on glassy carbon disc electrodes. They have stated that, from the analytical point of view, it is important that the charging of the electrical double layer does not affect the course of the E—t curves [94]. It turned out that good resolution is possible; two metals

with a difference of about 40 mV in the dissolution potentials can be determined. The limit of determination is equal to, or even somewhat lower than, that available by stripping voltammetry under equal conditions.

In most cases the sensitivity and the reproducibility could be improved by the simultaneous deposition of mercury with the other metals, but this influences the E—t curves depending on the solubility of the metals in mercury. With metals readily soluble in mercury, the transition time, τ, increases, whereas with metals sparingly soluble in mercury the value of τ decreases. The dependence of τ on the concentration is linear in the range 10^{-8}—10^{-4} M [95]. An extensive survey of the basic parameters such as medium, pre-electrolysis time, stripping current as well as the concentration range has been presented [96].

An interesting variant of stripping analysis has been described by Jagner and Årén [97]. The technique, which they call derivative (chrono-) potentiometric stripping analysis, is based on the preconcentration of metal analytes directly onto glassy carbon or in a thin film of mercury on glassy carbon and subsequent measurement of the electrode potential subject to controlled transport of oxidant to the electrode surface. This oxidant strips the metal from the mercury film. To avoid oxidation of the mercury itself, iron(III) or mercury(II) can be used as mild oxidants. Of course, if mercury or other noble metals, e.g. silver, have to be determined, strong oxidizing agents such as acidic permanganate must be used. One of the great advantages of this technique is that in the stripping phase no current is drawn and, therefore, the methods can be used in samples with low ionic strength or in organic solutions which exhibit a low conductivity. Heavy metals can be analysed in the concentration range 0.1—10 ppm.

FLOW-THROUGH DETECTORS

During the last decade there has been a greatly enhanced interest in flow-through detectors, and especially electrochemical flow cells. Particularly, attempts have been made to develop detectors of sufficiently small volumes to be compatible with modern high-performance liquid chromatography (h.p.l.c.) and systems for continuous analysis, for example flow injection analysis (f.i.a.). Detectors based on electrochemical reactions can be subdivided in two categories: amperometric and coulometric detectors. This nomenclature is rather misleading because in both cases the current is usually measured. However, in coulometric cells one is aiming at a quantitative conversion of all the analyte and electrodes with a relatively large area are therefore used, whereas in amperometric cells much smaller electrodes are used and the current will depend on the limited transport determined by the hydrodynamic conditions.

Fleet and Little [98] have discussed some of the requirements that have to be fulfilled by an amperometric flow-through detector to make it suitable as a h.p.l.c. detector. They claim that a detector based on the "wall-jet"

principle using a glassy carbon working electrode offers some unique features. Of special importance is the very small effective cell volume of about 0.5 μl. Lund et al. [99] have designed a cell based on the same principle. They found that some commercial detectors did not function properly because of excessive uncompensated resistances. These authors as well as Dieker et al. [100] have found constant-potential amperometry to be preferable to normal-pulse measurements; the latter technique gave excessive background currents because of chemical changes at the glassy carbon surface. With the differential pulse technique, the calibration graph often showed a deviation from linearity probably caused by small shifts of the peak potential. Dieker et al. [100] have found that, at the expense of some loss in detection limit, the normal-pulse technique can give some improvement when strong adsorption takes place provided that the rest potential is adjusted to a value at which desorption takes place.

An amperometric cell with a small uncompensated resistance has been developed by Bollet et al. [101]; for the rest, this cell is similar to that suggested by Kissinger et al. [102].

A differential amperometric detector provided with GCEs has been described by Brunt and Bruins [103]. They have used the detector in f.i.a. as well as in combination with anion-exchange chromatography [104]. Brunt et al. [105] have designed a detector with a rotating glassy carbon electrode. An evaluation of the parameters that are important in operating an amperometric detector with a glassy carbon electrode has also been given by Ivaska and Smyth [106]. Several authors have described coulometric cells. A working electrode of carbon cloth, a material made of glassy carbon fibres, was used by Takata and Muto [107]; this material has a large active surface facilitating 100% current efficiency together with 100% conversion. In this case the preparation of a calibration curve is unnecessary and variations in the flow rate and temperature of the effluent hardly affect the results. Such a mass-flow sensitive device made of large flat glassy carbon working and auxiliary electrodes has also been designed by Lankelma and Poppe [108]. The applicability of this detector was shown in the chromatographic analysis of biogenic amines and other biomedical mixtures [109, 110].

Strohl and Curran [111, 112] have made an electrochemical flow-through cell in which reticulated vitreous carbon (RVC) is used as the working electrode. This material combines a large surface with a low fluid flow resistance. The cell could operate in an amperometric and a coulometric mode. A relative precision of a few ng l^{-1} was achieved in the latter mode, but the sampling rate was limited to 20—30 samples per hour. Much higher sampling rates (up to 264 samples per hour) were achieved in the amperometric mode, the relative precision being about 0.5%. Blaedel and Wang [113] have also used RVC. Their cell can contain a variable number of RVC discs thus increasing the conversion yield. However, increased electrode length leads to a proportionally increased background.

Special attention has been paid to the development of flow-through cells

for stripping analysis. Wang and Ariel [114] have described a.s.v. with a mercury-coated glassy carbon electrode in a flow-through system for the analysis of sea water. An improvement could be realized by measuring in a differential mode with two GCEs [115]. A remarkably constant background in stripping analysis can be attained when the conventional a.s.v. is supplemented, during the stripping step, by simultaneous re-deposition (collection) at the ring of a ring-disc electrode. The collection current is measured at a suitable, constant cathodic potential so that no change in the surface condition and no charging of the double layer occurs [116]. A similar procedure was suggested by Schieffer and Blaedel [117] who described a cell consisting of a pair of tubular glassy carbon electrodes in series for a.s.v. with collection at thin mercury films.

A technique that can be considered to be in a direct line with the coulometric cell is the technique termed electrolytic chromatography and developed by Fujinaga and Kihara [118—120]. This technique makes use of a column electrode with glassy carbon grains. A full account is beyond the scope of this review.

CHEMICALLY MODIFIED GLASSY CARBON ELECTRODES

In the previous sections ample evidence has been presented that glassy carbon surfaces can be oxidized to carbonyl or even carboxyl groups. The occurrence of these carboxyl groups forms the basis of a class of chemically modified electrodes introduced by Lennox and Murray [121, 122]. The desired modification proceeds according to the following reaction scheme:

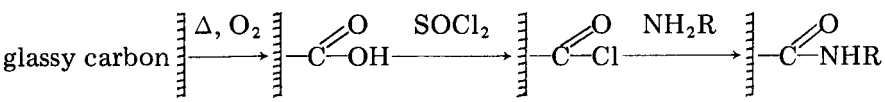

where R is an electrochemically reactive moiety, for instance a tetraphenylporphyrin ring. It was shown by Rocklin and Murray [123] that the thionyl chloride can be replaced by acetyl chloride. Because subsequent metallation of the immobilized porphyrine is possible, systems can be synthesized which exert interesting and potentially useful electrocatalytic effects. Bettelheim et al. [124] have made use of the specifically adsorbed cobalt(III) tetrapyridylporphyrin on a GCE for electrocatalysis of reduction of oxygen.

In a preliminary note, Murray and co-workers [125] demonstrated that it was possible to activate the glassy carbon surface by mechanical abrasion and by etching with a radiofrequency argon plasma. In this case the "surface oxides" are removed and, at the same time, the reactivity of the surface carbon is increased so that ferrocene or pyridine can be attached directly via vinyl ferrocene or vinyl pyridine, respectively. Further research seems to be in progress.

ELECTROSYNTHESIS AT GLASSY CARBON ELECTRODES

In electrosynthesis, platinum and graphite electrodes have already frequently been used. During the last decade glassy carbon has also received some attention, because at carbon electrodes there seems to be a tendency for further oxidation of the primarily produced carbon radicals to carbonium ions. In general, this leads to more side-products [126].

According to Plzak and Wendt [127], who studied the azide-anion oxidation in acetonitrile and drew a parallel to the Kolbe reaction, the unique role played by platinum (and platinum group metals) is due to the fact that on platinum, carbon radicals are adsorbed to a much lesser extent than on carbon. This low adsorbability of the radicals at platinum gives rise to typical homogeneous consecutive reactions such as dimerization reactions. In contrast, at carbon anodes, heterogeneous reactions can occur which involve a further oxidation to carbonium ions and finally the formation of monomers. A good example is the oxidation of carboxylate anions:

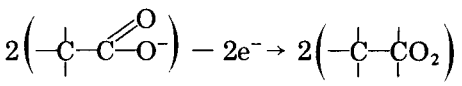

on platinum

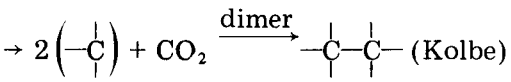

on carbon

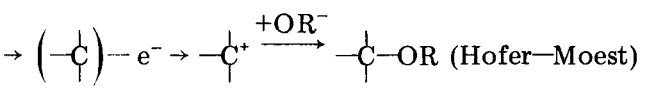

The conclusions drawn by Plzak and Wendt from their experiments in acetonitrile do not seem to be valid for all solvents. Brennan and Brettle [128] who examined the oxidation of heptanoate in protic solvents such as methanol, ethanol and water, found that the Kolbe-dimer dodecane is formed at glassy carbon.

Cauquis and Serve [129] have observed that in acetonitrile the oxidation of hydroxy-4-diphenylamine at a GCE differs from that at a platinum electrode. They attribute this to a deprotonating step preceding the oxidation, which step proceeds much faster on glassy carbon than on platinum.

The reduction of organic chlorides at the GCE has been reported by Lambert et al. [130, 131]. They showed that, in contrast to the dropping mercury electrode, alkyl monochlorides could be reduced at a GCE in dimethyl formamide. They discovered that even carbon tetrachloride could be reduced in four consecutive steps. Bard and Merz [132] re-investigated the reduction of allyl halides in non-aqueous solvents, e.g. acetonitrile.

They found that at glassy carbon the reduction is free of substrate and product surface interactions, and represents a purely diffusion-controlled one-step electroreduction, whereas at platinum and mercury the surface plays an active role leading to multiple peaks. Quaal et al. [133] studied the substituent effects on reductive cleavage of *N*-methylarenesulphonanilide by means of sodium anthracene as well as electrochemically at the GCE. The electrochemical reduction of aromatic sulphenyl and sulphonyl chlorides was studied by Johansson and Persson [134]. At glassy carbon, disulphides and thiosulphonates are formed as intermediates. According to van Effen and Evans [135] the oxidation at a GCE of aliphatic aldehydes occurs in acetonitrile at very positive potentials (+3 V vs. SCE). The peak potentials correlate with the ionization potentials. Adsorption phenomena in the NAD^+/NADH system at GCEs have recently been reported by Moiroux and Elving [136].

A group of Russian investigators has studied the electrochemical properties of different grades of glassy carbon in electrosynthesis reactions at high anode potentials. They have found that adipate ions and to a somewhat lesser extent acetate ions retard the oxidation of solvent, for instance methanol. Therefore, adipate ions are added to the solution used for the electrochemical preparation of sebacic acid diester [137].

PRETREATMENT OF GLASSY CARBON ELECTRODES

From the discussion in the preceding sections, it is evident that glassy carbon electrodes need some kind of pretreatment to obtain reproducible results. It is virtually impossible to summarize all the procedures described in the literature, because there seem to be as many different procedures as there are investigators who have used GCEs. However, some general aspects can be considered.

Glassy carbon has a very low porosity but, depending on the quality of the glassy carbon, microscopic pitting can be observed at the polished surface. Presumably, these cavities are due to excessively fast heating during the carbonization process so that the gases formed have too little time to diffuse to the surface. The more careful the heating procedure, the fewer the cavities and the better the electrode will function. To obtain well-defined surfaces, the electrodes have to be abraded with emery paper of increasing fineness followed by polishing with, for instance, alumina or chromium(III) oxide suspensions (particle size 0.3 μm).

An electrode surface pretreated in this way is virtually free of functional groups. When the electrode is immersed in a solution, chemical or electrochemical attack can take place. If the electrode surface has to be maintained without any oxygen-containing groups, the electrode must be washed after polishing with acids which have no oxidizing properties (e.g. 1 + 1 HCl) [138], the solution has to be free of oxidizing agents, and the potential must be kept slightly negative with respect to a SCE. As soon as the solution contains

strong oxidizing agents and/or the potential is made positive, carbonyl groups and even carboxyl groups can be formed. Subsequent scanning in the negative direction leads to a reduction of the carbonyl groups, possibly to hydroxyl groups. No stripping of the oxygen-containing groups seems to occur and hence the electrode surface which has been once oxidized can only be freed from functional groups by abrading again. Electrodes fouled by adsorption of reactants or reaction products can often be cleansed by rinsing with ethanol or chloroform, or by wiping the surface carefully with a wet paper tissue. When the electrode has to be brought to a special chemical condition, it has been recommended to apply several polarization cycles. Eggli [139] who studied the influence of the electrode pretreatment on the detection limit of anodic stripping voltammetry at a mercury-coated GCE, has found the following procedure to be suitable: after mechanical pretreatment, including abrading and polishing, 5 polarization cycles are applied in which in each cycle the potential is kept at −1.0 V vs. SCE for 10 min and subsequently scanned to 0 V at a rate of 20 mV s^{-1}.

The above discussion has been restricted to processes which change the surface, but which do no irreparable damage to the electrode. Irreversible deterioration of the glassy carbon was observed by Dodson and Jennings [140] when the electrode operates with large current densities when anodically polarized. With a current density of 1 mA cm^{-2} in a solution of 0.05—1 M sulphuric acid, the electrode shows a shiny black surface; an increase of the current density to 20 mA cm^{-2} causes a black product to flake off after about one hour. They have drawn a parallel with graphite where a similar reaction is used to produce a black form of graphitic oxide.

Commercial availability of glassy carbon

Several manufacturers of glassy carbon are mentioned in the literature. At the risk of being incomplete, these firms are mentioned here: Tokai Electrode Manufacturing Co., Ltd., Tokyo, Japan; Le Carbone Lorraine, Paris, France; Vitreous Carbon, Ltd., United Kingdom; VEB Elektrokohle, Berlin-Lichtenberg, G.D.R.; Sigridur, Firma Sigri, Meitingen bei Augsburg, F.R.G.; Chemotronics International, Inc., Ann Arbor, MI, U.S.A. (manufacturer of reticulated vitreous carbon).

REFERENCES

1 S. Yamada and H. Sato, Nature, 193 (1962) 261.
2 J. C. Bokros, Carbon, 15 (1977) 355.
3 G. M. Jenkins and K. Kawamura, Nature, 231 (1971) 175; Polymeric Carbons — Carbon Fibres, Glass and Char, Cambridge University Press, Cambridge, 1976.
4 J. P. Randin and E. Yeager, J. Electroanal. Chem., 58 (1975) 313.
5 D. Laser and M. Ariel, J. Electroanal. Chem., 52 (1974) 291.
6 B. D. Epstein, E. Dolle-Malle and J. S. Mattson, Carbon, 9 (1971) 609.
7 J. W. Dieker, W. E. van der Linden and H. Poppe, Talanta, 25 (1978) 151.
8 L. Dunsch and R. Naumann, Z. Chem., 14 (1974) 31.
9 V. Majer, J. Veselý and K. Štulík, J. Electroanal. Chem., 45 (1973) 113.

10 M. Březina and A. Hofmanová, Collect. Czech. Chem. Commun., 38 (1973) 985.
11 R. J. Taylor and A. A. Humffray, J. Electroanal. Chem., 64 (1975) 63.
12 R. J. Taylor and A. A. Humffray, J. Electroanal. Chem., 64 (1975) 85, 95.
13 Yu. B. Vasil'ev, L. S. Kanevskii, V. I. Lushikov and A. M. Skundin, Sov. Electrochem., 19 (1977) 377.
14 M. Štulíková and F. Vydra, J. Electroanal. Chem., 38 (1972) 349.
15 M. Štulíková and F. Vydra, J. Electroanal. Chem., 44 (1973) 117.
16 M. Štulíková, J. Electroanal. Chem., 48 (1973) 33.
17 D. Laser and M. Ariel, J. Electroanal. Chem., 52 (1974) 474.
18 L. Dunsch, Z. Chem., 19 (1979) 77.
19 D. M. Kolb, M. Przasnyski and H. Gerischer, J. Electroanal. Chem., 54 (1974) 25.
20 V. V. Pnev, L. A. Moskovskikh and V. S. Putrova, J. Anal. Chem. USSR, 28 (1973) 1704.
21 Z. Yoshida and S. Kihara, J. Electroanal. Chem., 95 (1979) 159.
22 R. G. Daneshwar and A. V. Kulkarni, J. Electroanal. Chem., 99 (1979) 207.
23 F. Palmisano, E. Desimoni, L. Sabbatini and G. Torsi, J. Appl. Electrochem., 9 (1979) 517.
24 D. D. Lyungrin, V. V. Pnev and M. S. Zakharov, J. Anal. Chem. USSR, 30 (1975) 1032.
25 R. J. Taylor and A. A. Humffray, J. Electroanal. Chem., 42 (1973) 347.
26 W. J. Blaedel and G. W. Schieffer, J. Electroanal. Chem., 80 (1977) 259.
27 J. Weber and J. Volke, Electrochim. Acta, 24 (1979) 113.
28 H. W. Salzberg, J. Electrochem. Soc., 121 (1974) 1451.
29 M. P. J. Brennan and O. R. Brown, J. Appl. Electrochem., 3 (1973) 231.
30 O. R. Brown and S. Clarke, J. Electroanal. Chem., 70 (1976) 349.
31 M. Abraham, M. C. Trudelle and M. Poirier, J. Appl. Electrochem., 6 (1976) 183.
32 B. V. Tilak and B. E. Conway, Electrochim. Acta, 21 (1976) 745.
33 C. L. Hussey, L. A. King and J. K. Erbacher, J. Electrochem. Soc., 125 (1978) 561.
34 W. K. Behl, J. Electrochem. Soc., 118 (1971) 889.
35 J. Thonstad, Electrochim. Acta, 15 (1970) 1581.
36 R. D. Armstrong, T. Dickinson and M. Reid, Electrochim. Acta, 20 (1975) 709.
37 R. D. Armstrong, T. Dickinson and M. Reid, Electrochim. Acta, 21 (1976) 935.
38 J. Phillips, R. J. Gale, R. G. Wier and R. A. Osteryoung, Anal. Chem., 48 (1976) 1266.
39 S. C. Levy and P. R. Farina, Anal. Chem., 47 (1975) 604.
40 R. D. Armstrong, T. Dickinson and P. M. Willis, J. Electroanal. Chem., 48 (1973) 47.
41 H. E. Zittel and F. J. Miller, Anal. Chem., 37 (1965) 200.
42 H. Monien, H. Specker and K. Zinke, Z. Anal. Chem., 225 (1967) 342.
43 J. F. Alder, B. Fleet and P. O. Kane, J. Electroanal. Chem., 30 (1971) 427.
44 C. E. Plock, Anal. Chim. Acta, 43 (1968) 281.
45 C. E. Plock, Anal. Chim. Acta, 47 (1969) 27.
46 C. E. Plock, J. Inorg. Nucl. Chem., 30 (1968) 3023.
47 C. E. Plock, Anal. Chim. Acta, 53 (1971) 249.
48 M. Štulíková and F. Vydra, J. Electroanal. Chem., 39 (1972) 229.
49 P. Peták and F. Vydra, J. Electroanal. Chem., 33 (1971) 161.
50 D. H. Holtzen and A. S. Allen, Anal. Chim. Acta, 69 (1974) 153.
51 A. M. Bond, T. A. O'Donnell and R. J. Taylor, Anal. Chem., 46 (1974) 1063.
52 F. Vydra, M. Štulíková and P. Peták, J. Electroanal. Chem., 40 (1972) 99.
53 B. Fleet and N. B. Fouzder, J. Electroanal. Chem., 99 (1979) 227.
54 V. J. Jennings, T. E. Forster and J. Williams, Analyst, 95 (1970) 718.
55 J. F. Coetzee, G. H. Kazi and J. C. Spurgeon, Anal. Chem., 48 (1976) 2170.
56 H. K. Chan and A. G. Fogg, Anal. Chim. Acta, 105 (1979) 423.
57. J. Ballantine and A. D. Woolfson, J. Pharm. Pharmacol., 30 (1978) 46P.
58 T. Yao, T. Wasa and S. Musha, Bull. Chem. Soc. Jpn., 51 (1978) 1235.
59 T. Yao, T. Wasa and S. Musha, Bull. Chem. Soc. Jpn., 50 (1977) 2917.

60 W. J. Blaedel and R. A. Jenkins, Anal. Chem., 46 (1974) 1952.
61 M. Kopánicá and F. Vydra, J. Electroanal. Chem., 31 (1971) 175.
62 B. Hircq and S. Lafontan, Anal. Chim. Acta, 93 (1977) 183.
63 E. Temmerman and F. Verbeek, Anal. Chim. Acta, 58 (1972) 263.
64 O. L. Kabanova and S. M. Beniaminova, J. Anal. Chem. USSR, 26 (1970) 94.
65 S. M. Beniaminova and O. L. Kabanova, J. Anal. Chem. USSR, 30 (1975) 55.
66 G. Dian, J. Huguet and C. Caullet, Analusis, 5 (1977) 408.
67 L. Luong and F. Vydra, J. Electroanal. Chem., 50 (1974) 379.
68 M. Štulíková and F. Vydra, J. Electroanal. Chem., 42 (1973) 127.
69 M. Taddia, Microchem. J., 23 (1978) 64.
70 K. Štulík and M. Štulíková, Anal. Lett., 6 (1973) 441.
71 T. M. Florence, J. Electroanal. Chem., 27 (1970) 273.
72 D. R. Kendall, Anal. Lett., 5 (1972) 867.
73 A. H. Miguel and C. M. Jankowski, Anal. Chem., 46 (1974) 1832.
74 M. Geiszler, B. Schiffel and C. Kuhnhardt, Z. Chem., 15 (1975) 408.
75 J. Dieker and W. E. van der Linden, Fresenius Z. Anal. Chem., 274 (1975) 97.
76 L. Sipos, S. Kozar, I. Kontušić and M. Braniča, J. Electroanal. Chem., 87 (1978) 347.
77 G. Subramanian and G. P. Rao, J. Electroanal. Chem., 70 (1976) 133.
78 J. A. Cox and K. H. Cheng, Anal. Lett., 7 (1974) 659.
79 P. M. J. Coenegracht, A. Bult and H. J. Metting, Z. Anal. Chem., 284 (1977) 273.
80 F. Vydra and P. Peták, J. Electroanal. Chem., 24 (1970) 379.
81 E. Samcová, J. Štulík and J. Dolezăl, Collect. Czech. Chem. Commun., 37 (1972) 60.
82 V. J. Jennings, A. Dodson and A. M. Atkinson, Analyst, 97 (1972) 923.
83 V. J. Jennings, A. Dodson and G. Tedds, Talanta, 20 (1973) 681.
84 V. J. Jennings, A. Dodson and D. Colbourne, Anal. Chim. Acta, 75 (1975) 478.
85 V. J. Jennings, A. Dodson and G. Tedds, Talanta, 21 (1974) 622.
86 V. J. Jennings, A. Dodson and R. J. Eastman, Anal. Chim. Acta, 76 (1975) 143.
87 V. J. Jennings, A. Dodson and A. Harrison, Analyst, 99 (1974) 145.
88 C. E. Plock and J. Vasquez, Talanta, 16 (1969) 1490.
89 O. L. Kabanova and E. A. Zalogina, J. Anal. Chem. USSR, 26 (1970) 726.
90 J. Doležal and K. Štulík, J. Electroanal. Chem., 17 (1968) 87.
91 A. Dodson and V. J. Jennings, Anal. Chim. Acta, 72 (1974) 205.
92 V. J. Jennings, A. Dodson and D. Colbourne, Anal. Chim. Acta, 75 (1975) 481.
93 H. E. Zittel and F. J. Miller, J. Electroanal. Chem., 13 (1967) 193.
94 F. Vydra and L. Luong, J. Electroanal. Chem., 54 (1974) 447.
95 L. Luong and F. Vydra, Collect. Czech. Chem. Commun., 40 (1975) 1490.
96 L. Luong and F. Vydra, Collect. Czech. Chem. Commun., 40 (1975) 2961.
97 D. Jagner and K. Arén, Anal. Chim. Acta, 100 (1978) 375.
98 B. Fleet and C. J. Little, J. Chromatogr. Sci., 12 (1974) 747.
99 W. Lund, M. Hannisdal and T. Greibrokk, J. Chromatogr., 173 (1979) 249.
100 J. W. Dieker, W. E. van der Linden and H. Poppe, Talanta, 26 (1979) 511.
101 C. Bollet, M. Claude and R. Rosset, Analusis, 6 (1978) 54.
102 P. T. Kissinger, C. Refshauge, R. Dreiling and R. N. Adams, Anal. Lett., 6 (1973) 465.
103 K. Brunt and C. H. P. Bruins, J. Chromatogr., 161 (1978) 310.
104 K. Brunt and C. H. P. Bruins, J. Chromatogr., 172 (1979) 37.
105 K. Brunt, B. Oosterhuis and D. A. Doornbos, Anal. Chim. Acta, 114 (1980) 257.
106 A. Ivaska and W. F. Smyth, Anal. Chim. Acta, 114 (1980) 283.
107 Y. Takata and G. Muto, Anal. Chem., 45 (1973) 1864.
108 J. Lankelma and H. Poppe, J. Chromatogr., 125 (1976) 375.
109 U. R. Tjaden, J. Lankelma, H. Poppe and R. G. Muusze, J. Chromatogr., 125 (1976) 275.
110 J. Lankelma and H. Poppe, J. Chromatogr., 149 (1978) 587.
111 A. N. Strohl and D. J. Curran, Anal. Chem., 51 (1979) 353.
112 A. N. Strohl and D. J. Curran, Anal. Chem., 51 (1979) 1045.

113 W. J. Blaedel and J. Wang, Anal. Chem., 51 (1979) 799.
114 J. Wang and M. Ariel, J. Electroanal. Chem., 83 (1977) 217.
115 J. Wang and M. Ariel, J. Electroanal. Chem., 85 (1977) 289.
116 D. Laser and M. Ariel, J. Electroanal. Chem., 49 (1974) 123.
117 G. W. Schieffer and W. J. Blaedel, Anal. Chem., 49 (1977) 49.
118 T. Fujinaga, Pure Appl. Chem., 25 (1971) 709.
119 S. Kihara, J. Electroanal. Chem., 45 (1973) 31.
120 T. Fujinaga and S. Kihara, CRC Crit. Rev. Anal. Chem., (1977) 223.
121 J. C. Lennox and R. W. Murray, J. Electroanal. Chem., 78 (1977) 395.
122 J. C. Lennox and R. W. Murray, J. Am. Chem. Soc., 100 (1977) 3710.
123 R. D. Rocklin and R. W. Murray, J. Electroanal. Chem., 100 (1979) 271.
124 A. Bettelheim, R. J. H. Cham and T. Kuwana, J. Electroanal. Chem., 99 (1979) 391.
125 R. Nowak, F. A. Schultz, M. Umaña, H. Abruña and R. W. Murray, J. Electroanal. Chem., 94 (1978) 219.
126 J. P. Randin (Ed.), Encyclopedia of Electrochemistry of the Elements, Vol. VII, M. Dekker, New York, 1976, Ch. 1.
127 V. Plzak and H. Wendt, Ber. Bunsenges. Phys. Chem., 83 (1979) 481.
128 M. P. J. Brennan and R. Brettle, J. Chem. Soc. Perkin Trans. 1 (1973) 257.
129 G. Cauquis and D. Serve, J. Electroanal. Chem., 34 (1972) App. 1.
130 F. L. Lambert and G. B. Ingall, Tetrahedron Lett., 36 (1974) 3231.
131 F. L. Lambert, B. L. Hasslinger and R. N. Franz, J. Electrochem. Soc., 122 (1975) 737.
132 A. J. Bard and A. Merz, J. Am. Chem. Soc., 101 (1979) 2959.
133 K. S. Quaal, J. Sungehul, Y. M. Kim, W. D. Clossan and J. A. Zubieta, J. Org. Chem., 43 (1978) 13111.
134 B. L. Johansson and B. Persson, Acta Chem. Scand., Ser. B, 32 (1978) 431.
135 R. M. van Effen and D. H. Evans, J. Electroanal. Chem., 103 (1979) 383.
136 J. Moiroux and P. J. Elving, J. Electroanal. Chem., 102 (1979) 93.
137 Z. P. Bezrukova, Yu. B. Vasil'ev, L. S. Kanevskii, E. P. Kovsman, V. I. Lushnikov, N. I. Presnova, R. G. Pryadkina, G. A. Tarkhanov and V. D. Chekanova, J. Anal. Chem. USSR, 12 (1976) 737.
138 L. S. Chulkina and V. A. Zarinskii, J. Anal. Chem. USSR, 27 (1972) 2044.
139 R. Eggli, Anal. Chim. Acta, 97 (1978) 195.
140 A. Dodson and V. J. Jennings, Nature, 240 (1972) 15.

Analytica Chimica Acta, 119 (1980) 25—32

A CESIUM-SELECTIVE ELECTRODE PREPARED FROM A CRYSTALLINE SYNTHETIC ZEOLITE OF THE MORDENITE TYPE

GILLIS JOHANSSON*, and LARS RISINGER

Department of Analytical Chemistry, University of Lund, P.O. Box 740, S-220 07 Lund (Sweden)

LARS FÄLTH

Department of Inorganic Chemistry 2, University of Lund, P.O. Box 740, S-220 07 Lund (Sweden)

(Received 2nd April 1980)

SUMMARY

Cesium-selective electrodes were prepared from a synthetic zeolite molecular sieve of the mordenite type. The membrane was made from zeolite crystals embedded in an epoxy resin. The response towards cesium ions was linear from about 3×10^{-5} to at least 0.1 mol l^{-1}, with almost Nernstian slope. The usable pH range was 3.5—9 for 0.01 mol l^{-1} cesium solutions. The selectivity order was Cs > Ag, K > Na > Li for univalent ions. The response for divalent ions was not Nernstian, Cs ≫ Ba > Ca > Cu. About two weeks after the hydration, there was a degradation of electrode performance indicated by increased detection limit and decreased slope.

The ion-exchange processes of zeolite molecular sieves are interesting because there are unusual mechanisms for providing ion selectivity. The cation selectivities do not follow the rules that typify other inorganic and organic exchangers [1]. For steric reasons, the ions may have to give up some of their water of hydration to pass through openings, or to fit into their positions in the vicinity of the fixed negative charges of the crystal lattice.

Marshall and co-workers [2—5] have made extensive studies of membranes prepared from natural zeolites. Initially, they ground membranes from large single crystals of chabazite or apophyllite; later they used films made from colloidal clays, e.g. montmorillonite and beidellite. The properties could be changed by heat treatment. Their studies were an integrated part of the effort undertaken at that time to clarify the theory of membrane potentials and membrane transport. Part of the work was also directed towards an understanding of the chemistry of the clays themselves. Nevertheless, they were able to prepare membranes with which ionic activities could be measured. Good permselectivity was obtained, resulting in a near-Nernstian slope when a single cation was present. Plastic compounds were developed as supports for zeolitic materials [6], but embedding in polystyrene, polyethylene, polymethylmethacrylate or in a phenolic resin all resulted in less than ideal wetting of the crystals [7]. Barrer and James [7]

used synthetic zeolites of NaX (faujasite-type) and of NaA (A-type). An acid—base titration with analcite membranes has also been reported [8].

Although near-Nernstian response for some cations has been clearly demonstrated, almost all other information normally sought in choosing an ion-selective electrode is not available. Selectivities between different cations have not been determined, even though their size can be indirectly deduced from the data in a few scattered cases. Very few measurements have been done at low concentrations, so that generally there are no data about the limits of detection.

Zeolites are crystalline, hydrated aluminosilicates made up from a three-dimensional network of AlO_4 and SiO_4 tetrahedra linked to each other by sharing of all the oxygens. The framework contains channels and interconnected voids which are occupied by exchangeable cations and water molecules. The water can be removed at high temperatures from several of the zeolites and it will be replaced, reversibly, at lower temperatures. Thirty-four species of crystalline zeolite minerals and more than one hundred types of synthetic crystalline zeolites are known [1]. Non-crystalline materials like glass, coal and the amorphous permutites can also be used as molecular sieves.

Synthetic zeolites are better suited for research because of their greater purity and uniformity in composition. Impurities or stacking faults may restrict diffusion in the channels: in mordenite minerals this occurs regularly with the b-channel. For this exploratory investigation, a synthetic zeolite of the mordenite-type was selected: for brevity it will be referred to as mordenite, $NaAlSi_{6.4}O_{14.8} \cdot nH_2O$. There are two types of channels in a mordenite crystal; a projection showing the largest channels is shown in Fig. 1. The free apertures are of two kinds, 12-rings orthogonal to the c-axis and 8-rings orthogonal to the b-axis; the dimensions are 6.7 × 7.0 Å

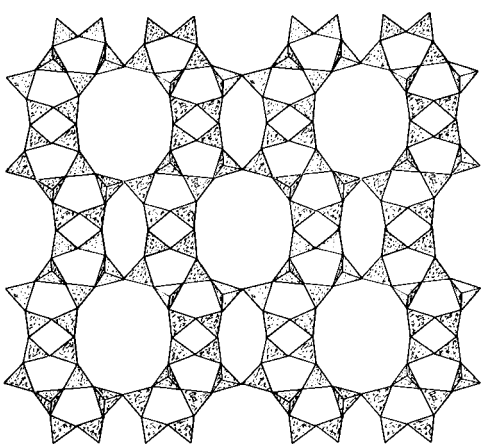

Fig. 1. Projection of the mordenite structure drawn to show the largest channels. Several kinds of smaller voids, or channels, can also be seen.

and 2.9 × 5.7 Å, respectively. There are eight sodium ions in each unit cell, four of which are located in restrictions with one dimension of 2.8 Å; the positions of the remaining ions or the water molecules are not known. The largest molecule adsorbed in dry mordenite is C_2H_4 and the kinetic diameter is 3.9 Å. A synthetic variety known as large-port mordenite has been prepared [9]. It can absorb molecules as large as C_6H_6 and has a kinetic diameter of 6.2 Å. This mordenite is known to have excellent capacity for retaining cesium in treatment of radioactive wastes.

EXPERIMENTAL

Synthesis

The raw materials were sodium hydroxide, aluminium hydroxide and amorphous silica with a batch composition corresponding to 7.7 Na_2O—Al_2O_3—28 SiO_2—165 H_2O. Crystallization was done in a stainless-steel autoclave at 120°C over 14 days. Initially, there is an induction period but once the crystallization has started there is a rapid growth until most of the amorphous material is converted into the crystalline phase [9]. The crystals were uniform and prismatic with a length of ca. 40 μm. There were no other crystalline phases, apart from mordenite; this was proved by the absence of extra lines in the Guinier powder pattern. Analysis showed a Si/Al ratio of 6.4:1. The crystals were filled into a column and the sodium was exchanged for cesium with an 1 mol l^{-1} cesium chloride solution. Dissolution and analysis of a sample showed that the ion exchange was 99.0% complete. The total ion-exchange capacity was 1.65 meq. g^{-1} (dry weight). If the remaining 1.0% of sodium is neglected, the chemical composition of the material used can be written as $CsAlSi_{6.4}O_{14.8} \cdot nH_2O$. The zeolite was dried at 300°C for 2 h.

Membrane preparation

Several polymeric materials were tested in order to find one which wetted the zeolite well and gave a membrane with acceptable mechanical properties. Preliminary tests were made with PVC which gave rather brittle membranes and inadequate adherence to the zeolite crystals. Polyurethane membranes produced potentials themselves and were therefore ruled out, at least at this stage of the investigation. Silicone rubbers were very viscous and produced spongy casts. Tests with various epoxy resins were all successful. An epoxy resin mixture with low viscosity (60 cP) and high chemical resistance was selected. The embedding solution [10] was made from vinyl chlorhexanedioxide (10 g), propyleneglycol diglycidyl ether (6 g), nonenylsuccinic anhydride (26 g), and dimethylaminoethanol (0.4 g).

Desiccated mordenite crystals (130—200 mg) were filled into a press die, i.d. 13 mm, and pressed under vacuum with 10 tons for 15—20 min. The brittle cast was removed with care and transferred to a vacuum desiccator which also contained a vessel with embedding resin mixture. A small piece

of unglazed porcelain was put into the resin mixture. Vacuum was then applied until the degassing of the embedding mixture stopped, which usually took about 30 min. The mordenite disc was then dropped into the resin mixture and allowed to soak for 10 min. The vacuum was broken and the impregnated disc was removed after a few more minutes. It was put on a polypropylene plate and kept at 70°C overnight for curing. Excess of polymer was removed with wet emery paper (grade 600) and the disc faces were polished until the zeolite layer was free from polymer. The operations were checked in a metal microscope. Fine polishing was then made in a polishing machine, by using either silicon carbide grinding powder or aluminium oxide powder.

The end of a glass tube (o.d. 12 mm, i.d. 6.5 mm) was ground smooth and coated with the embedding resin mixture. The polished membrane was pressed gently to the glass tube; it was then kept at 70°C overnight for curing.

Electrode preparation

The membrane was hydrated with 0.1 mol l^{-1} cesium chloride on both sides. It takes about 24 h for the water to penetrate the disc so that an electrical connection can be established. The electrode properties are improved if the disc is soaked for one or two days more.

Some mordenite discs with the zeolite water remaining inside were also embedded by the same procedure. The polymer adhered well to the crystals and working electrodes could be produced. The results reported below, however, were all obtained with membranes prepared from dehydrated zeolite. It was also possible to cast membranes from a mixture of zeolite and resin, but hydration was slow and their behaviour was erratic, depending on unreliable conduction paths. The pressing step ensured good contact between crystals before the resin could isolate them from each other. An inner Ag/AgCl electrode was made, as described by Brown and MacInnes [11] and its potential was compared to the external reference electrode (Radiometer K401 calomel electrode) in a 0.1 mol l^{-1} CsCl solution. All reported potentials were normalized by subtracting this potential from the readings. The internal filling solution was 0.1 mol l^{-1} CsCl. It was replaced frequently and the reference electrode potential difference was also checked periodically. All measurements were made at 25.2 (±0.1)°C.

Chemicals

Chemicals for the embedding resin were obtained from Taab Laboratories, 52 Kidmore End Road, Reading, England. Cesium chloride and sulphate were of optical grade (Sigma Chemical Co.). Benzenesulphonic acid was recrystallized from toluene. The sulphonates were then prepared by titrating weighed amounts of the sulphonic acid with alkali metal hydroxide solutions.

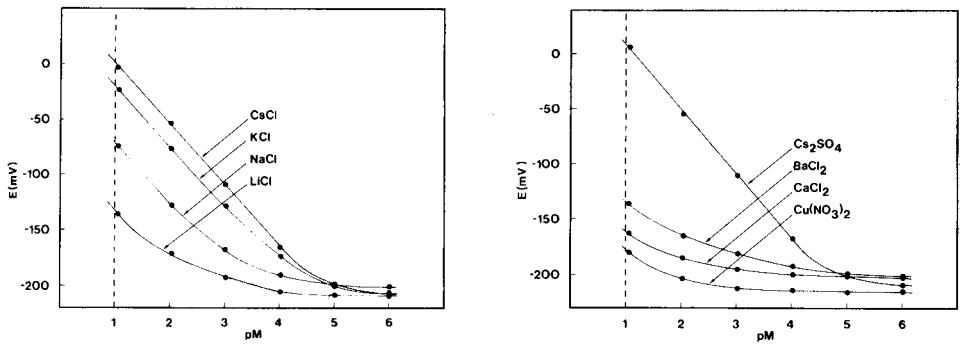

Fig. 2. Calibration curves for a cesium-saturated mordenite membrane electrode in solutions of some univalent cations. The membrane potential difference is plotted versus the logarithm of the metal ion concentration.

Fig. 3. Response of the mordenite membrane electrode to some divalent cations compared with the response to the membrane-filling ion, cesium. Concentration units are used.

RESULTS

Figure 2 shows calibration curves for a mordenite electrode in CsCl, KCl, NaCl, and LiCl solutions. Five electrodes were studied but all results reported in this paper were obtained on the same electrode. All the electrodes in the set gave similar slopes and selectivities, but one of them had a larger asymmetry potential (20 mV) than the others (less than 5 mV). The slope of the CsCl line in Fig. 2 is 55.4 mV/decade because the logarithm of the concentration is plotted on the abscissa. If the slope is calculated with activities in the range above 10^{-4} it becomes 57.7 mV/decade, i.e. almost Nernstian. The limit of detection, for cesium ions, defined according to IUPAC rules [12], is 2×10^{-5} mol l^{-1}.

Calibration curves were also prepared for cesium sulphate solutions (Fig. 3) and in potassium, sodium and lithium sulphate solutions (not shown), as well as in cesium and sodium benzenesulphonate solutions. This sulphonate anion was selected because it should be too large to enter into the zeolite lattice. The response and the selectivity were independent of the anion when activity changes were taken into account.

Figure 3 shows the electrode response in calcium and barium chloride and copper nitrate solutions. At low concentrations the potential remains close to the level set by the cesium ions dissolved from the mordenite membrane. At higher concentrations, there is an increase in potential but the rise is much slower than a normal Nernstian response. Silver nitrate solutions were also studied (not shown) using a double-junction external reference electrode. The selectivity coefficient towards cesium ions was small and the detection limit similar to that for cesium. For silver ions, there were rather large differences between the five electrodes, indicating

TABLE 1

Selectivity coefficients at ionic activities of 0.1 and ion-exchange selectivities, S [15]

M	Cs	Ag^+	K^+	Na^+	Li^+	Ba^{2+}	Ca^{2+}	Cu^{2+}
$k^{pot}_{Cs^+, M}$	1.0	0.47	0.47	0.067	0.0062	0.0017	0.0005	0.0005
S	81	16	12.6	1.0	0.123	4.3	0.86	—
S_M/S_{Cs}	1.0	0.20	0.15	0.012	0.0015	0.053	0.011	—

less reproducible properties, possibly caused by traces of chloride transported through the membrane or trapped in it during the soaking. Table 1 shows the selectivity coefficients determined with the separate solution method and calculated as recommended [12].

The pH response of the membranes in 0.01 mol l^{-1} cesium chloride solution was studied by adding small increments of either hydrochloric acid or tetrabutylammonium hydroxide. The pH was measured simultaneously with a glass electrode. The tetrabutylammonium cation should be too large to pass into the lattice. It was found that a plot of potential versus pH was flat within 1 mV from pH 3.5 up as far as pH 9, the highest investigated. On the acidic side, the potential rose rapidly below pH 2.5 indicating a hydrogen response.

The mordenite electrodes reached a stable potential in less than a minute except in the most dilute solutions in which a few minutes were required. The internal resistance of the electrode varied from about 1 MΩ to 70 kΩ. It was high immediately after preparation and decreased continually with ageing. The d.c. resistance was the same in both directions and it was independent of the composition of the outer solution.

The lifetime of a mordenite electrode was around two weeks. At the end of its life, the detection limit became higher. The slope also decreased and could be as low as 30 mV/decade after about 4 weeks. Attempts to rejuvenate the electrodes by storing them in 1 mol l^{-1} CsCl were unsuccessful, indicating that the degraded performance was not due to exchange of cesium.

DISCUSSION

The slope of the mordenite membrane electrode was almost Nernstian in cesium chloride solutions, which indicates a very good permselectivity. Mordenite is considered to be very stable chemically, even in acidic solution. The rapid ageing as indicated by the decreased slope was therefore unexpected. The epoxy resin is also very stable and seemed to adhere well to the crystals. Barrer and James [7] reported similar decreases in permselectivity and they suspected that leaks developed between the crystals and the polymers. In addition to this possibility, there might be changes in the zeolite structure (cf. the preparation of large-port mordenite [9]).

The detection limit varies somewhat with age; it can be seen that the

calibration curves sometimes cross each other. This depends on the order in which the measurements are made. There is probably a common cause of the increased cesium ion dissolution from the membrane, resulting in an increase in detection limit and the non-Nernstian slope developed with age. This also gives some hope that the detection limit can be decreased further, if a remedy can be found for the rapid ageing.

The ion-exchange isotherms of zeolites are generally very complex [1,13]; they may be highly convex, concave or S-shaped, and in many cases complete exchange is impossible. The ion exchange of modernite has been studied by Ames [14] and by Wolf et al. [15]. The selectivity coefficients vary with composition and show a very deep minimum when 50% or more of the original sodium ions have been exchanged [15]. This behaviour is a consequence of the steric restrictions imposed on four of the eight cations in the unit cell. Table 1 also shows the ion-exchange selectivity coefficients (S) determined by Wolf et al. [15]. They are not directly comparable to the potentiometric selectivity coefficients, partly because they are defined differently, and partly because they relate to an ion exchanger initially saturated with sodium ions, whereas the potentiometric coefficients were determined with a membrane almost completely saturated with cesium ions. Despite these reservations, it can be seen that there is a marked parallelism between the two. From ion-exchange data [15] it can be predicted that there should be very little interference from Ni^{2+}, Co^{2+}, Mn^{2+}, Sr^{2+} and Mg^{2+} ions.

The radius of the hydrated cesium ion (3.38 Å) is larger than the diameter of the smallest ports (2.8—2.9 Å). Sodium ions (hydrated radius, 1.90 Å) diffuse fifty times faster than cesium ions [1], but nevertheless cesium ions are preferentially bound by the zeolite. The explanation [15] is that the small ions have larger hydration numbers and the water molecules are bound more tightly because of the larger field strength. A large ion like cesium can easily be stripped of its water of hydration. Water in the lattice may assist in the final binding of the large ions. The crystal radius of cesium is 1.67 Å.

Financial support from the Swedish Natural Research Council is gratefully acknowledged.

REFERENCES

1 D. W. Breck, Zeolite Molecular Sieves, Structure, Chemistry and Use, J. Wiley, New York, 1974.
2 C. E. Marshall and W. E. Bergman, J. Am. Chem. Soc., 63 (1941) 1911.
3 C. E. Marshall and C. A. Krinbill, J. Am. Chem. Soc., 64 (1942) 1814.
4 C. E. Marshall and A. D. Ayers, J. Am. Chem. Soc., 70 (1948) 1297.
5 C. E. Marshall and L. O. Eime, J. Am. Chem. Soc., 70 (1948) 1302.
6 M. R. J. Wyllie and H. W. Patnode, J. Phys. Chem., 54 (1950) 204.
7 R. M. Barrer and S. D. James, J. Phys. Chem., 64 (1960) 417, 421.
8 M. Adhikari and D. Ghosh, J. Inst. Chem. Calcutta, 44 (1972) 194.
9 L. B. Sand, Molecular Sieves, Society of Chemical Industry, London 1968, p. 71.
10 A. R. Spurr, J. Ultrastruct. Res., 26 (1969) 31.

11 A. S. Brown and D. A. MacInnes, J. Am. Chem. Soc., 57 (1935) 1356.
12 IUPAC Compendium of Analytical Nomenclature, Pergamon, Oxford, 1978.
13 D. W. Breck and H. S. Sherry, in R. F. Gould (Ed.), Molecular Sieve Zeolites Vol. I (Adv. Chem. Ser., no. 101), Am. Chem. Soc., Washington, DC, 1971, pp. 1—18 and 350—378.
14 L. L. Ames, Jr., Am. Mineral., 46 (1961) 1120; 49 (1964) 127.
15 F. Wolf, H. Fürtig and H. Knoll, Chem. Technol., 23 (1971) 273.

Analytica Chimica Acta, 119 (1980) 33—38

DETERMINATION OF L-THYROXINE SODIUM AND L-TRIIODOTHYRONINE SODIUM IN TABLETS BY DIFFERENTIAL PULSE POLAROGRAPHY

E. JACOBSEN* and W. FONAHN

University of Oslo, Institute of Pharmacy P.O. Box 1068, Blindern, Oslo 3 (Norway)

(Received 16th April 1980)

SUMMARY

Differential pulse polarograms of thyroxine and of triiodothyronine recorded from 0.1 M sodium carbonate exhibit a well-defined peak at −1.060 and −1.050 V vs. Ag/AgCl, respectively, and the peak current is proportional to the concentration in the range 10^{-6}—5 × 10^{-5} M. A simple and rapid method is proposed for the determination of the drugs in tablets. The procedure does not involve time-consuming extractions or decomposition of organic matter, and it is suitable for control of content uniformity in pharmaceutical formulations.

Chemical methods for the determination of thyroxine are generally based on measuring the organically combined iodine. The organic matter is destroyed by ignition and the liberated iodide determined directly or, more frequently, by subsequent oxidation to iodate which is determined by titration, spectrophotometry or polarography [1—5]. The chemical methods are not sufficiently sensitive for determination of the active ingredient in single tablets and the instrumental methods suggested are very tedious for large numbers of determinations [4, 6]. The object of the present work was to investigate the application of differential pulse polarography to faster and simpler determinations of these drugs in single tablets.

EXPERIMENTAL

Instrumentation

All polarograms were recorded with a Princeton Applied Research Model 174 Polarographic Analyzer connected to a Houston Omnigraph 2000 XY recorder. Conventional types of dropping mercury electrode and of electrolysis cell were used. Cyclic voltammetry was done with a versatile solid-state instrument constructed to the design of Goolsby and Sawyer [7]; this was used with a Moseley 7030AM XY recorder. A Metrohm E410 hanging mercury drop served as working electrode, with a Ag/AgCl-saturated KCl reference electrode and a platinum coil auxiliary electrode in all experiments. Dissolved air was removed from the solutions by bubbling oxygen-free nitro-

gen through the cell for 5 min and passing it over the solution during the electrolysis. All experiments were conducted at 25 ± 0.1°C.

Materials

L-Thyroxine sodium and L-triiodothyronine sodium (pharmaceutical grade), tablets and placebos were obtained from Nyegaard & Co. A/S, Oslo, Norway. All other chemicals were of reagent grade and used without further purification.

Stock solutions (5×10^{-5} M) were prepared by dissolving the appropriate amount of the drug in 0.1 M sodium carbonate and heating the solution at 40°C for 24 h. The stock solutions were stored in the dark at room temperature.

RESULTS AND DISCUSSIONS

Polarographic behaviour of thyroxine

Preliminary experiments showed that differential pulse polarograms of triiodothyronine and of thyroxine recorded from neutral or slightly alkaline buffers exhibited three or four peaks overlapping each other. However, when the pH of the supporting electrolyte was increased above 11, only one well-defined peak was observed on the polarogram. The peak potential of this peak was independent of a further increase in pH, indicating that hydrogen ions are not consumed in the electrode reaction. The most well-defined peak and the highest peak current (i.e. the most reversible electron transfer) was obtained from 0.1 M sodium carbonates (pH 11.6). Hence, 0.1 M sodium carbonate was used as supporting electrolyte in the following experiments. The peak potentials of thyroxine and of triiodothyronine recorded from this electrolyte were −1.060 and −1.050 V vs. Ag/AgCl, respectively.

Further experiments showed that the most well-defined peak and relatively high peak current were obtained when a drop time of 1 s, scan rate 2 mV s^{-1} and pulse amplitude 50 mV were used.

Thyroxine sodium is only slightly soluble in water and stock solutions were prepared by adding small portions of 0.1 M sodium carbonate to the appropriate amount of the drug under vigorous shaking. In order to complete the dissolution, the solution was then heated at 40°C for 24 h. Experiments showed that the stock solutions of L-thyroxine sodium were stable for 30 days provided that they were stored in the dark at room temperature. When exposed to daylight, the solutions were stable for only one hour. Solutions of triiodothyronine sodium decomposed even more rapidly and only freshly prepared stock solutions of this drug should be used.

Differential pulse polarograms recorded from 0.1 M sodium carbonate with various amounts of thyroxine or triiodothyronine present, showed that the peak current increased linearly with concentration in the range 10^{-6}—5×10^{-5} M. At higher concentrations the standard curve was no longer a straight line and the peak potential was shifted to more negative values, indicating strong adsorption on the electrode surface.

D.c. polarograms of the drugs recorded from 0.1 M sodium carbonate were ill-defined and exhibit both first- and second-order maxima. Attempts to depress the maxima with small amounts of Triton X-100 resulted in great distortion of the wave. Obviously, d.c. polarography is not a suitable method for the determination of these drugs.

The adsorption of the drugs on the electrode surface was verified by drop-time measurements. As indicated in Fig. 1, the presence of either of these drugs caused a large decrease in the drop time over a considerable potential range, indicating that both the oxidized and the reduced form of both drugs are surface-active and are strongly adsorbed on the electrode surface.

Cyclic voltammetry

Cyclic voltammetry experiments were done with a hanging mercury drop electrode. Reproducible results were obtained provided that the mercury drop was changed between each experiment and just before the next potential sweep. No anodic peak was observed at any scan rate or any switching potential, indicating an irreversible electrode reaction. As indicated in Fig. 2, there are two peaks on the voltammogram, the first peak having the characteristic symmetrical shape of an adsorption wave. Experiments showed that the ratio of the two peak currents increased rapidly with increasing scan rate and that the value i_p/C increased rapidly with decreasing concentration. This is a characteristic feature for surface-active depolarizers and indicates that the first peak is a "prewave" resulting from strong adsorption of the reduction product [8].

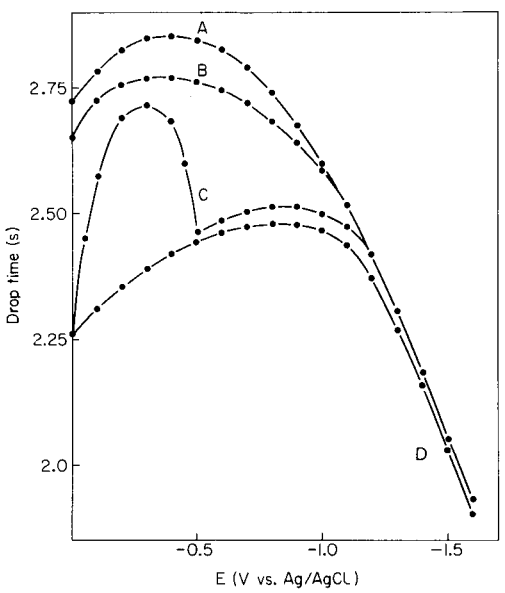

Fig. 1. Electrocapillary curves of 0.1 M sodium carbonate in the absence (curve A) and in the presence of 4.76×10^{-5} M thyroxine sodium (curve B), 5.00×10^{-4} M thyroxine sodium (curve C) and 5.00×10^{-4} M triiodothyronine sodium (curve D).

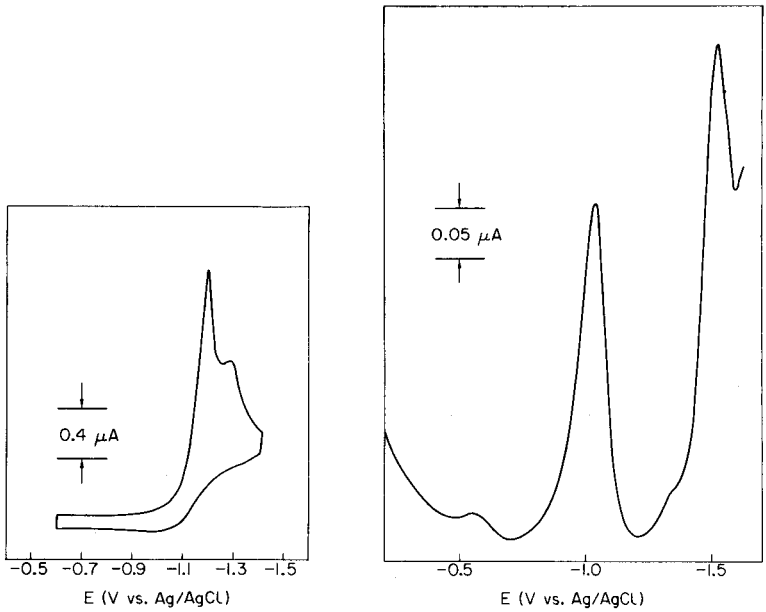

Fig. 2. Cyclic voltammogram of 5×10^{-5} M L-thyroxine sodium in 0.1 M sodium carbonate. Scan rate 50 mV s^{-1}.

Fig. 3. Differential pulse polarogram of a Levaxine Mite tablet (declared amount of L-thyroxine sodium 61 μg) dissolved in 20 ml of 0.1 M sodium carbonate. Drop time 1 s, scan rate 2 mV s^{-1} and pulse amplitude 50 mV.

The voltammetric experiments indicate an irreversible electrode reaction whereas the well-defined pulse polarographic curve indicates a fast step in the overall electrode reaction. The peak potential is independent of pH of the supporting electrolyte and implies that hydrogen ions are not consumed in the electron transfer reaction. Based on the above experiments the following electrode reaction is proposed:

$$RI_4 + e \xrightarrow{\text{slow}} (RI_3)_{ad} + I^-$$

$$(RI_3)_{ad} + e \xrightleftharpoons{\text{fast}} (RI_3)_{ad}$$

$$(RI_3)^-_{ad} + H^+ \longrightarrow RHI_3$$

where RI_4 denotes thyroxine.

Analytical applications

The cyclic voltammetric experiments and drop-time measurements showed that both thyroxine and triiodothyronine are strongly adsorbed at the electrode surface. Hence, it should be possible to determine these drugs by polarography without any preceding separation from surfactants usually present in pharmaceutical formulations.

Experiments showed the active ingredient in the thyroid tablets dissolved in 0.1 M sodium carbonate provided that the tablet was finely ground in an agate mortar. As indicated in Fig. 3, a very well-defined pulse polarogram of a single tablet was obtained from this electrolyte without any preceding separation of insoluble matter or surfactants in the tablet. The second peak on the polarogram is the reduction wave of lactose which is present in these tablets. In addition to lactose the tablets contain starch, gelatine, magnesium stearate and talcum. None of these inactive compounds causes any interference in pulse polarographic determination of thyroxine. Based on the above experiments the following procedure is recommended.

Recommended procedure. Dissolve one finely ground tablet (containing 20—125 μg of L-thyroxine sodium or L-triiodothyronine sodium) in 20.00 ml of 0.1 M sodium carbonate. Transfer a suitable amount of the suspension to a polarographic cell, deaerate with pure nitrogen and record a differential pulse polarogram with starting potential −0.6 V, scan rate 2 mV s^{-1}, pulse amplitude 50 mV and drop time 1 s. Measure the peak current and determine the concentration from a calibration curve obtained by the same procedure in the presence of a placebo.

The results of a few determinations of L-thyroxine and of L-triiodothyronine in single tablets are given in Tables 1 and 2. The proposed method is very simple and sensitive and gives satisfactory accuracy in the determination of these drugs in single tablets.

TABLE 1

Determination of L-thyroxine sodium in tablets

Tablet no.	Peak current (μA)	Found (μg)	Tablet no.	Peak current (μA)	Found (μg)
Levaxine Mite tablets: declared amount, 61 μg[a]					
1	0.335	56.1	6	0.358	60.1
2	0.365	61.2	7	0.360	60.5
3	0.365	61.2	8	0.360	60.5
4	0.355	59.6	9	0.368	61.8
5	0.370	62.1	10	0.365	61.2
L-Thyroxin-Natrium tablets: declared amount, 122 μg[b]					
1	0.690	114.0	6	0.700	115.8
2	0.720	119.2	7	0.715	118.3
3	0.715	118.3	8	0.700	115.8
4	0.700	115.8	9	0.715	118.3
5	0.725	120.0	10	0.735	121.8

[a]Mean 60.4; St.dev. 2.8%. [b]Mean 117.7; St.dev. 2.0%.

The authors thank cand.real. T. Jacobsen, Nyegaard & Co, Oslo, Norway, for valuable discussions and for supply of the drugs used in this investigation.

TABLE 2

Determination of L-triiodothyronine sodium in Triiodthyronin tablets (declared amount 22 μg)

Tablet no.	Peak current (μA)	Found (μg)	Tablet no.	Peak current (μA)	Found (μg)
1	0.143	22.5	6	0.160	25.7
2	0.153	24.4	7	0.140	21.9
3	0.138	21.5	8	0.150	23.8
4	0.145	22.9	9	0.147	23.2
5	0.145	22.9	10	0.137	21.3

Mean 23.0; St.dev. 5.9%.

REFERENCES

1 W. W. Hilty and D. T. Wilson, Ind. Eng. Chem., Anal. Ed., 11 (1939) 637.
2 T. S. Sappington, N. Halperin and W. T. Salter, J. Pharmacol., 81 (1944) 331.
3 D. C. M. Adamson, A. P. Domleo, J. P. Jefferies and W. H. C. Shaw, J. Pharm. Pharmacol., 4 (1952) 760.
4 W. Holak and D. Shostak, J. Pharm. Sci., 68 (1979) 338.
5 The Joint Committee of Pharm. Soc. and The Soc. for Anal. Chem., Analyst, 92 (1967) 328.
6 I. Alsos, Medd. Nor. Farm. Selsk., 29 (1967) 91.
7 A. D. Goolsby and D. T. Sawyer, Anal. Chem., 39 (1967) 411.
8 R. H. Wopschall and I. Shain, Anal. Chem., 39 (1967) 1514.

Analytica Chimica Acta, 119 (1980) 39—45

DONNAN DIALYSIS MATRIX NORMALIZATION FOR THE VOLTAMMETRIC DETERMINATION OF METAL IONS

J. A. COX* and Z. TWARDOWSKI

Department of Chemistry and Biochemistry, Southern Illinois University at Carbondale, Carbondale, IL 62901 (U.S.A.)

(Received 5th February 1980)

SUMMARY

The efficacy of Donnan dialysis for removal of interferences by surfactants, complexing agents, and electroactive organic compounds on anodic stripping voltammetry and differential pulse polarography is demonstrated. Up to at least 0.05% gelatin and 0.005% Triton X-100 do not alter the rate of dialysis of Cd(II), Pb(II), Zn(II), and Cu(II). As the ion-exchange membrane is not permeable to the surfactants, subsequent voltammetric determinations can be performed by a working curve method. Recoveries of metals from a variety of real samples were generally above 90%. The presence of humic acid (50 mg l^{-1}) does not alter the transport of Cu(II), Pb(II), or Cd(II) from pH 3 solution but does at pH 8. The transport is related to the free and labile-complexed ion concentration which suggests that Donnan dialysis can be used for speciation as well as for enrichment and matrix normalization.

Application of voltammetric methods to the determination of metals in real samples often requires a pretreatment. The suppression of faradaic currents by surfactants, the shifting of the electrolysis potentials of electrode processes by complexing agents, and the faradaic contribution of electroactive organic species to voltammograms can otherwise complicate the data interpretation.

Earlier work has demonstrated that Donnan dialysis can provide quantitative enrichment of cations [1]. From other studies [2—4] it can be expected that Donnan dialysis could provide enrichments which are independent of sample matrices over a wide variety of conditions and thus simplify the evaluation of voltammetric results. This promise is examined in the present paper by using differential pulse polarography (d.p.p.) and anodic stripping voltammetry (a.s.v.) as the test methods.

EXPERIMENTAL

The cation-exchange membranes were type P-1010 (RAI Research Corporation, Hauppauge, Long Island, New York). They were pretreated as in our previous work [1].

Pulse polarography experiments were performed with either a PAR

Model 170 or a Model 174 system (Princeton Applied Research, Princeton, New Jersey). Stripping determinations utilized a conventional 3-electrode potentiostat, which was constructed in-house with Philbrick Model P25AU operational amplifiers. A Metrohm Model E140 hanging mercury drop electrode served as the indicator. All potentials are reported vs. a saturated calomel reference electrode.

Except as noted below, reagent grade chemicals were used without purification. Those which served as receiver electrolytes for Donnan dialysis and as supporting electrolytes were purified by controlled potential electrolysis at a stirred Hg pool electrode at −1.3 V to remove electroactive metals. The 1% (w/w) Triton X-100 (polyoxyethylene-*p*-t-octylphenol; Sigma Chemical Co., St. Louis) was conditioned with Chelex-100 ion-exchange resin for 2 days. Sodium humate (Aldrich Chemical Co., Milwaukee) solutions (0.05%) were treated likewise.

Donnan dialysis was performed as detailed elsewhere [1]. Unless otherwise noted, 200 ml samples were contacted to the receiver system for 30 min during which magnetic stirring was used. The stirring rate (7 ± 1 Hz) was controlled with the aid of stroboscopic monitoring. The receiver system was a 4.9-cm^2 membrane-enclosed glass cylinder which contained 5 ml of the receiver electrolyte (0.2 M magnesium sulfate—5 × 10^{-4} M aluminum sulfate mixture). After dialysis the electrolyte was transferred and diluted to 10 ml for the voltammetric experiments. The latter step corrects for osmotic dilution which occurs during the dialysis.

The d.p.p. experiments used a 2 mV s^{-1} scan rate and a 1-s drop time. With a.s.v. a 300-s electrolysis in stirred solution at −1.2 V at a 0.03-cm^2 Hg drop followed by a 30-s rest period in unstirred solution was employed. The stripping step was performed at a 20 mV s^{-1} scan rate. For direct a.s.v. and d.p.p. the supporting electrolyte was 0.1 M $MgSO_4$—2.5 × 10^{-4} M $Al_2(SO_4)_3$.

The real samples which were studied were suction-filtered through Whatman No. 40 paper and used within 24 h. For some experiments the samples were spiked with known quantities of Cu, Zn, Pb, and/or Cd salts just prior to dialysis.

RESULTS AND DISCUSSION

Initial experiments were performed with synthetic samples so that the matrix factors could be individually investigated. Cu(II), Cd(II), Pb(II) and Zn(II) were used as the test ions. Differential pulse polarography and anodic stripping voltammetry were the methods employed. Earlier work [1] had shown that the $MgSO_4$—$Al_2(SO_4)_3$ receiver electrolyte eliminated the effect of various sample ions on the Donnan dialysis of the test species, and so the present study was mainly concerned with complexing agents and surfactants.

Surfactants are well-known to affect the responses of the above methods

TABLE 1

Effect of surfactants on the electrolysis current for the determination of selected ions. All values are given in μA.

Surfactant[a]	Cu(II), d.p.p.	Pb(II), d.p.p.	Cu(II), a.s.v.	Pb(II), a.s.v.	Cu(II), D.d./d.p.p.[b]	Pb(II), D.d./d.p.p
	0.26	0.28	1.45	1.95	0.84	0.89
0.001% G	0.26	0.28	1.45	1.90	0.84	0.88
0.01% G	0.26	0.28	1.35	1.90	0.84	0.88
0.05% G	0.25	0.27	1.25	1.80	0.85	0.88
0.001% T	0.36	0.24	1.00	1.52	0.83	0.88
0.003% T	0.44	0.18	0.72	1.28	0.84	0.90
0.005% T	0.62	0.11	0.70	1.20	0.84	0.88

[a]G, gelatin; T, Triton X-100. [b]D.d., Donnan dialysis.

[5, 6]. From Table 1 it is apparent that gelatin only slightly decreases the response of d.p.p. and a.s.v., but Triton X-100 has a marked influence. In the case of Cu(II), the latter surfactant gives a positive interference in the case of d.p.p. because of a tensammetric peak which is superimposed on the reduction current. The Cu(II) a.s.v. current is suppressed by Triton X-100.

The data in Table 1 also demonstrate that Donnan dialysis eliminates the interference of surfactants by blocking their entry into the receiver electrolyte. In support of this conclusion, the Donnan dialysis—a.s.v. combination yields currents of 4.65 ± .07 μA and 6.12 ± .08 μA for Cu(II) and Pb(II), respectively, in the presence of Triton X-100 over the tabulated concentration range. Cd(II) and Zn(II) as test metals yielded results which were analogous to those which are tabulated and discussed above.

In addition to eliminating the effect of surfactants, the 30-min Donnan dialysis provides a three-fold enrichment of the metals under the conditions employed (see Table 1). Since the enrichment factor is proportional to time, a 10-min dialysis would be sufficient if the only objective is to eliminate matrix effects.

The effect of complexing agents was studied for two reasons. When an excess of a relatively strong complexing agent is present, the electrolysis potentials of metal ion electrode reactions are influenced so that qualitative identifications are complicated. Further, even small quantities of complexing agents could possibly affect the Donnan dialysis enrichment by altering the ratio of the free metal ion to the total metal concentration in the sample. The latter was of greater concern since a large excess of a strong complexing agent would be an atypical situation in a natural sample. The humic acid system was selected for this investigation because it is a common component of natural water and has been recently studied by other workers [7—10].

Additions of up to 12 mg l^{-1} sodium humate to 10^{-6} M Pb(II), Cu(II), and Cd(II) solutions influenced neither the d.p.p. peak current nor potential. With a.s.v. on the 12 mg l^{-1} solutions, Cu(II), Pb(II) and Cd(II) showed 18%, 28%, and 40% decreases in the stripping peak current and positive peak potential shifts of 23 mV, 13 mV, and 45 mV, respectively. Adsorption of

humic acid on the stationary electrode probably caused the greater influence in the a.s.v. case.

It should be noted that the above d.p.p. results are not consistent with those in recent reports [9, 10]. Buffle and Greter [10] found a marked influence of fulvic and humic substances on the polarographic current and potential for the reduction of lead(II). In their work the naturally-occurring humic and fulvic substances in a water sample were used whereas a purified commercial product was used in our work. Given the heterogeneity of humic acid it is probable that the active components were different. That the commercial product has less influence on the electrochemical behavior is indicated by our work on natural samples which is reported below. The need for matrix normalization of natural samples is, therefore, more pressing than suggested by the above data.

Whether the humic acid system affects the Donnan dialysis of metal ions depends upon the sample pH. For example, the Table 2 data show that when the samples are acidified, Cu(II), Pb(II), and Cd(II) transport across the membrane is not decreased by humic acid. At low pH values, metal humate complexes are not formed. The decrease in the quantity of metals which are dialyzed in the presence of humate at pH 8 reflects the percentage of the metal which is in the non-labile complex form: Cu (43%), Pb (51%), and Cd (52%) with 0.01 g l^{-1} humic acid. The free ion as well as the fraction of the metal which is labile in the experimental time period will still be transferred. These results are in good agreement with those of Figura and McDuffie [8] considering the difference in the experimental approaches.

The data in Table 2 demonstrate that adjustment of the sample pH can lead to Donnan dialysis transfer which reflects the total concentration of a metal in a sample. Digestion of a sample could probably provide the same result. Direct Donnan dialysis yields only the free and labile fraction, but in many instances this result may be desired. Thus, in terms of complexes as a matrix effect in electroanalytical studies on real samples, Donnan dialysis pretreatment is an especially significant method when the free and labile

TABLE 2

Influence of humic acid on the Donnan dialysis of metal ions

Humic acid (g l^{-1})	pH[a]	A.s.v. peak current (μA)		
		Cu(II)	Pb(II)	Cd(II)
0	6	1.40	1.94	1.78
0.01	8	0.80	0.95	0.86
0.01	3	1.35	1.82	1.74
0.05	8	0.34	0.57	0.43
0.05	3	1.38	1.95	1.80

[a]pH refers to that of the sample.

metal concentration is desired but other matrix factors such as surfactants may complicate a direct analysis.

The veracity of Donnan dialysis pretreatment for metal determinations was tested on three categories of samples. Lake water which did not contain metals which were detectable by d.p.p. or a.s.v. (electrolysis for 1 h at a mercury drop electrode) was spiked with metals to see whether Donnan dialysis in conjunction with d.p.p. or a.s.v. gave correct recovery results with this matrix. Likewise, the laboratory effluent from the SIU Chemistry Building was used. Although metals were present in the sample, spiking was employed to calculate the recovery (the initial quantity was considered a correctable background concentration). Finally, effluent from a municipal sewage treatment plant was used as a sample.

The experiments which employed spiked samples are summarized in Table 3. It is apparent that the sample matrix did not affect the Donnan dialysis experiment. The recoveries were greater than those obtained with nitric acid digestions on the same spiked samples (70—80%). The dialyses also took much less time than the acid digestions. Moreover, as exemplified by Figs. 1 and 2, Donnan dialysis greatly clarified the d.p.p. and a.s.v. current—voltage curves. The elimination of electroactive organic components was probably the main factor in Fig. 1 whereas surfactants and organic impurities probably both affected the a.s.v. data in Fig. 2.

With the municipal sewage treatment plant effluents which were tested, d.p.p. did not yield evidence of electroactive metals when used directly on the samples. With a.s.v. applied to a typical sample with a 30-min electrolysis time, the following metal ions were found by direct analysis with a standard addition method: 1.5 (±0.4) × 10^{-8} M Cu(II) (E_p, 50 mV); 5 (±4) × 10^{-9} M Pb(II) (E_p, −400mV); 7 (±3) × 10^{-9} M Cd(II) (E_p, −540 mV); and 2.2 (±0.5) × 10^{-7} M Zn(II) (E_p, −830 mV). When Donnan dialysis pretreatment was used in conjunction with a.s.v., the same concentrations

TABLE 3

Efficiency of Donnan dialysis of metal ions from real samples

Sample[a]	Recovery[b]		
	Pb	Cd	Zn
Cedar Lake, Jackson Co., IL	0.97	1.09	0.89
Campus Lake, SIU	0.88	0.91	0.82
Chemistry Building sewage	0.92	1.04	1.22
Carbondale, IL sewage treatment plant effluent	1.02	0.97	0.92

[a]Samples were filtered and spiked with 1.25 × 10^{-7} M Pb(II), Cd(II), and Zn(II). The stripping currents due to the initial concentrations of the metals in the samples were treated as a correctable background. [b]The recoveries were calculated as the corrected Donnan dialysis—a.s.v. peak currents from the spiked, real samples divided by the Donnan dialysis—a.s.v. peak currents obtained from identical experiments with single component laboratory standards, 1.25 × 10^{-7} M, used as samples.

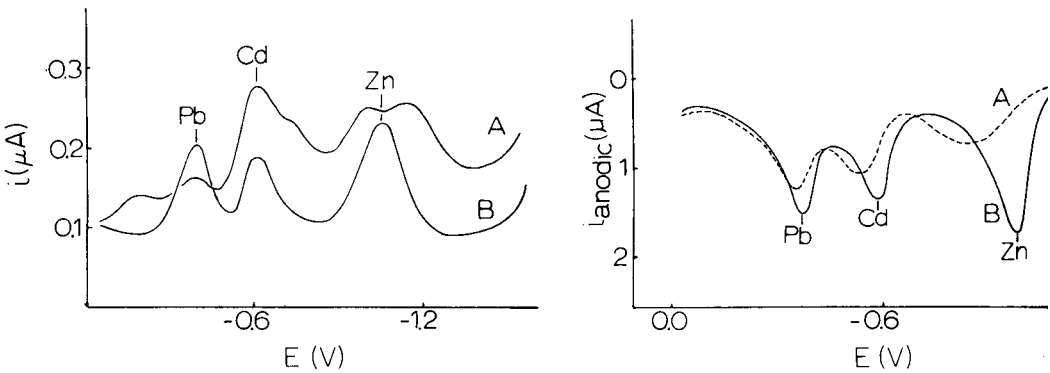

Fig. 1. Effect of Donnan dialysis on the d.p.p. determination of metal ions in sewage. (A) Direct d.p.p.; (B) Donnan dialysis—d.p.p. Sample: Chemistry Building sewage effluent spiked with 3×10^{-6} M Pb(II) and Cd(II). Experimental conditions described in text.

Fig. 2. Effect of Donnan dialysis on the a.s.v. determination of metal ions in sewage. (A) Direct a.s.v.; (B) Donnan dialysis—a.s.v. Sample same as Fig. 1.

were obtained; however, the peak potentials were more typical for the $MgSO_4$—$Al_2(SO_4)_3$ electrolyte which was employed: Cu(II), 65 mV; Pb(II), —365 mV; Cd(II), —560 mV; and Zn(II), —880 mV. Further, the peak currents prior to standard addition were those expected for the subsequently-determined concentrations. Thus, a working curve can be used with the Donnan dialysis—a.s.v. combination whereas standard addition is required for direct a.s.v.

In cases where many samples have to be analyzed, the ability to use a working curve will more than offset the time required for Donnan dialysis pretreatment in terms of overall efficiency. A.s.v. experiments will require a shorter electrolysis time because of the enrichment from the dialysis. Moreover, as indicated in Table 1, surfactant exclusion may increase the sensitivity of Donnan dialysis—a.s.v. relative to a.s.v. more than expected on the basis of the Donnan dialysis enrichment factor.

With d.p.p. the addition of a dialysis step will often slow the overall method. Nevertheless the Donnan dialysis—d.p.p. combination may be useful relative to a standard addition approach to matrix correction because it provides increased sensitivity, as discussed above. The enrichment and the exclusion of electroactive organic species permit this combination to be applied to a greater range of sample types than is possible for d.p.p. alone. Certainly, other separation methods and/or digestions could be coupled to d.p.p. for complicated samples, but Donnan dialysis is quite attractive since it is rapid, minimizes the chance of chemical contamination, and results in the test species being in an aqueous electrolyte which is ideal for electro-analytical chemistry.

This work was supported by the National Science Foundation under grant CHE 7908660. Partial Support was received by Z.T. from the Eastern European Universities Exchange Program grant to SIU-C from the U.S. State Department.

REFERENCES

1 J. A. Cox and J. E. DiNunzio, Anal. Chem., 49 (1977) 1272.
2 G. L. Lundquist, G. Washinger and J. A. Cox, Anal. Chem., 47 (1975) 319.
3 J. A. Cox and K. H. Cheng, Anal. Lett., A11 (1978) 653.
4 J. A. Cox and K. H. Cheng, Anal. Chem., 50 (1978) 601.
5 E. Jacobsen and H. Lindseth, Anal. Chim. Acta, 86 (1976) 123.
6 D. R. Canterford and R. J. Taylor, J. Electroanal. Chem., 98 (1979) 25.
7 F. J. Stevenson, Soil Sci., 123 (1977) 10.
8 P. Figura and B. McDuffie, Anal. Chem., 51 (1979) 120.
9 F. L. Greter, J. Buffle and W. Haerdi, J. Electroanal. Chem., 101 (1979) 211.
10 J. Buffle and F. L. Greter, J. Electroanal. Chem., 101 (1979) 231.

Analytica Chimica Acta, 119 (1980) 47—54

DETERMINATION OF TELLURIUM(IV) IN PERCHLORIC ACID BY STRIPPING VOLTAMMETRY WITH COLLECTION

RICHARD W. ANDREWS

Department of Chemistry, University of Alabama in Birmingham, Birmingham, AL 35294 (U.S.A.)

(Received 17th December 1979)

SUMMARY

The deposition and stripping of tellurium(IV) at a rotating gold ring—gold disk electrode is described. Tellurium(IV) is reduced to the metal by two cathodic procedures, and three activity states of electrodeposited tellurium are observed. For sub-monolayer depositions, a single stripping peak is observed. Determination of tellurium(IV) by stripping voltammetry and by stripping voltammetry with collection is described. The detection limits are 1×10^{-9} M and 5×10^{-11} M, respectively.

Rotating ring-disk electrodes have been used to determine Ag(I) [1], Hg(II) [2], Cu(II) [3, 4], Zn(II) [4] and Pb(II) [4] by stripping voltammetry with collection. Blaedel and Schieffer [5, 6] have used this technique at tubular electrodes to determine Cd(II), Pb(II) and Cu(II) in tap water at sub-nanomolar concentrations. Because the ring potential is held constant during the measurement the contribution of charging current is significantly reduced; and the collection technique possesses greater sensitivity than conventional stripping voltammetry. The primary requirements are that the observed collection efficiency of a given rotating ring disk electrode (RRDE) remain constant over a wide range of analyte concentrations and that the deposited metal be oxidized to a soluble species. Here the determination of tellurium(IV) in 0.1 M perchloric acid by stripping voltammetry with collection is described.

The determination of tellurium(IV) by stripping voltammetry has been accomplished at the hanging mercury drop electrode [7, 8], graphite electrodes [9, 10], and gold electrodes[11]. Gold electrodes have also been used in the determination of Se(IV) [12], Hg(II) [13], As(III) [14], and Ni(II) [15] by anodic stripping voltammetry. Because gold has a low hydrogen overvoltage and does not form an oxide film at potentials less positive than +1.0 V vs. SCE in mineral acid [16], gold is especially well suited to the determination of metals more electropositive than mercury. In this study, a rotating gold disk—gold ring electrode (RAuRDE) was used to determine tellurium(IV) at concentrations less than 10^{-10} M in 0.1 M perchloric acid.

EXPERIMENTAL

Apparatus and reagents

The RAuRDE used (Pine Instrument Co., Grove City, PA) had the following geometric parameters: r_1 = 0.379 cm; r_2 = 0.393 cm; r_3 = 0.418 cm; N_0 = 0.118; $\beta^{2/3}$ = 0.474. A model PIR rotator and a model RDE3 bipotentiostat based on the operational amplifier circuit of Napp et al. [17] were used; both were obtained from Pine Instruments. A Houston Omnigraphic XY recorder was used to record the *I—E* curves, and a Keithley Model 163 digital multimeter was used to measure all voltages. Peaks were integrated with a Keuffel and Esser compensating planimeter.

A Metrohm titration cell served as the electrolysis vessel. It was necessary to ream the centre hole of the cell cap to accommodate the RAuRDE. A Beckman saturated calomel reference electrode and a platinum wire spiral auxiliary electrode were used. Both were separated from the main electrolysis chamber by salt bridges containing supporting electrolyte and fine glass frits. The cell bottom, salt bridges and purge tubes were soaked in 50% nitric acid for no less than 3 h prior to all experiments.

All solutions were prepared from Fischer Analyzed Reagents unless otherwise specified. The water used to prepare all solutions was deionized, distilled from alkaline permanganate and redistilled under nitrogen. Tellurium(IV) solutions were prepared from 99.99% tellurium metal (Alpha Ventron) as described by Marshall [18].

Procedures

The RAuRDE was polished with 30 μm, 6 μm and 1 μm Buehler diamond polishing compound followed by polishing with 0.1 μm and 0.05 μm Buehler alumina. During deaeration, the potentials of the ring and disk electrodes were sequentially held at +1.4 V and −0.40 V for 5 min. After anodization and cathodization the electrode potentials were cycled between the desired potential limits until reproducible *I—E* curves were recorded. The ring electrode potential was held at 1.20 V during all deposition experiments and switched to the desired potential 30 s prior to recording a I_r—E_d curve. All potentials are reported in V vs. SCE.

RESULTS AND DISCUSSION

Current—potential curves for tellurium(IV)

Current—potential curves obtained from a 10^{-7} M Te(IV) solution are shown in Fig. 1. The effects of reversing the potential sweep are also illustrated in Fig. 1. The *A* family of *I—E* curves shows the effect of reversal of the anodic potential sweep while the *B* family shows the effect of reversal of the cathodic potential sweep. After each potential reversal, the potential of the electrode was cycled between +1.2 V and −0.4 V until the original *I—E* curve could be reproduced. The anodic processes are labeled as peaks A, B and C while the

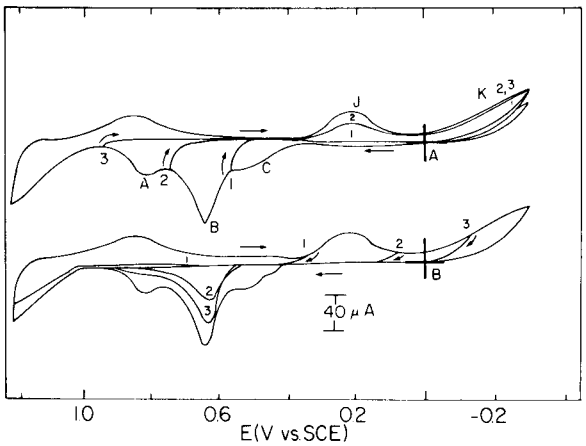

Fig. 1. I_d–E_d curves for 1 × 10^{-4} M tellurium(IV) at the RAuRDE (900 r.p.m., 5 V min^{-1}, 0.1 M $HClO_4$). Curves A: anodic potential limit study. Curves B: cathodic potential limit study.

cathodic processes are labeled peak J and wave K for convenience. Tellurium(0) is deposited on the gold electrode in the formation of both peak J and wave K. When the *B* family of *I*–*E* curves is examined, it is clear that Te(0) is not deposited for $E > 0.35$ V. Scan reversal at 0.10 V (point 2) results in the deposition of Te(0) which is subsequently anodically stripped in peaks B and C. Holding the potential at 0.10 V results in the growth of peaks A and B. Sweep reversal at $E < -0.15$ V (point 3) restores anodic peak C. The quantity of charge consumed during peak B never exceeds the equivalent of a monolayer of tellurium. Deposition of Te(0) at $E \leq -0.15$ V results in the growth of peaks A, B and C; and the appearance of anodic peak C in the fourth *I*–*E* curve in the *B* family of *I*–*E* curves (Fig. 1) is primarily the result of the increased scan time required to reach −0.30 V. The quantity of charge consumed in the three anodic peaks, A, B, and C, exceeds a monolayer equivalent only when the deposition of tellurium is performed with $E \leq -0.15$ V, i.e., in the region of cathodic wave K.

In the *A* family of curves of Fig. 1, the sweep was reversed after each of the anodic peaks. Reversal after peak C (point 1, 0.57 V) resulted in the disappearance of peak J and the magnitude of wave K was significantly reduced. Cathodic peak J was restored when the reversal occurred at 0.75 V or 0.95 V (points 2 and 3, respectively). The product of the oxidation occurring during anodic peaks A and B is concluded to be the species undergoing reduction in cathodic peak J. The Te(0) formed during cathodic peak J also enhances the rate of deposition during wave K.

It is concluded that tellurium(IV) is formed during anodic peaks A and B and subsequently adsorbed on the gold electrode. The adsorbed Te(IV) is reduced in peak J and enhances the rate of reduction of Te(IV) from solution. Adsorbed Te(IV) is not formed as a result of peak C.

Anodic peak C is not observed unless the Te(IV) concentration exceeds 10^{-5} M or the deposition at potentials less than −0.20 V is continued for an extended period of time. Anodic peak A is concluded to result from the oxidation of bulk deposited tellurium; its peak potential is closest to the thermodynamic value [16] of the $TeOOH^+/Te$ couple, indicating the smallest degree of interaction with the gold electrode surface. The voltammetric behavior of tellurium(IV) is remarkably similar to that of selenium(IV) in 0.1 M perchloric acid [12].

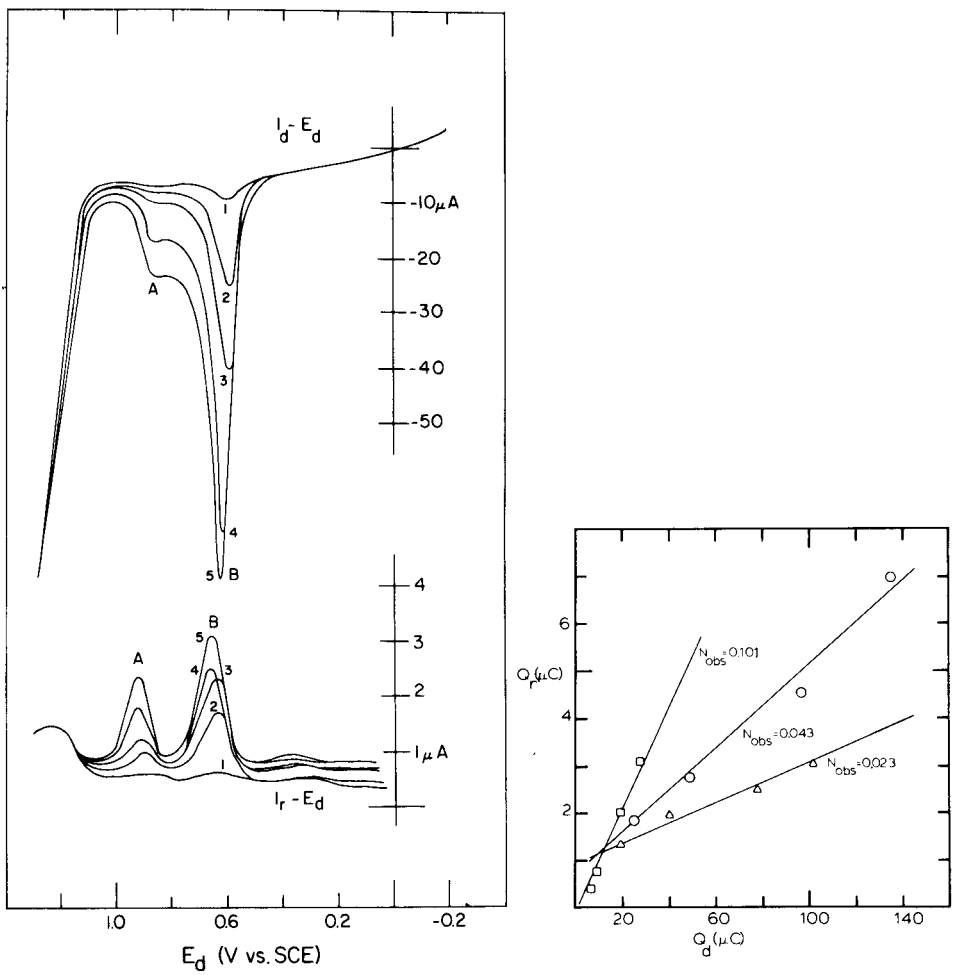

Fig. 2. Stripping and collection curves for 2×10^{-7} M tellurium(IV) for several values of deposition time at the RAuRDE (400 r.p.m., 5 V min^{-1}, 0.1 M $HClO_4$, $E_{d,dep} = -0.20$ V, $E^r = -0.20$ V). Deposition time: (1) 0; (2) 1; (3) 2; (4) 5; (5) 11 min.

Fig. 3. Collection efficiency of 2×10^{-7} M tellurium(IV) at the RAuRDE. Conditions as for Fig. 2, except for deposition time. (□) Peak A; (△) peak B; (○) total process.

Ring-disk electrode studies

Figure 2 shows a series of I_r—E_d and I_d—E_d curves recorded after deposition of tellurium at −0.20 V. The ring potential was −0.20 V during the recording of the I_r—E_d curves. Several features should be noted in Fig. 2. The ring collection peaks A and B are somewhat better resolved than their counterparts in the I_d—E_d curve and the relative peak areas of A and B are not equal in the I_r—E_d and I_d—E_d curves. A plot of ring charge vs. disk charge will have a slope equal to the observed collection efficiency [19]. Figure 3 shows such a plot for peak A, peak B and the total stripping—collection process. The geometric collection efficiency calculated from radius ratios [19] for the electrode is 0.118. Only for peak A is this value approached. The observation of collection efficiencies less than the geometric value clearly implies that not all of the tellurium oxidized at the disk electrode is available for subsequent reduction and collection at the ring electrode. This observation is consistent with the results of the scan limit studies (Fig. 1) where the tellurium(IV) formed in anodic peaks A and B was observed to be adsorbed on the gold electrode surface. The products of anodic peaks A and B appear to differ in the degree of adsorption and/or in their kinetic stabilities in the solution gap separating the ring and disk electrodes. The total charge consumed at the disk electrode is substantially less than that equivalent to a monolayer, and anodic peak C was not observed in these experiments.

In order to determine whether peaks A and B resulted from the transfer of the same number of equivalents, the influence of ring collection potential was studied. The results are shown in Figs. 4 and 5. In Figs. 2 and 4 collection peaks A and B are clearly visible as well as a third collection peak at +1.2 V which probably corresponds to the reduction of gold oxide formed at the disk electrode. The product of peak A is reduced with an $E_{1/2}$ value of 0.05 V in a single step while the product of peak B is reduced with an $E_{1/2}$ value of −0.15 V. The products of anodic peaks A and B do not appear to differ in oxidation state and the difference in $E_{1/2}$ values is a consequence of the different degrees of coverage of the ring electrode surface by Te(0) for collection peaks A and B. The observed collection efficiencies for peaks A and B differ by a factor of five with values of 0.101 and 0.023, respectively. The influence of rotational velocity (ω) upon collection efficiency was investigated. The observed collection efficiency was not a linear function of $\omega^{1/2}$, ω, or ω^{-1}. The observed collection efficiency of peak B decreased with increasing rotational velocity, but the observed collection efficiency for peak A remained constant. A simple reaction sequence is not suggested by the observed data, but adsorption of the product of peak B on the electrode surface is probably significant.

Anodic stripping voltammetry of tellurium(IV) at gold electrodes

At tellurium(IV) concentrations less than 1×10^{-7} M and for relatively short deposition periods (less than 3 min), a single anodic stripping peak is observed for tellurium deposited at gold electrodes at a potential less than

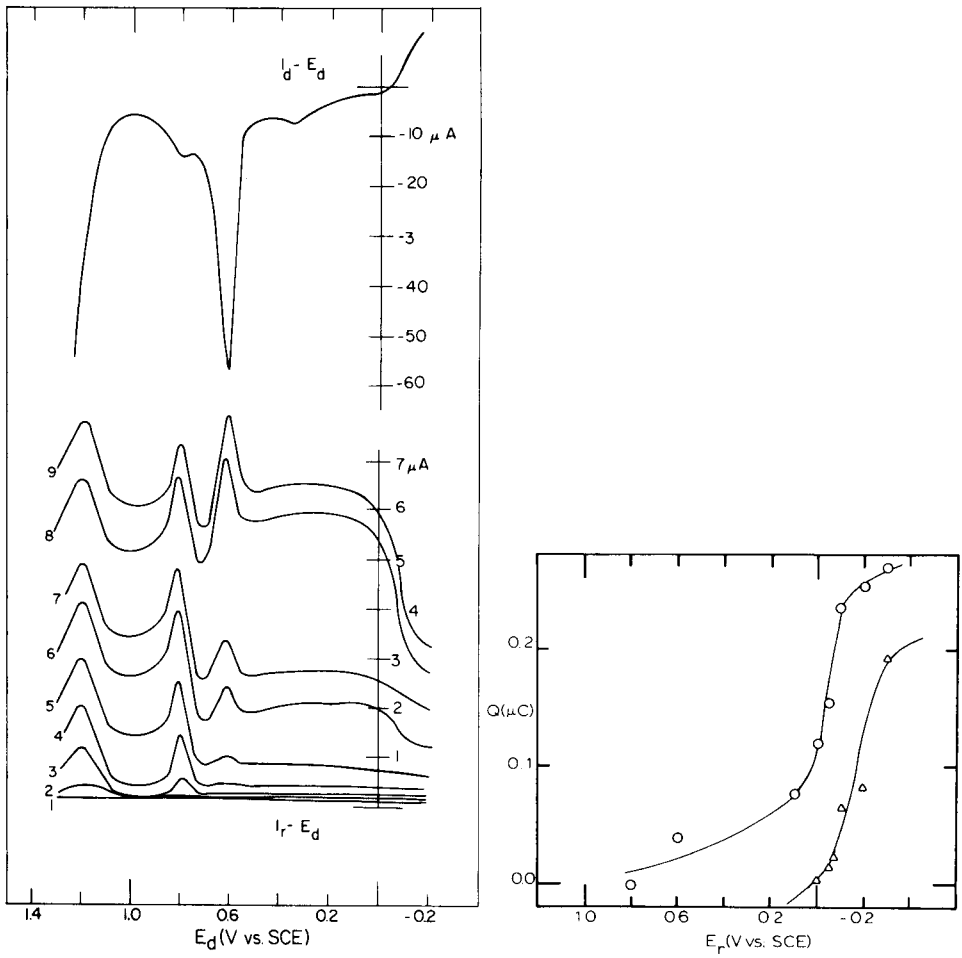

Fig. 4. Ring potential study for 2×10^{-7} M tellurium(IV) at the RAuRDE (3600 r.p.m., 5 V min^{-1}, $E_{d,dep} = -0.20$ V, deposition time 1 min, 0.1 M $HClO_4$). E_r: (1) 1.00; (2) 0.80; (3) 0.60; (4) 0.40; (5) 0.10; (6) 0.00; (7) −0.10; (8) −0.15; (9) −0.20 V.

Fig. 5. Charge vs. ring potential for 2×10^{-7} M tellurium(IV) at the RAuRDE. Conditions as for Fig. 4. (○) Peak A; (△) peak B.

−0.20 V. This is shown in Fig. 6. The quantity of charge consumed in the oxidation of the deposited tellurium increases linearly with rotational velocity and deposition time. The minimum detectable quantity of tellurium(IV) by anodic stripping voltammetry at a RAuDE is 1×10^{-9} M (signal/background = 3:1) and the calibration curve is linear for three orders of magnitude with a correlation coefficient of 0.998.

In an effort to reduce the minimum detectable quantity of tellurium(IV), stripping voltammetry with collection was investigated. Figure 7 shows a

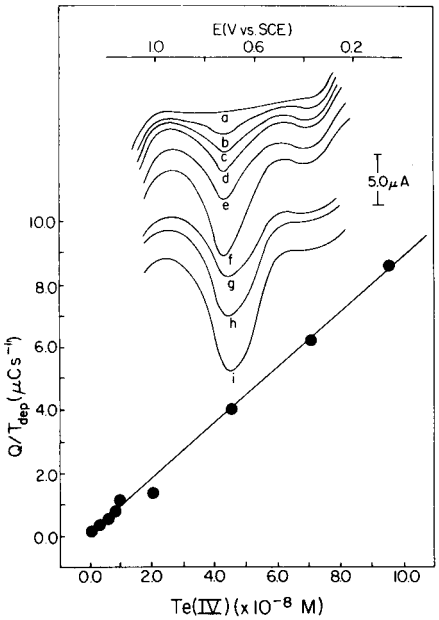

Fig. 6. Anodic stripping voltammetry of tellurium(IV) at the RAuRDE (3600 r.p.m., 5 V min^{-1}, $E_{d,dep}$ = −0.40 V, 0.1 M $HClO_4$). Deposition times: (a) — (f) 10 min; (g) — (i) 5 min. Te(IV) concentration: (a) 0, residual with 10-min deposition; (b) 1×10^{-9}; (c) 3×10^{-9}; (d) 6×10^{-9}; (e) 8×10^{-9}; (f) 1×10^{-8}; (g) 2×10^{-8}; (h) 5×10^{-8}; (i) 7×10^{-8} M.

series of collection curves recorded from a solution 1×10^{-8} M in tellurium(IV) for several values of deposition time. The collection efficiency is 0.062 and remains constant as the quantity of tellurium deposited is varied by changing the tellurium(IV) concentration or deposition time. Plots of charge consumed vs. deposition time and tellurium(IV) concentration are linear with correlation coefficients of 0.998 and 0.999, respectively. The minimum detectable quantity of tellurium(IV) by this collection technique was 5×10^{-11} M. Figure 8 shows the I_d—E_d and I_r—E_d curves for a 1×10^{-9} M Te(IV) solution following a 10-min deposition period.

Conclusion

Tellurium(IV) can be determined by stripping voltammetry at gold electrodes either by conventional anodic stripping voltammetry or by stripping voltammetry with collection. Detection limits are 0.1 ppb and 0.006 ppb, respectively. Tellurium(IV) is reduced to Te(0) at gold electrodes and multiple activity states are observed. The oxidation of electrodeposited tellurium leads to the formation of a layer of adsorbed tellurium(IV) and then at least two tellurium(IV) species are produced as the result of oxidation of electrodeposited tellurium.

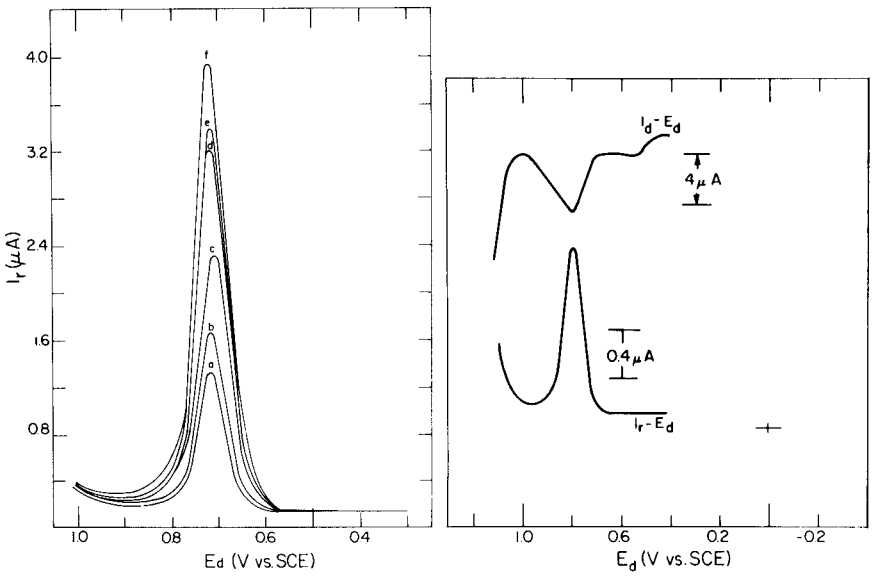

Fig. 7. Stripping voltammetry with collection of 1×10^{-8} M tellurium(IV) at the RAuRDE (1600 r.p.m., 7 V min^{-1}, $E_{d,dep} = -0.40$ V, $E_r = 0.00$ V, 0.1 M $HClO_4$). Deposition times: (a) 15; (b) 30; (c) 60; (d) 90; (e) 120; (f) 150 s.

Fig. 8. Stripping and collection curves for 1×10^{-9} M tellurium(IV) at the RAuRDE (3600 r.p.m., 5 V min^{-1}, $E_{d,dep} = -0.40$ V, $E_r = 0.40$ V, deposition time 10 min, 0.1 M $HClO_4$).

REFERENCES

1 R. E. Allen and D. C. Johnson, Talanta, 20 (1973) 305.
2 R. E. Allen and D. C. Johnson, Talanta, 20 (1973) 799.
3 G. W. Tindall and S. Bruckenstein, Anal. Chem., 22 (1969) 367.
4 D. Laser and M. Ariel, J. Electroanal. Chem., 49 (1974) 123.
5 G. W. Schieffer and W. J. Blaidel, Anal. Chem., 49 (1977) 49.
6 G. W. Schieffer and W. J. Blaidel, Anal. Chem., 50 (1978) 99.
7 G. Henge, P. Monks, G. Tolg, F. Umland and E. E. Wessling, Frezenius Z. Anal. Chem., 295 (1979) 1.
8 B. Ya. Kaplan and A. S. Rezakova, Zh. Anal. Khim., 21 (1966) 1268.
9 E. Ya. Kaplan and L. N. Trukhacheva, Zavod. Lab., 38 (1972) 1058.
10 M. Kapanica and V. Stara, J. Electroanal. Chem., 91 (1978) 351.
11 R. S. Posey and R. W. Andrews, Anal. Chim. Acta, 119 (1980) 55.
12 R. W. Andrews and D. C. Johnson, Anal. Chem., 47 (1975) 294.
13 R. W. Andrews, J. H. Larochelle and D. C. Johnson, Anal. Chem., 48 (1976) 212.
14 G. Forsberg, J. W. O'Laughlin, R. G. Megargle and S. R. Koirtyohann, Anal. Chem., 47 (1975) 1586.
15 M. M. Nicholson, Anal. Chem., 32 (1960) 1058.
16 D. T. Sawyer and J. L. Roberts, Experimental Electrochemistry for Chemists, Wiley—Interscience, New York, 1974, p. 67.
17 D. T. Napp, D. C. Johnson and S. Bruckenstein, Anal. Chem., 39 (1967) 481.
18 H. Marshall, Inorganic Synthesis, Vol. 3, McGraw-Hill, New York, 1950, pp. 143—145.
19 W. J. Albery and M. L. Hitchman, Ring—Disk Electrodes, Clarendon Press, Oxford, 1971, p. 18.

Analytica Chimica Acta, 119 (1980) 55—66

STRIPPING VOLTAMMETRY OF TELLURIUM(IV) IN 0.1 M PERCHLORIC ACID AT ROTATING GOLD DISK ELECTRODES

ROBERT S. POSEY and RICHARD W. ANDREWS*

Department of Chemistry, University of Alabama in Birmingham, University Station, Birmingham, AL 35294 (U.S.A.)

(Received 17th December 1979)

SUMMARY

The stripping voltammetry of tellurium(IV) in 0.1 M perchloric acid at gold electrodes is described. Detection limits for solid gold, in situ gold-plated and externally gold-plated rotating glassy carbon disk electrodes are presented. There is no significant increase in sensitivity for the use of solid gold electrodes; 0.25 ppm tellurium(IV) can be determined by anodic stripping voltammetry at an in situ gold-plated rotating glassy carbon disk electrode. The determination of tellurium in NBS SRM 1632a (Trace Elements in Coal) is described.

The use of the rotating disk electrode in stripping voltammetry has been discussed by several authors [1, 2]. Various forms of carbon such as glassy carbon, pyrolytic graphite and wax-impregnated graphite have been recommended as suitable working electrode materials. The noble metals such as platinum and gold have limited application in anodic stripping voltammetry primarily because of their low hydrogen overvoltage, the formation of surface oxide films in potential regions where deposited metals are oxidized [3], the necessity of developing pretreatment procedures which insure constant active surface area [1], and the formation of intermetallic compounds on the electrode surface which may lead to the presence of multiple stripping peaks [4]. Electrode pretreatment can be especially problematic; Griess et al. [5] observed that the deposition potential for silver(I) on platinum electrodes can shift by as much as 100 mV after ignition and that traces of silver were not removed from platinum electrodes by anodization in cyanide media. Selenium is not completely removed from gold electrodes unless the electrode is held at +1.8 V vs. SCE in 0.1 M perchloric acid for at least 5 min [6]. A thin film electrode significantly simplifies pretreatment. The electrode surface can be renewed for each experiment; and the thin film can be formed in situ, thereby decreasing the number of operations and eliminating exposure of the electrode surface to air. The enhanced sensitivity associated with mercury film electrodes is largely a consequence of the greater surface area to volume ratio which results in the formation of a more concentrated amalgam [7]. A gold film electrode would not be expected to behave in a similar manner unless the analyte is highly mobile in the gold deposit.

In this paper, the use of gold-plated glassy carbon electrodes in the determination of tellurium(IV) is discussed.

The polarographic behavior of tellurium(IV) in ammoniacal and citrate buffers was studied by Lingane and Niedrach [8]; the two polarographic waves observed corresponded to reduction of Te(IV) to Te(0) and Te(2−), respectively. Volaire et al. [9] studied the electrode reaction $Te(0)_{ads} \rightarrow Te(-2)$, by pulse, a.c., and linear-sweep voltammetry at mercury electrodes and reported a detection limit of 10^{-8} M for Te(IV) in 1 M $HClO_4$. Henze et al. [10] used cathodic stripping voltammetry to determine Se(IV) and Te(IV) in the low $\mu g\ l^{-1}$ range. A graphite electrode was used [11] to determine tellurium in indium antimonide powder and crystals by anodic stripping voltammetry with a detection limit of 10^{-8} M. The formation of Cu—Te alloys has been studied by anodic stripping voltammetry [12], while Kraki et al. [13] utilized the co-deposition of tellurium with copper at a rotating platinum wire electrode to determine Te(IV) by anodic stripping voltammetry.

The principal metals determined by anodic stripping voltammetry (a.s.v.) at gold electrodes include Se, As, Sb, Hg and Ni. The advantages of gold electrodes for a.s.v. include a greater anodic working range making it suitable for the determination of metals more electropositive than mercury [7]; the absence of significant oxide film formation in mineral acid solution at potentials less positive than ca. 1.0 V vs. SCE [14]; and, in some cases, highly reversible plating and stripping electrode reactions. Forsberg et al. [15] found gold to be superior to platinum for the determination of As(III), the detection limit being 0.02 ng As ml^{-1}, while Andrews observed similar results for Se(IV) [6]. Andrews et al. [16] determined Hg(II) from 0.02 to 20 ppb, using differential pulse a.s.v. at a rotating gold disk electrode. A single anodic stripping peak was obtained for submonolayer equivalent depositions of mercury. Submonolayer equivalent deposition of selenium at rotating gold disk electrode was used by Andrews and Johnson for the determination of Se(IV) with a detection limit of 0.04 ng ml^{-1} [17]. Nicholson determined 5×10^{-8} M Ni(II) by a.s.v. at gold electrodes [18].

Complete removal of deposited metals from gold electrodes is often quite difficult (see above). A gold-plated electrode on an inert substrate largely circumvents this difficulty. Glassy carbon is especially attractive as a substrate material because of its low porosity and high electrical conductivity [19, 20]. Davis et al. [21, 22] have demonstrated the utility of gold-plated electrodes for the determination of sub-ppb As(III) by a.s.v. while Forsberg et al. [15] showed that the sensitivity for As(III) is enhanced by co-deposition with gold at platinum electrodes [15]. Andrews and Johnson [17] demonstrated that gold-plated glassy carbon electrodes yield stripping voltammograms similar to these obtained at solid gold electrodes. In this report the use of gold-plated electrodes for the determination of 0.3 ppb Te(IV) is discussed and the application of a.s.v. for the determination of tellurium in NBS SRM 1632 coal is described.

EXPERIMENTAL

Apparatus and instrumentation

A model RDE 3 Bipotentiostat (Pine Instrument Co., Grove City, PA) was used with an Omnigraphic 2000 XY recorder (Houston Instruments, Bellaire, TX). A Keithley model 168 digital multimeter was used to measure all voltages and a Keuffel and Esser compensating planimeter was used to integrate peak areas.

The disk electrodes and model PIR rotator were obtained from Pine Instrument Co. The glassy carbon disk electrode had a projected surface area of 0.452 cm^2 while the gold disk electrode had a projected surface area of 0.553 cm^2. A spiral of platinum wire separated from the main electrolysis chamber by a fine glass frit served as the auxiliary electrode; a Ag/AgCl (4 M NaCl) reference electrode was used throughout. The electrolysis vessel was a 100-ml Metrohm titration cell with a cap modified to accommodate the rotating disk electrodes. The glass cell bottom, purge tube and salt bridge chambers were soaked in 50% (v/v) nitric acid for at least 3 h before use and rinsed with distilled demineralized water.

Reagents

All solutions were prepared from Fisher Reagent chemicals, except as noted. The water used was demineralized and doubly distilled, the first distillation being from alkaline permanganate solution. The stock plating solution was prepared from 99.99% gold wire (Alpha Ventron), and the Te(IV) stock solution was prepared from 99.99% tellurium metal (Alpha Ventron) as described by Marshall [23]. The stock solutions were stored in polyethylene bottles.

Procedures

Pretreatment of the rotating glassy carbon disk electrode (RGCDE) consists of consecutive polishing with 5.0, 0.3 and 0.05-μm Buehler alumina on Buehler microcloth moistened with distilled deionized water. After this polishing, the electrode was rotated in the test solution which was purged with nitrogen while the potential was cycled between +1.20 V and −0.40 V (vs. Ag/AgCl). When deaeration was complete, the nitrogen flow was diverted over the solution, and *I—E* curves were recorded until a reproducible curve was obtained.

When an externally gold-plated electrode was required, a 1.0×10^{-6} M Au(III) solution in 0.4 M HCl—0.4 M KCl was used as the plating solution and the deposition potential was −0.400 V. In situ plating of the RGCDE required only the addition of sufficient Au(III) to make the solution 2.0×10^{-6} M in Au(III).

Analysis of NBS SRM 1632 (Trace Elements in Coal). Weigh the sample into the digestion flask. Add a suitable quantity of a 5:1:1 mixture of concentrated nitric, perchloric and sulfuric acids, connect the reflux head and

heat vigorously until perchlorate fumes are evolved. Cool and dilute with distilled deionized water. Dilute an aliquot 10-fold with 0.1 M $HClO_4$ and transfer to the electrolysis cell. Deaerate for 10 min while scanning between 1.20 and −0.40 V with the RGCDE rotated at 2500 r.p.m., using a sweep rate of 5 V min^{-1}. Add enough gold solution to give 2×10^{-6} M Au(III). When mixing is complete, cycle the electrode potential to −0.40 V and deposit for 10 min. Sweep the working electrode potential to 1.20 V and record the stripping voltammogram. Then add 0.01 μg of Te(IV) and repeat the deposition and sweeping steps. Repeat these two steps with two further standard additions of 0.01 μg of Te(IV).

RESULTS AND DISCUSSION

Current—potential curves for tellurium(IV) at solid gold electrodes

Current—potential curves recorded for several Te(IV) concentrations in 0.1 M $HClO_4$ at a rotating gold disk electrode (RAuDE) are shown in Fig. 1. Two cathodic processes, peak J and wave K, are observed, and three anodic processes, peaks A, B and C, are observed. These results parallel the voltammetric behavior of Se(IV) under similar conditions [17]. Only anodic peak B is observed for Te(IV) concentrations less than 10^{-5} M without depositing Te(0) at E < +0.20 V vs. SCE. Figure 2 shows the stripping voltammograms

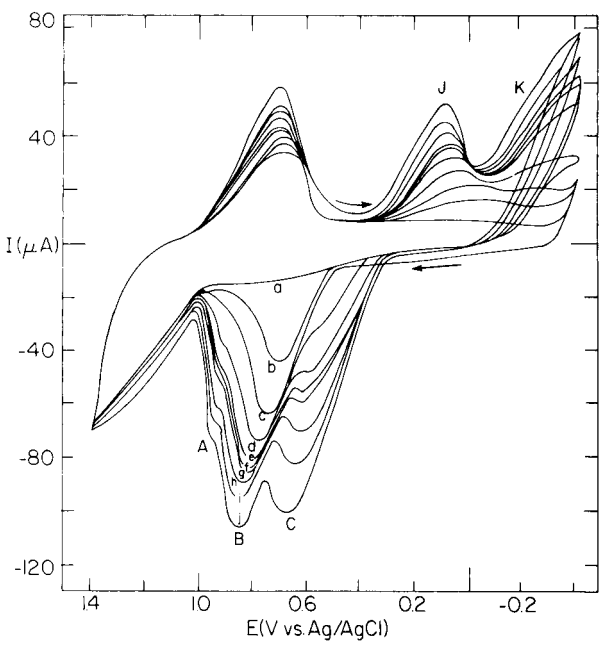

Fig. 1. *I—E* curves for several Te(IV) concentrations at the RAuDE in 0.1 M $HClO_4$ with 1600 r.p.m. and scan rate 5 V min^{-1}. Molarity of Te(IV): (a) 0.0; (b) 5×10^{-6}; (c) 1×10^{-5}; (d) 2×10^{-5}; (e) 4×10^{-5}; (f) 6×10^{-5}; (g) 1×10^{-4}; (h) 1.25×10^{-4}; (i) 2.50×10^{-4}; (j) 5×10^{-4}.

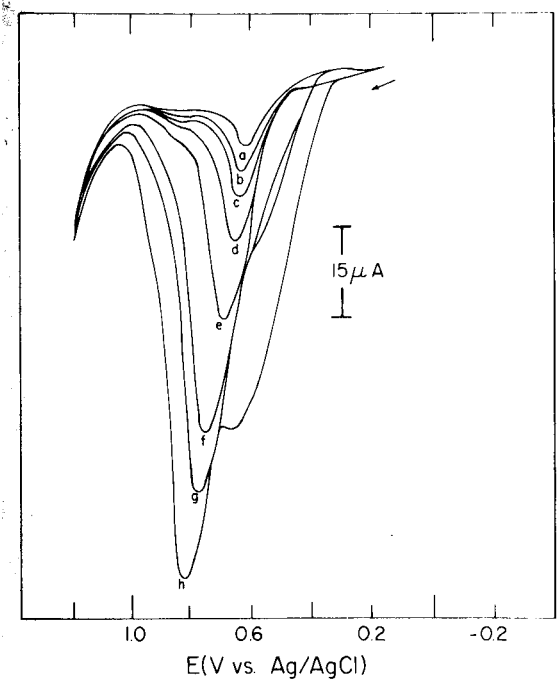

Fig. 2. Stripping voltammograms for 1×10^{-6} M Te(IV) for several deposition times at the RAuDE with 1600 r.p.m. snd scan rate 5 V min^{-1}; $E_{dep} = -0.40$ V. Deposition time (s): (a) 0; (b) 10; (c) 20; (d) 40; (e) 80; (f) 150; (g) 240; (h) 300.

recorded for a 1×10^{-6} M Te(IV) solution with increasing deposition periods. Once again, only anodic peak B is observed for relatively short deposition periods (<120 s). Peak C appears after longer deposition while peak A is identifiable only when peak C is present. It is concluded that these three anodic stripping peaks result from the presence of three distinct activity states of electrodeposited Te(0). The current-time integral of peak B never exceeded the equivalent of a single monolayer of deposited Te(0) calculated on the basis of a perfectly smooth electrode surface and a 1:1 correspondence of tellurium and gold. Peak B is concluded to result from the oxidation of Te(0) which has formed a monolayer on the gold surface. Peak C is observed before peak B reaches its limiting value, indicating a non-uniform deposition pattern [24]. Peak C continues to increase as either the Te(IV) concentration or the deposition period is increased and is concluded to result from deposition of Te(0) on sites occupied by Te(0), i.e., a deposit of bulk Te(0). The peak potential of peak C is closest to the standard reduction potential of Te(IV) in acidic media [25]; this is consistent with the proposed activity state requiring the smallest Au—Te interaction. Peak A appears here primarily as a shoulder on peak B only when peak C is also observed. This suggests that tellurium diffuses into the gold when the concentration gradient of tellurium provides the free energy. Peak A has a peak potential which clearly indicates

a significant Au—Te interaction, and is concluded to represent the oxidation of Te(0) from a Te—Au intermetallic compound.

It is significant that a single anodic stripping peak is recorded when the quantity of deposited Te(0) does not exceed a monolayer. That condition is easily satisfied for dilute solutions and short deposition periods. Plots of charge vs. deposition period for 0.5×10^{-6} M Te(IV) and charge (normalized by deposition time) vs. Te(IV) molarity are linear (correlation coefficients ≥ 0.999 from linear least-squares analysis). The detection limit for the determination of Te(IV) by a.s.v. at the RAuDE is 10^{-9} M or 0.13 ppb Te with a 10-min deposition period.

Gold-plating conditions for RGCDE

In order to simplify the pretreatment conditions, the utility of gold-plated glassy carbon electrodes was investigated. Davis et al. [21] have described gold-plating conditions for the hydrodynamic electrode of Environmental Science Associates, and Vydra et al. have reported the determination of Au(III) by a.s.v. at RGCDE's [26]. A point of initial concern was the possibility of multiple activity states of the electrodeposited gold as the quantity of gold exceeded several monolayers.

Initial experiments with Au(III) in 0.1 M H_2SO_4 resulted in complex stripping voltammograms, and a gold oxide reduction peak was observed on the succeeding negative potential sweep. Consequently, a 0.4 M NaCl—0.4 M HCl mixture was chosen as the supporting electrolyte. In the chloride media, no gold oxide reduction peak was observed, and a suitable collection peak for the electro-oxidized Au(III) was observed at the platinum ring of a platinum-ring/glassy carbon disk RRDE. Figure 3 shows a plot of charge vs. deposition potential; $E_{1/2}$ is approximately −0.175 V. The deposition potential was

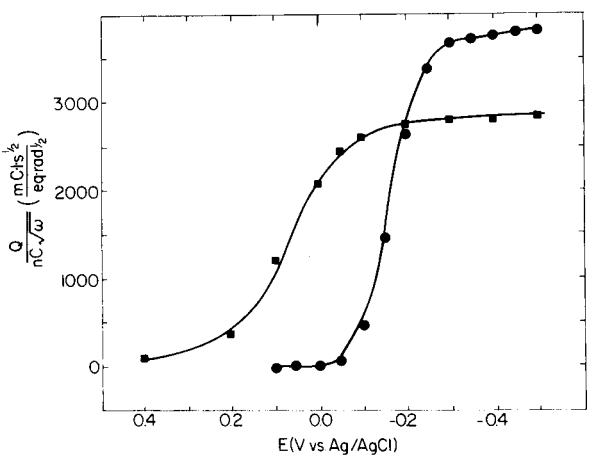

Fig. 3. Charge vs. deposition potential curves for (•) 10^{-6} M Au(III) at the RGCDE (1600 r.p.m., 5 V min^{-1}, deposition time, 60 s, 0.4 M HCl—0.4 M NaCl) and (▪) 5×10^{-7} M Te(IV) with 2×10^{-6} M Au(III) (2500 r.p.m., 5 V min^{-1}, deposition time 60 s, 0.1 M $HClO_4$).

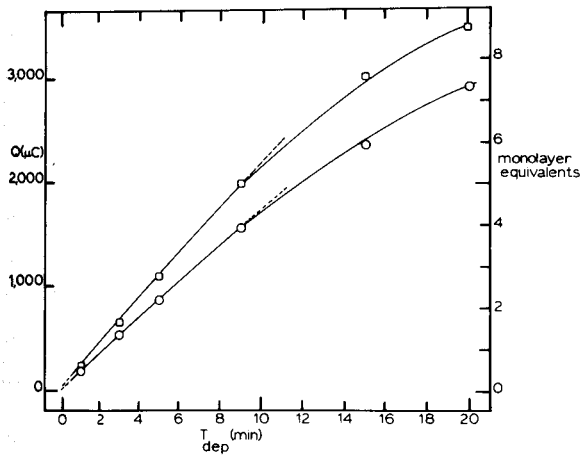

Fig. 4. Charge and monolayer equivalents vs. deposition time for 10^{-6} M Au(III) at the RGCDE (1600 r.p.m., 5 V min^{-1}, E_{dep} −0.40 V, 0.4 M HCl—0.4 M NaCl).

chosen as −0.40 V in all succeeding experiments. Plots of charge vs. square root of rotational velocity were linear. The reduction is mass-transport controlled and behaves reversibly. Figure 4 is a plot of charge vs. deposition period and monolayer equivalents vs. deposition period. The plots are linear for deposition periods less than 10 min, and only a single stripping peak was observed for deposition periods as long as 20 min. There was no indication of multiple activity states of the electrodeposited gold.

Current—potential curves for Te(IV) at the gold-plated RGCDE

Tellurium(IV) can be determined by a.s.v. at carbon electrodes [11]. Figure 5A demonstrates such a determination of Te(IV) with a RGCDE. When Au(III) was added to the solution the *I—E* curves shown in Fig. 5B resulted. The quantity of deposited Te(0) increased substantially, and multiple activity states of the deposited Te(0) are shown. The similarity of Figs. 1 and 5A when the concentration of Te(IV) exceeds 10^{-5} M should be noted. A comparison of Figs. 1 and 5 indicates that the glassy carbon electrode offers a significant advantage over gold electrodes when Te(IV) is to be determined by a.s.v. at concentrations exceeding 10^{-5} M insofar as a single stripping peak is recorded. However, when the concentration of Te(IV) is less than 10^{-6} M, a single stripping peak is recorded with gold-plated glassy carbon electrodes and that stripping peak is significantly larger than the stripping peak obtained from unplated glassy carbon electrodes.

Anodic stripping voltammetry of Te(IV) at a gold-plated RGCDE. The suitability of gold-plated electrodes for the determination of Te(IV) by a.s.v. was assessed by examining the influence of deposition potential, deposition period, rotational velocity, sweep rate and finally concentration of Te(IV) on the stripping voltammograms. Figure 3 shows a plot of charge vs. deposition potential; and $E_{1/2}$ is +0.07 V for the reduction of Te(IV) to Te(0). The

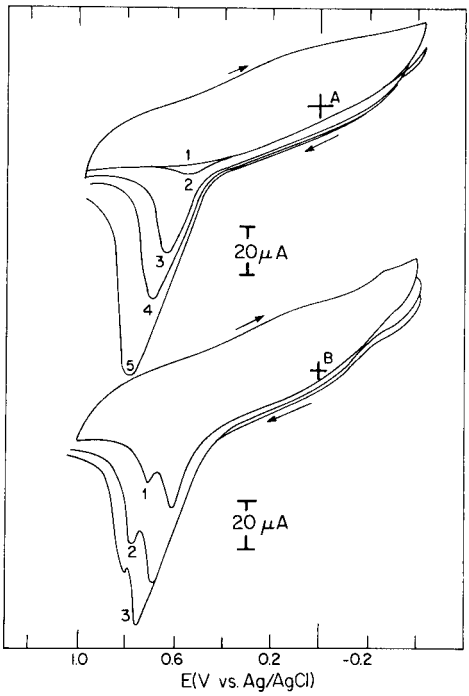

Fig. 5. *I—E* curves for 10^{-5} M Te(IV) in 0.1 M $HClO_4$ at the RGCDE (1600 r.p.m., 5 V min^{-1}, 0.1 M $HClO_4$, E_{dep}—0.40 V). (A) No Au(III) added. Deposition time (s): (1) residual, without Te(IV) added; (2) 0; (3) 5; (4) 10; (5) 20. (B) 2 × 10^{-6} M Au(III) added. Deposition time (s): (1) 0; (2) 5; (3) 10.

deposition potential in all experiments was chosen to be $\leqslant -0.40$ V. Plots of charge vs. deposition period and square root of rotational velocity were linear, demonstrating the mass-transport control of the Te(IV) reduction.

Figure 6 shows the influence of sweep rate upon the stripping voltammograms. Peak current increases linearly with sweep rate while the charge consumed remains nearly constant (±5%). The first-order dependence is predicted by Branina's peak current equation for RDE's [27]. Finally, calibration curves of charge (normalized by deposition period) vs. Te(IV) concentration were linear (correlation coefficients $\geqslant 0.995$). In a separate series of experiments, the detection limit for the determination of Te(IV) by a.s.v. was evaluated for the externally gold-plated RGCDE. The concentration of Te(IV) which resulted in a stripping peak the height of which exceeded the noise level by a factor of three was taken to be the detection limit. The gold film thickness was varied from 1 to 5 monolayers.

The results, summarized in Table 1, clearly indicate no significant advantage for the externally gold-plated electrodes and no significant loss of sensitivity in the use of gold-plated electrodes relative to the solid gold electrode for the determination of Te(IV) by a.s.v. Consequently, the in situ gold-plated electrode was selected for further use because of its greater experimental simplicity.

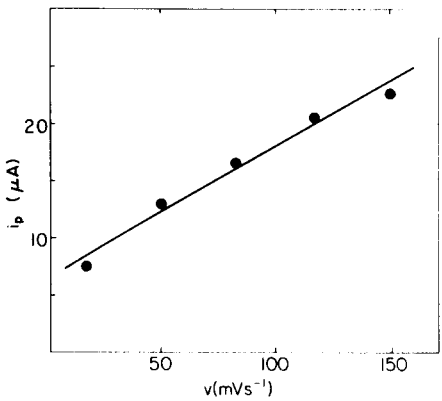

Fig. 6. Scan rate dependence of anodic dissolution of Te(IV) at the RGCDE (1600 r.p.m., E_{dep} = −0.40 V, deposition time, 60 s, 0.1 M $HClO_4$, 2 × 10^{-6} M Au(III), 1 × 10^{-6} M Te(IV)).

Interferences

Interference in stripping voltammetry is generally the result of codeposition of the interfering metal which either forms an intermetallic compound leading to incomplete stripping and/or multiple stripping peaks, or is oxidized at potentials similar to the analyte with a resulting loss of resolution of the stripping peaks. The effects of Cu(II), Pb(II), Hg(II), Se(IV) and As(III) on the area of the stripping peak recorded for a 10^{-7} M Te(IV) solution are summarized in Table 2.

In the case of Pb(II) and Cu(II), interference is observed only when a significant excess of the metal is present, so that resolution of the Te(IV) peak becomes difficult or impossible. In the cases of As(III), Hg(II) and Se(IV), the stripping peak potentials are sufficiently close that only when very small fractions of monolayer equivalents are deposited can the stripping peaks be clearly resolved. Since mercury is easily lost from samples that are wet-ashed in perchloric—nitric acid mixtures [28], the consequences of co-deposition of mercury are less serious in the analysis of samples requiring vigorous wet ashing.

TABLE 1

Detection limits

Electrode	Detection limit (M)
Solid Au	1×10^{-9}
In situ Au-plated	2×10^{-9}
1 monolayer Au-plated	3×10^{-9}
2 monolayer Au-plated	1×10^{-8}
5 monolayer Au-plated	4×10^{-9}

TABLE 2

Interference study for a 10^{-7} M Te(IV) solution

Metal	E_p(V vs. Ag/AgCl)	% Deviation caused by		
		1×10^{-8} M	1×10^{-7} M	1×10^{-6} M
Pb(II)	+0.05	0.0	+3.0	−16.0
Cu(II)	+0.40	+5.0	+11.0	+36.0
As(III)	+0.40	0.0	−4.0	−14.0
Se(IV)	+0.95	−2.0	−12.0	−78.0
Hg(II)	+0.85	−1.0	+3.0	—[a]

[a]Tellurium peak could not be resolved.

Determination of tellurium in NBS Coal (SRM 1632a)

The Standard Reference Materials available from the National Bureau of Standards [29] do not contain an environmental standard which has a certified tellurium assay. For SRM 1632a (Trace Elements in Coal) there is an uncertified value of 0.1 μg Te g^{-1} based on a single determination. Consequently, SRM 1632a was chosen as a model sample for a practical demonstration of the proposed method. The dried coal sample was dissolved in mixed acids [30] and treated as described in the Experimental section. The sample was found to contain 0.19 ± 0.09 μg Te g^{-1} (95% confidence limits based upon Student's t test and four determinations). Stripping voltammograms recorded during a determination are shown in Fig. 7. The coal sample contains significantly greater quantities of As, Cu, Se, and Pb than tellurium. The molar ratios of metal to tellurium range from 330:1 for Cu:Te to 41:1 for Se:Te, and significant interference would be expected. Consequently, the technique of standard additions was chosen for quantification, as the calibration plots had been shown to be linear with zero intercept, and the degree of linearity of the standard addition plots was good (correlation coefficients were typically 0.996 or greater). The interferences from As, Cu, Se, and Pb are not unidirectional (Table 2) and are least significant in dilute solution. The nominal concentrations of the interfering metals following the dissolution of a 1-g sample, dilution and aliquotting ranged from 3×10^{-8} M for selenium to 3×10^{-7} M for copper based on the certificate values. Consequently, interference would be expected to occur, but was not observed to be significant. It should be noted that much of the uncertainty in the reported value for the tellurium content is the result of a significant blank value (0.05 μg Te) from the digestion reagents. Samples requiring less vigorous oxidizing conditions should have correspondingly smaller blank values. The use of mineral acids purified by sub-boiling point distillation would be expected to reduce the blank as well [31].

The results of the determination of tellurium in NBS SRM 1632a indicate that a.s.v. with in-situ gold-plated RGCDE's provides an accurate assay. In order to extend the methodology to samples containing large excesses

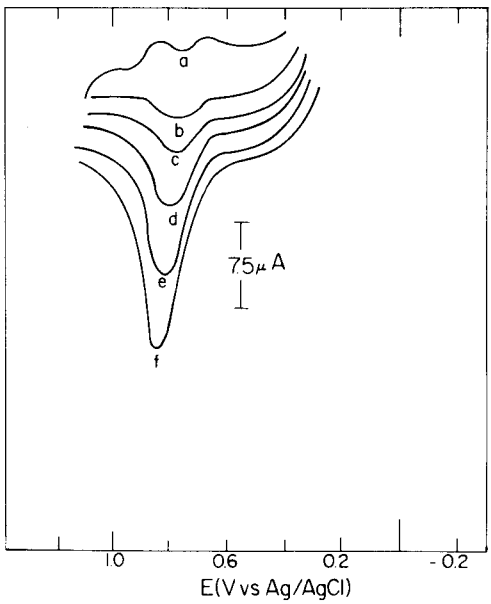

Fig. 7. Analysis of Coal SRM at the RGCDE (2500 r.p.m., 5 V min^{-1}, E_{dep} = −0.40 V, deposition time 10 min). Curves: (a) sample; (b) +0.128 μg Te(IV); (c) +0.255 μg Te(IV); (d) +0.574 μg Te(IV); (e) +1.21 μg Te(IV); (f) +2.42 μg Te(IV).

of interfering metals, a preliminary separation of the Te(IV) would be required. The technique possesses adequate sensitivity for sub-ppm amounts of tellurium and is experimentally simple to perform, requiring only minimal electrode pretreatment.

The generous support of the Faculty Research Council of the University of Alabama in Birmingham is gratefully recognized.

REFERENCES

1 F. Vydra, Electrochemical Stripping Analysis, Halsted Press, New York, 1976.
2 F. Opekar and P. Beran, J. Electroanal. Chem., 69 (1976) 68.
3 R. N. Adams, Electrochemistry at Solid Electrodes, M. Dekker, New York, 1969.
4 G. W. Tindall and S. Bruckenstein, Anal. Chem., 40 (1968) 1051.
5 J. C. Griess, J. T. Byrne and L. B. Rodgers, J. Electrochem. Soc., 98 (1951) 447.
6 R. W. Andrews, Ph.D. Dissertation, Iowa State University, 1975.
7 T. R. Copeland and R. K. Skogerboe, Anal. Chem., 46 (1974) 1257A.
8 J. J. Lingane and L. Niedrach, J. Am. Chem. Soc., 71 (1949) 196.
9 M. Volaire, O. Vittori and M. Porthault, Anal. Chim. Acta, 71 (1974) 185.
10 G. Henze, P. Monks, G. Toelg, F. Umland and E. Wessling, Fresenius Z. Anal. Chem., 295 (1979) 1.
11 V. F. Gridaev, A. A. Kaplan and A. G. Stromberg, Izv. Tomsk. Politekh. Inst., 257 (1973) 187.
12 E. Ya. Nieman and G. B. Ponomarenko, Zh. Anal. Khim., 30 (1975) 1132.
13 S. Kraki, S. Suzuki and T. Kuwabara, Bunseki Kagaku, 22 (1973) 700.
14 D. T. Sawyer and J. L. Roberts, Experimental Electrochemistry for Chemists, Wiley—Interscience, New York 1974, pp. 66—69.

15 G. Forsberg, J. W. O'Laughlin, R. G. Megargle and S. R. Koirtyohann, Anal. Chem., 47 (1975) 1586.
16 R. W. Andrews, J. H. Larochelle and D. C. Johnson, Anal. Chem., 48 (1976) 212.
17 R. W. Andrews and D. C. Johnson, Anal. Chem., 47 (1975), 294.
18 M. M. Nicholson, Anal. Chem., 32 (1960) 1058.
19 T. M. Florence, J. Electroanal. Chem., 27 (1970) 273.
20 R. E. Allen and D. C. Johnson, Talanta, 20 (1973) 799.
21 P. H. Davis, G. R. Delude, R. M. Griffin, W. R. Matson and E. W. Zink, Anal. Chem., 50 (1977) 137.
22 P. H. Davis, F. J. Berlaudi, G. R. Delude, R. M. Griffin, W. R. Matson and E. W. Zink, J. Am. Ind. Hyg. Assoc., 39 (1978) 480.
23 H. Marshall, Inorganic Synthesis, Vol. 3, McGraw-Hill, New York, 1950, pp. 143—145.
24 J. A. Harrison and H. R. Thirsk, in A. J. Bard (Ed.), Electroanalytical Chemistry, Vol. 5, M. Dekker, New York, 1971, pp. 125—130.
25 W. M. Latimer, Oxidation States of the Elements and Their Potentials in Aqueous Solutions, 2nd edn., Prentice-Hall, Englewood Cliffs, NJ.
26 T. V. Nghi and F. Vydra, J. Electroanal. Chem., 64 (1975) 163.
27 Kh. Z. Branina, Elektrokhimiya, 2 (1966) 1006.
28 T. T. Gorsuch, Analyst, 84 (1959) 135.
29 National Bureau of Standards, Catalog of NBS Standard Reference Materials, NBS Special Publication No. 260, 1975—76 edn.
30 G. F. Smith, Wet Chemical Oxidation of Organic Compositions, G. F. Smith Chemical Co., Columbus, OH, 1965, pp. 85—87.
31 E. C. Kuehner, R. Alvarez, P. J. Paulsen and T. J. Murphy, Anal. Chem., 44 (1972) 2050.

Analytica Chimica Acta, 119 (1980) 67—74

DIRECT DETERMINATION OF LEAD IN POLLUTED SEA WATER BY CARBON-FURNACE ATOMIC ABSORPTION SPECTROMETRY

M. C. HALLIDAY and C. HOUGHTON

Department of Biological Sciences, Napier College of Commerce and Technology, Colinton Road, Edinburgh EH10 5DT (Gt. Britain)

J. M. OTTAWAY*

Department of Pure and Applied Chemistry, University of Strathclyde, Cathedral Street, Glasgow G1 1XL (Gt. Britain)

(Received 10th April 1980)

SUMMARY

A simple and rapid method is described for the direct determination of lead in polluted sea water by carbon furnace atomic absorption spectrometry. Filtered sea water is diluted (1 + 1) with deionised distilled water and ammonium nitrate is added to act as a matrix modifier. Aliquots of this mixture are injected into a tantalum-coated graphite tube in a HGA-2200 furnace atomiser operated under gas-stop conditions. With the standard addition method, a detection limit (2σ) of 1 μg Pb l^{-1} is achieved. Good agreement between the proposed method and results obtained by anodic stripping voltammetry was achieved for samples taken from the Firth of Forth.

The determination of the concentrations of trace elements in both coastal and oceanic waters, has received increasing attention in pollution studies. Rapid, sensitive methods are required to measure accurately the low concentrations found in these environments, to enable the environmental hazards of these pollutants to be more readily assessed. The average level of lead in sea water has been reported by Riley and Skirrow [1] to be within the range 0.03—9.0 μg l^{-1} in the open ocean. Values for the outer Firth of Forth, in comparison, are reported to be in the range 0.3—70 μg l^{-1} [2]. The latter range is higher, partly because samples were taken from the intertidal zone. It has been shown by Preston [3] that shoreline waters possess higher concentrations of trace metals than offshore waters.

Atomic absorption spectrometry (a.a.s.) is one of the most widely used techniques for the determination of trace metals in natural waters, including sea water. Lead cannot at present be determined directly in sea water, either by flame (f.a.a.s.) or carbon furnace (c.f.a.a.s.) atomic absorption spectrometry. In the case of f.a.a.s. this is due both to the low levels found in sea water, which are below the detection limit of the instrument, and the matrix interference effects of the salts present. Hence the lead must be preconcentrated and separated from the interfering components. The two main techniques employed are solvent extraction and ion-exchange, which have recently

been reviewed by Wilson [4]. These operations are time-consuming and increase the possibility of contamination unless considerable time and care is taken.

Recently, other trace elements, including cadmium and zinc [5], iron, manganese, copper and cadmium [6], copper [7] and iron, manganese and zinc [8] have been determined directly by c.f.a.a.s. Thus the development of a method to determine lead in this way would be desirable in order to achieve faster analysis and avoid contamination. However, although this technique is capable of directly determining small amounts of lead, the interference from the major ions in sea water makes this impossible owing to the suppression of the lead signal. Suppression by sodium chloride has been observed by several workers [5, 9, 10] and is probably due to the large background molecular absorption signal of sodium which is too great for the background correction system to overcome efficiently [5]. The suppressive effect of magnesium chloride, which appears to be a vapour phase effect, has also been reported [5, 11]. Similar effects have been observed with a number of other elements [10, 12, 13]. Interference by sulphate has also been reported [9, 11, 14] and has been attributed to the formation of a non-volatile sulphide [15].

In an attempt to overcome suppression by these ions, matrix modifiers such as ammonium nitrate and ascorbic acid have been used. Copper has been determined directly in sea water by c.f.a.a.s. after addition of ammonium nitrate [7]. Sturgeon et al. [8] found this to be unsuccessful for the determination of iron and manganese, but suitable for zinc. The effect of ammonium nitrate on the removal of sodium chloride interference has been discussed by Ediger et al. [7]; sodium nitrate and ammonium chloride are formed and removed by volatilization during ashing at 500°C. Ascorbic acid is applicable to the determination of lead in drinking water [16], by overcoming interference from magnesium chloride, which, according to Fuller [17], is achieved by the reduction of lead oxide to lead by certain organic compounds.

The treatment of graphite tubes with solutions of metals capable of forming interstitial carbides is of increasing interest. Coating tubes with these metals can alleviate sensitivity problems, because the type, structure and reactivity of the graphite influence sensitivity [18]. Molybdenum has been used as a coating in the direct determination of lead in blood and urine by Hodges [9], while the use of tantalum [19], tantalum and tungsten [20] and tungsten [21] has also been described. The use of tantalum, lanthanum and molybdenum as coatings for the L'vov platform has been reported by Slavin and Manning [22] for the determination of lead in chloride, sulphate and phospate matrices.

In the method described in this paper an unmodified commercial instrument is used for direct determinations of lead in filtered, diluted sea-water samples, containing added ammonium nitrate. The graphite tubes are coated with tantalum and the lead determined by the standard addition method. The results obtained by the proposed method are in close agreement with those obtained by anodic stripping voltammetry (a.s.v.).

EXPERIMENTAL

Reagents

Analytical-grade chemicals were used throughout, and deionised distilled water was used in the preparation of all solutions. Stock solutions of lead 1000 μg ml^{-1}) as nitrate (atomic absorption grade) were obtained from BDH Chemicals Ltd. The stock solution was diluted as required to give working solutions of 1 or 5 μg ml^{-1} immediately before use. Ammonium nitrate was purified by extraction with ammonium pyrrolidinedithiocarbamate—methyl isobutyl ketone (APDC—MIBK) as follows: 200 ml of a 50% (w/v) solution of ammonium nitrate was extracted with 20 ml of water-saturated MIBK plus 2 ml of APDC (previously purified with MIBK) by shaking in a polypropylene separating funnel with a teflon stopper for ca. 10 s. The procedure was repeated five times.

Sample collection, storage and treatment

Sea-water samples were collected from the outer Firth of Forth at high tide in 1-l polyethylene bottles. Concentrated (Aristar) nitric acid (1 ml) was added to each litre of sea water immediately after collection to stabilise it with respect to lead. The sea water was filtered through a Sartorius cellulose nitrate membrane filter (pore size 0.45 μm, presoaked in 5% (v/v) nitric acid) on a Sartorius glass vacuum filter holder and kept at 4°C prior to analysis.

Immediately prior to analysis by c.f.a.a.s., 2.5 ml of acidified sea water was diluted with 2.5 ml of deionised distilled water and 2.5 ml of 50% (w/v) ammonium nitrate solution. A calibration graph for each sample was prepared by the standard addition method by adding 7.5, 15.0 and 30.0-μl aliquots of a lead solution (5 μg ml^{-1}) to the diluted sea water—ammonium nitrate mixture. Blank solutions were prepared by adding 5 ml of deionised distilled water to 2.5 ml of the ammonium nitrate solution.

Apparatus

A Perkin-Elmer 373 atomic absorption spectrometer equipped with a heated graphite atomiser HGA 2200, a deuterium arc background corrector and a Servoscribe potentiometric chart recorder were used. The argon purge gas flow-rate was 40 ml min^{-1} at 40 lb in^{-2}.

Tantalum-coated tubes were prepared as described by Zatka [19]; the uncoated tubes were supplied by Perkin-Elmer. A Gilson Pipetman adjustable micropipette was employed for injecting small volumes into the graphite tube, and a Jencons adjustable Finn pipette (5 ml) to prepare the samples for analysis. All glassware, sample collection bottles and other containers were thoroughly cleaned with 5% (v/v) nitric acid and rinsed with deionised water prior to use. Sterilin universal containers were used for sample preparation.

A multiple anodic stripping analyser model 2014 (Environmental Sciences Associates) was also used.

TABLE 1

Instrumental conditions

C.f.a.a.s.		A.s.v.	
Wavelength (nm)	217.0	Initial potential (mV)	−700
Spectral bandwidth (nm)	0.7	Autosweep hold (mV)	590
Lamp current (mA)	10	Plating potential (mV)	−700
Drying temp. (°C)	110	Sweep rate (mV s^{-1})	+20
Drying time (s)	22	Standby potential (mV)	−100
Ashing temp. (°C)	500		
Ashing time (s)	30		
Atomisation temp. (°C)	2100		
Atomisation time (s)	6		
Sample volume (μl)	25		
Argon flow rate (ml min^{-1})	40		

Instrumental conditions

Carbon-furnace atomic absorption spectrometry. Aliquots (25-μl) were injected into the graphite furnace and atomised under the conditions given in Table 1. The gas-stop facility was used during the atomisation stage which increases sensitivity for volatile elements such as lead, and the deuterium arc background corrector was used at all times. The tubes were fired at maximum temperature at intervals for 10 s to clear the sample matrix from the tube surfaces.

Anodic stripping voltammetry. The lead present in 5 ml of acidified sea water was plated onto a composite mercury graphite electrode for 7—15 min, depending on the concentration of lead present. Nitrogen was bubbled through the sample at a rapid but uniform rate at 7 lb in^{-2} to aid plating. The standard addition method was used to determine the amount of lead present in samples and suitable aliquots of a working standard solution (1 μg Pb ml^{-1}) were added as required. Instrumental conditions are given in Table 1.

RESULTS AND DISCUSSION

The major constituents of sea water that are most likely to affect the determination of trace elements such as lead are Na^+, K^+, Mg^{2+}, Ca^{2+}, Cl^-, SO_4^{2-} and PO_4^{3-}. Their effects on the c.f.a.a.s. lead signal were examined in both pyrolytic graphite and tantalum-coated tubes. The results are given in Tables 2 and 3 respectively. Potassium chloride, calcium chloride and sodium hydrogenphosphate had little effect on the signal in either type of tube, even in the absence of the matrix modifier, ammonium nitrate. However, at the concentrations found in sea water, sodium chloride caused some interference, particularly in the pyrolytically coated tube, probably because of the large background molecular absorption signal of sodium, as mentioned previously, although the addition of ammonium nitrate relieved the suppression to some

TABLE 2

Interference of major sea-water elements on the determination of lead in a pyrolytic graphite coated tube, with and without addition of ammonium nitrate (15%).
(Values are expressed as % suppression of the peak height from 25 μl of 20 ng ml^{-1} lead solution, except where a positive sign indicates enhancement.)

Conc.[a] (mg ml^{-1})	Ca^{2+}		K^+		Mg^{2+}		Na^+		SO_4^{2-}		PO_4^{3-}	
	−AN[b]	+AN[c]	−AN	+AN	−AN	+AN	−AN	+AN	−AN	+AN	−AN	+AN
0.01											1	0
0.05											24	+9
0.1	10	16.0	22	+20	5	19	14	+3			9	1
0.25	8.0[d]	17.0[d]	9[d]	+18[d]	9	13	10	+2				
0.5	13.0[d]	28.0[d]	4[d]	+19[d]	24		8	5			28	1
0.75	13.0	28.0	6	+23	35	3	12	11			0	13
1.0	25.0	29.0	22	+28	64[d]	+ 13[d]	13	4	89	11	3	1
1.5	14.0	31.0	7	1	80[d]	+ 11[d]	6	10	89	30		
2.0	17.0	31.0	17	4					92[d]	53[d]		
2.5									92	56		
3.0					96	23	13	10	95	60		
4.0									94	71		
5.0					100	30	35	12				
10.0					96	66	46[d]	26[d]				
30.0					100	72	76	43				

[a]Sodium, magnesium, calcium and potassium were added as their chlorides, phosphate as sodium hydrogenphosphate and sulphate as sodium sulphate. [b]Without ammonium nitrate. [c]With addition of ammonium nitrate. [d]Normal sea-water concentration. Phosphate levels in the Firth of Forth are lower than those investigated, i.e. 0.0004—0.0665 × 10^{-3}% [2].

extent. Magnesium chloride suppressed the signal in the pyrolytically coated tube to an even greater extent than sodium chloride, presumably because of chemical reaction between the lead and magnesium chloride [5, 10—12]. The addition of ammonium nitrate relieved this effect completely, even enhancing the signal at certain concentrations. The suppression of the signal in the tantalum-coated tube at normal sea water concentrations, however, was hardly noticeable, even in the absence of ammonium nitrate. Sodium sulphate, which is believed to form a non-volatile lead sulphide [15], had the most marked effect on the lead signal of all the salts investigated; in both types of tube the suppression was 80—100%. The addition of ammonium nitrate largely removed this suppression, the effect being most marked in the tantalum-coated tube.

Thus the use of matrix modifier and tube coatings, although it does not totally remove the suppressive effects of all salts at the concentrations present in sea water, reduces their effects to a degree that the quantity of lead can be determined by the method of standard additions in the presence of any of the salts tested. The determination of lead in sea water was best done by addition of ammonium nitrate and dilution (1 + 1) of the sea water, in tantalum-coated tubes.

TABLE 3

Interference of major sea water elements on the determination of lead in a tantalum-coated tube
(Conditions and footnotes as in Table 2)

Conc. (mg ml^{-1})	Ca^{2+}		K^+		Mg^{2+}		Na^+		SO_4^{2-}		PO_4^{3-}	
	–AN	+AN	–AN	+AN	–AN	+AN	–AN	+AN	–AN	+AN	–AN	+AN
0.01											+2	11
0.05											16	2
0.1	+3	1	+4	14							10	16
0.25	18[d]	5[d]	18[d]	+3[d]								
0.5	10[d]	10[d]	10[d]	22[d]	+5	30					28	12
0.75											10	18
1.0	20	7	36	14	5[d]	27[d]			75	8	16	8
1.5					9[d]	30[d]			82	12		
2.0									82	19		
2.5									82[d]	22[d]		
3.0							39	6	86	35		
4.0									86	49		
5.0					74	+10	35	11				
10.0							23[d]	32[d]				
30.0							33	42				

When the sea water was not filtered prior to analysis, the variability in the results was excessive (Table 4). The values given by c.f.a.a.s. and a.s.v., however, correlated significantly (correlation coefficient, 0.84; $p < 0.01$) and were not significantly different ($t = 0.93$) by the paired 't' test. Each sample was analysed six times by c.f.a.a.s. and three times by a.s.v. Filtration of sea water resulted in a marked improvement in reproducibility (Table 4) and gave a detection limit of 1 μg Pb l^{-1} (2σ). The values given by the two methods again correlated significantly (correlation coefficient 0.97; $p < 0.01$) and were not significantly different ($t = 0.58$) by the paired 't' test.

The tantalum coating was preferred to the pyrolytic coating for the following reasons. Firstly, the pyrolytic coating allowed the sample to spurt out of the injection port during the drying and charring stages; the use of a ramp accessory may alleviate this problem. Secondly, the tantalum-coated tube was found to have a life of over 1000 injections compared with around 500 for the pyrolytically coated tube. This increased lifetime, reported by Zatka [19] and Norvel et al. [20], is probably related to the observed degradation effects of ammonium nitrate on pyrolytically coated tubes.

Attempts were made to overcome the interference effects by other methods, including the use of the rapid heating mode on the graphite furnace, utilisation of molybdenum tube coatings and addition of ascorbic acid as matrix modifier, all of which were without effect. It has been reported by Welz et al. [23] that lead can be determined in a 2% sodium chloride matrix when the sample is heated rapidly; the lead then atomises at 1100°C prior to sodium chloride volatilisation at 1413°C, thus overcoming the serious back-

TABLE 4

Determination of lead in unfiltered and filtered Firth of Forth sea water by c.f.a.a.s. and a.s.v.

Sample No.	Unfiltered sea water			Filtered sea water		
	Pb conc. ($\mu g\ l^{-1}$)		RSD (HGA-2200) (%)	Pb conc. ($\mu g\ l^{-1}$)		RSD (HGA-2200) (%)
	HGA-2200	A.s.v.		HGA-2200	A.s.v.	
1	8.4	10.5	49	10.5	11.5	5.5
2	8.2	10.8	51	9.1	8.7	5.9
3	10.2	10.0	36	12.1	12.6	7.5
4	18.2	15.8	20	10.4	11.5	5.4
5	9.7	8.4	16	7.9	9.1	5.4
6	8.6	5.8	38	15.7	16.2	4.4
7	13.0	12.8	13	11.8	11.2	8.5
8	8.6	9.0	38	14.9	14.9	2.4
9	13.7	10.6	21	16.5	15.6	5.1
10	6.0	5.2	24	16.6	15.7	6.3

ground interference. When sea water was heated rapidly, although there was an increase in absorbance in coated and uncoated tubes, the addition of lead produced no further absorbance and the initial effect was found to be due to decreased background absorption produced as a result of the lower temperature used. This technique therefore did not allow the determination of lead in sea water. The use of a molybdenum-coated tube in conjunction with ammonium nitrate as matrix modifier was also investigated, as this method has been used to determine lead in a chloride matrix with no analytical interference [24]. This method did little to remove matrix interference, however, from the sea water. In further tests, the addition of ascorbic acid [16] did not increase the absorbance when lead was added to sea water in both pyrolytically coated and tantalum-coated tubes. Ascorbic acid enhanced the lead signal in the presence of magnesium chloride and removed the suppression caused by sodium chloride but not sodium sulphate; this is presumably the reason for the lack of success with sea water.

Campbell and Ottaway [5] reported a detection limit for lead in sea water of 40 $\mu g\ l^{-1}$; the high value was largely due to the depressive interference of magnesium chloride. The detection limit of lead in pure solution using c.f.a.a.s. is 0.4—0.5 $\mu g\ l^{-1}$. A value of 1 $\mu g\ l^{-1}$ was achieved in the present investigation for the sea-water matrix as a result of the (1 + 1) dilution with deionised distilled water. The marked improvement from Campbell and Ottaway's results is due to the combined effects of the tantalum coating and the matrix modifier in removing the magnesium chloride interference. These two modifications allow the full detection ability of the carbon furnace to be realised.

The proposed c.f.a.a.s. method allows the rapid screening of a large number of samples (approximately 50 per day) with minimal effort if an automatic sampling device is employed.

We are grateful to the Lothian Regional Council and to the Department of Chemistry, Napier College, for the use of facilities and the W. C. Graham, Marine Laboratory, Department of Agriculture and Fisheries for Scotland, for assistance with the a.s.v. analysis.

REFERENCES

1 J. P. Riley and G. Skirrow (Eds.), Chemical Oceanography, Vol. 2, Academic Press, London, 1965, p. 351.
2 Napier College of Commerce and Technology. Report for the period prior to the introduction of the Sewage Scheme (1977). An investigation of the effects of Edinburgh City Sewage Scheme on the ecology of the Firth of Forth. Report to Lothian Regional Council, pp. 406. Annual Report for the period April (1978) to March (1979), pp. 213.
3 A. Preston, Nature (London), 242 (1973) 13.
4 D. L. Wilson, At. Absorpt. Newsl., 18 (1979) 13.
5 W. C. Campbell and J. M. Ottaway, Analyst, 102 (1977) 495.
6 D. A. Segar and A. Y. Cantillo, in T. R. P. Gibb (Ed.), Analytical Methods in Oceanography, Adv. in Chem. Ser., Washington, DC Am. Chem. Soc., 1975, p. 147.
7 R. D. Ediger, G. E. Peterson and J. D. Kerber, At. Absorpt. Newsl., 13 (1974) 61.
8 R. E. Sturgeon, S. S. Berman, A. Desaulniers and D. S. Russell, Anal. Chem., 51 (1979) 2364.
9 D. J. Hodges, Analyst, 102 (1977) 66.
10 W. B. Barnett and M. M. Cooksey, At. Absorpt. Newsl., 18 (1979) 61.
11 L. R. Hageman, J. A. Nichols, P. Viswanadham and R. Woodriff, Anal. Chem., 51 (1979) 1406.
12 W. C. Campbell, PhD Thesis, University of Strathclyde, 1975.
13 R. C. Hutton, PhD Thesis, University of Strathclyde, 1977.
14 K. C. Thompson, K. Wagstaff and K. C. Wheatstone, Analyst, 102 (1977) 310.
15 S. Bäckman and R. W. Karlsson, Analyst, 104 (1979) 1017.
16 J. G. T. Regan and J. Warren, Analyst, 103 (1978) 447.
17 C. W. Fuller, At. Absorpt. Newsl., 16 (1977) 106.
18 G. Volland, G. Kölblin, P. Tschöpel and G. Tölg, Fresenius Z. Anal. Chem., 284 (1977) 1.
19 V. J. Zatka, Anal. Chem., 50 (1978) 538.
20 E. Norvel, H. G. C. Human and L. R. P. Butler, Anal. Chem., 51 (1979) 2045.
21 P. Bailey, E. Norval, T. A. Kilroe-Smith, M. I. Skikne and H. B. Röllin, Microchem. J., 24 (1979) 107.
22 W. Slavin and D. C. Manning, Anal. Chem., 51 (1979) 261.
23 B. Welz, E. Wiedenking and W. Sigl, Appl. At. Absorpt. Spectrosc., 7E (1977) 3.
24 D. C. Manning and W. Slavin, Anal. Chem., 50 (1978) 1234.

Analytica Chimica Acta, 119 (1980) 75—89

INVESTIGATIONS OF REACTIONS INVOLVED IN ELECTRO-THERMAL ATOMIC ABSORPTION PROCEDURES
Part 8. A Theoretical and Experimental Study of Factors Influencing the Determination of Phosphorus

JAN-ÅKE PERSSON* and WOLFGANG FRECH

Department of Analytical Chemistry, University of Umeå, S-901 87 Umeå (Sweden)

(Received 11th April 1980)

SUMMARY

Ideal conditions for the determination of phosphorus by graphite-furnace atomic absorption spectrometry are investigated by the use of high-temperature equilibrium calculations. All reasonable reaction products resulting from the reaction between P, C, O, H, N, Ca and Ar are considered. The calculations show that phosphorus forms the volatile monoxide and dioxide molecules below 1800 K ($P_{O_2} \geqslant 10^{-13}$ atm.). At higher temperatures the relative amount of atomic phosphorus is mainly controlled by the equilibrium between monatomic and diatomic phosphorus. The significance of the theoretical study was investigated experimentally. The relative amounts of P_2 and PO were monitored by molecular absorption using vaporization under isothermal conditions; the interfering effects of Ca, N_2, H_2 and O_2 on the atomic absorption signal for phosphorus were also studied. The sensitivity was greatly dependent on graphite tube conditions as well as the heating rate of the furnace. For $CaHPO_4$ the sensitivity for phosphorus was 4.5×10^{-8} g. If samples were introduced into a preheated tube, this value was improved to 2×10^{-9} g.

Several problems are involved in the determination of phosphorus by atomic absorption spectrometry (a.a.s.). Like other non-metals, phosphorus has its resonance lines in the vacuum u.v. and in this region special difficulties arise as the strong absorption by the oxygen of the air requires an optical system which can be evacuated or purged with an inert gas. The use of a.a.s. with flames presents an additional problem as the flame gases strongly absorb the radiation from the light source [1]. With graphite furnaces as atomizers this absorption is eliminated and, compared to flames, reduced noise levels as well as higher sensitivities can be achieved [2]. In order to circumvent the difficulties arising from work in the vacuum u.v., use of the less sensitive non-resonance lines at 213.55/213.62 nm has been proposed [3—7]. At such lines the sensitivity becomes highly temperature-dependent.

Apart from the problems connected with the analytical lines, difficulties arise as phosphorus tends to form gaseous compounds even at high temperatures. The latter characteristic has been utilized for methods based on

the molecular emission of HPO and PO [8—13] as well as the molecular absorption of PO [14].

Very many interference effects have been observed in phosphorus determinations by graphite-furnace a.a.s. For example, Ediger et al. [3] have found that the absorbance obtained from 200 ng of phosphorus as phosphoric acid varied from 0.09 to 0.00 A s for solutions with and without lanthanum, respectively. For practical work the addition of lanthanum to all solutions was suggested. The sensitivity for phosphorus was also found to be critically dependent on graphite tube conditions [5, 7]. The investigations mentioned above were made at non-resonance lines and furnaces without close control of the heating properties were used. As a consequence, some of the interference effects obtained might have been caused by uncontrollable changes in heating rates or final temperatures. Good control of the atomization conditions was obtained by introducing the samples into a preheated furnace by means of a tungsten wire [15]. In this way diffusion losses of molecular phosphorus species were minimized and a sensitivity of 2×10^{-9} g was obtained.

In this work, optimum conditions for the formation of phosphorus atoms have been established by using high-temperature equilibrium calculations. The theoretical study was made alongside experimental work in order to obtain a continuous feed-back. The experimental study included determinations of the relative amounts of monoatomic and diatomic phosphorus as well as phosphorus monoxide. The latter two species were determined by graphite furnace molecular absorption under isothermal conditions.

EXPERIMENTAL

Instrumentation

For the determination of atomic phosphorus, a Perkin-Elmer spectrometer model 372 equipped with a HGA 74 furnace was used. The furnace was connected to a home-made power supply with facilities for close temperature control of the graphite tube as described earlier [16]. For the measurements of the molecular absorption of phosphorus monoxide and diatomic phosphorus a Varian-Techtron spectrometer model AA6 fitted with a carbon cup atomizer model 63 was used. Facilities for close temperature control of the graphite cup were installed as described earlier [17]. The instrumental parameters for the determinations are summarized in Table 1.

Reagents and materials

Orthophosphoric acid (p.a., Riedel-de Haen) and calcium orthophosphate (p.a., Mallinckrodt) were used for the preparation of phosphoric acid standards. High-purity gases were SR-grade (AGA Gas AB, Sweden).

Preparation of gas mixtures. Nitrogen and hydrogen were added to the internal flow of argon leading into the graphite tube (HGA 74). Flow rates were measured by use of a closed-vent system (Leybold-Heraeus, Cat. No.

TABLE 1

Instrumental parameters

	Phosphorus (HGA 74)			Phosphorus monoxide (CRA 63)		Diatomic phosphorus (CRA 63)	
	Time (s)	Temp. (K)	Heating rate ($K\ s^{-1}$)	Time (s)	Temp. (K)	Time (s)	Temp. (K)
Drying	40	370	4	—	—	—	—
Ashing	40	1450[a]	45	—	—	—	—
Atomization	5	2770[a]	1800	7	1200—2600	7	1300—2800
Cleaning	3	Max.	—	—	—	—	—
Wavelength (nm)		213.55/213.62			246.449		216.45/216.58
Spectral band width (nm)		0.7			0.5		0.5
Lamp source		EDL[b]			HCL[c]		HCL[d]
Background correction		Used			Not used		Not used
Argon flow							
Internal ($l\ min^{-1}$)		0.16			—		—
External ($l\ min^{-1}$)		1.5			1.4 or 5.1		5.1[a]
Signal evaluation[e]							
Integration time (s)		4.9			6.9		6.9
Integration delay (s)		0.1			0.5		0.5

[a]Varied in some experiments. [b]Electrodeless discharge lamp (Perkin-Elmer) operated at 8 W. [c]Yb hollow-cathode lamp (Varian-Techtron) operated at 7 mA. [d]Fe hollow-cathode lamp (Pye-Unicam) operated at 14 mA. [e]Peak areas as well as peak heights were recorded for all determinations.

17317). The gas flows were calibrated by use of a soap-bubble meter or a rotameter. The accuracy of the concentration of the prepared gas mixture was expected to be within 10% by this procedure.

High temperature equilibrium calculations

The calculations were performed as described in Part 1 [18]. The elements as well as the compounds considered are given in Table 2. In order to obtain a survey of the extent of interfering effects caused by C, H, O, N and Ca, the amounts of these elements as well as the equilibrium temperature were varied over a wide range. In this way a general idea of the critical parameters controlling the formation of P(g) was obtained. In some calculations a low input amount of carbon was chosen in order to be able to simulate its incomplete reaction with oxygen.

Determination under isothermal conditions

Graphite of quality RWO (Ringsdorff Werk GmbH) was cut into pieces of 3 ± 0.3 mg and cleaned by heating in a graphite tube at its maximum temperature for 10 s. The appropriate standard solution (1 μl) was pipetted onto these pieces and then carefully dried under an electric bulb. The graphite pieces were dropped into the furnace or cup after the preset temperature was reached. Using the HGA 74 introduction was facilitated by placing a graphite tube (3.0 mm i.d.) onto the sample part after enlarging the injection hole to 3.0 mm i.d. The lowest part of the light beam was masked in order to prevent its obstruction by the graphite pieces. No precautions were necessary when the Varian-Techtron graphite cup was used.

Measurements of molecular absorption by P_2 and PO

The P_2 absorption was measured using the emission lines of an iron hollow-cathode lamp at 216.45 and 216.58 nm. Strong absorption bands for P_2 have been reported at 216.43 nm [19]. The amount of absorption not caused by P_2 was measured by using calcium nitrate instead of calcium hydrogenphosphate. Owing to the rapid development of the P_2 signals, a modified Varian AA6 [20] with a time constant of 47 ms was used.

The PO absorption was measured using the emission line of a ytterbium hollow-cathode lamp at 246.50 nm. This line coincides completely with a reported absorption band of PO [21]. The amount of absorption not caused by PO was measured by using calcium nitrate instead of phosphoric acid.

TABLE 2

Species considered in the equilibrium calculations

Gaseous
Ar, H_2, H, O_2, O, N_2, N, C, CO, CO_2, H_2O, CN, CH_2, HCO, NO, NH_3, P_4, P_2, P, PH, PH_3, PN, PO, PO_2, Ca, CaH, CP, (HCP)
Condensed
C, Ca, CaO, CaC_2, $Ca_2P_2O_7$, Ca_3P_2, $Ca_3P_2O_8$, $CaHPO_4$, CaO_2H_2

RESULTS AND DISCUSSION

General survey

The determination of phosphorus with commercial graphite furnaces yields a poor sensitivity [3]. One reason is that the resonance lines for phosphorus are in the vacuum u.v. and hence non-resonance lines have to be used. Another reason can be understood by studying the high-temperature equilibrium calculations shown in Fig. 1. The input amounts in these calculations were chosen to simulate the reactions involved during the vaporization of pure phosphoric acid in a graphite furnace. In earlier experiments [22] it was found that the reaction between carbon and oxygen was incomplete below 2300 K. These conditions were simulated in the calculations by decreasing the input amounts of carbon. As can be seen, the fraction of volatile phosphorus-containing molecules is large at, and below those temperatures at which atomic phosphorus is formed. This means that losses of phosphorus are likely to occur during the heating of the tube. In fact phosphorus in the form of phosphoric acid has not been successfully determined by graphite furnace a.a.s. (non-isothermal atomization). Useful analytical signals for phosphorus can be obtained only if the vaporization of phosphorus compounds proceeds at higher temperatures. This can be accomplished by vaporizing thermally stable phosphorus salts or by using isothermal conditions.

Phosphorus in the presence of calcium

The interference effects of phosphorus on the determination of calcium by a.a.s. with an air—acetylene flame are well documented [23]. The formation of thermally stable calcium—phosphorus compounds is assumed to cause decreased amounts of calcium atoms in the flame, and can be utilized for phosphorus determinations by graphite-furnace a.a.s. Figure 2 shows the

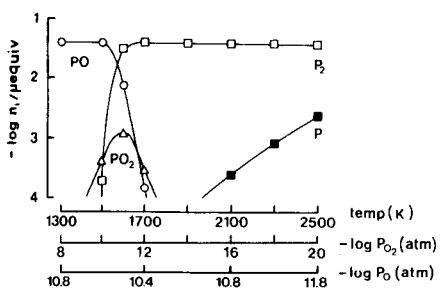

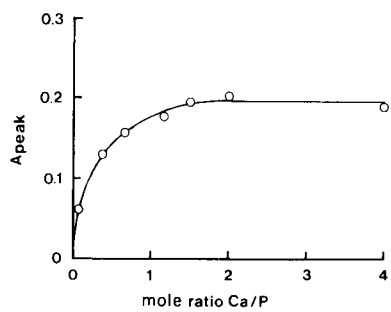

Fig. 1. The distribution of phosphorus compounds as a function of temperature and partial pressure of oxygen. The input amounts (μmol) used in the calculations were: Ar = 4, C = 0.2, H = 0.08, N = 0, Ca = 0 and P = 0.04. n_i = amount of compound.

Fig. 2. Peak height absorbances for 1 μg of phosphorus (H_3PO_4) in the presence of different amounts of calcium.

signals for phosphorus for increasing calcium/phosphorus ratios. As can be seen no significant increase in the signal is obtained for calcium/phosphorus ratios exceeding 1.5, indicating that a compound of the general form $Ca_{1.5}PX_y$ is formed.

During the course of these experiments, difficulties were experienced in obtaining reproducible results. It was found that the sensitivity for phosphorus was highly dependent on the type as well as the age of the graphite tubes used. In order to obtain a better understanding of these phenomena, high-temperature equilibrium calculations were used to simulate the vaporization of phosphorus in a graphite tube containing calcium. The calcium/phosphorus compounds assumed to be present in the condensed phase were $Ca_2P_2O_7$, $Ca_3(PO_4)_2$ and Ca_3P_2. According to the calculations, $Ca_3(PO_4)_2$ was the only phosphorus compound formed in the condensed phase. The maximum temperature at which this compound is stable was found to be increased by increasing the partial pressure of oxygen. The results of these calculations are summarized in Fig. 3(a). The total amount of phosphorus left in the condensed phase is given as a function of temperature for oxygen/carbon equilibrium ($P_{O_2} = 10^{-21}$ atm.) as well as for $P_{O_2} = 10^{-17}$ and 10^{-15} atm.

The relevance of these theoretical results was checked experimentally by obtaining thermal decomposition curves for a solution of $CaHPO_4$. In order to accomplish thermal decomposition of the phosphorus compound at different partial pressures of oxygen, two types of tubes were chosen, ordinary graphite and glassy carbon. The reactivity of the glassy carbon is known to be lower than that of ordinary graphite, and as a consequence higher partial pressures of oxygen are expected to be present in the glassy carbon tube. The thermal decomposition curves obtained for the two tubes are presented in Fig. 3(b). It can be seen that the calcium—phosphorus compound decomposes at 1700 K in glassy carbon and at 1600 K in the ordinary graphite tube. According to the calculations at equilibrium the

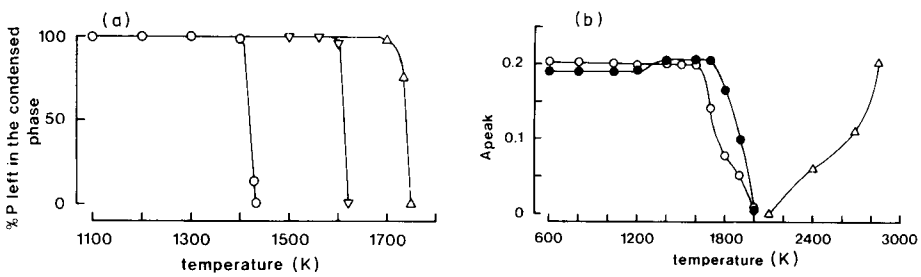

Fig. 3(a) Calculated amounts of phosphorus in the condensed phase as a function of temperature at P_{O_2} values of (○) 10^{-21} atm., (▽) 10^{-17} atm., (△) 10^{-15} atm. The input amounts (μmol) used in the calculations were: Ar = 4, C = 0.2, H = 0.002, N = 0, Ca = 0.04 and P = 0.02. (b) Thermal decomposition curves for 1 μg of phosphorus in (○) ordinary graphite and (●) glassy carbon tubes. Curve (△) gives the peak height absorbances as a function of the atomization temperature.

partial pressure of oxygen inside a graphite tube is 10^{-21} atm and at this low pressure $Ca_3(PO_4)_2$ decomposes at 1400 K. These theoretical results contradict the experimental findings which means that oxygen/carbon equilibrium is not obtained at these temperatures (provided the assumptions made for the calculations are correct). A comparison of the experimental results with the theoretical calculations suggests that the partial pressure of oxygen should be of the order of 10^{-16} atm.

In order to investigate the temperature dependence of the formation of excited phosphorus atoms in the presence of calcium the peak absorbances were measured at different atomization temperatures. The right-hand curve in Fig. 3(b) shows the peak absorbances obtained as a function of the atomization temperatures after ashing of the samples at 1600 K. It should be observed that temperature-controlled heating was used, which means that the tube was heated at almost the same rate to achieve different final temperatures. By comparison with the left-hand curves, it can be seen that losses of phosphorus occur above 1600 K whereas an absorption signal cannot be obtained at temperatures lower than 2100 K. From a thermodynamic point of view only minute amounts of P(g) should be formed at 1600—1700 K. This means that phosphorus vaporizes mainly in molecular forms at these temperatures. Theoretically the most stable species are $P_2(g)$, PO(g) and $PO_2(g)$.

Monatomic and diatomic phosphorus

In the general survey it was shown that in graphite furnace systems $P_2(g)$ should be the major phosphorus species at temperatures above 1600 K. The distribution of phosphorus between P(g) and $P_2(g)$ is controlled by the sum of their partial pressures as well as an equilibrium constant K_1. This can be better understood by considering the equation $P_P/P_{P_2}^{1/2} = K_1$. An increase of the sum of the partial pressures of phosphorus ($P_P + P_{P_2}$) at a given temperature will result in a decreased P_P:P_{P_2} ratio. On the other hand, the equilibrium constant K_1 increases with temperature giving rise to an increase in the relative amount of atomic phosphorus. The calculated distribution between monatomic and diatomic phosphorus is shown in Fig. 4. The temperatures at which the partial pressures of monatomic and diatomic phosphorus are equal are given as a function of their total pressures. For example, if 10 ng of phosphorus is assumed to occupy the inner volume of a HGA 74 graphite tube, the sum of the partial pressures of monatomic and diatomic phosphorus at 2500 K will be in the range 10^{-4}—10^{-5} atm. At this temperature for a total pressure of 10^{-4} atm. the partial pressure of atomic phosphorus equals that of diatomic phosphorus (see Fig. 4). This means that only 33% of the phosphorus will be present as free atoms. At lower total pressures, the relative amount of atomic phosphorus will be greater if the same temperature is used.

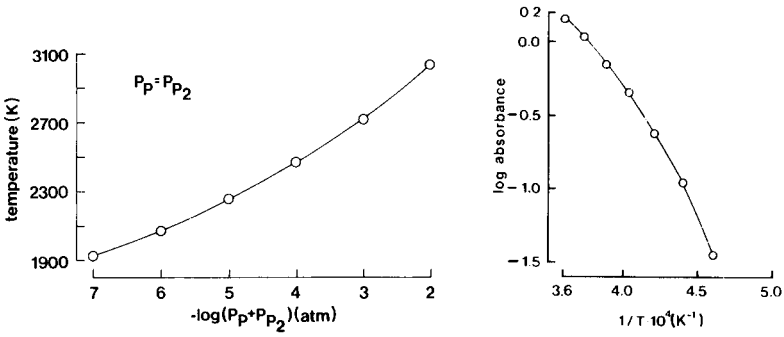

Fig. 4. Temperatures at which the partial pressures of monatomic and diatomic phosphorus are equal as a function of the total pressure of phosphorus.

Fig. 5. A plot of the logarithm of the peak area for 0.7 μg of phosphorus against the inverse of temperature in the atomization interval 2170—2770 K. Isothermal conditions were used. All values are corrected for the change of the diffusion coefficient with temperature.

Excited phosphorus atoms

The high-temperature dependence of the sensitivity for phosphorus (see Fig. 3b) can be explained by considering not only the change of K_1 with temperature but also the fact that a non-resonance line is used. For a non-resonance line the number of atoms (N^*) populating the energy level of interest follows the Maxwell—Boltzmann distribution: $N^*/N^0 = A \cdot \exp - (E^* - E^0)/kT$, where N^0 is the number of atoms in the ground state, A is a statistical constant for the particular electron transition, k is the Boltzmann constant and T is the temperature. The ΔE value for the transition of the phosphorus atoms from the ground state (E^0), to the excited state (E^*) was calculated to be 2.26×10^{-12} erg. Data for the transitions from the ground configuration $3p^3\,{}^4S^0_{3/2}$ to the excited levels $3p^3\,{}^2D^0_{3/2,5/2}$ were taken from Gmelin [24]. The absorption at the doublet 213.547/213.618 nm arises from the latter energy levels. A plot of log N^* against $1/T$ should yield a straight line with a slope corresponding to ΔE provided that the number of free atoms is constant over the temperature interval studied. As was discussed above, this condition is not fulfilled for phosphorus. Theoretically the slope of such a plot should reflect ΔE as well as the increased fraction of free phosphorus atoms formed at higher temperatures. In order to find out whether equilibrium with regard to the reactions $1/2P_2 \rightleftharpoons P$ as well as $P^* \rightleftharpoons P^0$ is obtained or not (other equilibria were not considered), the theoretical slope of log P^* against $1/T$ was calculated considering ΔE as well as the increased number of phosphorus atoms with temperature. This theoretical slope was compared with the experimentally obtained values. A typical plot of the log of the peak area against $1/T$ is given in Fig. 5. The samples were vaporized at a constant temperature. The integrated absorbance values

were corrected for their temperature dependence caused by the change in the diffusion coefficient (D) with temperature. This change is given by $D = D_0(T/T_0)^n$, where D_0 is the diffusion coefficient at temperature T_0. The value of n was assumed to be 1.6, according to measurements made by L'vov [25].

The best fit of the data represented in Fig. 5 was obtained by a first-order equation; equations up to third-order were evaluated. The slight bending of the curve might be due to increased temperature variations along the graphite tube at the higher temperatures. In order to minimize such variations, samples were atomized by using mini-flow conditions, i.e. the tube was flushed with a small inner flow of argon during atomization. In this way, the atomic vapour was confined to the central volume of the tube. Another reason for using the mini-flow was to eliminate possible condensation and re-evaporation of phosphorus atoms. In order to test whether the mini-flow changed the slopes or not, the experiments were repeated for lead at its 280.2-nm non-resonance line. Lead was chosen because the likelihood of its condensation and re-evaporation is very small and it is an element for which the number of ground-state atoms can be assumed to be relatively unchanged with temperature. This means that the slope obtained should reflect only ΔE. The results of these experiments are given in Table 3; it can be seen that the slopes obtained are not significantly changed by using different flow conditions and the agreement with the theoretical value is excellent. For phosphorus, however, the experimentally obtained value is lower by 18%. The reason for this may be that the formation of HCP(g) was not considered. This compound was not included in the calculations because the $\Delta_f H^0_{298}$ value for its formation is very uncertain ($\Delta_f H^0_{298}$ = 40 ± 15 kcal mol^{-1}). If HCP(g) is included in the calculations a slope of -1.46×10^4 is obtained ($P_{H_2} = 10^{-4}$ atm., $P_{O_2} = 10^{-20}$ atm.). The value of the calculated slope will also depend on the accuracy of the estimation of the partial pressure of phosphorus (see Fig. 4). In the calculations represented in Table 3 the partial pressure of phosphorus was estimated to be 5×10^{-3} atm. A decrease of this value to 5×10^{-4} atm. will result in a

TABLE 3

Evaluations of ΔE values (excitation energies) for lead and phosphorus
(The formation of diatomic species is considered in some of the theoretical calculations.)

Element	λ(nm)	Experimental slopes[a]		Theoretical slopes	
		Gas stop	Mini-flow (65 ml min^{-1})	Dimers considered	Dimers neglected
Pb	280.2	-0.62×10^4	-0.65×10^4	-0.66×10^4	-0.66×10^4
P	213.55/213.62	—	-1.60×10^4	-1.96×10^4 (-1.46×10^4)[b]	-0.71×10^4

[a]Isothermal conditions used. [b]HCP(g) also considered.

slope of -1.88×10^4 instead of -1.96×10^4. In conclusion, the experimental results indicate that the formation of excited phosphorus atoms is controlled mainly by the equilibria between P and P_2 as well as the excitation energy corresponding to the non-resonance line used.

Diatomic phosphorus

According to the calculations, $P_2(g)$ is the major phosphorus compound in the temperature range 1500—2500 K. In order to check the relevance of theoretical work it was found to be essential to measure the relative change of formation of diatomic phosphorus with temperature, so that comparisons with the values obtained using the high-temperature equilibrium calculations could be made.

Graphite furnaces have been successfully employed for the measurement of molecular species [26, 27]. Several absorption bands for $P_2(g)$ have been reported [19]. Since the bands listed were found to be rather narrow, the measurements were made at an emission line of an iron hollow-cathode lamp very close to an absorption band of diatomic phosphorus. In this way relatively good sensitivity was obtained without employing a monochromator with high resolution. In order to facilitate the comparison with the calculations, samples were vaporized under isothermal conditions. The integrated absorbances were corrected for the variation of diffusion with temperature. Figure 6 shows the results obtained for diatomic phosphorus in the temperature interval 1300—2500 K for phosphoric acid as well as $CaHPO_4$.

The integrated absorption not caused by diatomic phosphorus was found to be less than 0.03 A s. It can be seen that the experimental results obtained for phosphoric acid are in good agreement with the theoretical calculations shown in Fig. 1. For $CaHPO_4$, the lowest temperature at which a signal

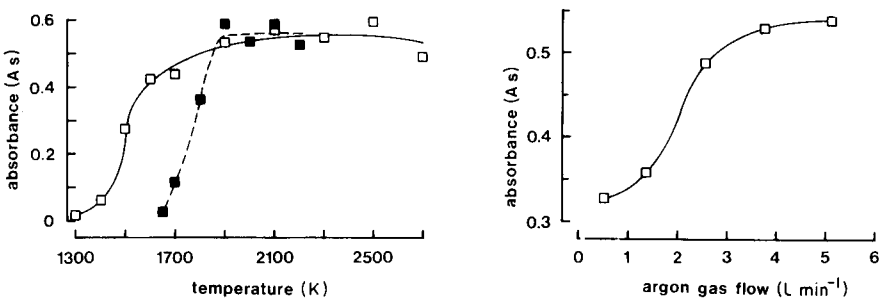

Fig. 6. Peak area absorbance of diatomic phosphorus as a function of temperature. Isothermal conditions were used; all values are corrected for the change of the diffusion coefficient with temperature; (□) 10 μg of phosphorus as H_3PO_4 or (■) $CaHPO_4$.

Fig. 7. Peak area absorbance of diatomic phosphorus at 1700 K as a function of the inert gas flow rate. Isothermal conditions were used; 10 μg of phosphorus as H_3PO_4 was vaporized.

for $P_2(g)$ can be detected is 1600 K. This is the temperature at which losses of phosphorus are observed if an ordinary graphite tube is used (see Fig. 3b). The agreement between theoretical and experimental results indicates that equilibrium between P(g) and $P_2(g)$ is obtained and that the predictions made in the calculations are correct.

According to the calculations the amount of $P_2(g)$ formed should be strongly dependent on the partial pressure of oxygen for pressures higher than 10^{-11} atm. Owing to the open nature of the Varian furnace, the partial pressure of oxygen is likely to be increased at the lower flow rates of the inert gas. Further control of the calculations was made by measuring the P_2 signal as a function of the inert gas flow rate. The results are given in Fig. 7. The shape of this curve can be explained by considering Fig. 8 (see below).

Phosphorus oxides

In addition to $P_2(g)$, phosphorus forms oxides even at relatively low partial pressures of oxygen. As a consequence the amount of free phosphorus atoms formed in graphite furnaces might be affected by changes of the partial pressure of oxygen inside the atomizer. Figure 8 gives the theoretical conditions for the formation of PO(g) as well as $PO_2(g)$ as a function of the partial pressure of oxygen at two temperatures. For all partial pressures of oxygen, the total amount of oxides formed decreases as the temperature is raised. At higher temperatures the formation of phosphorus monoxide becomes more significant.

The equilibrium calculations were followed up by measuring the molecular absorption of phosphorus monoxide. These experiments were made in the same way as those described for $P_2(g)$, by using an ytterbium hollow-cathode lamp. The results of the measurements are shown in Fig. 9 for two different inert gas flows. The integrated absorption not caused by phosphorus monoxide was found to be less than 0.02 A s. Only at temperatures above 2000 K did the use of a low inert flow rate significantly increase the PO

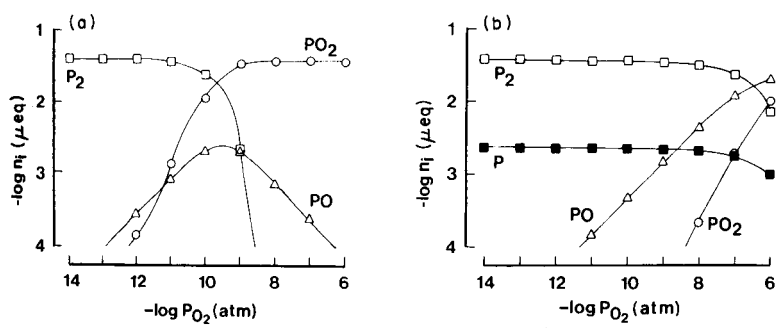

Fig. 8. The distribution of phosphorus compounds as a function of the partial pressure of oxygen at (a) 1700 K and (b) 2500 K. The input amounts (μmol) used in the calculations were: Ar = 4, C = 0.2, H = 0.08, N = 0, Ca = 0, and P = 0.04.

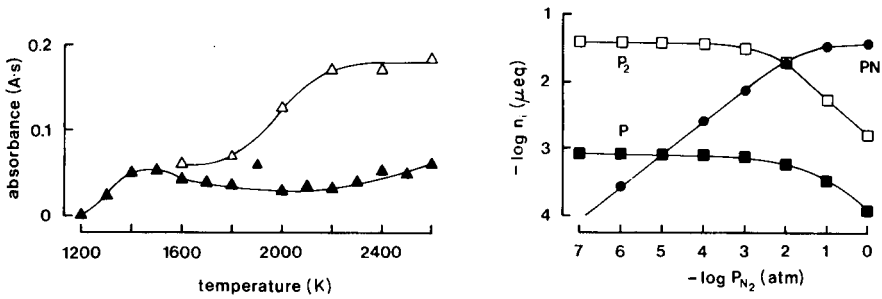

Fig. 9. Peak area absorbance for phosphorus monoxide as a function of temperature. Inert gas flow rates: (△) 1.4 l min^{-1}, (▲) 5.1 l min^{-1}; 10 μg of phosphoric acid was vaporized under isothermal conditions. All values are corrected for the change of the diffusion coefficient with temperature.

Fig. 10. The distribution of phosphorus compounds at 2300 K as a function of the partial pressure of nitrogen. The input amounts (μmol) used in the calculations were: Ar = 4, C = 0.2, H = 0.08, C = 0.2, Ca = 0.08, and P = 0.04. The partial pressure of oxygen was held constant at 10^{-18} atm.

signals. This result can be explained by considering Fig. 8. Larger amounts of PO(g) are formed with increased partial pressures of oxygen at 2500 K. On the other hand, at 1700 K an increase in the partial pressure of oxygen can even lead to decreased amounts of PO(g) if the partial pressure of oxygen is kept higher than 10^{-10} atm. At this temperature the experimentally obtained absorbance values for PO(g) were not significantly influenced by changing the inert gas flow rate. According to the calculations, this means that the partial pressure of oxygen at 1700 K should be around 10^{-9} atm. for the lower flow rate of argon.

The role of the graphite in reducing the atmosphere was tested by measuring the PO absorbance in a CRA 90 graphite cup, the inner surface of which was covered with tantalum foil. The signals obtained were insignificant below 2300 K. At higher temperatures, a signal was obtained only for the highest flow rates of argon. According to the calculations, these results indicate that the partial pressure of oxygen is of the order of 10^{-6} atm., which means that the use of tantalum foil favours the formation of PO_2(g).

The precision of the PO(g) measurements was found to be 15—20%. This poor precision might be caused by small variations in the amounts of oxygen present since a controlled atmosphere in the CRA 90 is not likely to be obtained because of its open nature.

The system phosphorus, carbon and nitrogen

The sensitivity for phosphorus has been reported to be decreased by 23—50% if nitrogen is used instead of argon as a purge gas [3, 7, 28]. This rather large effect of nitrogen cannot be explained by the difference in the

diffusion coefficients of the two gases. The lower signals in the presence of nitrogen are most probably due to the formation of phosphorus nitride. Figure 10 shows a theoretical calculation of the phosphorus system in the presence of various amounts of nitrogen; the formation of phosphorus nitride is indeed significant. In order to investigate experimentally the influence of nitrogen on the phosphorus signal, phosphoric acid was vaporized in the presence of different amounts of nitrogen under isothermal conditions. The results of these experiments are given in Table 4. It can be seen that the interference effect at 2400 K is only −20% for 18% of nitrogen added. Theoretically, the amounts of free phosphorus atoms should be decreased by 85% for these conditions. The reason for the small depressive effect of nitrogen has been discussed by L'vov and Pelieva [28], who assumed that equilibrium between N_2 and P is not reached because of the high stability of the N_2 molecules.

The system phosphorus, carbon and hydrogen

As has been discussed above, reliable thermodynamic data for the formation of methinophosphide (HCP(g)) are not available. In order to test if this compound is formed or not, the effect of hydrogen on the phosphorus signal was investigated by using an ordinary graphite tube and a glassy carbon tube. In the latter tube, the reactivity of the carbon is known to be relatively low and consequently the formation of HCP(g) should be less. The results obtained are shown in Table 5. Hydrogen lowered the signals least in the glassy carbon tube. The same degree of interference effect as in an ordinary tube is obtained if carbon is added to the surface of the glassy carbon tube. This means that HCP(g) is likely to be formed. A theoretical calculation in which HCP(g) is included is given in Fig. 11. If HCP(g) is excluded from the calculations, variations in the input amounts of hydrogen do not significantly change the distribution of the phosphorus species.

Combined effects

The theoretical and experimental results given above have shown that the relative amount of phosphorus atoms formed is critically dependent on the

TABLE 4

Interference effects of nitrogen on the signal obtained for phosphorus at two different temperatures[a]

Nitrogen in argon[b] (vol %)	Peak area (A s) (2400 K)[c]	Peak area (A s) (2800 K)[d]
0	0.117	0.196
5.2	0.102	0.165
17.8	0.094	0.160

[a]Isothermal conditions. [b]Inner argon gas flow was 65 ml min^{-1}. [c]10 μg phosphorus. [d]1 μg phosphorus.

TABLE 5

Interference effects of hydrogen on the signal obtained for 1 μg of phosphorus with different graphite tubes

Gas used	Ordinary graphite	Glassy carbon	Glassy carbon with graphite powder
Argon	0.142	0.051	0.066
Argon with 70% H_2	0.070	0.049	0.038

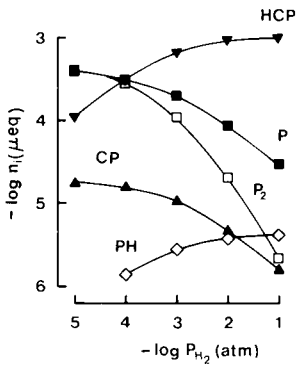

Fig. 11. The distribution of phosphorus compounds at 2600 K as a function of the partial pressure of hydrogen. The input amounts (μmol) used in the calculations were: Ar = 4, O = 0.004, N = 0, C = 0.1, Ca = 0 and P = 0.001.

partial pressures of oxygen, carbon, hydrogen and nitrogen. A change in the partial pressure of one of these elements will affect all the other elements and hence the phosphorus signal. The interdependent action of the interfering elements will be illustrated by an example.

The vaporization of phosphorus has to proceed under reducing conditions in order to minimize the formation of phosphorus oxides. Non-pyrolytically coated graphite tubes can provide sufficiently low partial pressures of oxygen but nevertheless they do not provide an ideal atmosphere because during the heating of such tubes, hydrogen will be developed from trace amounts of water remaining on the graphite [29], thus enabling the formation of HCP(g).

Isothermal atomization

The usefulness of atomizing phosphorus at a constant temperature was tested for H_3PO_4 and $CaHPO_4$. The sensitivity for both phosphorus compounds was found to be 2×10^{-9} g. The fact that the same sensitivity was obtained shows that interference effects are minimized. Using non-isothermal conditions no signal could be obtained for H_3PO_4; for $CaHPO_4$ the sensitivity was found to be 45×10^{-9} g.

Conclusions

Reproducible results can be obtained only if the heating rate and the final temperature of the furnace as well as the atmosphere inside the graphite tube can be controlled during the course of the determination. In practice, this control is very difficult to achieve and therefore the most suitable system for phosphorus determinations should permit the introduction of the sample into an atomizer preheated to a high temperature.

The experimental results given in this paper show that high-temperature equilibrium calculations can be successfully used in order to obtain a general idea of the complex reactions involved in the graphite-furnace a.a.s. determination of phosphorus.

The authors thank Prof. Anders Cedergren, Dr. Erik Lundberg and Dr. Gunnar Eriksson for valuable discussions.

REFERENCES

1 G. F. Kirkbright and M. Marshall, Anal. Chem., 45 (1973) 1610.
2 B. V. L'vov, Atomic Absorption Spectrochemical Analysis, A. Hilger, London, 1970, p. 255.
3 R. D. Ediger, A. R. Knott, G. E. Peterson and R. D. Beaty, At. Absorpt. Newsl., 17 (1978) 28.
4 P. J. Whiteside and W. J. Price, Analyst, 102 (1977) 618.
5 A. Prévot and M. Gente-Jauniaux, At. Absorpt. Newsl., 17 (1978) 1.
6 M. S. Vigler, A. Strecker and A. Varnes, Appl. Spectrosc., 32 (1978) 60.
7 D. J. Driscoll, D. A. Clay, C. H. Rogers, R. H. Jungers and F. E. Butler, Anal. Chem., 50 (1978) 767.
8 M. Lam Thanh and M. Peyron, J. Chem. Phys., 60 (1963) 1289.
9 R. M. Dagnall, K. C. Thompson and T. S. West, Analyst, 3 (1968) 72.
10 C. Veillon and J. Y. Park, Anal. Chim. Acta, 60 (1972) 293.
11 R. Belcher, S. L. Bogdanski, O. Osibanjo and A. Townshend, Anal. Chim. Acta, 84 (1976) 1.
12 K. M. Aldous, R. M. Dagnall and T. S. West, Analyst, 95 (1970) 417.
13 R. K. Skogerboe, A. S. Gravatt and G. H. Morrison, Anal. Chem., 39 (1967) 1602.
14 H. Haraguchi and K. Fuwa, Anal. Chem., 48 (1976) 784.
15 B. V. L'vov and L. A. Pelieva, Zh. Anal. Khim., 33 (1978) 1572.
16 E. Lundberg and W. Frech, Anal. Chim. Acta, 104 (1979) 67.
17 E. Lundberg and W. Frech, Anal. Chim. Acta, 104 (1979) 75.
18 W. Frech and A. Cedergren, Anal. Chim. Acta, 82 (1976) 83.
19 R. W. B. Pearse and A. G. Gaydon, The Identification of Molecular Spectra, 3rd Edn., Chapman and Hall, London, 1965.
20 E. Lundberg, Chem. Instrum., 8 (1978) 197.
21 H. Massmann, Z. El Gohary and S. Gucer, Spectrochim. Acta, Part B, 31 (1976) 399.
22 W. Frech and A. Cedergren, Anal. Chim. Acta, 113 (1980) 227.
23 G. F. Kirkbright and M. Sargent, Atomic Absorption and Fluorescence Spectroscopy, Academic Press, London, 1974, p. 516.
24 Gmelin, Handbuch der Anorganische Chemie, 16, Teil B, Verlag Chemie, Weinheim.
25 B. V. L'vov, Atomic Absorption Spectrochemical Analysis, Adam Hilger, London, 1970, p. 287.
26 K. Dittrich, Anal. Chim. Acta, 97 (1978) 59.
27 K. Tsunoda, K. Fujiwara and K. Fuwa, Anal. Chem., 50 (1978) 861.
28 B. V. L'vov and L. A. Pelieva, Zh. Anal. Khim., 33 (1978) 1695.
29 W. Frech and A. Cedergren. Anal. Chim. Acta, 82 (1976) 83.

Analytica Chimica Acta, 119 (1980) 91—97

KINETIC DETERMINATION OF ALCOHOLS AND THEIR BINARY MIXTURES WITH A STOPPED-FLOW SPECTROPHOTOMETRIC TECHNIQUE

EDOARDO MENTASTI* and CLAUDIO BAIOCCHI

Istituto di Chimica Analitica, Università di Torino, Via P. Giuria 5, 10125 Torino (Italy)

(Received 13th November 1979)

SUMMARY

The kinetic method described for the determination of a single alcohol ($\geq 5 \times 10^{-4}$ M), or of a binary mixture of alcohols in aqueous solution is based on fast oxidation by silver(II), monitored spectrophotometrically by using a stopped-flow technique. Mixtures of alcohols having rate constants differing by a factor of ≥ 3 can be resolved. The lower limit of determination is ca. 5×10^{-4} M.

Many spectrophotometric methods have been developed for the determination of alcohols. For example, alcohols react with 3,5-dinitrobenzoyl chloride in pyridine to form the corresponding benzoates, which, when extracted with cyclohexane and treated with sodium hydroxide in acetone, produce intensely coloured quinonoid ions [1]. Phenyl isocyanate reacts with alcohols to form phenylcarbamates that absorb intensely in the u.v. region [2]. The relative rates for these reactions have been measured for a series of alcohols, and kinetic methods can be applied to the analysis of binary alcohol mixtures [3]. A kinetic method for the resolution of binary mixtures of alcohols has also been described, based on the different rates of acetylation by acetic anhydride in pyridine [4].

The kinetics of oxidation of several alcohols by silver(II) perchlorate have been investigated [5]. These reactions are rapid and reproducible, and can be followed by monitoring the variation of silver(II) concentration in the visible region; their rates are strongly affected by the structure of the alcohol. These features have enabled a kinetic method to be developed for the determination of single alcohols and their binary mixtures.

Gas—liquid chromatography (g.l.c.) has also proven to be a powerful technique for the determination of alcohols and their mixtures [6, 7]. It has some reproducibility problems for routine analysis from gas flow variations and the physical condition of the solid and liquid phases [6]. Also although g.l.c. is one of the best techniques for higher aliphatic alcohols, low-molecular-weight alcohols, such as those examined here, are more difficult to differentiate [7]. Thus the present kinetic method should be very useful for low-molecular-weight alcohols.

Aquosilver(II) ions are powerful oxidants with a formal reduction potential of 2.0 V for the half-reaction $Ag^{2+} + e^- \rightleftharpoons Ag^+$ in 1 M perchloric acid [8]. Silver(II) undergoes hydrolysis: $Ag^{2+} + H_2O \rightleftharpoons AgOH^+ + H^+$ with a hydrolysis constant of 0.15 M at 8°C [9], and disproportionates to give silver(III) and silver (I) [10]. The former, as well as silver(II), oxidizes the solvent.

Aqueous solutions of silver(II) are stabilized in $\geqslant$1.0 M perchloric acid; formation of $AgOH^+$, which is more reactive toward the reductants and the solvent, is repressed. In solutions containing an excess of silver(I) ions, ([Ag(I)]/[Ag(II)] $\geqslant$ 100) both the reduction potential and the tendency to disproportionate are lowered. Solutions of silver perchlorate (0.1 M) can be partially oxidized by electrolysis at a platinum anode, and are stable for hours at 0°C.

Figure 1 shows the visible spectrum for a typical silver(II) solution. The great oxidizing power of silver(II) allows most organic compounds to be readily oxidized [11], even those which show sluggish behaviour with other analytical reagents. The reaction can be monitored by the decrease in absorbance at 470 nm. The molar absorptivity of silver(II) at this wavelength is 138 ± 2 l mol^{-1} cm^{-1} [11].

EXPERIMENTAL

Apparatus

A Durrum-Gibson stopped-flow spectrophotometer was used, with a teflon-quartz cell of 2.00-cm optical path. A Tektronix 564 storage oscilloscope was used to record the signals.

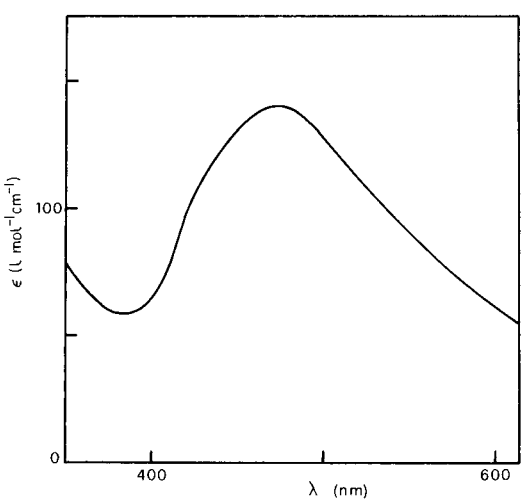

Fig. 1. Visible spectrum (molar absorptivity) of silver(II) perchlorate in 4.0 M perchloric acid.

Procedure

A silver(I) perchlorate solution (0.2 M in Ag^+ and 4.0 M in $HClO_4$), prepared by dissolving Ag_2O in perchloric acid was oxidized at a platinum gauze electrode (0°C, 200 mA); the cathode compartment was separated by a glass frit and contained 4.0 M perchloric acid. The oxidation was stopped (ca. 10 min) when the silver(II) concentration was 5×10^{-4}—10^{-3} M.

The solution for analysis was made 4.0 M in perchloric acid by adding the concentrated acid (70%, d = 1.67). The two solutions were thermostatted at 8.0°C in the stopped-flow apparatus, and then mixed. The change in transmittance at 470 nm was monitored on the oscilloscope screen as a function of time. The appropriate transmittance readings were converted to absorbance for plotting the various graphs below.

(a) Individual alcohol determination. A graph of $\ln A_t$ (A_t = absorbance at time t) as a function of time t was plotted. It gave a straight line, the slope of which gave the observed rate constant, k_{obs} [12]. The alcohol concentration was obtained from the ratio k_{obs}/k^{II} (see below).

(b) First-order integration method for binary mixtures. The k_{obs} value was obtained as in (a); the equations given below for C_A and C_B were used to evaluate the components. The total alcohol concentration was determined by reaction of a portion of the sample solution with an excess of silver(II) in the stopped-flow apparatus; the amount of silver(II) consumed was evaluated from the initial and final absorbance readings, silver(II) being the sole absorbing species at 470 nm; $C_{tot} = \frac{1}{2}C_{Ag(II)}$.

(c) Single-point method for binary mixtures. From the transmittance-time trace on the oscilloscope, $t(1/e)$ the time taken for the absorbance to decrease by $1/e$ from its initial value, was evaluated. This procedure was carried out with standard solutions of constant total alcohol concentration, to give a calibration curve (see below) from which unknown concentrations were evaluated.

RESULTS AND DISCUSSION

Determination of individual alcohols

In the aqueous acidic perchlorate medium, the alcohols are oxidized to the corresponding aldehydes (primary), ketones (secondary) and other products (tertiary alcohols) by silver(II), with a 1:2 stoichiometry [5]

$$\text{Alcohol} + \text{Ag(II)} \overset{k^{II}}{\rightleftarrows} \text{Radical} + \text{Ag(I)} + H^+$$

$$\text{Radical} + \text{Ag(II)} \xrightarrow{\text{fast}} \text{Products} + \text{Ag(I)}$$

The kinetics follow the simple equation

$$\text{Rate} = -\text{d[Ag(II)]}/dt = k^{II}[\text{alcohol}][\text{Ag(II)}]$$

With ten-fold excess of alcohol with respect to the oxidant

$$\text{Rate} = -\text{d[Ag(II)]}/dt = k_{obs}[\text{Ag(II)}] \qquad (1)$$

where $k_{obs} = k^{II}$(alcohol). The silver(II) species in the above equations involve both Ag^{2+} and $AgOH^{+}$, therefore k^{II} and k_{obs} are a composite function of acidity and vary with temperature and ionic strength. Thus, by performing kinetic measurements at constant acidity, temperature and ionic strength, the rate of disappearance of silver(II) is a linear function of the alcohol concentration [5].

Table 1 collects the overall second-order rate constants, k^{II}, measured at 8.0°C in 4.0 M perchloric acid and R, the relative rates (methanol = 1) for the alcohols investigated. The alcohol concentration can be evaluated from k_{obs}/k^{II}. Table 2 summarizes the results for the determination of some alcohols on this basis. The smallest amount of alcohol that can be determined, whilst retaining the pseudo first-order kinetics, is a 5-fold molar excess over silver(II), which is 5×10^{-4} M. This also applies to C_{tot} for the determination of mixtures.

Determination of binary mixtures

First order integration method [13]. For the oxidation of a binary mixture of alcohols A and B, the observed rate, k_{obs}[Ag(II)], has an observed rate constant

$$k_{obs} = k_A^{II} C_A + k_B^{II} C_B \quad (2)$$

where k_A^{II} and k_B^{II} are the overall second-order rate constants for reaction of alcohols A and B, and C_A and C_B are their concentrations. By evaluating k_{obs}, the single components can be determined from

$$C_A = (k_{obs} - k_B^{II} C_{tot})/(k_A^{II} - k_B^{II}) \quad (3)$$

and

$$C_B = (k_{obs} - k_A^{II} C_{tot})/(k_B^{II} - k_A^{II}) \quad (4)$$

where $C_{tot} = C_A + C_B$. Knowledge of C_{tot} is needed for determining the two components. This parameter can be obtained as described under Experimental.

The results obtained for mixtures of constant total concentration of n-butanol/t-butanol and cyclohexanol/cyclopentanol as examples and given

TABLE 1

Second-order rate constants k^{II}, and reactivity ratios R for the oxidation of alcohols by silver(II) at 8.0°C in 4.0 M perchloric acid

Alcohol	k^{II} (l mol^{-1} s^{-1})	R	Alcohol	k^{II} (l mol^{-1} s^{-1})	R
CH_3OH	54.5	1.0	iso-C_4H_9OH	855	15.7
CD_3OD	10.2	0.19	sec-C_4H_9OH	435	8.0
C_2H_5OH	219	4.0	t-C_4H_9OH	6.9	0.13
C_2D_5OD	54.7	1.0	2-$C_5H_{11}OH$	560	10.3
n-C_3H_7OH	285	5.2	Cyclohexanol	349	6.4
iso-C_3H_7OH	162	3.0	Cyclopentanol	6090	112
n-C_4H_9OH	425	7.8	$C_6H_5CH_2OH$	3420	62.8

TABLE 2

Kinetic determination of individual alcohols by oxidation with silver(II)

Alcohol	Conc. added ($\times 10^{-3}$ M)	k_{obs} (s^{-1})	Conc. found ($\times 10^{-3}$ M)	Error (%)	Alcohol	Conc. added ($\times 10^{-3}$ M)	k_{obs}	Conc. (s^{-1}) ($\times 10^{-3}$ M)	Error (%)
Methanol	0.50	0.029	0.53	+6.4	n-Propanol	1.00	0.29	1.02	+2.0
	1.00	0.059	1.08	+8.0		2.00	0.55	1.93	−3.5
	2.00	0.103	1.89	+5.5		3.00	0.77	2.70	−10.0
	3.00	0.155	2.84	−5.3		5.00	1.63	5.72	+14.4
	5.00	0.268	4.92	−1.6		8.00	2.26	7.93	−0.9
Ethanol	1.00	0.228	1.04	+4.0	Pentan-2-ol	0.50	0.30	0.54	+7.2
	2.00	0.465	2.12	+6.0		1.00	0.56	1.00	—
	3.00	0.665	3.04	+1.3		2.00	1.11	1.98	−1.0
	5.00	1.12	5.11	+2.2		3.00	1.67	2.98	−0.7
	8.00	1.71	7.81	−2.4		5.00	3.00	5.36	+7.2

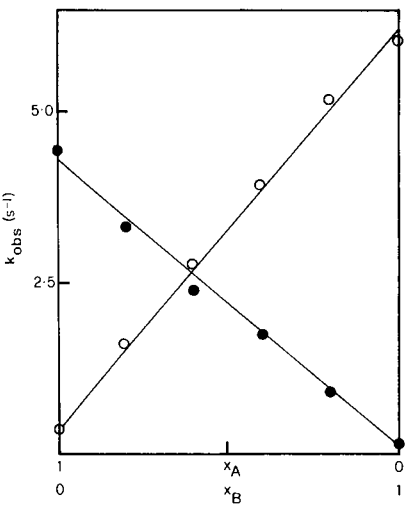

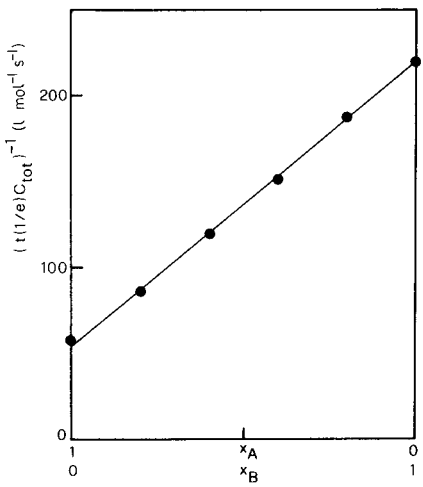

Fig. 2. Plots of k_{obs} as a function of mole fraction x for mixtures of alcohols. (•) A = n-butanol, B = t-butanol (C_{tot} = 10^{-2} M); (○) A = cyclohexanol, B = cyclopentanol (C_{tot} = 10^{-3} M).

Fig. 3. Single-point calibration graph for the determination of methanol (A)—ethanol (B) mixtures (C_{tot} = 1.0×10^{-2} M).

in Fig. 2. The straight lines show the theoretical behaviour; the experimental data lie close to the line, showing the absence of synergic effects.

Table 3 presents the kinetic and analytical data obtained for some typical mixtures. As can be seen, closely related structures like cyclohexanol/cyclopentanol can easily be resolved.

The analysis of mixtures of unknown total composition gives a further uncertainty, in addition to those arising from the kinetic data, which derives

TABLE 3

First-order integration method for determination of binary mixtures of alcohols by oxidation with silver(II)

	Added ($\times 10^{-3}$ M)	k_{obs} (s^{-1})	Found ($\times 10^{-3}$ M)	Error (%)	Found ($\times 10^{-3}$ M)	Error (%)
Methanol	*Ethanol*		*Methanol*		*Ethanol*	
10.0	0.0	0.58	9.8	−2.1	0.00	0.0
8.0	2.0	0.83	8.3	+2.8	1.7	−13.5
6.0	4.0	1.15	6.3	+5.3	3.7	−8.0
4.0	6.0	1.49	4.3	+6.5	5.7	−4.3
2.0	8.0	1.83	2.2	+9.5	7.8	−2.3
0.0	10.0	2.14	0.0	0.0	9.7	−3.0
n-Butanol	*t-Butanol*		*n-Butanol*		*t-Butanol*	
10.0	0.0	4.45	10.5	+4.8	0.00	0.0
8.0	2.0	3.85	7.6	−4.9	2.4	+19.5
6.0	4.0	2.39	5.6	−7.5	4.5	+11.3
4.0	6.0	1.77	4.1	+1.8	5.9	−1.2
2.0	8.0	0.94	2.1	+4.0	7.9	−1.0
0.0	10.0	0.09	0.0	0.0	9.95	−0.5
Cyclo-hexanol	*Cyclo-pentanol*		*Cyclo-hexanol*		*Cyclo-pentanol*	
1.00	0.00	0.35	1.00	0.0	0.0	0.0
0.80	0.20	1.65	0.77	−3.4	0.23	+13.5
0.60	0.40	2.80	0.57	−4.5	0.43	+6.8
0.40	0.60	3.90	0.38	−4.8	0.62	+3.2
0.20	0.80	5.15	0.16	−18.0	0.84	+4.5
0.00	1.00	5.90	0.00	0.0	0.97	−3.3

from the error in the evaluation of C_{tot}. This error is smaller (1—3%) than the kinetic errors (3—5%). The results reported in Table 3 were obtained from samples of known total composition; therefore the reported error is related only to the uncertainties in the kinetic data, which affect the individual values C_A and C_B of the components.

(b) Single-point method. The method described above enables the two components to be determined with the aid of k_A^{II}, k_B^{II} and C_{tot}. This procedure can be modified to a single data-point method, by using a calibration curve [13]. The rate equations (eqns. 1—4), after integration and substitution, yield

$$C_A/C_{tot} = \{\ln ([Ag(II)]_t/[Ag(II)]_0)/(k_B^{II} - k_A^{II})tC_{tot}\} + k_B^{II}/(k_B^{II} - k_A^{II}) \qquad (5)$$

where t is the time and the subscripts t and 0 refer to time t and time zero. This equation predicts that at constant $[Ag(II)]_t/[Ag(II)]_0$, a plot of $(tC_{tot})^{-1}$ vs. C_A/C_{tot} should be linear. For the least error in the evaluation of C_A and C_B, the fraction $[Ag(II)]_t/[Ag(II)]_0$ should be $(1/e)$ [13]. Therefore, for a series of calibration solutions, a single time is determined which is that

needed to decrease the silver(II) concentration by $1/e$. The linear plot obtained is used for calibration. Figure 3 shows such a calibration plot for methanol—ethanol mixtures.

This method is very convenient since the evaluation of a single time enables both components of the mixture to be determined, provided that the total alcohol concentration is known. Moreover, the calibration graph is obtained from mixtures of known composition, without the tedious determination of k_A^{II} and k_B^{II}.

For both methods, any binary mixture of components which have rate constants with a ratio of $\geqslant 3$ can be analyzed. A general treatment for the evaluation of errors has been described previously [14].

REFERENCES

1 D. P. Johnson and F. E. Critchfield, Anal. Chem., 32 (1960) 865.
2 J. C. Malm, Anal. Chem., 26 (1954) 188.
3 L. P. Hammett, Physical Organic Chemistry, McGraw-Hill, New York, 1940.
4 S. Siggia and J. G. Hanna, Anal. Chem., 33 (1961) 896.
5 C. Baiocchi and E. Mentasti, Int. J. Chem. Kinet., in press.
6 R. K. Kulkarni, E. C. Johnson and C. W. R. Wade, Anal. Chem., 46 (1974) 749.
7 J. B. Pias and L. Gasco, Anal. Chim. Acta, 75 (1975) 139.
8 A. McAuley, Coord. Chem. Rev., 5 (1970) 245; K. Kustin and D. L. Toppen, Inorg. 12 (1973) 1404.
9 E. Pelizzetti and E. Mentasti, J. Chem. Soc. Dalton Trans., (1975) 2086.
10 A. A. Noyes, D. Devault, C. D. Coryell and T. J. Deahl, J. Am. Chem. Soc., 59 (1937) 1326 and refs. therein; A. Viste, D. A. Holm, P. L. Wang and G. D. Veith, Inorg. Chem., 10 (1971) 631.
11 E. Mentasti, E. Pelizzetti and C. Baiocchi, J. Chem. Soc. Perkin Trans. 2, (1976) 1841; (1978) 77.
12 See, for example K. J. Laidler, Chemical Kinetics, McGraw-Hill, London 1965, Ch. 1; A. A. Frost and R. G. Pearson, Kinetics and Mechanism, J. Wiley, New York, 1961; Ch. 2 and 3.
13 H. B. Mark, Jr. and G. A. Rechnitz, Kinetics in Analytical Chemistry, Interscience, New York, 1968, pp. 121 and 218.
14 E. Mentasti, E. Pelizzetti and G. Saini, Anal. Chim. Acta, 86 (1976) 303.

Analytica Chimica Acta, 119 (1980) 99—111

EFFECT OF ACIDITY AND ALKALINITY ON THE DISTILLATION OF PHENOL: INTERFERENCES OF AROMATIC AMINES AND FORMALDEHYDE WITH THE 4-AMINOANTIPYRINE SPECTROPHOTOMETRIC METHOD FOR PHENOL

GEORGE NORWITZ and PETER N. KELIHER*

Chemistry Department, Villanova University, Villanova, PA 19085 (U.S.A.)

(Received 24th February 1980)

SUMMARY

As determined by the 4-aminoantipyrine (4-AAP) spectrophotometric method, the distillation of phenol is quantitative over the range from about pH 6 to very strongly acidic solutions. Recovery from alkaline solutions decreases with increasing alkalinity. Aromatic amines can interfere with the 4-AAP method by producing colors. The extent of the interference varies markedly with different aromatic amines and is much greater for the extraction method than the direct method. The interference can be considerably reduced by distillation from a strongly acidic solution (10 ml of concentrated sulfuric acid per 500 ml); for large amounts of aromatic amines, double distillation may be necessary. Formaldehyde can interfere by reacting with phenol and repressing the color development. This interference can be eliminated by treatment with ammonium sulfate and sodium hydroxide to form hexamethylenetetramine, followed by acidification and distillation.

It is customary in determining phenol in water and wastes to separate the phenol by distillation prior to its determination by the 4-aminoantipyrine (4-AAP) or other spectrophotometric method. In the most frequently used distillation technique, the pH of the solution is adjusted to about 4 (using methyl orange indicator) with phosphoric, sulfuric, or hydrochloric acid, prior to the distillation [1—5]. However, solutions of stronger acidity have also been used [6—8]. Since phenol distills slowly, it is customary to distil a volume of solution approximately equal to that originally present [1—5]. A double distillation has been used when the first distillate is turbid [1—3]. Apparently, no systematic study has been made of the effect of acidity and alkalinity on the distillation of phenol.

Aromatic amines interfere with the 4-AAP spectrophotometric method for phenol by producing interfering colors and this interference decreases with increasing alkalinity of the solution used in the color development [9—11]. The interference of aromatic amines with the determination of 2,4-dinitrophenol by the 4-AAP method has been overcome by prior extraction of the 2,4-dinitrophenol with petroleum ether from an acidic solution [1, 12]. This procedure is not applicable to the determination of

phenol because that substance is not completely extractable with petroleum ether [13, 14].

It is known that formaldehyde interferes with the determination of phenol but data on the extent of interference are sparse [15, 16]. A procedure has been proposed for the elimination of the interference whereby a 500-ml sample is treated with sodium hydroxide and hydroxylammonium chloride. The solution is boiled down to about 350 ml, acid is added, the solution is distilled, and the phenol determined by titration using potassium bromate—bromide solution [15].

It is the purpose of this paper to study the effect of acidity and alkalinity on the distillation of phenol and to investigate the interference of aromatic amines and formaldehyde with the 4-AAP method and ways to eliminate this interference.

EXPERIMENTAL

Apparatus and reagents

Distillation apparatus consisted of a 1-l round-bottom flask with a Graham condenser (with a jacket 40 cm in length and an outer 24/40 joint at top) joined together by a connecting tube (Fisher No. 15-323D) with the thermometer opening sealed off with a 10/30 ground glass stopper. The flask was heated by an electric mantle.

Distilled water and reagent chemicals were used.

Phenol solution No. 1 (1.00 mg ml^{-1}) was prepared by dissolving 1.000 g of phenol in water and diluting to 1 l in a volumetric flask. Phenol solution No. 2 (0.10 mg ml^{-1}) and phenol solution No. 3 (0.005 mg ml^{-1}) were prepared fresh daily by appropriate successive dilutions of phenol solution no. 1.

The 4-AAP solution (2%) and potassium hexacyanoferrate(III) solution (8%) were both prepared fresh weekly. Standard aniline and *N*,*N*-dimethylaniline solutions (10.0 and 0.10 mg ml^{-1}) were prepared in ethanol. Formaldehyde solution (35—37%) was assayed by the sodium hydroxide—hydrogen peroxide method [17] and found to contain 37.2% formaldehyde (by weight).

Preparation of calibration curves

Direct method. Transfer 0.00, 1.00, 2.00, 3.00, and 4.00 ml of standard phenol solution no. 2 to 125-ml Erlenmeyer flasks (calibrated at 100 ml) and dilute to 100 ml. Add 2.0 ml of ammonium chloride solution (5%) and adjust to pH 10.0 ± 0.2 with (1 + 1) ammonia solution, using a pH meter. Add 2.0 ml of 4-AAP solution (2%) and 2.0 ml of potassium hexacyanoferrate(III) solution (8%) and mix. After 5 min measure the absorbance at 510 nm against distilled water (1-cm cell). Deduct the blank and plot absorbance against mg of phenol (per 100 ml).

Extraction method [1]. Transfer 0.00, 2.00, 5.00, 8.00, and 10.00 ml of phenol solution No. 3 to 600-ml beakers and dilute to about 500 ml with

water. Add 10 ml of ammonium chloride solution (5%) and adjust to pH 10.0 ± 0.2 with (1 + 1) ammonia solution. Add 3.0 ml of 4-AAP solution (2%) and 3.0 ml of potassium hexacyanoferrate(III) solution (8%), mix, and allow to stand for 5 min. Wash into 1-l separatory funnels, add exactly 25 ml of chloroform, and shake vigorously for 60 s. Allow to settle, swirl vigorously, and allow to settle again. Filter 21—23 ml of the chloroform layers through dry 9-cm no. 40 Whatman filter papers containing about 2 g of anhydrous sodium sulfate into dry flasks. Within 5 min, measure the absorbance at 460 nm against chloroform (1-cm cell). Deduct the blank and plot absorbance against mg of phenol (per 500 ml of solution).

Procedures

General procedure. For the direct method (applicable to samples containing more than 0.05 mg of phenol per 100 ml), proceed as follows. Transfer 500 ml of the sample to a 1-l round-bottom flask that has been calibrated at 550 ml. If it is suspected that oxidants are present, add 10 ml of sodium arsenite solution (10%) [4]. Add about 5 drops of 0.05% methyl orange indicator. Add sulfuric acid (1 + 9) until the color changes to a definite pink and then add about 5 drops in excess. If the indicator is destroyed, use pH paper (to a pH of 2.5—3). If it is suspected that sulfide is present, add 10 ml of copper(II) sulfate pentahydrate solution (10%) [1]. Dilute to about 550 ml and distil 500 ml to a 500-ml Erlenmeyer flask, calibrated at 500 ml. For samples containing 0.05—0.4 mg of phenol per 100 ml, transfer a sufficient amount of the distillate to attain the 100-ml mark in the calibrated 125-ml Erlenmeyer flask; for samples containing more than 0.4 mg of phenol per 100 ml, dilute an appropriate aliquot of the distillate to the 100-ml mark in the calibrated 125-ml Erlenmeyer flask. Proceed as described in the preparation of the calibration curve for the direct method.

For the extraction method (applicable to samples containing 0.000—0.05 mg of phenol per 100 ml), distil the sample as in the direct method. For samples containing 0.000—0.01 mg of phenol per 100 ml, transfer the entire 500 ml of distillate to a 600-ml beaker; for samples containing 0.01—0.05 mg of phenol per 100 ml, dilute an appropriate aliquot of the distillate to about 500 ml in the 600-ml beaker. Proceed as described in the preparation of the calibration curve for the extraction method.

The above method is not applicable to samples containing more than very small amounts of interfering aromatic amines; for example, the maximum amount of aniline (mg 100 ml^{-1}) that can be present, is about 2 for the direct method and about 0.1 for the extraction method. The maximum amount of formaldehyde (ml of 37% solution per 100 ml) that can be present is about 1.5 for the direct method and 1.0 for the extraction method. In analyzing samples containing formaldehyde, allow the solutions to stand for about 5 min after adjusting to pH 10.0 ± 0.2 with ammonia solution and if the pH has decreased add more ammonia solution.

Procedure for samples containing aromatic amines. Proceed as described in the general procedure, but instead of adding methyl orange indicator and neutralizing with sulfuric acid (1 + 9), add 10 ml of concentrated sulfuric acid. If a re-distillation is necessary, add 10 ml of concentrated sulfuric acid to the distillate and distil again.

The maximum amounts of aniline and *N,N*-dimethylaniline that can be handled in the direct and extraction methods (single and double distillation) are shown in Table 1. The following aromatic amines are insensitive to 4-AAP and therefore have interference limits at least several times greater than for aniline: chloroanilines, nitroanilines, anilines with a substituent group in the *para* position, and polycyclic amines. Anilines with alkyl groups in the *ortho* or *meta* position tend to have interference limits approximately equal to those for aniline. The effect of interfering aromatic amines is cumulative.

Procedure for samples containing formaldehyde. Proceed as described in the general procedure up to the addition of the sodium arsenite. Add 15 g of ammonium sulfate and 12 g of sodium hydroxide pellets and swirl to dissolve. Allow to stand 1.5 h. Add about 5 drops of methyl orange indicator (0.05%). Add concentrated sulfuric acid until the solution turns pink, then neutralize with dilute sodium hydroxide solution (10%) until just yellow. Add sulfuric acid (1 + 9) until the solution turns pink and then add about 5 drops in excess. Add the copper(II) sulfate and proceed as described in the general procedure.

This procedure is recommended for samples containing more formaldehyde than can be handled in the general procedure. Observe the same precautions about allowing to stand for 5 min after adjusting to pH 10.0 ± 0.2, as described in the general procedure.

RESULTS AND DISCUSSION

Effect of acidity and alkalinity on the distillation of phenol

The recovery of phenol on distillation under various conditions of acidity and alkalinity was studied by adding different amounts of acid or sodium hydroxide to solutions containing 1.5 mg of phenol, diluting to 550 ml, dis-

TABLE 1

Maximum permissible amounts of aniline and *N,N*-dimethylaniline (mg per 100 ml) that may be present without causing significant interference in the distillation procedures

Compound	Direct method		Extraction method	
	Single distillation	Double distillation	Single distillation	Double distillation
Aniline	200	600	3	30
N,N-Dimethylaniline	50	200	2	30

tilling, and analyzing for phenol by the direct 4-AAP method. The results (Table 2) show that complete recovery of phenol was obtained over the range of about pH 6 to very strongly acidic solutions. High acidity in itself did not affect the distillation but the different acids had their own peculiarities insofar as interference with the 4-AAP method was concerned. When larger amounts of sulfuric, hydrochloric, or perchloric acid were present, some acid distilled and necessitated the use of an increased amount of ammonia solution (1 + 1) in the neutralization. The resultant increase in volume had to be taken into consideration in calculating the phenol recovery. (The technique used in developing the color was to add the reagents to a 100-ml aliquot, as recommended by the American Public Health Association [1] and ASTM [2]). More than a few ml of nitric acid caused the color to fade. The recommended maximum permissible amounts of the acids (ml per 500 ml) are: phosphoric, 25; sulfuric, 20; hydrochloric, 5; perchloric, 15; nitric, 5. These figures represent the acidity at the start of the distillation; of course, the acidity increases as the distillation proceeds.

The recovery of phenol steadily decreased with increasing alkalinity from pH 7.5 to strongly alkaline (Table 2). However, a considerable amount of alkali had to be present to eliminate the distillation of phenol entirely (Table 2).

Although phenol can be distilled quantitatively over a wide range of acidity, it is generally recommended that a solution with a pH of about 2.5—3 be used. This pH is readily obtained by neutralizing with sulfuric acid (1 + 9) to the pink color of methyl orange indicator and then adding about 5 drops in excess.

Interference of aromatic amines with the 4-AAP method for phenol

The interference of aniline and *N,N*-dimethylaniline with the direct method without distillation and aniline with the extraction method without distillation was studied (Table 3). Both these amines interfere by producing colors with 4-AAP. The maximum amounts (mg per 100 ml) that could be present without causing significant interference were: aniline direct, 0.7; *N,N*-dimethylaniline direct, 0.3; aniline extraction, 0.04. In setting limits for interferences, the permissible error for phenol was arbitrarily taken as ±0.015 when 0.300 mg of phenol was present and ±0.0006 when 0.0060 mg of phenol was present.

No study was made of the interference of other aromatic amines with the non-distillation procedures for two reasons. Firstly, distillation would almost certainly have to be used in any case in a practical procedure. Secondly, the work of El-Dib et al. [18] who determined aromatic amines at pH 7.4—7.6 without distillation and the work of Emerson [9, 10] furnish a clear indication of the interference relative to aniline that might be expected. Their data on the molar absorptivity or sensitivity of the colors obtained for the reaction of aromatic amines and 4-AAP are summarized in Table 4. It is seen that the 4-AAP—amine colors are very insensitive insofar as chloroanilines, nitroanilines, *p*-substituted anilines, and polycyclic aromatic amines

TABLE 2

Effect of acidity and alkalinity on the recovery of phenol by distillation (1.5 mg of phenol present per 500 ml)

Present/500 ml		Phenol found (mg/100 ml)	Present/500 ml		Phenol found (mg/100 ml)	pH	Phenol found (mg/100 ml)	ml 20% NaOH/ 500 ml	Phenol found (mg/100 ml)
Acid	ml		Acid	ml					
H_3PO_4	5	0.295	$HClO_4$	5	0.295	4	0.295	1.25	0.065
	15	0.295		15	0.295	5	0.295	5	0.032
	25	0.295		25[c]	0.288	6	0.288	10	0.019
H_2SO_4	5	0.295	HNO_3	5	0.295	7.5	0.248	20	0.000
	15	0.301		10	0.275[d]	9	0.210		
	25[a]	0.295				11	0.157		
HCl	5	0.295							
	10[b]	0.288							

[a]0.25 ml of NH_4OH (1 + 1) required. [b]1.2 ml of NH_4OH (1 + 1) required. [c]2.5 ml of NH_4OH (1 + 1) required. [d]Absorbance read within 2 min; absorbance decreased about 50% in 15 min.

TABLE 3

Interference of aniline and *N,N*-dimethylaniline with the 4-AAP method for phenol without distillation

Present (mg/100 ml)			Phenol found (mg/100 ml) Direct method	Present (mg/100 ml)			Phenol found (mg/100 ml) Direct method	Present (mg/100 ml)		Phenol found (mg/100 ml) Extn. method
Phenol	Aniline	*N,N*-Dimethyl-aniline		Phenol	Aniline	*N,N*-Dimethyl-aniline		Phenol	Aniline	
0 300	0.5		0.301	—	1.0		0.019	0.0060	0.02	0.0058
0.300	1.0		0.327	—	10		0.084	0.0060	0.05	0.0068
0.300	10		0.380	—	20		0.164	0.0060	0.10	0.0076
0.300	20		0.481	—	30		0.288			
0.300		0.2	0.308	—	50		>0.9			
0.300		0.5	0.321	—		1.0	0.059			
0.300		1.0	0.340	—		2.0	0.177			
0.300		5.0	0.63	—		5.0	0.327			
				—		10	0.574			

are concerned. Anilines with a methyl group in the *o*- or *m*-position give colors of an intensity approximately equal to that obtained for aniline. *N,N*-Dimethylaniline gives a much more intense color than that obtained for aniline. It is not feasible to make corrections for the 4-AAP—amine colors, which tend to fade.

The effect of acidity during distillation on interference of aniline with the 4-AAP phenol method was investigated. The results (Table 5) were in many ways surprising. The interference was very marked when the distillation was conducted at pH 2.5—4, but decreased considerably as the acidity increased (the maximum amount of acid tested was 25 ml of concentrated phosphoric acid per 500 ml). The interference was less with sulfuric acid than phosphoric acid.

It is therefore obviously desirable to employ a strongly acidic solution for the distillation when aromatic amines are present. The use of 10 ml of concentrated sulfuric acid per 500 ml is recommended. It was felt that use of 20 ml of concentrated sulfuric acid or 25 ml of concentrated phosphoric acid would be rather drastic. Also, the use of this amount of acid is undesirable because it produces difficulties with the copper(II) sulfate procedure for the elimination of sulfide, by causing some copper sulfide to dissolve. The use of 10 ml of concentrated sulfuric acid has no effect in this regard. Sodium arsenite or copper(II) sulfate had no significant effect on the interference of aromatic amines.

The results obtained for phenol by the direct and extraction methods for aniline and *N,N*-dimethylaniline, using the distillation procedure with 10 ml of concentrated sulfuric acid (single and double distillation), are shown in Table 6. From these data, the maximum permissible amounts of aniline and *N,N*-dimethylaniline that could be present without causing significant interference was established (Table 1). As would be expected, the interference is far greater for the extraction method than the direct method. *N,N*-Dimethylaniline interferes more than aniline but the difference is less for the extraction method than the direct method. Double distillation increases the permissible limit for aniline by a factor of 3 for the direct method and a factor of 10 for the extraction method; it increases the permissible limit for *N,N*-dimethylaniline by a factor of 4 for the direct method and a factor of 15 for the extraction method.

It was not feasible to establish the exact permissible limits for all the common aromatic amines. However, it would be expected that the limits would have roughly the same ratio to the limits for aniline as discussed earlier in the non-distillation procedure. Results for phenol in the presence of some of these aromatic amines (Table 6) bear this out. The effect of interfering aromatic amines is cumulative.

The marked decrease in interference from aromatic amines when the distillation is conducted from a strongly acidic solution is due to the tendency of aromatic amines to react with acids to form salts, e.g. dianilinium sulfate $(C_6H_5NH_3)_2SO_4$ [19]. Apparently, the amine is more tightly bound to the inorganic ion when a large excess of acid (particularly sulfuric acid) is present. It is not known whether the amine that distils from an acidic

TABLE 4

Molar absorptivity (ϵ) of aromatic amine—4-AAP colors by the direct method (determined at pH 6.5—7.5) [9, 10, 18]

Amine	ϵ[a]	Amine	ϵ[a]	Amine	ϵ[a]
Aniline	18.8	2,5-Dimethylaniline	22.9	2-Phenylenediamine	8.4
2-Chloroaniline	0.6	2,6-Dimethylaniline	13.0	4-Phenylenediamine	10.1
3-Chloroaniline	2.5	2-Methyl-5-chloroaniline	11.5	1-Naphthylamine	8.0
4-Chloroaniline	—[b]	6-Methyl-2-chloroaniline	1.0	2-Naphthylamine	1.9
2,4-Dichloroaniline	—[b]	4-Methyl-2-chloroaniline	—[b]	*N,N*-Dimethyl-1-naphthylamine	9.8
3,4-Dichloroaniline	—[b]	*N,N*-Dimethylaniline	33.0	Diphenylamine	2.3
2-Methylaniline	20.3	2-Aminobenzoic acid	20.5	Nitroanilines	—[b]
3-Methylaniline	25.0	3-Aminobenzoic acid	7.0	Benzidine	—[b]
4-Methylaniline	0.9	4-Aminobenzoic acid	0.4	Sulfanilic acid	—[b]
2,4-Dimethylaniline	1.3			Polycyclic amines	—[b]

[a]($\times 10^3$ l mol^{-1} cm^{-1}). [b]Insensitive reaction.

TABLE 5

Effect of acidity of distillation on the interference of aniline with the 4-AAP method for phenol (0.300 mg of phenol present per 100 ml)

Aniline present (mg/100 ml)	Phenol found (mg/100 ml)							
	pH 4	pH 2.5	H_3PO_4			H_2SO_4		
			5 ml[a]	10 ml	25 ml	5 ml	10 ml	20 ml
2	0.308	0.301						
10	0.481		~0.7			0.295		
40			>0.9	0.295		0.366		
100				0.472	0.321	0.463	0.295	
200							0.308	
400							0.366	0.321
100 (no phenol)							0.000	

[a]All acids are concentrated acid per 500 ml.

solution volatilizes as the salt or as the amine formed in a hydrolysis reaction. Diphenylamine is unusual in that it is practically a neutral substance that does not form a stable salt. When a solution containing diphenylamine is distilled, that compound distils and precipitates in the distillate. When the precipitate is filtered off, there is no interference (Table 6). All the aromatic amines tested dissolved in the hot solution containing the 10 ml of concentrated sulfuric acid.

The procedure for phenol in the presence of aromatic amines should be useful in determining phenol in effluents from the many industries that use various aromatic amines. Also, it should be useful in process control when phenol and aromatic amines are used together. Insofar as the analysis of usual river water is concerned, the general procedure would probably be applicable in most cases. Meijers and Van der Leer [14] in a study of the

TABLE 6

Results for phenol by the 4-AAP method in the presence of aromatic amines after distillation from solutions containing 10 ml of concentrated sulfuric acid per 500 ml

Present (mg/100 ml)				Phenol found (mg/100 ml) Direct method		Present (mg/100 ml)				Phenol found (mg/100 ml Extraction method	
Phenol	Aniline	*N,N*-Dimethyl-aniline	Other amines	Single distillation	Double distillation	Phenol	Aniline	*N,N*-Dimethyl-aniline	Other amines	Single distillation	Double distillation
0.300	100			0.295		0.0060	2.0			0.0062	
0.300	200			0.308		0.0060	4.0			0.0073	
0.300	400			0.366	0.295	0.0060	10			0.0082	0.0060
0.300	600				0.301	0.0060	20			0.0090	0.0062
0.300	800				0.481	0.0060	30			0.0099	0.0066
0.300		25		0.301		0.0060	50			0.0110	0.0073
0.300		50		0.308		0.0060		2.0		0.0066	
0.300		100		0.407	0.295	0.0060		4.0		0.0097	0.0058
0.300		200			0.301	0.0060		10		0.0110	0.0062
0.300		600			0.427	0.0060		20			0.0062
0.300			200[a]	0.308		0.0060		30		>0.02	0.0066
0.300			1000[b]	0.301		0.0060			3.0[a]	0.0058	
0.300			400[c]	0.301		0.0060			50[b]	0.0058	
0.300			300[d]	0.295		0.0060			10[c]	0.0060	
						0.0060			50[d]	0.0058	

[a]2-Methylaniline. [b]4-Chloroaniline. [c]3-Aminobenzoic acid. [d]Diphenylamine: a portion of the distillate was filtered to remove precipitated diphenylamine.

organic constituents in the Rhine river over a period of a year (principally by gas chromatography after preliminary separation) found that several chloro- and alkyl-anilines were present but the total was less than 0.1 mg l^{-1}. They found that aniline was present but in an amount that was barely detectable. Aniline in river water would be expected to be quite unstable, owing to oxidation and substitution reactions. A solution in river water containing 1 mg l^{-1} deteriorated to such an extent that aniline could not be detected after 3 days [20].

Some experiments were conducted on the elimination of the interference of aniline by treating 500 ml of sample with 20 ml of sodium hydroxide solution (20%), boiling to about 300 ml to drive off the aniline, cooling, neutralizing with concentrated sulfuric acid, adding 10 ml of concentrated sulfuric acid in excess, and distilling. The amount of amine that could be handled by this method was not much more than could be handled by distillation with 10 ml of concentrated sulfuric acid alone. Apparently, distillation from a strongly alkaline solution is not optimum for aniline. Another disadvantage of this alkaline distillation procedure is that Cu^{2+} must be absent, since the copper(II) hydroxide that would precipitate in the alkaline solution would oxidize phenol [1, 2].

Interference of formaldehyde with the 4-AAP method for phenol

The interference of formaldehyde with the 4-AAP method for phenol was studied by adding standard phenol and 37% formaldehyde solutions to water and proceeding as in the various methods. The results (Table 7) show that formaldehyde can cause low results. The maximum amounts of formaldehyde (ml of 37% solution per 100 ml) that could be present in the direct method without causing significant interference were as follows: without distillation, 1.5; distillation at pH 3, 1.5; distillation in the presence of 10 ml of concentrated sulfuric acid per 500 ml, <0.2. For the extraction method, the amounts were as follows: without distillation, 0.7; with distillation at pH 3, 1.0. Sodium arsenite or copper(II) sulfate had no significant effect on the interference of formaldehyde at pH 3 or 4, but did increase the interference somewhat in the presence of several ml of concentrated sulfuric acid per 500 ml.

The mechanism of the interference of formaldehyde is complex. One factor involved that has nothing to do directly with the development of the color is the possible loss of phenol by a reaction between phenol and formaldehyde. When solutions containing phenol and formaldehyde of approximately equal strength are mixed at room temperature, no significant reaction takes place even on standing for several days [21]. However, if the mixture is treated with an excess of acid or alkali, the phenol and formaldehyde react (especially on heating) to form *o*- and *p*-hydroxybenzyl alcohol ($HOC_6H_4CH_2OH$), which can then react in a complex manner with more formaldehyde to form phenol-formaldehyde resins [21]. Of course, in the present analytical method, there is ordinarily not sufficient phenol for the

TABLE 7

Interference of formaldehyde with the 4-AAP method for phenol

Phenol (mg/100 ml)	Formaldehyde[a] (mg/100 ml)	Phenol found (mg/100 ml)			
		Direct method		Extraction method	
		Without distillation	With distillation	Without distillation	With distillation
0.300	0.2	0.301	0.295 (pH 4) 0.203 (10 ml H_2SO_4[b])		
0.300	1.0	0.295	0.295 (pH 4) 0.295[c] 0.150 (10 ml H_2SO_4)		
0.300	1.5	0.295	0.295 (pH 4) 0.288[c] 0.150 (10 ml H_2SO_4)		
0.300	2.0	0.228	0.275[c] 0.184 (5 ml H_2SO_4) 0.118 (10 ml H_2SO_4)		
0.300	3.0	0.150	0.275[c]		
0.300	3.5		0.118[c]		
0.300	4.0		0.045[c]		
0.300	10.0	0.032	0.032[c]		
0.0060	0.5			0.0060	0.0058[c]
0.0060	1.0			0.0051	0.0054[c]
0.0060	2.0			0.0045	0.0045[c]
0.0060	4.0			0.0028	0.0045c

[a]37% solution. [b]Concentrated acid per 500 ml. [c]pH 3.

reaction to proceed past the hydroxybenzyl alcohol stage. The marked effect of acid in causing a reaction between phenol and formaldehyde explains the pronounced effect of excess sulfuric acid in increasing the interference in the distillation procedure.

Insofar as the actual interference of formaldehyde with the development of the color is concerned, there are probably two reactions involved. One is the reaction between ammonia and formaldehyde to produce hexamethylenetetramine ($6HCHO + 4NH_3 \rightarrow (CH_2)_6N_4 + 6H_2O$) [22]. This reaction results in the consumption of ammonia and a lowered pH and consequently less color development. The second reaction involves the oxidation of formaldehyde by the potassium hexacyanoferrate(III) to produce acetic acid. This reaction not only consumes hexacyanoferrate(III) but also lowers the pH. The change in pH of the solution was readily observed. After samples containing formaldehyde had been adjusted to pH 10 with the ammonia solution, the pH decreased after several minutes standing, necessitating the addition of more ammonia.

The method for the determination of phenol in the presence of formaldehyde mentioned earlier [15] was found to be unsatisfactory when applied to

TABLE 8

Results for phenol in the presence of formaldehyde by the 4-AAP method after treatment with ammonium sulfate and sodium hydroxide followed by distillation

Phenol (mg/100 ml)	Formaldehyde[a] (ml/100 ml)	Phenol found (mg/100 ml)	
		Direct method	Extraction method
0.300	2.0	0.295	
0.300	4.0	0.295	
0.300	6.0	0.262	
0.300	8.0	0.228	
0.300	10.0	0.228	
0.0060	2.0		0.0058
0.0060	4.0		0.0052
0.0060	6.0		0.0038
0.0060	8.0		0.0036

[a]37% solution.

the 4-AAP procedure. Attention was therefore turned to a method that would make use of the reaction between formaldehyde and ammonia. Attempts to use ammonia solutions were unsatisfactory, so a mixture of ammonium salt and sodium hydroxide was tested. Such a combination has been used previously in the determination of formaldehyde in a procedure involving titration of the excess alkali with standard acid [22]. Ammonium sulfate was found to be more satisfactory than ammonium chloride. It was necessary to allow the solution to stand for 1.5 h after the addition of the sodium hydroxide because the reaction between formaldehyde and ammonia is slow. Heating the solution in an attempt to speed up the reaction caused the results for phenol to be very low.

The results obtained for the determination of phenol in the presence of formaldehyde by the recommended ammonium sulfate—sodium hydroxide treatment are shown in Table 8. The method gives accurate results for the direct and extraction methods in the presence of up to 4.0 and 3.0 ml of 37% formaldehyde solution (per 100 ml), respectively. More than this amount of formaldehyde causes low results. However, the results are enormously better than those that would be obtained in the regular procedure. For example, it is seen from Tables 7 and 8 that with 4—10 ml of 37% formaldehyde per 100 ml, the recoveries in the direct method after using the ammonium sulfate—sodium hydroxide treatment were 98—76%, as contrasted with recoveries after distillation at pH 3 without the treatment of 15—11%. There are probably two reasons why the ammonium sulfate—sodium hydroxide method gives low results when large amounts of formaldehyde are present. The first is the reaction between phenol and formaldehyde in the strong sodium hydroxide solution that was mentioned earlier. The second reason is the partial decomposition of the hexamethylenetetra-

mine in a hydrolysis reaction with boiling water to form a variety of products, including methylamine, carbon dioxide, ammonia, and formaldehyde [23]. This formaldehyde (identifiable by its odor) apparently causes the low results. An obvious way to reduce the interference from larger amounts of formaldehyde in the ammonium sulfate—sodium hydroxide method is to dilute the samples prior to the treatment.

The method for phenol in the presence of formaldehyde will be useful for the determination of phenol in effluents from the industries that use formaldehyde, and possibly for process-control in the manufacture of phenol—formaldehyde resins. The general procedure would be applicable to the analysis of ordinary river water insofar as the interference of formaldehyde is concerned, since the amount of formaldehyde found in such samples is usually quite small.

REFERENCES

1 American Public Health Assoc., Standard Methods for the Examination of Water and Wastewater, 14th Edn., Washington, DC, 1975, pp. 574—584.
2 American Society for Testing and Materials, Standard Methods of Test for Phenolic Compounds in Water, Designation D-1723-70, Philadelphia, PA, 1979.
3 U.S. Environmental Protection Agency, Methods for Chemical Analysis of Water and Wastes, Cincinnati, OH, 1974, pp. 241—248.
4 G. Norwitz, J. Farino and P. N. Keliher, Anal. Chem., 51 (1979) 1632.
5 M. Dannis, Sewage Ind. Wastes, 23 (1951) 1516.
6 G. W. Ströhl, Mikrochim. Acta, (1969) 130.
7 P. D. Goulden, P. Brooksbank and M. B. Day, Anal. Chem., 45 (1973) 2430.
8 M. E. Gales, Jr. and R. L. Booth, J. Am. Water Works Assoc., 68 (1976) 540.
9 E. Emerson (Eisenstaedt), J. Org. Chem., 3 (1938) 153.
10 E. Emerson (Eisenstaedt), J. Org. Chem., 8 (1943) 417.
11 M. B. Ettinger, C. C. Ruchhoft and R. I. Lishka, Anal. Chem., 23 (1951) 1783.
12 S. D. Faust and O. M. Aly, J. Am. Water Works Assoc., 54 (1962) 235.
13 B. K. Afghan, P. E. Belliveau, R. H. Larose and J. F. Ryan, Anal. Chim. Acta, 71 (1974) 355.
14 A. P. Meijers and R. Chr. Van der Leer, Water Res., 10 (1976) 597.
15 J. O. Dziegielewski, Chem. Anal. (Warsaw), 6 (1961) 237.
16 V. T. Kaplin, S. E. Panchenko and N. G. Fesenko, Gidrokhim. Mater., 41 (1966) 104.
17 American Chemical Society, Reagent Chemicals, 5th Edn., Washington, DC, p. 274.
18 M. A. El-Dib, M. O. Abdel-Rahman and O. A. Aly, Water Res., 9 (1975) 513.
19 Rodd's Chemistry of Carbon Compounds, 2nd Edn., Vol III, Part B, Elsevier, New York, 1974, p. 231.
20 A. I. Kuper and V. F. Ozerova, Prom. Zagryaz. Vodoemov., No. 8 (1967) 156.
21 Kirk-Othmer Encyclopedia of Chemical Technology, 2nd Edn., Vol. 15, Interscience, New York, 1968, p. 179.
22 I. M. Kolthoff and V. A. Stenger, Volumetric Analysis, Vol. II, Interscience, New York, 1947, p. 217.
23 Rodd's Chemistry of Carbon Compounds, 2nd edn., Vol. I, Part C, Elsevier, New York, 1965, p. 42.

Analytica Chimica Acta, 119 (1980) 113—119

SPECTROPHOTOMETRIC DETERMINATION OF TRACES OF COBALT IN WATER AFTER PRECONCENTRATION ON REAGENT-LOADED POLYURETHANE FOAMS

T. BRAUN* and M. N. ABBAS

Institute of Inorganic and Analytical Chemistry, L. Eötvös University, P.O.B. 123, Budapest 1443 (Hungary)

(Received 30th March 1980)

SUMMARY

Open-cell polyurethane foam loaded with 1-(2-pyridylazo)-2-naphthol (PAN) is used for the preconcentration of traces of cobalt from water at the ppb level with a preconcentration factor of 1000 or more. Cobalt is retained quantitatively from thiocyanate solution on the loaded foam placed in a column, at flow rates up to 100 ml min^{-1}, and then recovered completely from the foam by elution with acetone. Cobalt is determined spectrophotometrically with 4-(2-pyridylazo)-resorcinol at 510 nm, after the removal of interfering ions with a Dowex 1-X8 column. The amount of PAN leached by the water percolating through the column is too low to affect quantitative retention of traces of cobalt.

The determination of trace elements in water is usually carried out by various more or less sophisticated methods. The very low concentration of some trace metals makes preconcentration almost mandatory. The spectrophotometric determination of trace elements in water requires relatively simple and inexpensive equipment. It has however, the disadvantage that preconcentration is necessary to raise the concentration of trace elements to the sensitivity of the spectrophotometric method. In spite of this disadvantage, spectrophotometry remains an attractive method for trace element determination in water. A survey carried out by Thomas [1] showed that in the United States 46.2% of laboratories are equipped with u.v. spectrophotometers and 51.2% with visible spectrophotometers. No other analytical equipment (except pH meters) is so widely available.

Trace elements are usually present in water at $\mu g\ l^{-1}$ levels. The concentration of cobalt in natural waters is usually below 1 $\mu g\ l^{-1}$ (Table 1). The sensitivities of spectrophotometric methods, of course, vary very considerably depending on the element and on the reagent used. For cobalt, the sensitivities of the main procedures are shown in Table 2. As can be seen, there is a considerable gap between the concentration of cobalt in water and the sensitivity of the spectrophotometric methods. Crossing this gap needs a preconcentration factor of around one thousand; or expressed in volumes, a 10-ml sample for the spectrophotometric determination requires an initial sample volume of 10 l of water. Usually such concentration gaps can be circumvented by

using batch or flow preconcentration techniques. The batch methods such as co-precipitation [14—16], co-crystallization [17—20], adsorption, ion-exchange and chelate exchange usually yield high preconcentration factors but are tedious and time-consuming.

Liquid—liquid extraction [2, 4, 7] is very awkward practically when large volumes of water (10 l) are involved. In contrast, flow methods are usually simple and practical, though they are also time-consuming because of low flow rates (about 10 ml min^{-1} in most cases) when ion exchangers [5] or chelating exchangers [21] are used.

Experience with reagent-loaded polyurethane foam columns [22] showed that even very high flow rates can yield quantitative recoveries of trace elements in preconcentration processes. Moreover, because of the advantageous spherical (more precisely, regular dodecahedral) membrane structure of the foam, solid—liquid contact is ideal during the percolation.

The aim of this work was to establish a simple, inexpensive and rapid method for the preconcentration of traces of cobalt from large volumes of water on reagent-loaded polyurethane foam columns prior to spectrophotometric determination of the cobalt.

EXPERIMENTAL

Reagents, materials and columns

All chemicals used were of analytical reagent grade and demineralized water was used. For the cobalt stock solution (100 $\mu g\ ml^{-1}$), cobalt(II) chloride hexahydrate was dissolved in 1% (v/v) HCl. Iron(III) and nickel(II) solutions (100 $\mu g\ ml^{-1}$ in Fe or Ni) were prepared from iron(III) chloride and nickel chloride 1% (v/v) HCl.

TABLE 1

Concentration of cobalt in different natural waters

Type of sample	Concentration of cobalt ($\mu g\ l^{-1}$)	Ref.
Ocean water		
Northcentral Pacific	0.24	2
Northwest Coast of U.S.	0.13	2
Sea water		
Adriatic Sea	0.15	3
Shibukawa, Okayama, Japan sea shore	0.10	4
off shore	0.15	4
Kamrike Harbor, Kagoshima Bay	0.13	5
Koshiki Jima, East China Sea	0.15	5
Lake water		
Ikeda Lake, Kagoshima	0.19	5
River water (Danube)	0.10—0.50	3

TABLE 2

Sensitivity of some reagents for the spectrophotometric determination of cobalt(II)

Reagent	Sensitivity ($mg\ l^{-1}$)	Wavelength (nm)	Ref.
Nitroso-R salt	0.2	420	6
1-Nitroso-2-naphthol	0.1	417	7
1-(2-Pyridylazo)-2-naphthol (PAN)	0.1	640	8
4-(2-Pyridylazo)-resorcinol (PAR)	0.2	510	9
Dithiooxamide	0.16	400	10
2,3-Quinoxalinedithiol	0.2	505	11
2,2-Dipyridylketoxime	0.24	388	12
Phenanthraquinonemonoxime	0.6	420	13

Polyurethane foam of the polyether open-cell type was cut into cylindrical columns (25 mm diameter, 100 mm long), which were washed with 1 M HCl, distilled water and acetone, and then dried in air at room temperature. 1-(2-Pyridylazo)-2-naphthol (PAN) solution was prepared by dissolving 0.1 g of the reagent in 100 ml of chloroform. α Dinonyl phthalate (phthalic acid di-3,5,5-trimethylhexyl ester) was used as plasticizer without further purification. The reagent foam was prepared by soaking the foam cylinders in the appropriate amount of reagent solution (usually 10 ml of PAN solution and 0.2 ml of α-dinonyl phthalate).

The foam cylinder was placed in a glass column (25 mm diameter) by applying gentle pressure with a glass rod, and then the column was filled with water under vacuum.

For the PAR solution, 0.1 g of 4-(2-pyridylazo)-resorcinol was dissolved in 1 ml of 1% (w/v) NaOH and diluted to 500 ml with demineralized water. The citrate buffer solution (pH 6.8) was prepared by mixing 23 parts of 0.5 M sodium citrate and 0.3 parts of 0.5 M citric acid.

Carrier-free ^{58}Co isotope was obtained from the Institute of Isotopes, Budapest.

For the ion-exchange column [23], Dowex 1-X8 resin was slurried in demineralized water and packed into a glass column (10 mm diameter). The resin bed was 11.5 cm long.

Equipment

Activity measurements were done with a NaI(Tl) well-crystal and energy-selective counting device (NK 350/A, Gamma, Budapest). The spectrophotometric measurements were made with a Perkin-Elmer 124 double-beam instrument.

Preconcentration and separation procedure

To a 10-l water sample, add 192 g of potassium thiocyanate, and adjust the pH to about 5. Allow the water sample to flow through the PAN-loaded

foam column at a flow rate of 100 ml min^{-1}. Recover cobalt from the foam by elution with 50 ml of acetone at a flow rate of 3 ml min^{-1}. Evaporate the acetone, add 5 ml of concentrated nitric acid, heat to decompose the reagent and thiocyanate, and evaporate almost to dryness. Repeat the process with 1 ml of concentrated nitric acid. Take up the residue in 5 ml of 9 M HCl.

For the separation from interfering ions, condition the Dowex 1-X8 column by percolating 5 ml of 9 M HCl. Transfer the sample solution to the column and allow it to flow through at a rate of 0.75—1.0 ml min^{-1}. Then wash the column with 20 ml of 9 M HCl at the same flow rate. Elute cobalt with 30 ml of 4 M HCl and collect the eluate for determination. Before the next determination, wash the column with 30 ml of 0.01 M HCl.

Determination of cobalt [5]

Reduce the volume of the eluate containing cobalt by evaporation to 1—2 ml, dilute with a few ml of demineralized water, and then add 2.5 ml of citrate buffer and readjust the pH if necessary to 6.8 ± 0.2 with sodium hydroxide solution. Add 1 ml of PAR solution and mix well. Add 1 ml of both 0.05 M EDTA and 0.1 M potassium cyanide solutions and mix again. Transfer the mixture to a 25-ml volumetric flask and dilute to the mark with demineralized water. After 20 min measure the absorption at 510 nm against a similarly prepared blank.

Preliminary tests

The effect of the volume of the percolating sample on reagent leaching was studied for four series of foam columns packed with freshly prepared reagent-foam cylinders. The PAN concentrations in the loaded foams differed from one series to another. Demineralized water (5 l) was percolated through each column at a flow rate of 100 ml min^{-1}. The PAN-containing eluates were made 1% (v/v) in hydrochloric acid and the light absorbances of the acidic PAN solutions were measured at 440 nm [8].

The effect of pH on the retention of cobalt was studied as follows: 100 ml of solution which contained 0.01 μg of cobalt and was 0.2 M in potassium thiocyanate was adjusted to the required pH value with HCl or NaOH. The solution was spiked with carrier-free ^{58}Co isotope and then percolated through the foam column at a flow rate of 50 ml min^{-1}. The radioactivity of a 5-ml sample was compared to the initial activity of the solution and the percentage retention was calculated.

To study the effect of flow rate, 100-ml aliquots of solution each containing 0.01 μg of cobalt spiked with ^{58}Co, made 0.2 M in thiocyanate and adjusted to pH 5, were percolated through the loaded foam column at different flow rates. The percentage extraction was calculated by comparing the radioactivity of 5 ml of the sample solution after percolation to the initial radioactivity of the solution.

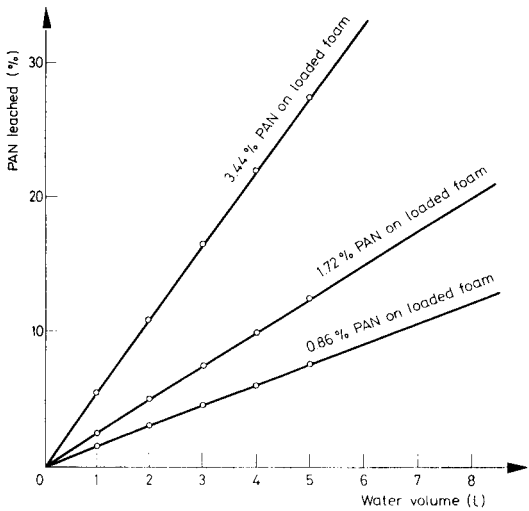

Fig. 1. PAN leached from loaded foam at different initial PAN concentrations.

RESULTS AND DISCUSSION

The relation between the amounts of the reagent leached from the foam and the volume of percolating water was determined spectrophotometrically as indicated above. PAN was found to be leached from the loaded foam at a constant rate; its concentration was found to be almost the same over the whole range of sample volume. The amount of PAN leached was dependent on the initial concentration of PAN on the loaded foam as shown in Fig. 1. From Table 3 it is clear that at a low concentration of PAN (0.86% w/w) in the foam, the amount of the reagent leached is relatively low, and the amount remaining on the foam is more than adequate for the quantitative retention of traces of cobalt.

The extraction of cobalt from 0.2 M thiocyanate solution is quantitative over the pH range 4—9. The effect of flow rate on the retention of 0.01 μg of cobalt from 100-ml samples (0.2 M thiocyanate) at pH 5 was also studied. Almost quantitative retention was obtained at flow rates as high as 100 ml min^{-1} (Table 4). The retained cobalt and the reagent itself are easily and completely eluted from the foam with acetone; 50 ml was found to be enough to recover cobalt completely at a flow rate of 3 ml min^{-1}.

TABLE 3

Leaching of PAN from loaded foams at different PAN concentrations after percolation of 5 l of demineralized water
(Each result is the mean of 4 determinations.)

PAN on foam (% w/w)	0.43	0.86	1.72	3.44
PAN leached (%)	not detected	7.5	12.5	27.5

TABLE 4

Effect of flow rate on the retention of 0.01 μg of cobalt on PAN-loaded foam
(Each result is the mean of 5 determinations.)

Flow rate (ml min^{-1})	Average percentage retention ($\bar{X}$) (%)	Standard deviation (s)	Confidence limit ($ts/n^{1/2}$; t= 99%)
38	99.05	0.55	± 1.34
50	98.79	0.01	± 0.03
75	98.04	0.08	± 0.21
100	96.76	0.20	± 0.51

Because of the lack of selectivity of PAN and the possibility of collecting other elements such as copper, iron, nickel, palladium, uranium, vanadium, mercury and zinc from water, as well as the possible interferences from these elements, PAR was used as reagent for the spectrophotometric determination of cobalt in citrate buffer after the elution from the loaded foam column. In this buffer and in the presence of EDTA and cyanide as masking agents, only iron and nickel interfere with the determination of cobalt. A Dowex 1-X8 column was used for the separation of cobalt from these elements.

The results for the determination of 1.0 μg of cobalt in the presence of 10.0 μg of nickel and 20.0 μg of iron before and after the Dowex column separation are shown in Table 5.

TABLE 5

Determination of 1.0 μg of cobalt with PAR, with and without column separation of interfering ions
(Each result is the mean of 5 determinations.)

	Amount of element added (μg)		Average found $\bar{X}$(μg)	Standard deviation (s)	Confidence limit ($ts/n^{1/2}$, t = 99%)
	Ni	Fe			
Without column separation	—	—	1.01	0.18	± 0.22
	10	—	1.94	0.26	± 0.28
	10	20	1.89	0.16	± 0.41
With column separation	—	—	0.99	0.16	± 0.20
	10	—	1.01	0.11	± 0.13
	10	20	1.01	0.12	± 0.16

REFERENCES

1 E. J. Thomas, R & D, Res. Dev., 29 (1978) 24.
2 B. Armitage and H. Zeitlin, Anal. Chim. Acta, 53 (1971) 47.
3 J. Korkisch and A. Sorio, Anal. Chim. Acta, 79 (1975) 207.
4 S. Motomizu, Anal. Chim. Acta, 64 (1973) 217.
5 T. Kiriyama and R. Kuroda, Fresenius Z. Anal. Chem., 288 (1977) 354.
6 E. B. Sandell, Colorimetric Determination of Traces of Metals, 3rd Ed., Interscience, New York, 1965.
7 E. Kenter and H. Zeitlin, Anal. Chim. Acta, 49 (1970) 587.
8 G. Goldstein, D. L. Manning and O. Menis, Anal. Chem., 31 (1959) 2, 192.
9 F. H. Pollard, P. Hanson and W. G. Geary, Anal. Chim. Acta, 20 (1959) 26.
10 W. D. Jacobs and J. H. Yoe, Anal. Chim. Acta, 20 (1959) 332.
11 R. W. Burke and J. H. Yoe, Anal. Chem., 34 (1962) 1378.
12 W. J. Holland and J. Bozic, Talanta, 15 (1968) 843.
13 K. C. Trikha, M. Katayal and R. P. Singh, Talanta, 14 (1967) 977.
14 M. Ishibashi et al., Rec. Oceanogr. Works Jpn., 1 (1953) 88.
15 G. Thompson and T. Laevastu, J. Mar. Res. 18 (1960) 189.
16 W. Forster and H. Zeitlin, Anal. Chim. Acta, 34 (1966) 211.
17 W. A. Black and R. L. Mitchell, J. Mar. Biol. Assoc. U.K., 30 (1952) 575.
18 E. G. Young, D. G. Smith and W. M. Laugille, J. Fish. Res. Board Can., 16(7), (1959) 7.
19 H. V. Weiss and J. A. Reed, J. Mar. Res., 18 (1960) 185.
20 J. P. Riley and J. A. Reed, J. Mar. Res., 18 (1960) 234.
21 M. Kubo, T. Yano, H. Kobayashi and K. Ueno, Talanta, 24 (1977) 519.
22 T. Braun, A. B. Farag and M. P. Maloney, Anal. Chim. Acta, 93 (1977) 191.
23 R. E. Thiers, J. F. Williams and J. H. Yoe, Anal. Chem., 27 (11), (1955) 1725.

Analytica Chimica Acta, 119 (1980) 121—127

THE DETERMINATION OF SULPHUR IN COPPER, NICKEL AND ALUMINIUM ALLOYS BY PROTON ACTIVATION ANALYSIS

C. VANDECASTEELE*, J. DEWAELE, M. ESPRIT and P. GOETHALS

Institute of Nuclear Sciences, Rijksuniversiteit Gent, Proeftuinstraat 86 B-9000 Gent (Belgium)

(Received 24th April 1980)

SUMMARY

The $^{34}S(p, n)^{34m}Cl$ reaction induced by 13-MeV protons is used for the determination of sulphur in copper, nickel and aluminium alloys. The ^{34m}Cl is separated by repeated precipitation as silver chloride. The results obtained were 3.08 ± 0.47, 1.47 ± 0.17 and <1 $\mu g\ g^{-1}$ for copper, nickel and aluminium alloys, respectively.

Sulphur is known to have an important influence on the properties of pure nickel [1] and its alloys [2], e.g. embrittlement [1] and magnetic properties [2]. Tentative specifications in some grades of primary nickel, e.g. DIN 1701 and BS 375, are at 5 μg S g^{-1} maximum. An accurate determination of sulphur at this concentration level is therefore required. Most industrial laboratories determine sulphur by combustion in an oxygen stream and measurement of the evolved sulphur dioxide. This technique works well for sulphur concentrations above 30 $\mu g\ g^{-1}$. At the 10 $\mu g\ g^{-1}$ level, or below, the results may be unreliable, because of incomplete combustion and adsorption of sulphur dioxide on metal oxides deposited in the apparatus. Moreover, no certified reference materials exist at this concentration level and practically no other techniques are available for comparison. A similar situation seems to exist for the determination of sulphur in aluminium and copper.

The present paper describes the determination of sulphur in copper, nickel and aluminium alloys by proton activation based on the $^{34}S(p, n)^{34m}Cl$ reaction. The relative excitation function for this reaction has been measured by Dabney et al. [3] and shows a maximum around 13.5 MeV. The threshold of the reaction is 6.5 MeV. At energies below 12 MeV, the interference of the $^{35}Cl(p, pn)^{34m}Cl$ (E_T = 12.9 MeV) and the $^{35}Cl(p, d)^{34m}Cl$ (E_T = 10.7 MeV) reactions, which are the only possible interfering reactions at these energies, is negligible. Chlorine-34m has a 32.2-min half-life and emits γ-rays of 145.7 (35.8%), 1177.4 (14.2%) and 2128.5 keV (48.4%).

*"Bevoegdverklaard navorser" of the NFWO.

EXPERIMENTAL

Samples and standards

The samples were cylindrical disks with 15 mm diameter and 1 mm thickness, prepared at BCMN, Geel. Two sorts of aluminium alloys, electrolytic tough pitch copper and nickel were analyzed. The copper was the same material as the BCR reference material for oxygen (RM 22); the nickel was the material used in a round-robin test for oxygen and nitrogen organized by BCR [4].

The standards used were sodium sulphate (UCB, p.a.) pellets, 20-mm diameter and 2 mm thick, pressed at 275 bar. It was verified that the sodium sulphate did not take up water on standing and did not lose weight when heated at 120°C.

Irradiation, chemical etching and energy degradation

The irradiations were carried out with 13-MeV protons extracted from the CGR-MeV 520 cyclotron of Ghent University. A 12-mm diameter collimator defined the irradiated area. Table 1 summarizes the irradiation conditions.

In front of the samples and standards was placed a copper foil (28.2 mg cm^{-2}, 15 or 20 mm diameter) which served as a beam intensity monitor.

After the irradiation, the samples were etched to remove surface contamination. Table 2 summarizes the etching conditions. After etching, the samples were rinsed with water and acetone and dried with a hair drier. The thickness removed was determined from the weight difference between the sample before the irradiation and after the etch.

As the chemical etch reduces the energy of the protons effectively incident on the samples, three series of standards were irradiated, placed behind a beam intensity monitor and a different number of copper foils (28.2 mg cm^{-2}) and of aluminium foils (4.9 mg cm^{-2}), so that the incident energies were 12.2, 11.9 and 11.5 MeV. As shown in Table 1, these energies span the energies effectively incident on the samples.

TABLE 1

Irradiation and measuring conditions

Conditions	Al	Cu	Ni	Standard
Intensity (μA)	2—3	0.8	1	0.020—0.035
Irradiation time (min)	30	15	30	5
Incident energy (MeV)	13	13	13	13
Energy after beam intensity monitor (MeV)	12.35	12.35	12.35	12.35
Energy corresponding to etching depth (MeV)	12.1—12.2	11.7—12.0	11.6—11.9	
Decay time (min)	70—80	45—60	45	80—90
Measuring time (min)	30	60	60	10

TABLE 2

Etching conditions

Sample	Solution	Temperature	Duration (min)	Thickness removed (mg cm^{-2})
Al	7:2:1 H_3PO_4(85%), HNO_3(14 M), H_2SO_4(35 M)	78—82°C	2 × 2.5	5—6
Cu	HNO_3(6 M)	Room	2 × 3	13—23
Ni	3:2 HF(40%), HNO_3(14 M)	Room	2 × 2.5	17—29

Chemical separations

Copper. The apparatus used is shown in Fig. 1. To 25 ml of a 14 M nitric acid solution containing 8 g of silver nitrate per l, 10 ml of an aqueous sodium chloride solution (3 g l^{-1}) were added in the separatory funnel (1). A silver chloride precipitate formed. The absorption vessels (2) were filled with a saturated hydrazine sulphate solution (10 ml in each) to trap chlorine gas. The sample was dissolved in the solution contained in the separatory funnel (1). After dissolution, the contents of the absorption vessels, 45 ml of distilled water and 10 ml of the sodium chloride solution (3 g l^{-1}) were added and the solution was agitated. The silver chloride precipitate was filtered off on a filter crucible (G4) (3) and washed with a 0.03 M nitric acid solution. The precipitate was dissolved in 15 ml of 6 M ammonia and the solution sucked through the filter. Then 15 ml of 14 M nitric acid was added and the silver chloride precipitate formed was filtered off on another, previously weighed filter crucible.

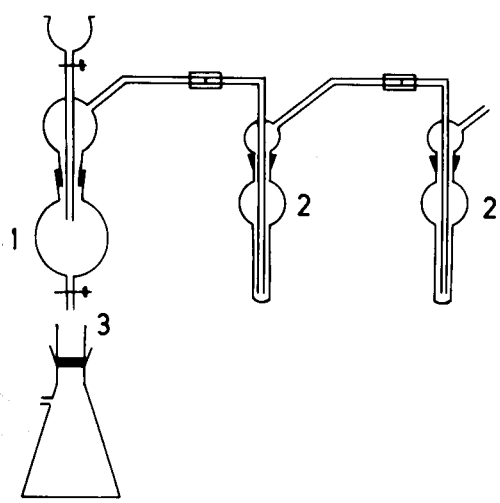

Fig. 1. Apparatus for the chemical separation.

Nickel. The chemical separation was similar to that for copper, except that for the dissolution, 10 ml of a solution of sodium chloride (3 g l^{-1}) in 14 M nitric acid and 1 ml of hydrofluoric acid (40%) were added to 25 ml of the nitric acid solution containing silver nitrate.

Aluminium. For the determination of sulphur in aluminium, the apparatus (Fig. 1) was slightly modified. The separatory funnel was replaced by a three-necked flask equipped with a condenser. The flask could be heated electrically. The condenser was connected to the two absorption vessels each containing 10 ml of a saturated solution of hydrazine sulphate.

40 ml of 14 M nitric acid, 50 mg of mercury(II) nitrate, 20 ml of silver nitrate solution (5 g l^{-1}) and 5 ml of sodium chloride solution (5 g l^{-1}) were added to the flask. A silver chloride precipitate formed. The sample was dissolved with slight heating. The contents of the absorption vessels and an additional 20 ml of silver nitrate solution were added. The precipitate was filtered, re-dissolved and filtered again on the same Seitz membrane filter (Typ M, pore size 5 μm).

Measurements

The precipitates were measured directly in the filter crucibles, or packed in an aluminium box for the determination of sulphur in aluminium, by means of a Ge(Li) detector (20% relative detection efficiency), coupled to an Intertechnique IN-90 γ-spectrometer. The standards were also measured in a filter crucible, with the irradiated side directed towards the detector. The measuring conditions are summarized in Table 1.

The areas of the 145.7-keV and the 2128.5-keV peaks of ^{34m}Cl and that of a pulser peak were calculated. The pulser peak was used to correct for count-losses caused by dead-time and pulse pile-up.

The beam intensity monitors for the samples and the standards were measured, respectively, for 5—20 min during the period 160—270 min after the irradiation, and for 10 min during the period 80—90 min after the irradiation, placed at a distance of 15 and 4 cm, respectively, from the detector. In addition, a 2-cm lead disk was interposed between the detector and the beam intensity monitors of the samples. The ratio of the detection efficiencies for the 669.6-keV peak was 48.5. The area of the 669.6-keV peak of 38.4-min ^{63}Zn formed by the ^{63}Cu(p, n)^{63}Zn reaction was calculated and used as a measure of the beam intensity.

Determination of the chemical yield

The chemical yield was determined by weighing the silver chloride precipitate after drying for 1.5 h at 150°C. For the determination of sulphur in aluminium, the yield was determined by activation with thermal neutrons using the ^{37}Cl(n, γ)^{38}Cl reaction. Chlorine-38 has a 37.3-min half-life and emits 2167-keV γ-rays, which were measured with a Ge(Li) γ-spectrometer. The chemical yields ranged from 65 to 99%.

Calculation of the results

As discussed elsewhere in a report dealing with standardization in charged particle activation [5], the concentration can be calculated from

$$C_X = C_S\,(a_X/a_S)(\Delta R_S/\Delta R_X)(1/Y)$$

where C is the concentration ($\mu g\ g^{-1}$); a the activity normalized for decay, irradiation time and beam intensity; ΔR the difference between the range at the incident energy and the threshold energy; and Y is the chemical yield. The subscripts X and S refer to the sample and the standard, respectively.

The ranges were obtained from Anderson and Ziegler [6]. For the energy corresponding to the depth of etching for the sample, a_S was deduced from a plot of the activity of the standard versus the energy. Over the energy range studied, a straight line could be fitted to the experimental points.

Two additional corrections were taken into account. First, the filter crucibles were not identical but contained glass disks of different thickness. A correction factor was determined by measuring a sulphur pellet, irradiated with protons, in each of the crucibles. All the activities measured were normalized to one crucible. The correction factor ranged from 0.95—1 (for 145.7 keV). Secondly, whereas the activity of the samples is distributed over the total area of the crucible (diameter, 30 mm), the activity of the standard is distributed only over the central area of the crucible (collimator diameter, 12 mm). This results in a higher detection efficiency for the standard. A correction factor was determined by measuring a sodium phosphate pellet, irradiated with 29-MeV α-particles, first as such (i.e. in a filter crucible) and then pulverized and homogeneously distributed over the filter. From sodium phosphate, ^{34m}Cl is formed according to the ^{31}P(α, n)^{34m}Cl reaction. The correction factor amounted to 1.043 ± 0.016 (for 145.7 keV).

RESULTS AND DISCUSSION

Chemical separation

The chemical separation described for copper was carried out with an inactive copper sample, to which a sodium phosphate pellet irradiated with α-particles was added before the dissolution. The sodium phosphate pellet (before the chemical separation) and the silver chloride precipitate were measured with the Ge(Li) detector, under the same conditions. The activity in the precipitate was corrected for decay, for the different detection efficiency (see above) and for the chemical yield. Six experiments showed that 97.2 ± 4.3% of the initial activity was recovered. It was verified that the first absorption vessel contained less than 0.1% of the ^{34m}Cl activity.

Figure 2 shows a Ge(Li) γ-spectrum of the silver chloride precipitate for a copper sample. The 145.7, 1177.4 and 2128.5-keV peaks of ^{34m}Cl appear in the spectrum together with the annihilation peak, the 669.6 and 961.9-keV peaks of ^{63}Zn formed by the ^{63}Cu(p, n)^{63}Zn reaction, and the 1460.7-keV peak of ^{40}K from the natural background.

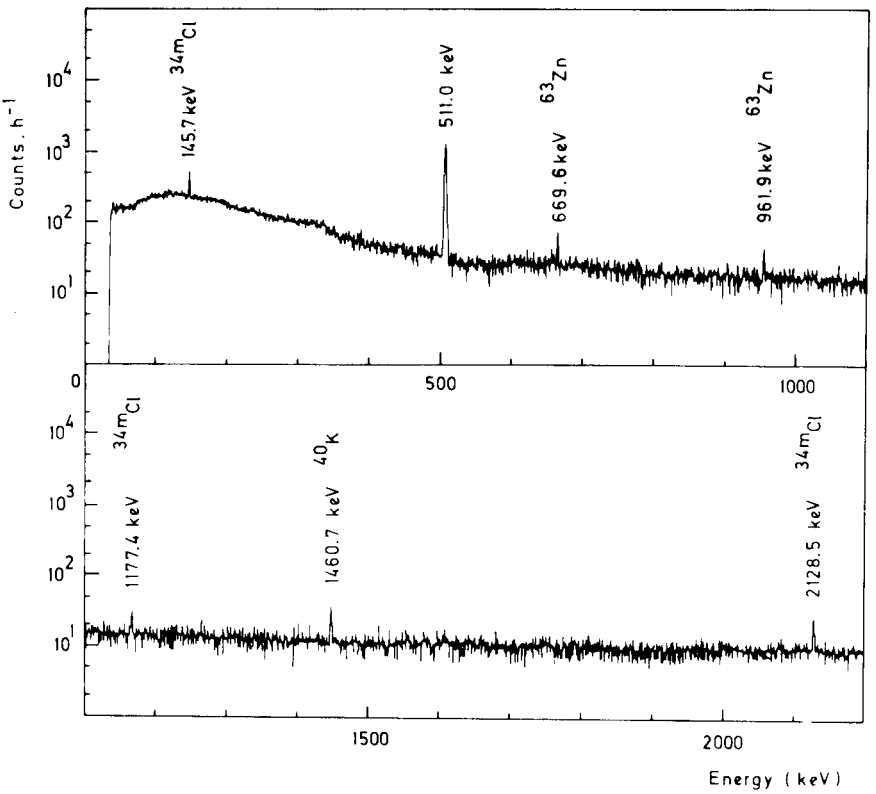

Fig. 2. Ge(Li) γ-ray spectrum of the silver chloride precipitate for a copper sample.

Results

Table 3 summarizes some results. For copper and nickel, each result is the weighted mean and the standard deviation on the mean of the results obtained via the 145.7 and 2128.5-keV peaks. The mean $\bar{x}$ and the standard deviation s were calculated from $\bar{x} = \Sigma_i x_i/s_i^2/\Sigma_i 1/s_i^2$ and $1/s^2 = \Sigma_i 1/s_i^2$, where s_i is the standard deviation expected from counting statistics for the 145.7 and 2128.5-keV peaks, respectively. For copper and nickel, the experimental relative standard deviation amounts to 15.4 and 11.5%, respectively. For copper, the experimental standard deviation is significantly greater (at the 95% confidence level) than the standard deviation calculated from counting statistics. This indicates an inhomogeneous distribution of the sulphur. For nickel, the experimental and the expected standard deviation are in good agreement.

The results for sulphur in aluminium alloys are based only on the 2128.5-keV peak. The detection limits given were calculated by the formulae given by Currie [7].

TABLE 3

Results obtained for sulphur in copper, nickel and aluminium

	S content found ($\mu g\ g^{-1}$)	Average ± s[a]
Copper	3.70 ± 0.16[b]; 3.18 ± 0.18; 3.36 ± 0.26; 2.63 ± 0.26; 2.42 ± 0.25; 3.16 ± 0.21	3.08 ± 0.47 (15.4%)
Nickel	1.40 ± 0.12; 1.73 ± 0.13; 1.42 ± 0.22; 1.61 ± 0.16; 1.26 ± 0.20; 1.41 ± 0.19	1.47 ± 0.17 (11.5%)
Aluminium		
A-U_4SG 19	0.71 ± 0.29	
20	<0.49	
A-Z_5GU 12	<2.21	
22	<0.77	

[a]Experimental standard deviation. [b]Calculated standard deviation (see text).

Grateful acknowledgement is made to J. Hoste for his interest in this work, to J. Pauwels (BCMN, Geel) and G. Beurton (Aluminium-Péchiney, Voreppe) for providing the samples, and to the IIKW and NFWO for financial support.

REFERENCES

1 K. Olsen, C. Larkin and P. Schmitt, Trans. Am. Soc. Met., 53 (1961) 349.
2 S. Ames, J. Appl. Phys., 41 (1970) 1032.
3 S. Dabney, D. Swindle, J. Beck, G. Francis and E. Schweikert, J. Radioanal. Chem., 16 (1973) 375.
4 J. Pauwels, The Analysis of Oxygen and Nitrogen in Nickel, EUR-6304 EN, 1979.
5 C. Vandecasteele and K. Strijckmans, J. Radioanal. Chem., 57 (1980) 121.
6 H. Anderson and J. Ziegler, The Stopping and Ranges of Ions in Matter, Vol. 3, Pergamon, New York, 1977.
7 L. Currie, Anal. Chem., 40 (1968) 586.

Analytica Chimica Acta, 119 (1980) 129—135

A DOUBLE QUADRUPOLE FOR MASS SPECTROMETRY/MASS SPECTROMETRY

D. ZAKETT and R. G. COOKS*

Department of Chemistry, Purdue University, West Lafayette, IN 47907 (U.S.A.)

W. J. FIES

Finnigan Corporation, Sunnyvale, CA 94086 (U.S.A.)

(Received 3rd March 1980)

SUMMARY

A double quadrupole mass spectrometer has been constructed to study unimolecular and collision-induced dissociation products from mass-selected ions. The two quadrupoles are closely coupled and the dissociation products sampled from a 2.5-mm inter-quadrupole region. Spectra obtained on the double quadrupole instrument are compared with published data obtained with triple quadrupole and reversed-sector (MIKE) mass spectrometers. The results indicate that the simple double quadrupole spectrometer is a highly efficient device which is a viable alternative to more complex quadrupole or sector instruments for obtaining dissociation spectra of mass-selected ions.

Bi- and multi-analyzer mass spectrometers have been in use for many years [1]. Perhaps the commonest configuration has been that in which an electric and magnetic sector are operated together to achieve high mass resolution. Uncoupling these analyzers so that they act independently and sequentially upon an ion beam is a more recent development. Trace organic analysis by the technique of sequential mass analysis has been accomplished over the past five years [2] by using a reversed-sector mass spectrometer (BE, magnetic field followed by electric field). These studies employed a mass-analyzed ion kinetic energy (MIKE) spectrometer [3] to separate individual ionized components and to characterize their fragments generated by collision-induced dissociation of the selected ions. The concept of ionization, ion separation, dissociation and fragment mass analysis as a method of mixture analysis has been adapted to quadrupole instruments in the form of a triple quadrupole (QQQ) device [4, 5]. In this instrument the center quadrupole is employed as a focusing device to contain the dissociation products formed in the low-energy (eV range) ion—molecule reactions.

In this and subsequent papers, the use of a double quadrupole (QQ) instrument is explored for mass spectrometry/mass spectrometry (m.s./m.s.) [6], i.e. for trace organic analysis without prior chromatographic separation and also for studies on the chemistry of individual ions selected from an ion mixture. Of particular interest is a comparison of the spectra obtained by

QQ with those generated by MIKE spectrometry on the one hand and by QQQ on the other. Both unimolecular and collision-induced dissociations are discussed. The former occur at longer times than those observed in typical sector instruments; the latter occur at about a thousand times lower axial energy than the analogous reactions in a sector instrument. In spite of these differences, very similar spectra will be shown to result (for electron ionization).

EXPERIMENTAL

A schematic diagram of the configuration of the QQ mass spectrometer is given in Fig. 1. The quadrupoles are standard Finnigan units, with rods (3-mm radius, 12.7-mm long) operated by using two Finnigan model 3000 electronic modules and a model 1015 preamplifier and display unit. The source is a Finnigan electron impact source, configured for vapor introduction and for probe introduction of the sample into the vacuum system. The detector is a Galileo Channeltron model 4700. The quadrupole assemblies are mounted in a holder such that the rods are separated by a grounded plate which is normally 2.5-mm thick with a centrally located aperture (6 mm diameter). In later experiments, target gas was introduced via a channel drilled radially through this aperture plate. The entire structure, however, is very open and the sample introduced into the source makes a considerable contribution to the target gas pressure. Pressure was read on an externally mounted ion gauge and was typically 6×10^{-5} torr. Higher pressure would have given more collision-induced dissociation but this was

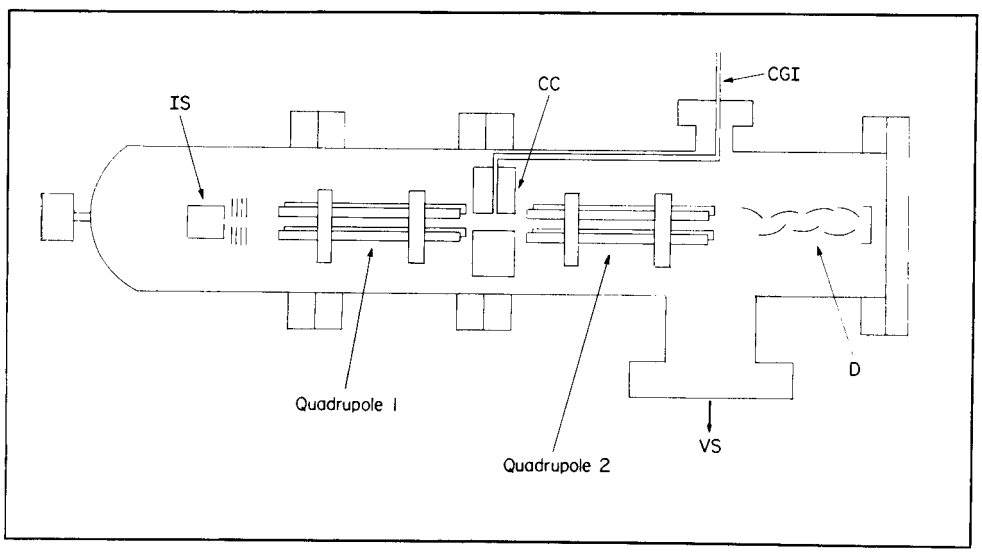

Fig. 1. Schematic diagram of the double quadrupole instrument: IS, ion source; CC, collision cell; CGI, collision gas inlet; VS, to vacuum system; D, detector.

precluded because of the lack of differential pumping and the danger of arcing in the multiplier.

An m.s./m.s. spectrum is obtained by setting Q_2 to pass all masses in the r.f.-only mode and then scanning Q_1 to locate the ion of interest. This ion is then transmitted at a fixed Q_1 setting and Q_2 is scanned in the mass analysis mode to obtain the m.s./m.s. spectrum.

RESULTS AND DISCUSSION

Studies on the diisopropyl ketone system

Figure 2 compares the dissociation spectrum of 114^+, the molecular ion of diisopropyl ketone, with the MIKE spectrum of the same ion. Both spectra were taken in the presence of target gas (the sample itself and nitrogen, respectively). The agreement is excellent, the only difference being in main beam intensity. The transition $114^+ \rightarrow 71^+$ is known [7] to be a collision-induced dissociation in MIKE spectrometry while $114^+ \rightarrow 70^+$ is known to be unimolecular. These features also hold true in the QQ experiment, as the data of Fig. 3 indicate. This result demonstrates that substantial unimolecular de-

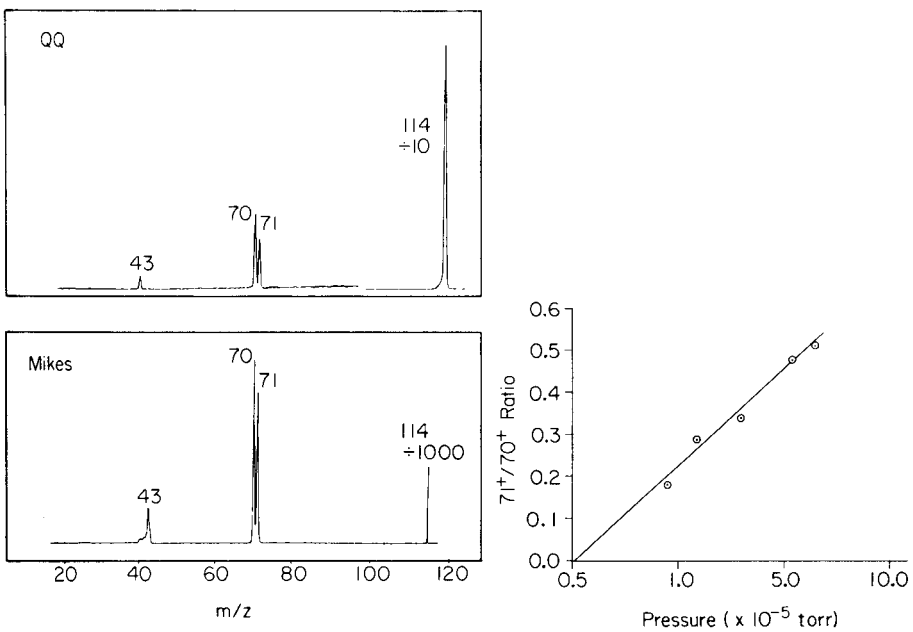

Fig. 2. Comparison of the fragments generated at high pressure from the diisopropyl ketone molecular ion (114^+) using the double quadrupole (upper) and the MIKE spectrometer (lower).

Fig. 3. Linear plot for the relative yields of 71^+ and 70^+ (from 114^+, diisopropyl ketone) against pressure. The individual reactions $114^+ \rightarrow 71^+$ and $114^+ \rightarrow 70^+$ are first and zero order, respectively, in pressure.

composition occurs some 30 μs (the transit time through Q_1) after ionization. While it has not been directly demonstrated, one assumes that some of the dissociations being sampled in the QQ experiment occur within the quadrupoles, near the interquadrupole region.

The diisopropyl ketone system was used to study the effects of instrumental and experimental variables on the m.s./m.s. spectrum. The diisopropyl ketone fragmentation processes did not change significantly except in relative main beam to fragment intensity as the interquadrupole spacing was increased from 1.6 mm to 8.4 mm, indicating poor fragment ion collection efficiencies at large spacings. The fragment ion collection efficiency and the overall transmission of the main beam ions were found to increase as the interquadrupole distance was decreased. In routine operation, Q_1 was operated at 2.14 MHz and Q_2 at 1.85 MHz. The frequency of Q_1 was varied from 2.49 MHz to 1.75 MHz; again there were no major changes in the relative intensities of the fragments in the spectrum. However, when Q_1 and Q_2 were operated at nearly identical frequencies the fragment ion signals were observed to show a 5—10% intensity modulation. The modulation frequency increased as the frequency difference between Q_1 and Q_2 increased, and may be the result of r.f.-phase discrimination during ion entry into Q_2. This modulation was not observable when Q_1 was operated at 2.14 MHz.

Comparison of spectra obtained on double quadrupole and triple quadrupole spectrometers

Comparisons were also made between spectra obtained on the double quadrupole spectrometer and published data for the triple quadrupole [7]. Some of these results are shown in Figs. 4—6. The QQ spectra for these figures were obtained without use of an added collision gas. The sample served as the collision gas and the instrument pressure was raised to the values indicated by increasing the sample gas flow rate. Except for the scaling of the main beam of ions, the agreement is excellent. Only two minor differences occur: (1) the QQQ spectrum of cyclohexanone molecular ion shows 81^+ which is absent in the QQ spectrum; (2) the QQ spectrum of benzene shows 63^+ which is much less intense in the QQQ spectrum. These differences probably reflect target gas and axial ion kinetic energy effects. For example, the cyclohexanone QQQ spectrum shows 99^+, i.e. an $(M + H)^+$ ion which is probably a consequence of the target gas used in that experiment. Protonated cyclic ketones should undergo extensive dehydration; this is the base peak of the MIKE spectrum for protonated cyclopentanone [8], and explains the presence of the 81^+ ion in the QQQ spectrum.

In later experiments, gas was introduced into a collision cell located between the quadrupoles. The pressure of the cell was monitored by using a capacitance manometer (Baratron 170-M). Collision cell pressures of 2—4 m torr were found to give about a five-fold increase in the absolute intensity of the fragment ion spectra when compared with spectra obtained without collision gas but at the same sample pressure. At a pressure of 3 mtorr the parent ion of diisopropyl ketone (m/z 114^+) was attenuated to approxi-

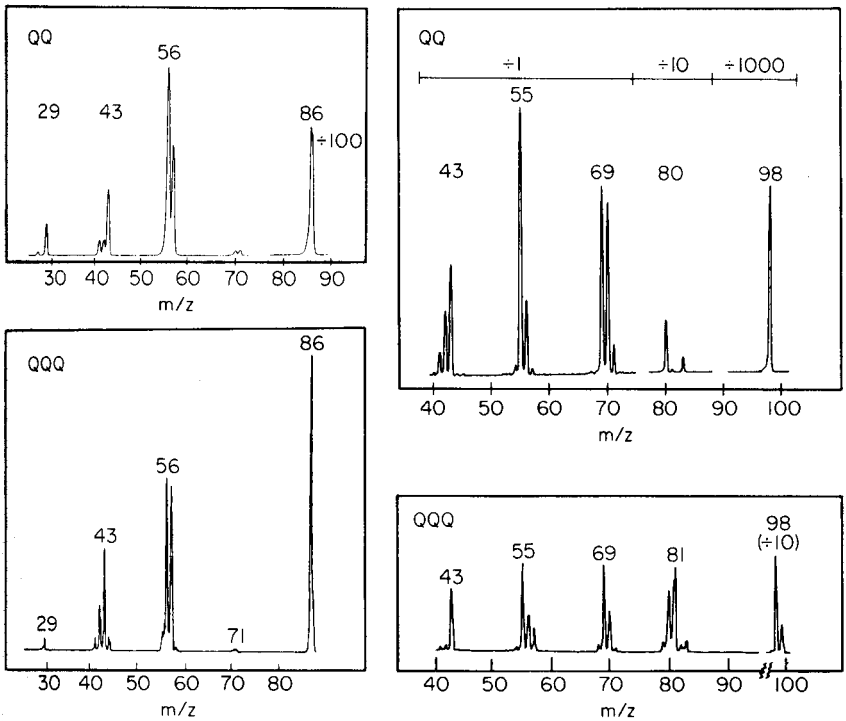

Fig. 4. Comparisons of the dissociations of n-hexane molecular ion (86^+) recorded on the double quadrupole (sample = target) and the triple quadrupole (Ar target) [9].

Fig. 5. Comparison of the m.s./m.s. spectra of cyclohexanone molecular ion (98^+) recorded using double and triple quadrupole mass spectrometers.

mately 15% of the intensity observed in the absence of collision gas (both Q_1 and Q_2 in mass-analysis mode). Presumably most of this loss is due to scattering. Figure 7 shows the m.s./m.s. spectrum of diisopropyl ketone *m/z* 114^+ using air as a collision gas where both the fragment ions and the parent ion were recorded on the same amplifier range setting.

Transmission efficiency

In the present configuration the transmission efficiency of Q_1 is estimated to be 10—15%. The transmission efficiency of Q_2 is also estimated at 10—15%. These values were determined by operating one quadrupole in the mass-analysis mode and the other in the r.f.-only mode. With the mass-analyzing quadrupole set to pass a given mass, the detector current was measured. The r.f.-only quadrupole was then switched to the mass-analysis mode and the detector current measured again, now with both quadrupoles performing mass analysis. The detector current decreased to 10—15% of the current for an m.s./r.f.-only or r.f.-only/m.s. configuration when going to an m.s./m.s. configuration (without collision gas).

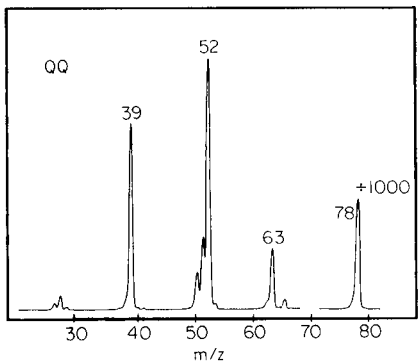

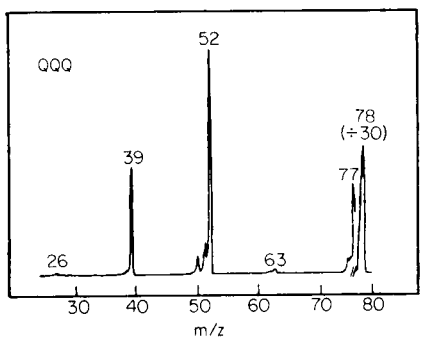

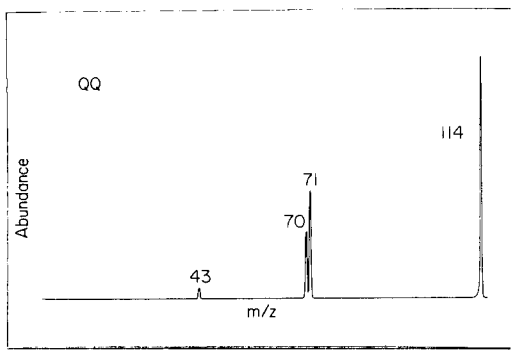

Fig. 6. Comparison of the m.s./m.s. spectra of $C_6H_6^{+\cdot}$ recorded using the double and triple quadrupole mass spectrometers.

Fig. 7. M.s./m.s. spectra of diisopropyl ketone recorded for a pressurized collision cell (2.3 mtorr air).

Transmission efficiency of ions from the exit of Q_1 to the entrance of Q_2 is estimated at approximately 50%. This value was determined by comparing detector currents in experiments which involved close-coupling of the two quadrupoles without a collision cell with the detector currents observed using the present collision cell. The transmission efficiency from Q_1 to Q_2 varies with the distance of separation, lensing, and/or aperture sizes of the particular collision cell used.

The fragment ions which reached the detector in Fig. 7 represent 10% fragmentation of the 114^+ ion in the collision region. Because of the 10—15% transmission efficiency of Q_2, approximately 1% of the 114^+ ion current exiting Q_1 was collected as detectable fragment ion current. Expressed differently, some 20% of the ion current arising from 114^+ recorded in the absence of collision gas and in the double mass-analyzing mode is collected and recorded in Fig. 7. This number compares favorably with that reported for the triple quadrupole [4].

Continuing experiments are underway to optimize the collision-region configuration and improve the collection efficiency of ions in the presence

of collision gas. The results suggest that the simple double quadrupole instrument described here is a viable alternative to more complex quadrupole or sector instruments in obtaining dissociation spectra of selected ions. These capabilities are explored further in subsequent papers.

This work was supported by the National Science Foundation CHE 77-01295.

REFERENCES

1 J. H. Futrell and T. O. Tiernan, in J. L. Franklin (Ed.), Ion Molecule Reactions, Plenum, New York, 1972, Ch. 11; E. Lindholm, in J. L. Franklin (Ed.), Ion Molecule Reactions, Plenum, New York, 1972, Ch. 10; J. P. L'Hote, J. Ch. Abbe, J. M. Paulus and R. Ingersheim, Int. J. Mass Spectrom. Ion Phys., 7 (1971) 309; M. L. Vestal and J. H. Futrell, Chem. Phys. Lett., 28 (1974) 559.
2 T. L. Kruger, J. F. Litton, R. W. Kondrat and R. G. Cooks, Anal. Chem., 48 (1976) 2113; R. W. Kondrat and R. G. Cooks, Anal. Chem., 50 (1978) 81A.
3 J. H. Beynon, R. G. Cooks, J. W. Amy, W. E. Baitinger and T. Y. Ridley, Anal. Chem., 45 (1973) 1023A.
4 R. A. Yost and C. G. Enke, J. Am. Chem. Soc., 100 (1978) 2274; Anal. Chem., 51 (1979) 1251A.
5 D. F. Hunt and J. Shabanowitz, 27th Annual Conference on Mass Spectrometry and Allied Topics, Seattle, Washington, June 1979, paper FAMOC2.
6 F. W. McLafferty and F. M. Bockhoff, Anal. Chem., 50 (1978) 69.
7 J. F. Litton, T. L. Kruger and R. G. Cooks, J. Am. Chem. Soc., 98 (1976) 2012.
8 M. L. Sigsby, R. J. Day and R. G. Cooks, Org. Mass Spectrom., 14 (1979) 273.
9 R. A. Yost, C. G. Enke, D. C. McGilvery, D. Smith and J. D. Morrison, Int. J. Mass Spectrom. Ion Phys., 30 (1979) 127.

Analytica Chimica Acta, 119 (1980) 137—144

ION STRUCTURE DETERMINATIONS AND ION—MOLECULE REACTIONS BY DOUBLE QUADRUPOLE MASS SPECTROMETRY

G. L. GLISH, P. H. HEMBERGER and R. G. COOKS*

Department of Chemistry, Purdue University, West Lafayette, IN 47907 (U.S.A.)

(Received 3rd March 1980)

SUMMARY

The QQ mass spectrometer is shown to be applicable to ion structure determination via collision-induced dissociations of mass-selected ions. The instrument can be scanned so as to record the products of dissociation as well as those of ion—molecule association reactions. The dissociations correspond to those observed at high kinetic energy in mass-analyzed ion kinetic energy spectrometers and the association reactions show parallels with reactions seen in ion cyclotron resonance spectroscopy and in high-pressure mass spectrometry.

This paper covers ion structure determination by double quadrupole [1] (QQ) mass spectrometry. The most important feature of the methodology is access, in a single scan, to both dissociative and associative ion—molecule reactions of individual mass-selected ions. It should be noted that the triple quadrupole (QQQ) mass spectrometer has been used [2] to characterize ion structures on the basis of collision-induced dissociations. The object is to demonstrate the parallel capability of the double quadrupole instrument and to broaden the overall method to include reactive as well as other inelastic collision processes.

EXPERIMENTAL

The QQ mass spectrometer has been described [1]. All reagents were used without prior purification. All liquids were thoroughly degassed through several freeze—pump—thaw cycles. In most experiments, the reagent gas (or gases) served also as the target gas effecting collision-induced dissociation and associative ion—molecule reactions. In these cases, the sample was allowed to diffuse throughout the instrument to a pressure of $2—6 \times 10^{-5}$ torr as indicated by a Bayard—Alpert ion gauge. For characterization of the $C_2H_5O^+$ isomers, a collision-cell was located between the two quadrupole assemblies so that the target gas could be introduced into the instrument independently of the sample gas.

The ion translational energy in the QQ mass spectrometer was calibrated by measurement of the relative abundance of the product ions $C_3H_3^+$ and $C_3H_5^+$ from the reaction of $C_2H_4^+$ with C_2H_4 at ion accelerating potentials

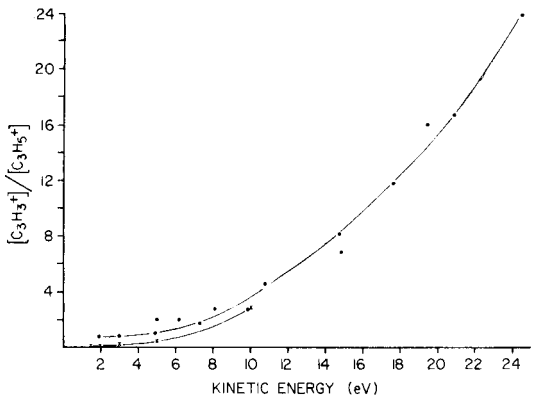

Fig. 1. Calibration of ion translational energies from the branching ratio $C_3H_3^+/C_3H_5^+$ in $C_2H_4^{+\cdot}$ collisions on C_2H_4. (•) QQ; (X) tandem mass spectrometer [3].

from 2 to 25 eV. Comparison of these results with those of tandem mass spectrometry [3] (Fig. 1) indicates that the measured ion kinetic energy in these experiments is low by approximately 2 eV, at least up to 10 eV.

RESULTS AND DISCUSSION

Keto (a) and enol (b) ions, $C_3H(D)_6O^{+\cdot}$

a b

were generated in the QQ by electron impact of a mixture of d_6-acetone and 2-hexanone. Structure a arises by direct ionization of d_6-acetone and structure b results from a McLafferty rearrangement of the molecular ion of 2-hexanone. Ion cyclotron resonance spectroscopy (ICR) has been used [4] to differentiate the isomers a and b by the reactions (1) and (2):

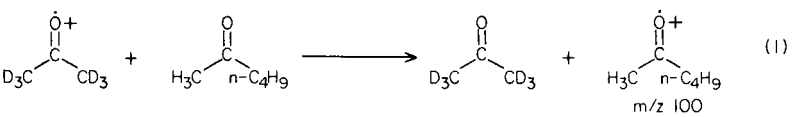

(1)

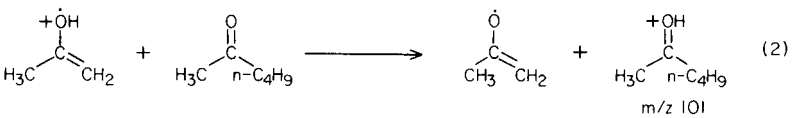

(2)

This method of assigning ion structures was attempted with the QQ spectrometer. The d_6-acetone molecular ion, m/z 64 (a) was mass-selected

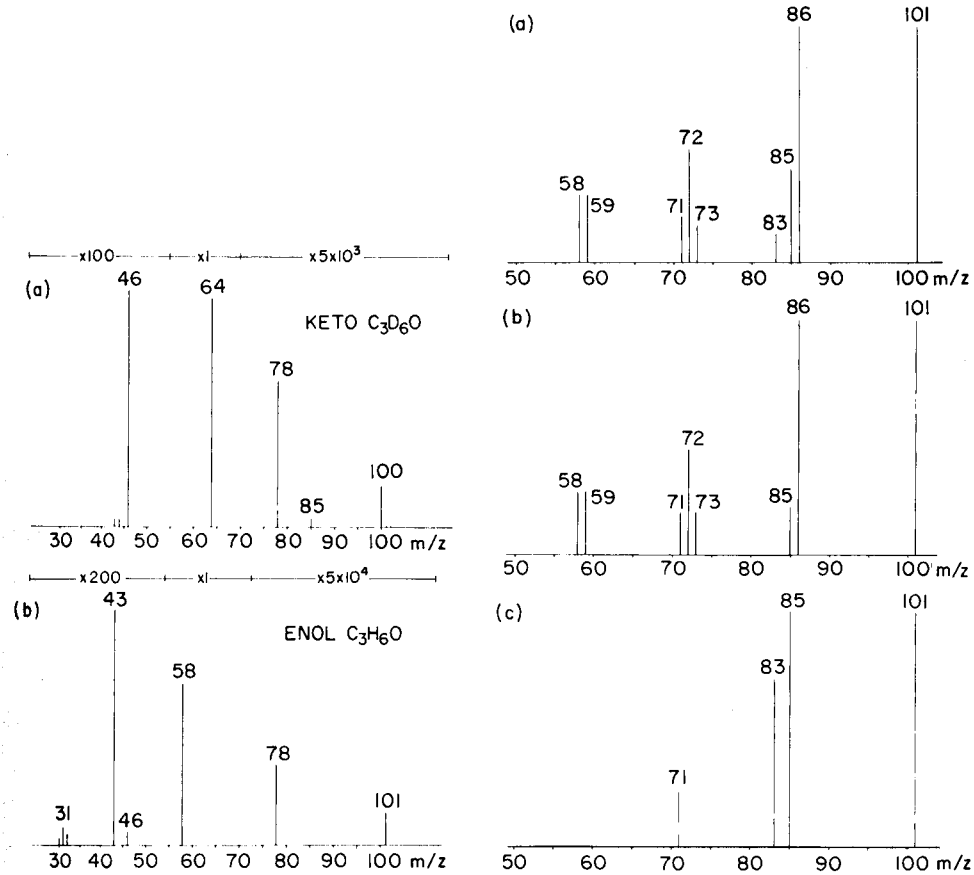

Fig. 2. Ion structure determination. (a) Spectrum of the dissociations and associations of $C_3D_6O^{+\cdot}$ from d_6-acetone. (Ion 78^+ arises by charge exchange of $C_3H_6O^{+\cdot}$ with residual benzene in the system; 85^+ is a fragment from $100^{+\cdot}$). (b) Spectrum of $C_3H_6O^{+\cdot}$ formed by McLafferty rearrangement of 2-hexanone. (78^+ is again the benzene charge exchange product.)

Fig. 3. (a) Dissociation spectrum of mass-selected 101^+. (b) Calculated ^{13}C contribution of 2-hexanone to 101^+. (c) The spectrum derived by subtracting the ^{13}C contribution from the actual spectrum of 101^+.

and the spectrum of its dissociative and associative reaction products was recorded (Fig. 2a). The ion corresponding to the other isomer (b) (m/z 58) was identically examined (Fig. 2b). The appearance of an ion at m/z 100 in Fig. 2(a) and at m/z 101 in Fig. 2(b) serves to differentiate the ion structures a and b according to reactions (1) and (2), respectively.

A more detailed inquiry into the above structural problem is possible by mass-selecting the products of reactions (1) and (2) and examining their spectra in the QQ spectrometer. The actual QQ spectrum of 101^+ is shown in

Fig. 3(a). When this is corrected for ^{13}C contributions of the 2-hexanone molecular ion (Fig. 3b), one obtains the spectrum given in Fig. 3(c) which shows mainly loss of 16 and 18 mass units. This behavior is consistent with the protonated ketone structure as shown by MIKE spectrometric studies [5]. Further evidence that the 100^+ product from reaction (1) between $C_3D_6O^{+\cdot}$ and 2-hexanone is indeed the molecular ion of 2-hexanone is the presence of 85^+ in the $C_3D_6O^{+\cdot}$ spectrum (Fig. 2a) and in the spectrum (not shown) of the molecular ion of 2-hexanone.

Isomeric $C_2H_5O^+$ ions, **c** and **d**, have been characterized by collision-induced dissociation [6] and by their low-energy ion-molecule reactions [7]. The reactions used in these earlier collisional activation and ion cyclotron resonance studies are shown in eqns. (3) and (4).

$$\begin{array}{l} CH_3CH = {}^{+}OH \xrightarrow{CID} H_3O^+ \ (m/z\ 19) \\ \mathbf{c} \quad \Big\downarrow + \text{i-PrOH} \\ (CH_3)_2CHOH_2^+ \ (m/z\ 61) \end{array} \qquad (3)$$

$$\begin{array}{l} CH_3-\overset{+}{O}=CH_2 \xrightarrow{CID} CH_3^+ \ (m/z\ 15) \\ \mathbf{d} \qquad\qquad\quad \hookrightarrow CHO^+ \ (m/z\ 29) \end{array} \qquad (4)$$

Precisely the same reactions are observed for the low kinetic energy collisions which occur in the QQ. This is shown in Fig. 4, which shows ions at higher mass (59^+ and 61^+) due to proton transfer and hydride abstraction, as well as fragments arising from collision-induced dissociation. Since the target gas was not confined to the interquadrupole region the spectrum of dimethyl ether on the 2-propanol target represents a composite of ions from both compounds. The ions at *m/z* 19 and 27 and a portion of the ions at *m/z* 29 are CID fragments of $H_3C-CH=OH^+$, a fragment of 2-propanol generated in the ion source. Ions at *m/z* 15 and the remaining ions at *m/z* 29 arise from the dissociation of $CH_3-O=CH_2^+$ from dimethyl ether. The association ion at *m/z* 59 has contributions from both precursor structures while *m/z* 61 arises exclusively from protonation of 2-propanol by $CH_3-CH=OH^+$. This is consistent with the fact that $CH_3-\overset{+}{O}=CH_2$ is a very poor proton donor.

In other systems, reactive collisions leading to transfer of larger units occur. For example, the spectrum of $C_6H_6^{+\cdot}$ on a benzene target shows adducts with carbon numbers 7 through 12, including $C_{12}H_{11}^+$. These ions presumably arise from dissociation of a $C_{12}H_{12}^{+\cdot}$ collision complex. This is supported by the MIKE spectrum of $C_{12}H_{12}^{+\cdot}$ prepared by high-pressure mass spectrometry [8]. Both spectra show cations at *m/z* 153—155, 141, 127—129, and 115 as the main high-mass species.

The ion—molecule reactions of two fragment ions from n-hexane with n-hexane itself were investigated with the QQ mass spectrometer (Fig. 5). Although abundant products at *m/z* 55 and 57 are observed for the reaction of both the closed shell $C_3H_7^+$ ion and $C_3H_6^{+\cdot}$ radical cation, these products probably arise by different mechanisms. It is suggested that $C_3H_6^{+\cdot}$ reacts with

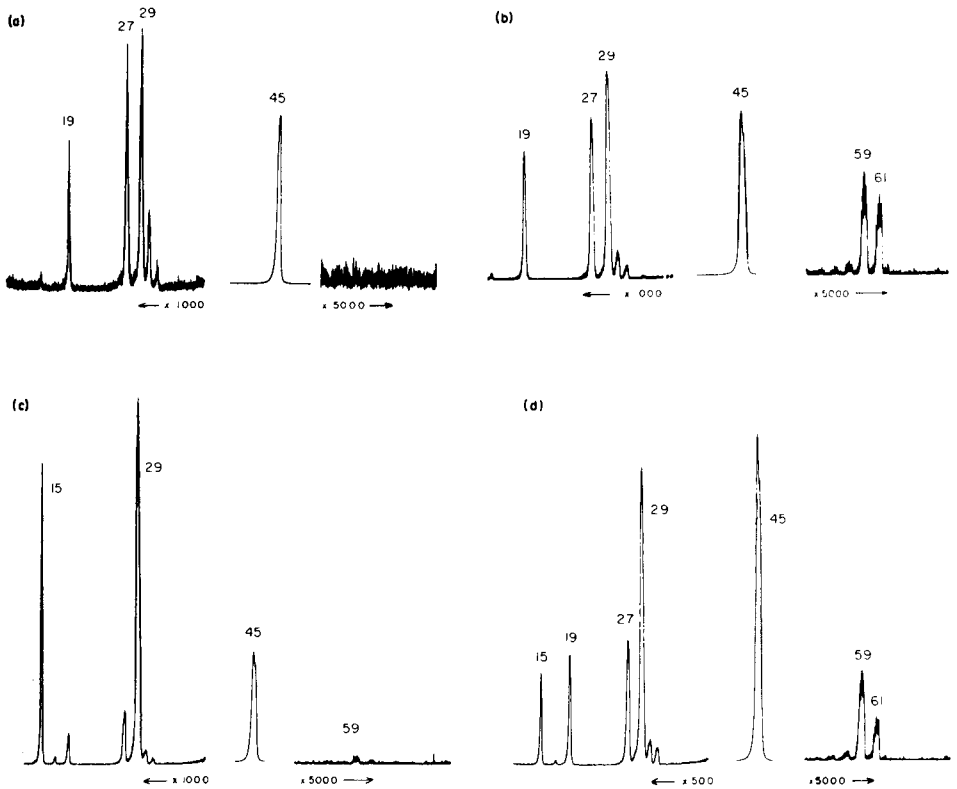

Fig. 4. Spectra showing the dissociations and associations of isomers of $C_2H_5O^+$ using air or 2-propanol as the target gas. (a) Ethanol sample, air target, ion CH_3—CH=OH^+; (b) ethanol sample, 2-propanol target, ion CH_3—CH=OH^+; (c) dimethyl ether sample, air target, ion CH_3—O^+=CH_2; (d) dimethyl ether sample, 2-propanol target, ions CH_3—O^+=CH_2 and CH_3—CH=OH^+.

n-hexane by first undergoing charge exchange to form the hexane molecular ion and propene. This ion then fragments by loss of H_2 and a neutral moiety giving not only 55^+ and 57^+ but also 56^+:

$$C_3H_6^{+\cdot} + C_6H_{14} \xrightarrow{-C_3H_6} C_6H_{14}^{+\cdot} \begin{cases} \longrightarrow C_4H_9^+ + C_2H_3 + H_2 \\ \longrightarrow C_4H_8^{+\cdot} + C_2H_4 + H_2 \\ \longrightarrow C_4H_7^+ + C_2H_3 + 2H_2 \end{cases} \quad (5)$$

By contrast the closed shell $C_3H_7^+$ ion abstracts hydride from n-hexane to form the hexyl cation and propane. Subsequent loss of C_2H_4 from the hexyl ion leads to the formation of $C_4H_9^+$. The $C_4H_7^+$ ion forms by sequential loss of C_2H_4 and H_2:

$$C_3H_7^+ + C_6H_{14} \xrightarrow{-C_3H_8} C_6H_{13}^+ \begin{cases} \longrightarrow C_4H_9^+ + C_2H_4 \\ \longrightarrow C_4H_7^+ + H_2 + C_2H_4 \end{cases} \quad (6)$$

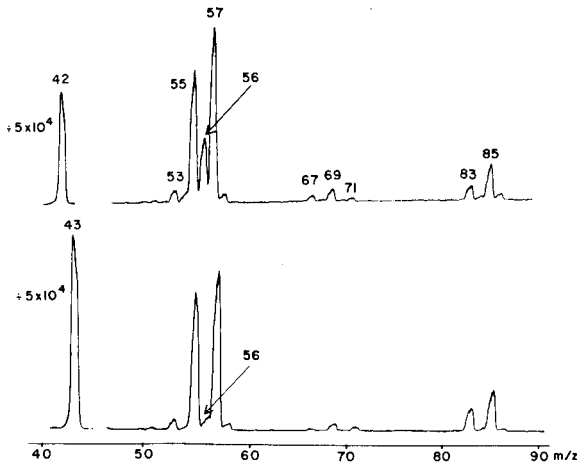

Fig. 5. QQ spectra showing the associative reactions of $C_3H_7^+$ and $C_3H_6^{+\cdot}$ generated from n-hexane with n-hexane target.

Precedence for the proposed hydride abstraction exists in the ion—molecule reactions of $C_2H_5^+$ with n-hexane as investigated by ion cyclotron resonance spectrometry [9].

The component of ion translational energy in the axial direction is readily varied in the QQ mass spectrometer and the effects of variation of this energy upon collision-induced dissociations and associative ion—molecule reactions were investigated. This was done for an ion, 27^+, from methane, which is itself the product of an associative ion—molecule reaction. The ion $C_2H_3^+$ was mass-selected through the first quadrupole mass filter and allowed to react with methane between the two quadrupole assemblies. Mass analysis of the products of these ion—molecule reactions gave the spectra shown in Fig. 6. Of particular interest is the increased abundance of lower mass ions as the axial ion energy is increased. This is true both for ions below the selected mass, and above it. These results show that initial translational energy can assist in driving both dissociation and associative reactions. In other cases, particularly charge exchange [10], negligible translational energy effects have been observed.

The QQ mass spectrometer is shown in this initial survey to provide both structural characterization of ions and the potential to supply information on the energetics of ion—molecule reactions. Data of the type shown should serve to supplement the wealth of information already gathered on ion—molecule reactions by ion cyclotron resonance spectroscopy [11]. The possibility of using axial ion kinetic energy as a variable for highly endothermic reactions in structural and other ion—molecule studies is attractive although there is no feature comparable to the time range and resolution achieved in ion cyclotron resonance. The combination of dissociation and ion—molecule reactions in a single spectral scan represents a unique capability.

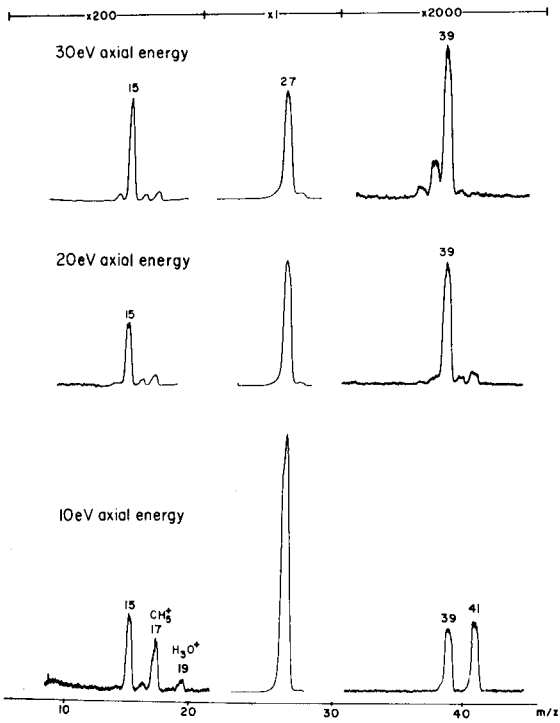

Fig. 6. The effect of ion energy upon the products of the reaction of $C_2H_3^+$ (27^+) with methane.

This work was supported by the National Science Foundation CHE 77-01295. We thank Dr. Mike Story and Finnigan Corporation for technical assistance.

NOTE ADDED IN PROOF

For recent discussions of translational energy effects on ion—molecule reactions in a triple quadrupole mass spectrometer see R. K. Latven, B. Newcome and C. G. Enke, paper RAMOA3 presented at the 28th Conference on Mass Spectrometry and Allied Topics, ASMS, New York, NY, May 1980.

REFERENCES

1 D. Zakett, W. J. Fies and R. G. Cooks, Anal. Chim. Acta, 119 (1980) 129.
2 R. A. Yost and C. G. Enke, 27th Annual Conference on Mass Spectrometry and Allied Topics, Seattle, Washington, June 1979.
3 D. L. Smith and J. H. Futrell, Int. J. Mass Spectrom. Ion Phys., 14 (1974) 171.
4 J. Diekman, J. K. MacLead, C. Djerassi and J. D. Baldeschwieler, J. Am. Chem. Soc., 91 (1969) 2069.
5 M. L. Sigsby, R. J. Day and R. G. Cooks, Org. Mass Spectrom., 14 (1979) 273.

6 F. W. McLafferty, R. Kornfeld, W. F. Haddon, K. Levsen, I. Sakai, P. F. Bente, S.-C. Tsai and H. D. R. Schuddemage, J. Am. Chem. Soc., 95 (1973) 3886.
7 J. L. Beauchamp and R. C. Dunbar, J. Am. Chem. Soc., 92 (1970) 1477.
8 J. F. Litton, Ph.D. Dissertation, Purdue University (1976).
9 R. Houriet, G. Parisod and T. Gaumann, J. Am. Chem. Soc., 99 (1977) 3599.
10 K. L. Busch, T. L. Kruger and R. G. Cooks, Anal. Chim. Acta, 119 (1980) 153.
11 T. A. Lehman and M. M. Bursey, Ion Cyclotron Resonance Spectrometry, Wiley-Interscience, New York, 1976.

Analytica Chimica Acta, 119 (1980) 145—148

Short Communication

DIRECT ANALYSIS OF MIXTURES BY DOUBLE QUADRUPOLE MASS SPECTROMETRY

G. L. GLISH and R. G. COOKS*

Department of Chemistry, Purdue University, West Lafayette, IN 47907 (U.S.A.)

(Received 3rd March 1980)

Summary. The double quadrupole mass spectrometer is shown to be applicable to differentiation of isomeric C_5 ketones and for the detection of camphor in a drug and a cosmetic. Detection limits in the picogram range are demonstrated. The similarity between the low-energy QQ collision-induced dissociations and those of high-energy MIKE spectrometry facilitates use of both techniques for mass spectrometry/mass spectrometry.

Direct analysis of mixtures by mass spectrometry/mass spectrometry (m.s./m.s.) is an alternative to g.c./m.s. [1]. The most desirable feature of m.s./m.s. is the need for little or no sample work-up, even in complex mixtures [2]. M.s./m.s. can be performed on any mass spectrometer with two or more analyzers which are independently settable. This has been demonstrated on the reversed-geometry MIKE (BE) spectrometer [3], conventional double focusing (EB) spectrometer [4], and triple quadrupole (QQQ) spectrometers [5].

This communication demonstrates the applicability of a new instrument, the double quadrupole (QQ) mass spectrometer [6], to direct analysis of mixtures by m.s./m.s. Examples are shown for analysis of isomer mixtures, detection of specific components in complex mixtures, and trace determinations.

Experimental

The instrument is described in detail in an accompanying paper [6]. All spectra were recorded using a collision cell with air as the target gas (indicated pressure of 4×10^{-5} torr; collision cell pressure of about 2—4 mtorr). The samples were introduced via a leak valve or on a direct insertion probe. Ionization was by electron impact with an electron energy of 70 eV.

Results and discussion

The most demanding problem in m.s./m.s. is the differentiation of isomers. It has been demonstrated by MIKE spectrometry that some isomers can be successfully differentiated [7], while others cannot [8] unless ionization is via a complex ion attachment process. To test whether isomers can be differentiated by using the QQ, the first example of mixture analysis by m.s./m.s. using MIKE spectrometry was repeated [9]. Three C_5 ketones, 2-

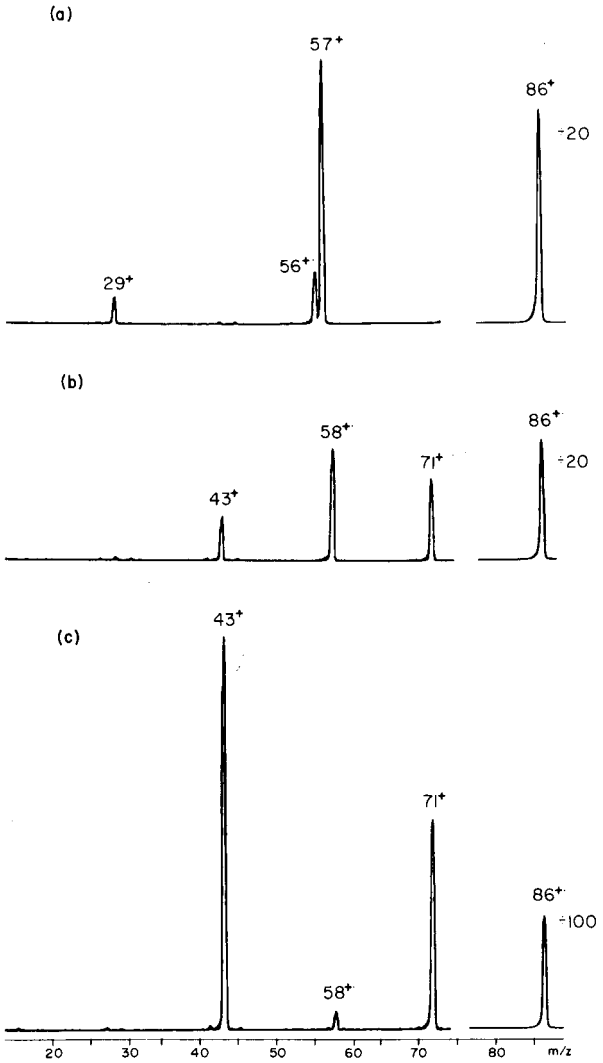

Fig. 1. QQ dissociation spectrum of the molecular ions of (a) 3-pentanone, (b) 2-pentanone, and (c) 3-methyl-2-butanone.

pentanone, 3-pentanone, and 3-methyl-2-butanone, were examined. The dissociation spectra of the compounds are shown in Fig. 1. It can be seen that 3-pentanone shows unique fragment ions, *m/z* 29, 56 and 57, compared to the two other ketones. The other two ketones, 2-pentanone and 3-methyl-2-butanone, show the same fragmentations, *m/z* 43, 58 and 71; however, the relative abundance of the fragment ions is quite different (Fig. 1). All the above fragments correspond to those seen in the MIKE spectrometric study [9]. Thus the presence in a mixture of the various isomers can be discerned

qualitatively as shown in Fig. 2. Since the system was not equipped with a heated inlet, quantification of the ketones relative to one another could not be performed, although this should be possible.

Another capability in m.s./m.s. is the analysis of crude mixtures without any sample work-up. An example of this is shown in Fig. 3; parts (a) and (b) show the QQ dissociation spectra for pure camphor and phenol, respectively. Figure 3(c) and (d) show the dissociation spectra for mass-selected 152^+ and 94^+, respectively, from a commercial skin cream. The presence of the $152^+ \rightarrow 108^+$ and $152^+ \rightarrow 81^+$ transitions in Fig. 3(c) indicate the presence of camphor in the preparation. (An identical spectrum was obtained for mass-selected 152^+ from a commercial decongestant.) In part (d) the $94^+ \rightarrow 66^+$ transition is indicative of the presence of phenol in the mixture. The difference in the ratio of 66^+ to 94^+ in the two spectra (b and d) suggests that another ion is present at *m/z* 94, either in the mixture itself or in the instrument background. This is further evidenced by the relative increase of 79^+ to 66^+ in the spectrum of the mixture.

The last example of the application of the QQ spectrometer to analysis of mixtures is in the field of trace determinations. The system studied was 3-pentanone in water. The complete dissociation spectrum was recorded in 2 min with a total consumption of 450 pg of 3-pentanone. The peak at 57^+ was recorded at a signal-to-noise ratio of 2. This corresponds to a detection limit of 5 pg for the $86^+ \rightarrow 57^+$ transition. This is quite good considering the unsophisticated nature of the present inlet system, where much of the sample may be lost during introduction.

This work was supported by the National Science Foundation CHE 77-01295. We thank Dr. Mike Story and Finnigan Corporation for technical assistance.

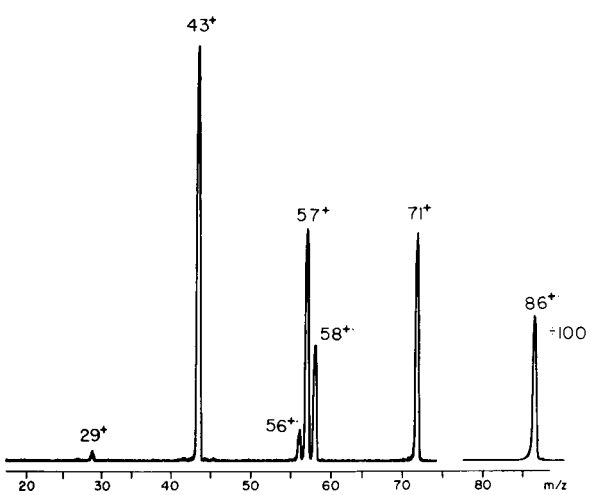

Fig. 2. M.s./m.s. spectrum of 86^+ in a 1:1:1 mixture of 3-pentanone, 2-pentanone, and 3-methyl-2-butanone.

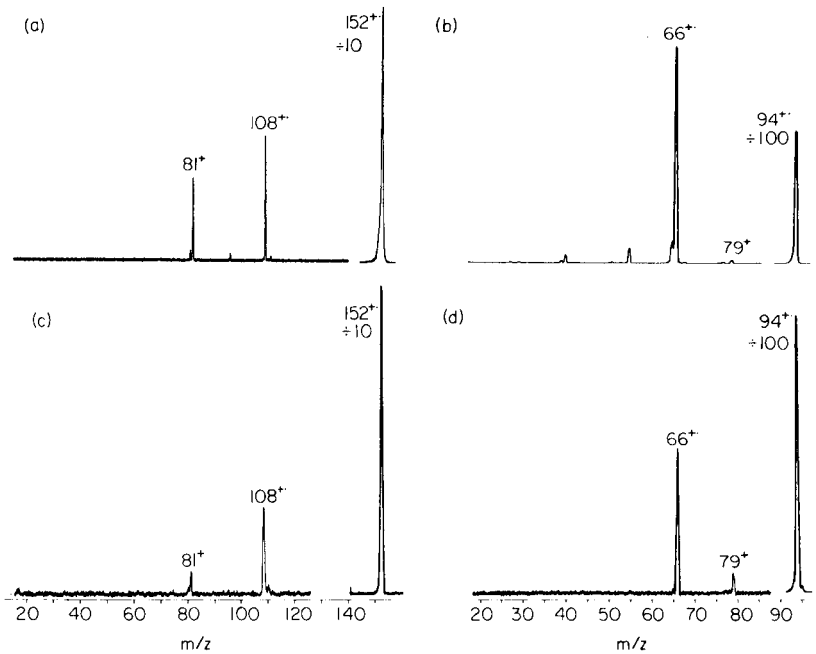

Fig. 3. QQ dissociation spectrum of (a) camphor molecular ion, (b) phenol molecular ion, (c) 152^+ from commercial skin cream, and (d) 94^+ from skin cream.

NOTE ADDED IN PROOF

Recently the QQ has been fitted with a chemical ionization (CI) source. M.s./m.s. spectra taken on the QQ using CI differ much more from their MIKE spectrometric counterparts than do the corresponding electron impact (EI) spectra. It has been determined using a new instrument, a BQ mass spectrometer (magnetic sector followed by a quadrupole), that this is due to effects of ion translational energy upon differences in energy deposition. Dissociation of the odd-electron molecular ions formed by EI often requires less energy and is therefore less affected by translational energy than is dissociation of the even-electron ions generated by CI.

REFERENCES

1 T. L. Kruger, J. F. Litton, R. W. Kondrat and R. G. Cooks, Anal. Chem., 48 (1976) 2113.
2 R. W. Kondrat, R. G. Cooks and J. L. McLaughlin, Science, 199 (1978) 978.
3 R. W. Kondrat and R. G. Cooks, Anal. Chem., 50 (1978) 81A.
4 W. F. Haddon, 178th ACS Meeting, Washington, D.C., September 1979.
5 R. A. Yost and C. G. Enke, 27th Annual Conference on Mass Spectrometry and Allied Topics, Seattle, Washington, June, 1979; D. F. Hunt, J. Schabanowitz and A. Giordani, 27th Annual Conference on Mass Spectrometry and Allied Topics, Seattle, Washington, June, 1979.
6 D. Zakett, W. J. Fies and R. G. Cooks, Anal. Chim. Acta, 119 (1980) 129.
7 A. E. Schoen, R. G. Cooks and J. L. Wiebers, Science, 203 (1979) 1249.
8 D. Zakett, V. M. Shaddock and R. G. Cooks, Anal. Chem., 51 (1979) 1849.
9 T. L. Kruger, J. F. Litton and R. G. Cooks, Anal. Lett., 9 (1976) 533.

Analytica Chimica Acta, 119 (1980) 149—152

Short Communication

FUNCTIONAL GROUP SCREENING OF COMPLEX MIXTURES WITH A DOUBLE QUADRUPOLE MASS SPECTROMETER

D. ZAKETT, P. H. HEMBERGER and R. G. COOKS*

Department of Chemistry, Purdue University, West Lafayette, IN 47907 (U.S.A.)

(Received 3rd March 1980)

Summary. A double quadrupole mass spectrometer is used to obtain mass spectra which represent only those species in a complex mixture which undergo fragmentation with loss of a constant neutral moiety. Examples are given where these spectra for $Br^{\bullet}$ loss and $NO_2^{\bullet}$ loss allow recognition of bromo compounds and the nitro functional group in complex mixtures. The method is easier to implement than the corresponding scans on a sector instrument.

The identification of particular constituents in complex mixtures can be achieved by mass spectrometry/mass spectrometry (m.s./m.s.) [1]. Examples of the application of the QQ mass spectrometer in identifying specific compounds in mixtures have been reported [2]. A more difficult problem occurs when possible mixture constituents cannot be specified in advance. In such cases rapid screening of complex mixtures for particular functional groups can be readily accomplished by using a mass spectrometer with two stages of quadrupole mass analysis.

This type of functional group screening is based on the detection of collision-induced or metastable ion fragmentations which result either in an ion at a characteristic mass or loss of a characteristic neutral fragment. The concept of a scan which detects only metastable or collision-induced fragmentations involving loss of a constant neutral mass (m_3, for the reaction $m_1^+ \rightarrow m_2^+ + m_3$) from each ion produced in a mass spectrometer source has recently been described [3]. This type of scan, termed a neutral loss scan, has been implemented on a reversed-geometry (BE) magnetic instrument [4] and on a normal-geometry (EB) mass spectrometer [5]. Both applications require computer control and non-linear linked scanning of the magnetic and electric sectors. The scan mode which detects charged fragments of a constant mass from all precursor ions has also proved useful in mixture analysis on both BE [4] and EB [5, 6] mass spectrometers. This scan mode, a selected fragment ion scan, is implemented on QQ (or QQQ) mass spectrometers merely by setting the final quadrupole mass filter, Q_2, to transmit the mass of the fragment of interest and by performing a normal mass scan of the first quadrupole, Q_1.

Experimental

The QQ mass spectrometer [7] uses two Finnigan 3000 r.f. units to power the quadrupoles. The experiments reported here were done using the earlier instrumental configuration which did not include a separate collision cell. The sample itself served as collision gas. An external voltage (0—10 V) can be used to control the mass scan of each r.f. unit. Likewise, a voltage monitor ("sweep-out") allows the mass to be monitored when the r.f. unit is operated in the internal mass scan mode. The neutral loss experiment consisted of operating Q_1 in the internal mass scan mode and using the "sweep-out" voltage monitor of Q_1 as an input to a simple linear amplifier which scaled the "sweep-out" voltage to the value required to transmit $(m_1 - m_3)^+$ through Q_2. This voltage was then used to control Q_2 through the Q_2 external mass set input. During the actual experiment, Q_1 was scanned automatically and repetitively, and Q_2 was driven by the amplifier circuit to track Q_1 with a fixed voltage difference appropriate to the value of the neutral mass selected.

Figure 1 shows a plot of external mass set voltage versus transmitted ion mass for both Q_1 and Q_2. The slopes differ because Q_1 and Q_2 were operated at different frequencies, 2.14 and 1.85 MHz, respectively. If both Q_1 and Q_2 were operated at the same frequency and had identical physical characteristics, the slopes would be the same and a neutral loss scan could be achieved by a simple voltage subtraction circuit. In practice, even at the same frequency the slopes differ enough to require a slightly more complicated circuit.

A linear regression of external mass set voltage versus transmitted mass was calculated for both Q_1 and Q_2 from experimentally measured values (Fig. 1) as $V_1 = -0.02710\ m + 0.06218$ and $V_2 = -0.01938\ m + 0.02862$, where V is the external mass set voltage (volts) and m is the mass of the ion transmitted through the quadrupole. The amplifier circuit used is given in Fig. 2. The first stage buffers the sweep monitor output from Q_1. Rearrangement of these equations leads to $V_2 = 0.71576\ V_1 - 0.01589$, which may be used to specify the circuit parameters in the second stage. This stage scales the buffered output of Q_1 to provide a control voltage which causes Q_2 to track exactly with Q_1. In the third stage, the neutral loss voltage $(0.01938\ m_3)$ is then

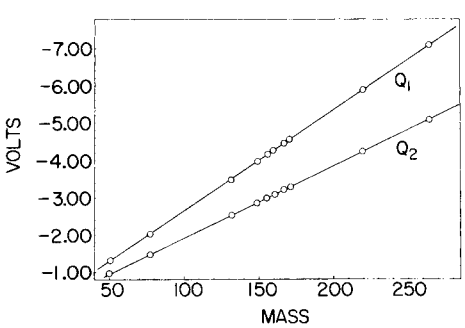

Fig. 1. Plot of external d.c. control voltage vs. transmitted ion mass for quadrupoles Q_1 (2.14 MHz) and Q_2 (1.85 MHz).

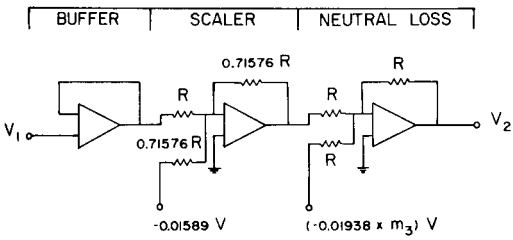

Fig. 2. Schematic diagram of the control circuit used to implement a constant neutral loss scan.

subtracted from the scaled control voltage to cause Q_2 to track Q_1 with a fixed difference in mass corresponding to the desired neutral loss.

Results and discussion

In a typical neutral loss experiment two spectra are acquired: the first is the normal mass spectrum of the mixture introduced into the source and the second is the neutral loss scan. A response in the second indicates that the precursor ion being transmitted by the first mass analyzer (Q_1) is undergoing loss of the selected neutral moiety in the interquadrupole region and the fragment ion corresponding to $(m_1 - m_3)^+$ is transmitted through the second mass analyzer (Q_2).

Figure 3 shows the EI mass spectrum of a mixture containing propyl bromide (*m/z* 122/124), bromobenzene (*m/z* 156/158) and perfluorotributylamine. It also shows a scan corresponding to loss of a neutral ^{79}Br radical. Only two peaks appear in the neutral loss scan above *m/z* 90; these correspond to the loss of $^{79}Br^+$ from the bromine-containing ions exiting Q_1. The peaks seen in the neutral loss spectrum below mass 90 are artifacts resulting from r.f.-only transmission through Q_2 which occurs at low mass values. For example, when Q_1 is passing *m/z* 80, Q_2 is passing *m/z* (80 — 79) = *m/z* 1. At these low *m/z* values, the d.c. component on Q_2 is nearly zero and Q_2 acts as an r.f.-only quadrupole, allowing undissociated precursor ions to be transmitted to the detector. Therefore, the significant portion of the neutral loss spectrum should be considered to be that region in which $(m_1 - m_3)^+ \geqslant 4$ amu, a precursor mass $\geqslant 84^+$ in Fig. 3.

A similar experiment is shown in Fig. 4 where a mixture containing several nitro compounds was ionized under EI conditions. A neutral loss scan for $(M - 46)^+$ clearly indicates all of the compounds present which lose NO_2 as a result of collision-induced dissociation.

Neutral loss scans hold the potential for rapid screening of complex mixtures for particular classes of compounds. This screening is optimal when a soft ionization method such as CI or FD is employed since fragment ions are then avoided in the first stage of mass analysis. This study has shown that neutral loss scans are easily implemented on tandem quadrupole mass spectrometers, and in fact the experiment is considerably simpler than that

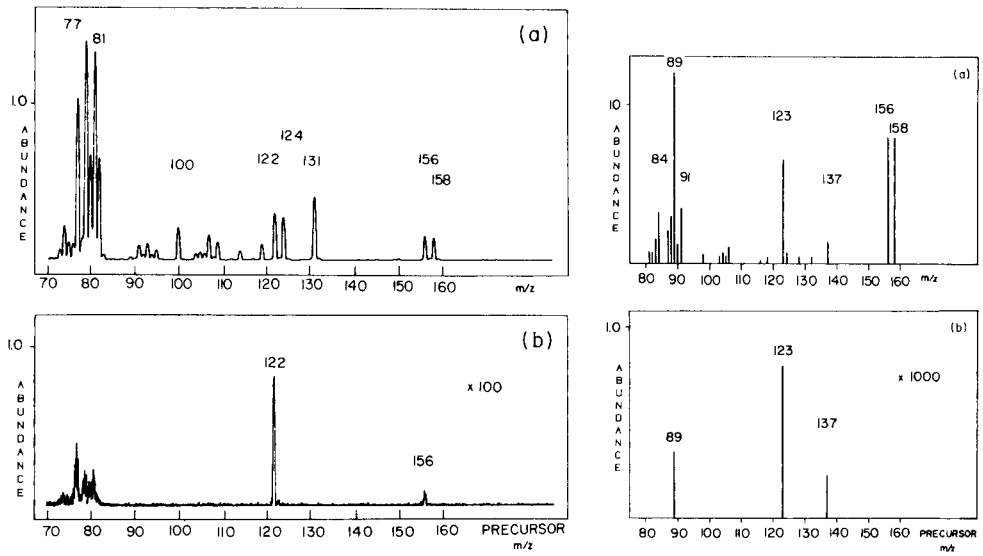

Fig. 3. Comparison of (a) the EI mass spectrum and (b) the neutral loss spectrum (loss of 79) for a mixture which included bromobenzene (M = 156, 158) and propyl bromide (M = 122, 124).

Fig. 4. Comparison of (a) the EI mass spectrum and (b) the neutral loss spectrum (loss of 46) for a mixture which included nitrobenzene (M = 123), m-nitrotoluene (M = 137), and 2-nitropropane (M = 89).

[4] on magnetic instruments. An analog scanning circuit was used in this application, but implementation of these scans under digital control should be straightforward.

This work was supported by the National Science Foundation CHE 77-01295. We thank Finnigan Corporation and Mr. W. J. Fies for assistance.

REFERENCES

1 R. W. Kondrat and R. G. Cooks, Anal. Chem., 50 (1978) 81A; R. A. Yost and C. G. Enke, J. Am. Chem. Soc., 100 (1978) 2274; P. F. Bente III and F. W. McLafferty, in C. Merritt, Jr. and C. N. McEwen (Eds.), Mass Spectrometry, M. Dekker, New York, 1979.
2 G. L. Glish, P. H. Hemberger and R. G. Cooks, Anal. Chim. Acta, 119 (1980) 137.
3 M. J. Lacey and C. G. MacDonald, Anal. Chem., 57 (1979) 691.
4 D. Zakett, A. E. Schoen, R. W. Kondrat and R. G. Cooks, J. Am. Chem. Soc., 101 (1979) 6781.
5 W. F. Haddon, Org. Mass Spectrom., in press.
6 E. Gallegos, Anal. Chem., 48 (1976) 1348.
7 D. Zakett, R. G. Cooks and W. J. Fies, Anal. Chim. Acta, 119 (1980) 129.

Analytica Chimica Acta, 119 (1980) 153—156

Short Communication

CHARGE EXCHANGE USING A DOUBLE QUADRUPOLE MASS SPECTROMETER

K. L. BUSCH, T. L. KRUGER and R. G. COOKS*

Department of Chemistry, Purdue University, West Lafayette, IN 47907 (U.S.A.)

(Received 3rd March 1980)

Summary. Charge exchange mass spectra obtained on a double quadrupole (QQ) mass spectrometer are compared with those obtained by other methods. The effects of reagent ion recombination energies and of axial ion translational energy on these spectra are followed.

The resonant charge exchange process $X^{+\cdot} + M \rightarrow M^{+\cdot} + X$, $\Delta E = 0$, yields a molecular ion $M^{+\cdot}$ whose internal energy is the difference between the ionization potential of the sample M and the recombination energy of the reagent ion $X^{+\cdot}$. Molecular ions of specified energies can thus be produced by appropriate choice of the reagent ion, and mass spectra recorded for well-defined internal energies [1—4]. Charge exchange mass spectrometry has usually required the use of complex tandem mass spectrometers, although the experiment has also been carried out with commercial double focusing mass spectrometers [5]. In addition, ionization by charge exchange can be effected using high pressure and other modified sources, although care must be taken to employ conditions which minimize ionization by extraneous species [6, 7].

To produce charge exchange mass spectra with a double quadrupole instrument [8], the first quadrupole is used to mass-select the reagent ion of interest and to pass this ion into a collision cell where the charge exchange reaction with the sample can take place. The second mass analyzer identifies fragments from the sample molecular ion.

Experimental

The double quadrupole instrument has been described [8]. Reagent ions were formed by 70-eV electrons in a standard Finnigan electron impact source. Reagent gas introduced into the source gave a pressure of 3×10^{-5} torr at the ion gauge mounted over the diffusion pump. Samples were introduced via a leak valve into the interquadrupole region until the total pressure at the ion gauge rose to 6×10^{-5} torr. No separate collision cell was used in these experiments.

Results and discussion

The charge exchange mass spectra of cyclohexene using $Xe^{+\cdot}$, $Ar^{+\cdot}$, and $Ne^{+\cdot}$ as reagent ions are shown in Fig. 1. The rare gases were chosen for this

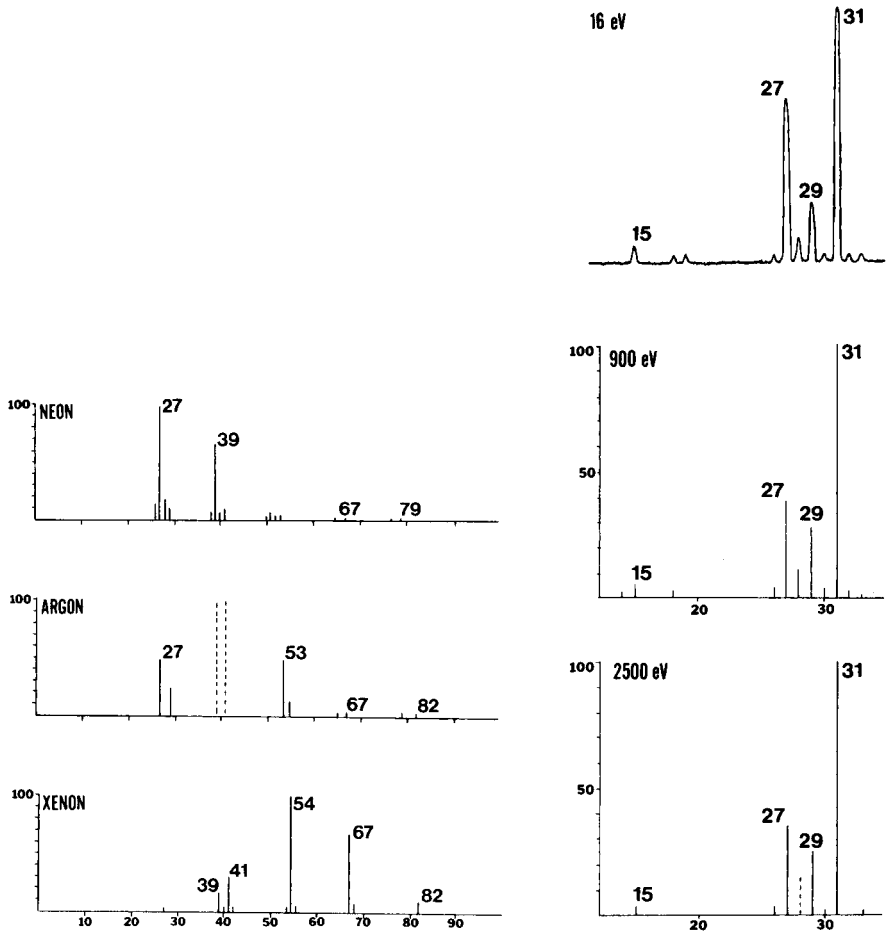

Fig. 1. Charge exchange mass spectra of cyclohexene with the reagent ions shown. These results, taken at an axial ion translational energy of 30 eV, agree with those obtained [5] at 2500 eV. The argon data are normalized to allow for the fact that the reagent ion (m/z 40) obscures the adjacent masses (dashed lines).

Fig. 2. Portion of the $Ar^{+\cdot}$ charge exchange mass spectrum of n-propanol which includes the abundant fragment ions. Spectra were taken using (a) a QQ spectrometer, axial $Ar^{+\cdot}$ translational energy 16 eV, (b) transverse tandem mass spectrometer, 900 eV [10], and (c) conventional high-resolution mass spectrometer, 2500 eV [5].

experiment because they have well-defined internal energies. For a resonant process, the recombination energies [9] of 12.1, 15.7, and 21.6 eV would result in 3.2, 6.8, and 12.7 eV of energy deposition in the molecular ion of cyclohexene (ionization potential of 8.9 eV), respectively. Greater fragmentation is expected from those molecular ions with more internal energy. Accordingly, the charge exchange mass spectrum formed by xenon contains

an observable molecular ion while that formed by neon does not. Fragmentations to form m/z 67 (loss of methyl) and m/z 54 (loss of ethylene) (predominate in the xenon charge exchange mass spectrum. Abundant fragment ions at m/z 27 ($C_2H_3^+$) and m/z 39 ($C_3H_3^+$) form from the more energetic molecular ion produced by neon. The argon charge exchange mass spectrum is intermediate between those of $Ne^{+\cdot}$ and $Xe^{+\cdot}$. A molecular ion is observed, but with a smaller relative abundance than in the spectrum obtained with xenon. In agreement with previous results [5], a fragment ion appears at m/z 53 rather than m/z 54. The argon reagent ion at m/z 40 precludes observation of the fragment ions from cyclohexene at m/z 39 and m/z 40, which are typically 1000 times less intense than the reagent ion. The $Xe^{+\cdot}$ and $Ar^{+\cdot}$ spectra agree well with those obtained on a double-focusing mass spectrometer at 2.5 keV [5].

The argon charge exchange mass spectrum of 1-propanol as determined on the double quadrupole mass spectrometer is shown in Fig. 2. Included for the sake of comparison are spectra obtained on other instruments [5, 10]. Despite the differences in the axial translational energy of the reagent ion, the spectra are quite similar. Conversion of the axial translational energy of the reagent ion beam to internal energy of the product ions seems not to occur to a significant extent.

Any ion which can be mass-selected by the first quadrupole can be used as the reagent ion in a charge exchange experiment, although polyatomic ions are not ideal charge exchange reagents because both products can be internally excited so that product ions of known internal energy are not formed. Figure 3 shows charge exchange spectra of benzene using $CH_3OH^{+\cdot}$, $N_2^{+\cdot}$, and $Ar^{+\cdot}$ as reagent ions. As expected, the degree of fragmentation is still a function of the recombination energy of the reagent ion. These reagent ions are expected [9] to deposit 2.8, 6.4, and 6.5 eV of energy into the products, with the bulk going to the larger benzene molecular ion [10].

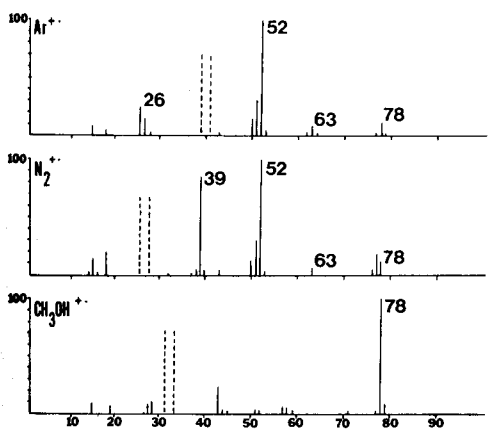

Fig. 3. Charge exchange mass spectra of benzene obtained using $CH_3OH^{+\cdot}$, $N_2^{+\cdot}$, and $Ar^{+\cdot}$ as reagent ions, with nominal energy depositions of 2.8, 6.4, and 6.5 eV, respectively [9]. Regions of the spectrum obscured by reagent ions are within the dashed lines.

TABLE 1

Charge exchange mass spectra of acetylene as a function of the translational energy of an $Ar^{+\cdot}$ reagent ion beam

m/z	Relative abundance at nominal ion energy (eV)								
	7[a]	10	20	25[a]	30	40	40[a]	50	60
26	100	100	100	100	100	100	100	100	100
25	35	22	64	75	78	68	50	61	58
13	0	1	2	20	4	6	25	7	10

[a]Data from ref. 11.

The ion energy in the double quadrupole mass spectrometer is independently variable over the range 1–100 V by use of an external d.c. power supply. Some charge exchange mass spectra are known to show dependence on the axial translational energy of the reagent ion beam [2, 11]. The effect of the ion energy on the appearance of the charge exchange mass spectrum was determined for the system $Ar^{+\cdot}$ and acetylene. Table 1 illustrates the spectral variation. The trends observed are similar to those reported in an earlier study [12]. Agreement is not quantitatively identical, however, presumably because of the wider energy bandpass in the quadrupole.

The utility of this relatively simple mass spectrometer for charge exchange studies has been demonstrated. The spectra obtained are similar to those determined with more complicated instruments.

This work was supported by the National Science Foundation CHE 77-01295. We thank Finnigan Corporation and Dr. Mike Story for assistance.

REFERENCES

1 E. Lindholm, in J. L. Franklin (Ed.), Ion Molecule Reactions, Vol. 2, Plenum, New York, 1972, p. 457.
2 E. Lindholm, Ion Molecule Reactions in the Gas Phase, Advances in Chemistry Series, No. 58, American Chemical Society, Washington, DC, 1966, p. 1.
3 J. H. Futrell and T. O. Tiernan, in J. L. Franklin (Ed.), Ion Molecule Reactions, Vol. 2, Plenum, New York, 1972, p. 485.
4 C. Lifshitz and T. O. Tiernan, J. Chem. Phys., 57 (1972) 1515.
5 C. S. Hsu and R. G. Cooks, Org. Mass Spectrom., 11 (1976) 975.
6 I. Jardine and C. Fenselau, Anal. Chem., 47 (1975) 730.
7 J. Turk and R. H. Shapiro, Org. Mass Spectrom., 5 (1971) 1373.
8 D. Zakett, R. G. Cooks and W. J. Fies, Anal. Chim. Acta, 119 (1980) 129.
9 H. M. Rosenstock, K. Draxl, B. W. Steiner and J. T. Herron, J. Phys. Chem. Ref. Data, 6 (1977) Suppl. 1.
10 M. L. Vestal, in P. Ausloos (Ed.), Fundamental Processes in Radiation Chemistry Interscience, New York, 1968, p. 59.
11 E. Pettersson, Ark. Fys., 25 (1963) 181.
12 W. B. Maier II, J. Chem. Phys., 42 (1965) 1790.

Analytica Chimica Acta, 119 (1980) 157—160

Short Communication

DETERMINATION OF TRACES OF CHROMIUM(VI) AS A THIOSEMICARBAZIDE COMPLEX BY SOLVENT EXTRACTION AND ATOMIC ABSORPTION SPECTROMETRY

WEN-JWU WANG

Department of Chemistry, Tamkang College, Tamsui, Taiwan 251 (Taiwan)

(Received 26th November 1979)

Summary. Extraction of chromium(VI) at pH 2—12 with thiosemicarbazide into methyl isobutyl ketone is described. The detection limit is 30 ng ml^{-1}, and the concentration which gives 1% absorbance is 60 ng ml^{-1}, when the organic phase is used directly.

One method frequently used for preconcentration in atomic absorption spectrometry (a.a.s.) is solvent extraction [1]. The determination of chromium(VI) can be made more sensitive by extracting chromium as its pyrrolidine dithiocarbamate [1—4] or diethyldithiocarbamate [5] complex into methyl isobutyl ketone (MIBK). However, the applications of these reagents are limited by the instability of the reagents in acidic solutions. Ichinose et al. [6] reported the quantitative extraction of chromium (1 ppm) into MIBK from sulfuric, hydrochloric or nitric acid solutions containing 0.03 M hydrogen peroxide at pH 1.2—2.5. However, extraction decreased rapidly at pH values higher than 2.5 and the solutions were stable for only 20—30 min.

Thiosemicarbazide was chosen for investigation as a chelating agent for chromium because it has both a hard base site (nitrogen) and a soft base site (sulfur), and is well known as a useful chelating agent for transition metal ions [7]. It will be shown that a one-step extraction can be used to concentrate traces of chromium from aqueous solutions over the wide pH range 2—12, prior to direct analysis of the extract by a.a.s.

Experimental

Apparatus. A Varian-Techtron Model 1200 atomic absorption spectrometer was used with a chromium hollow-cathode lamp operated at a lamp current of 5.0 mA. The wavelength used was 357.9 nm and the spectral bandpass 0.2 nm. The flow rates of air and acetylene were 14 and 1.8 l min^{-1}, respectively.

Reagents. A 1000 ppm chromium standard solution (potassium dichromate in water; Wako Pure Chemicals) was used to prepare a 1 ppm solution daily [8]. Thiosemicarbazide was recrystallized from ethanol and used as an aqueous 1000 ppm solution for the extraction. Distilled deionized water was used throughout. Analytical-grade chemicals were used for preparing buffer solutions and for interference studies.

Extraction procedure. Solutions (30 ml) containing 0—30 μg of chromium in hydrochloric acid (or sodium hydroxide) of various concentrations, and hydrogen peroxide (30%, 1 ml) were transferred to separatory funnels, and 10 ml of MIBK and 1 ml of the above thiosemicarbazide solution were added. After shaking for 30 min, the aqueous layer was discarded. The organic layer was used for a.a.s. There was no difference in absorbance between MIBK alone and MIBK which had been treated as above in the absence of chromium ion, hence untreated MIBK was used directly as a reference.

Results and discussion

Effect of reaction conditions on extraction. The pH dependence of the extraction of chromium with thiosemicarbazide (1 mg ml^{-1}) in MIBK was examined in the pH range 2—12. The pH was adjusted with sodium hydroxide and hydrochloric acid and monitored with a pH meter. The results (Fig. 1) show that pH has only a slight effect on extraction efficiency over this pH range. The optimal pH was 7; the small decline in efficiency at higher pH is probably due to decreased solubility of the chelate, and at lower pH to decomposition of the chelate or extraction of a protonated form.

The rate of extraction of 1 μg Cr ml^{-1} at pH 7 under the recommended conditions was examined by shaking the two phases for 0.5—100 min. At such a low concentration it was expected that fairly long shaking times would be necessary for appreciable extraction [9, 10]; maximum extraction was attained only after shaking for 20—30 min, after which prolonged extraction up to 100 min had no effect. Extraction efficiency and precision were adversely affected when the shaking time was less than 10 min, probably because a fine precipitate was formed in the aqueous phase when thiosemicarbazide was added, and dissolution of this precipitate was rather slow.

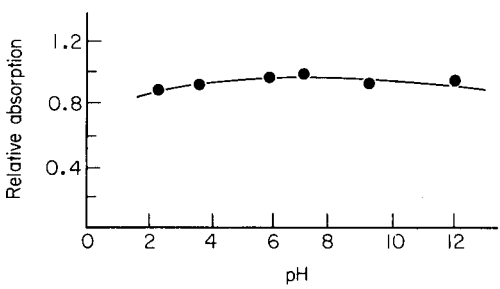

Fig. 1. pH dependence of the extraction of chromium (30 μg) by thiosemicarbazide—methyl isobutyl ketone. (Absorbance relative to pH 7 which is 0.161.)

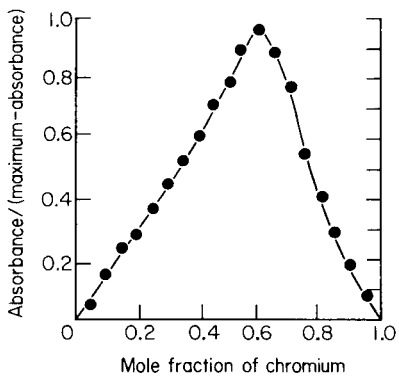

Fig. 2. Continuous variations plot for chromium(VI)—thiosemicarbazide complex (maximum absorbance ratio = 0.96; total concentration of metal and ligand = 1×10^{-4} M).

The effect of the reagent concentration on the extraction of 1 μg Cr ml^{-1} was studied. The absorbance increased linearly up to 15 μg ml^{-1} thiosemicarbazide and then became constant; a final concentration rather in excess of this value was therefore selected for routine use.

Calibration curve. When the recommended procedure was used, a.a.s. measurements gave a linear calibration graph for chromium over the range 0—1 μg ml^{-1}; the concentration which gave 1% absorbance was 0.060 μg Cr ml^{-1}. Comparison with results obtained for standard solutions prepared directly in the organic phase showed that more than 96% of the chromium was extracted from the aqueous solution. The relative standard deviation of the a.a.s. method, obtained from 5 determinations of 1 μg Cr ml^{-1}, was 1.5%. A comparison with the precision obtained by solvent extraction—a.a.s. procedures is given in Table 1. The detection limit (i.e., the concentration that corresponds to twice the standard deviation near the blank level) was 0.030 μg Cr ml^{-1} in the aqueous solution.

Stoichiometry of the extracted complex. The stoichiometry of the reaction was studied using a modified continuous variations method [11]. The absorbance of the extract prepared by following the recommended procedure with pure MIBK instead of the thiosemicarbazide mixture was zero. This shows that the chromium(VI) ion cannot be extracted into pure MIBK at pH 7, which simplifies the procedure. The continuous variations plot obtained (Fig. 2) confirms that the mole ratio of thiosemicarbazide to chromium in the reaction is 2:3. The distribution coefficient calculated is 5.43×10^{23}. These results indicate that thiosemicarbazide is a very strong extracting agent, and forms a strong complex.

Stability of extracted species. One of the shortcomings of the common ammonium pyrrolidine dithiocarbamate—MIBK extraction system is the instability of the complexes in the organic phase. To test the stability in the present system, several solutions were extracted as described under the recommended procedure, and the separatory funnels were left under diffuse daylight. The absorbances of the organic phases were measured at different

TABLE 1

Comparison of precision of various extraction—a.a.s. methods for chromium (1 μg ml^{-1})

Method	Ref.	Mean absorbance	S.d.[a]	R.s.d. (%)
Thiosemicarbazide	This work	0.161	0.0025	1.5
MIBK	4	0.15	0.033	22
MIBK—HNO_3	4	0.15	0.022	14
Diethyldithiocarbamate/MIBK	5	0.049	0.0018	3.7

[a] 5 measurements.

times after extraction. No change in their absorbance could be found for up to three days. After this, the absorbance decreased gradually.

Interferences. Various authors [12, 13] have found interference in air—acetylene flames from copper, barium, aluminium, magnesium, calcium, cobalt, iron and nickel. The reason for the iron and aluminium interferences is the ease of hydrolysis of iron and aluminium, even at rather low pH values, which causes coprecipitation of chromium. Since large excesses of transition metal could be expected in samples, the contribution of large excesses of such metals was investigated. The atomic absorption of solutions containing various metal ions (1 mg ml^{-1}) with 1 μg Cr ml^{-1} was measured. The results showed that manganese(II), iron(III), cobalt(II), nickel(II) and aluminium(III) did not interfere at this level.

The author wishes to thank Mr. I-Cher Shen for preparing the samples and measuring the absorption data.

REFERENCES

1 M. S. Cresser, Solvent Extraction in Flame Spectroscopic Analysis, Butterworth, London, 1978.
2 C. E. Mulford, At. Absorpt. Newsl., 5 (1966) 88.
3 R. E. Mansell and H. W. Emmel, At. Absorpt. Newsl., 4 (1965) 365.
4 T. K. Jan and D. R. Young, Anal. Chem., 50 (1978) 1250.
5 J. Nix and T. Goodwin, At. Absorpt. Newsl., 9 (1970) 119.
6 N. Ichinose, T. Inui, S. Terada and T. Mukoyama, Anal. Chim. Acta, 96 (1978) 391.
7 M. J. M. Campbell, Coord. Chem. Rev., 15 (1975) 279.
8 A. Glasner and M. Steinberg, Anal. Chem., 27 (1955) 2008.
9 L. G. Danielsson, B. Magnusson and S. Westerlund, Anal. Chim. Acta, 98 (1978) 47.
10 E. A. Jones, A. Warshawsky, K. Dixon, D. J. Nicolas and T. W. Steele, Anal. Chim. Acta, 94 (1977) 257.
11 W. Likussar and D. F. Boltz, Anal. Chem., 43 (1971) 1265, 1273.
12 M. Yanagisawa, M. Suzuki and T. Takeuchi, Anal. Chim. Acta, 52 (1970) 386.
13 L. Wilson, Anal. Chim. Acta, 40 (1968) 503.

Analytica Chimica Acta, 119 (1980) 161—166

Short Communication

THE DETERMINATION OF BARIUM, LANTHANUM AND MAGNESIUM IN PANCREATIC ISLETS BY ELECTROTHERMAL ATOMIC ABSORPTION SPECTROMETRY

PER-OLOF BERGGREN

Department of Histology, Biomedicum University of Uppsala, S-751 23 Uppsala (Sweden)

(Received 26th February 1980)

Summary. Barium and lanthanum are determined by direct injection of freeze-dried samples (1—15 μg), and magnesium by injection of 2-μl aliquots of a homogenized suspension. The amounts found are 5.5 (±0.7), 219 (±7) and 28±6 mmol kg^{-1} (dry weight) for Ba, La and Mg, respectively.

The determination in biological samples of traces of metals involved in the physicochemical reactions underlying many cellular functions can be achieved by atomic absorption spectrometry [1—6]. The high-sensitivity requirement is accentuated when only minute amounts of material are available, as exemplified by the endocrine part of the pancreas, the islets of Langerhans, which consist of only microgram amounts of tissue. However, even in this unfavourable situation it has been possible to determine zinc and calcium with an electrothermal atomizer [7, 8].

The calcium ion is involved in a variety of physiologically important processes including the regulation of insulin secretion from the β-cells located in the pancreatic islets [9—12]. Calcium analogues and antagonists are important tools in the exploration of Ca^{2+}-regulated mechanisms. Barium ions resemble calcium ions in penetrating cells and activating Ca^{2+}-dependent processes [9]. Lanthanum ions compete with calcium ions for negatively charged membrane sites, resulting in a hyperstabilization of the membrane and prevention of calcium transport [9]. Unlike barium and lanthanum ions, the magnesium ion is a physiological constituent of tissues. The action of magnesium ions is antagonistic to calcium ions in many biological systems [9].

The present communication describes the application of atomic absorption spectrometry with the Varian-Techtron carbon rod atomizer for direct determinations of barium, lanthanum and magnesium in microgram amounts of freeze-dried biological material.

Experimental

Apparatus. A Varian-Techtron AA-6 atomic absorption spectrometer, provided with background correction and fitted with a carbon rod atomizer (CRA-90), was used. The heating rate of the graphite furnace was controlled independently of the final temperature by the device described by Lundgren

[13]. A three-step temperature program was employed involving drying, ashing and atomization as shown in Table 1. The graphite furnace was flushed with argon at 5 l min^{-1}. To reduce gas consumption, a control unit was connected to the atomizer [14]. The signal damping of the AA-6 readout module was modified to obtain a faster response time. The value of the "DAMP A" time constant was thus altered from the original 260 ms to 47 ms [15]. A peak reader module was connected to the recorder output of the spectrometer [16], providing simultaneous recording of the peak height and peak area. For peak shape control a fast-response (250 ms) strip-chart recorder (Philips 8202) was used. Background correction was used only for magnesium measurements as the background absorption in the lanthanum and barium measurements was negligible.

Reagents and biological material. All chemicals were of analytical grade and were dissolved in distilled-deionized water. The standard solutions were prepared from $BaCl_2 \cdot 2H_2O$ (Merck), La_2O_3 and $MgSO_4 \cdot 7H_2O$ (British Drug Houses). The lanthanum oxide was dissolved in a minimal volume of (1 + 1) nitric acid. Islets of Langerhans were microdissected from adult non-inbred obese-hyperglycemic mice (*ob/ob*) [17].

Procedure. Calibration solutions (2 μl) were placed in the graphite furnace from a microsampler (Unimetrics) with a disposable teflon tip. After incubation for 60 min at 37°C in physiological media either with or without supplementation with barium (2.56 mM) or lanthanum (1 mM), the islets were freeze-dried and weighed on a quartz-fibre balance [18]. The dried samples (1—15 μg) were placed directly into the graphite furnace for measuring barium and lanthanum. In the magnesium measurements the islets were first homogenized in 50 μl of distilled-deionized water and 2-μl samples were then injected into the graphite furnace. Barium, lanthanum or magnesium was determined under the optimized operating conditions given in Table 1.

Interference studies. The recoveries of the metals studied were investigated

TABLE 1

Operating conditions

Element analyzed	Barium	Magnesium	Lanthanum
Wavelength (nm)	350.2	202.5	550.1
Spectral bandpass (nm)	0.15	0.20	0.15
Lamp current (mA)	17.5	7.5	15.0
Drying cycle	90°C for 50 s (22.6 s)[a]	90°C for 60 s (22.6 s)[a]	90°C for 50 s (22.6 s)[a]
Ashing cycle	1030°C for 60 s (2.6 s)[a]	800°C for 50 s (2.0 s)[a]	800°C for 60 s (2.6 s)[a]
Atomizing cycle	2250°C for 3.5 s (1.6 s)[a]	1900°C for 2.5 s (1.4 s)[a]	2000°C for 10.0 s (1.6 s)[a]

[a]Time required to reach set temperature; total time includes this period.

when the salts listed in Table 2 were present. The salts were added to aqueous solutions of barium (44 μM), lanthanum (1080 μM) and magnesium (6 μM). Table 2 shows the amount of each present in the sample solution on the carbon rod. The recoveries of the metals were also studied after addition of amounts equivalent to those found in incubated islets. Islets without added metals served as controls.

Results and discussion

Because of its greater sensitivity, electrothermal atomic absorption spectrometry was preferred to the flame method for direct measurements of barium, lanthanum and magnesium in minute amounts of dried, β-cell rich pancreatic islets. The amounts of these metals present, incubated under the present conditions, were in the range 25—125 pmol of barium, 720—3600 pmol of lanthanum and 4—20 pmol of magnesium per islet. Calibration graphs within these intervals were linear for barium, whereas the lanthanum graph curved upwards slightly, and the magnesium graph curved slightly downwards (Fig. 1). However, these moderate deviations from linearity were reproducible and presented no serious problem since they were reproducible. The coefficient of variation in measuring 7 samples of 60 pmol of barium on different occasions over a period of one month was 9%. The corresponding coefficients for 8 samples of 2200 pmol of lanthanum over one month and 10 samples of 8 pmol of magnesium over two months were 17% and 8%,

TABLE 2

Effect of various substances on the determination of barium (88 pmol), lanthanum (2160 pmol) and magnesium (12 pmol)

Salt added	Amount (nmol)	Ba response (%)[a]	La response (%)[a]	Mg response (%)[a]
NaCl	20	94.5 ± 3.0	95.4 ± 11.1	110.0 ± 3.0
$NaHCO_3$	20	92.0 ± 5.9	95.1 ± 8.7	111.0 ± 1.2
NaH_2PO_4	20	97.8 ± 3.6	99.4 ± 3.6	89.9 ± 2.8
$MgSO_4$	20	17.8 ± 6.1	86.5 ± 5.1	—
$MgSO_4$	2	89.3 ± 10.5	91.3 ± 9.2	—
$MgCl_2$	20	62.0 ± 19.2	93.0 ± 6.5	—
$MgCl_2$	2	98.5 ± 8.8	87.7 ± 6.3	—
KCl	20	106.2 ± 13.0	115.2 ± 10.6	94.9 ± 3.3
$CaCO_3$	20	95.8 ± 3.1	68.4 ± 16.7	102.3 ± 2.6
$CaCO_3$	2	100.8 ± 8.8	94.5 ± 2.1	109.5 ± 4.9
$LaCl_3$	20	19.5 ± 2.9	—	10.7 ± 3.6
$LaCl_3$	2	42.0 ± 4.8	—	55.3 ± 9.0
$La(NO_3)_3$	20	18.9 ± 1.3	—	126.0 ± 6.4
$La(NO_3)_3$	2	100.5 ± 4.0	—	110.9 ± 5.2

[a]Relative to response in absence of added component.
[b]Mean value ± standard error of the mean, for 3 or 4 measurements.

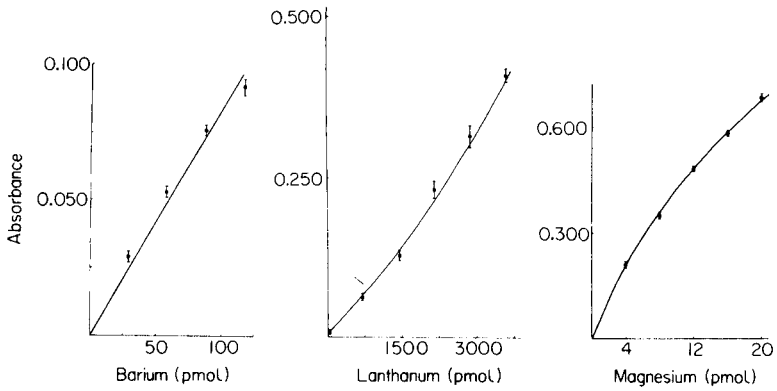

Fig. 1. Calibration graphs for barium, lanthanum and magnesium. (Mean peak absorbance ± standard error of the mean is given for 8—10 separate experiments.)

respectively. After known concentrations of standard solutions had been added to pancreatic islets, the recoveries for barium and lanthanum were 117 ± 10% and 90 ± 6% (mean values ± standard error of the mean, for 7 and 29 experiments, respectively). In the case of magnesium the high sensitivity of the analysis made it necessary to use only tiny fragments of tissue (<1 μg). The resulting variation was intolerably high, but was markedly reduced when 2-μl samples of the pancreatic islet homogenates were analysed. The recovery for this procedure was 106 ± 8% (6 experiments).

Chemical interferences were studied after high concentrations of different salts had been added to standard solutions of barium, lanthanum and magnesium (Table 2). Among the physiological salts, magnesium chloride and sulfate interfered with barium but not with lanthanum. High concentrations of chlorides have also been reported to suppress the absorption signal when measuring calcium [8] and other metals [19]. However, it should be noted that interference from magnesium chloride or sulfate is no problem in analyses of biological tissues for metals, because the physiological concentrations of these salts are much lower than those tested.

Lanthanum has been used for discriminating between superficial and intracellular calcium in various cell systems [20]. The effect of lanthanum on calcium analogues is so far poorly understood and merits further investigations. Lanthanum chloride suppressed the absorption signal for barium and magnesium. This type of interference has also been observed in measurements of calcium [8]. The interference was not due to chloride, since 2 nmol of lanthanum chloride, caused serious interference whereas 20 nmol of sodium chloride did not. This effect was unexpected since lanthanum is used as a releasing agent to improve sensitivity for calcium in flame atomic absorption spectrometry [21]. Lanthanum nitrate (20 nmol) also had a depressive effect on barium determination, but 2 nmol had no effect. The addition of 2 nmol of lanthanum nitrate to the standards approximately simulates the ratios between lanthanum and the other elements in the islets.

TABLE 3

Metal content of freeze-dried pancreatic islets

Element	Ba	La	Mg
Metal content (mmol kg^{-1}, dry wt.)[a]	5.5 ± 0.7 (7)	219 ± 7 (6)	28 ± 6 (6)

[a]Mean value ± standard error of the mean; number of results in parentheses.

Table 3 presents the amounts of barium, lanthanum and magnesium determined in pancreatic islets. The experimental variation is acceptable and the data on Ba^{2+} uptake compare favourably with ^{45}Ca studies in this laboratory [22]. The lanthanum content is in agreement with the uptake of ^{171}Tm, another member of the lanthanide series [23]. However, the amounts of magnesium in the islets were lower than in other tissues. There was even less magnesium than calcium [8], which might be a unique feature of the β-cells, for the reverse relationship was observed in other types of cells [24, 25].

This work was supported by the Swedish Medical Research Council (12x-562), the Swedish Diabetes Association and Längmanska Kulturfonden.

REFERENCES

1 B. G. Danielsson and A. Oberg, Uppsala J. Med. Sci., 80 (1975) 71.
2 G. Lundgren and G. Johansson, Talanta, 21 (1974) 257.
3 J. P. Matousek and B. J. Stevens, Clin. Chem., 17 (1971) 363.
4 F. J. Langmyhr and J. Aamodt, Anal. Chim. Acta, 87 (1976) 483.
5 D. A. Lord, J. W. McLaren and R. C. Wheeler, Anal. Chem., 49 (1977) 257.
6 K. Fujiwara, Y. Umezawa, Y. Numata, K. Fuwa and S. Fujiwara, Bunseki Kagaku 26 (1977) 735.
7 O. Berglund and B. Hellman, Diabetologia, 12 (1976) 380.
8 P.-O. Berggren, O. Berglund and B. Hellman, Anal. Biochem., 84 (1978) 393.
9 R. P. Rubin, Calcium and the Secretory Process, Plenum Press, New York, 1974, p 1.
10 J. E. Gerich, A. Charles and G. M. Grodsky, Ann. Rev. Physiol., 38 (1976) 353.
11 W. J. Malaisse, A. Herchuelz, G. Devis, G. Somers, A. C. Boschero, J. C. Hutton, S. Kawazu, A. Sener, I. J. Atwater, G. Duncan, B. Ribalet and E. Rojas, Ann. N.Y. Acad. Sci., 307 (1978) 562.
12 B. Hellman, T. Andersson, P.-O. Berggren, P. Flatt, E. Gylfe and K.-D. Kohnert, Hormones and Cell Regulation, Vol. 3, Elsevier/North-Holland Biomedical Press, Amsterdam, 1979, 69.
13 G. Lundgren, Dissertation, University of Umeå, Sweden, 1975.
14 E. Lundberg and L. Lundmark, Biomed. Environ. Instrum., 9 (1979) 91.
15 E. Lundberg, Chem. Instrum., 8 (1978) 197.
16 E. Lundberg, Appl. Spectrosc., 32 (1978) 276.
17 B. Hellman, Ann. N.Y. Acad. Sci., 131 (1965) 541.
18 B. Hellman, Diabetologia, 6 (1970) 110.
19 W. Frech and A. Cedergren, Anal. Chim. Acta, 82 (1976) 83.
20 G. B. Weiss, Ann. Rev. Pharmacol., 14 (1974) 343.
21 B. P. Adams and W. O. Passmore, Anal. Chem., 630 (1966) 38.

22 G. D. Bloom, B. Hellman, J. Sehlin and I.-B. Täljedal, Am. J. Physiol., 232 (1977) 114.
23 P. R. Flatt, E. Gylfe and B. Hellman, submitted for publication.
24 D. Bossi, A. Cittadini, F. Wolf, A. Milani, S. Magalini and T. Terranova, FEBS Lett., 104 (1979) 6.
25 F. Clemente and J. Meldolesi, J. Cell Biol., 65 (1975) 88.

Analytica Chimica Acta, 119 (1980) 167—169

Short Communication

THE USE OF MAGNESIUM PERCHLORATE AS DESICCANT IN THE SYRINGE INJECTION TECHNIQUE FOR DETERMINATION OF MERCURY BY COLD-VAPOUR ATOMIC ABSORPTION SPECTROMETRY

D. GARDNER

CSIRO Division of Fisheries and Oceanography, P.O. Box 21, Cronulla, N.S.W. 2230 (Australia)

(Received 21st April 1980)

Summary. The method developed earlier was found to suffer a loss in sensitivity when the magnesium perchlorate desiccant became damp. The most sensitive and consistent results were obtained when the magnesium perchlorate was removed from the sample injection manifold. Under most circumstances a desiccant is not required.

Recently, a simple syringe injection method was described for the cold-vapour atomic absorption determination of mercury in fish and hair, which gives rapid, precise and accurate results [1]. It is known that water vapour can cause problems in such techniques for mercury [2]. In most methods this is overcome by passing the mercury vapour through a tube of magnesium perchlorate desiccant which precedes the cell [1—4]. However, some workers have found that magnesium perchlorate tends to broaden absorption peaks, absorb mercury and cause memory effects [5, 6].

Further work has shown that the earlier initial assumption, that a desiccant is always required in the syringe technique, was wrong and can lead to errors. Because so little water vapour enters the cell, no drying procedure is necessary under the recommended experimental conditions [1].

Mercury determinations were carried out in a mercury-free clean room with constant temperature and humidity [7, 8]. Samples were injected every 90 s. The magnesium perchlorate drying agent was fresh at the beginning and was replaced when still in apparently good condition after 100 injections. The first 22 injections of a standard mercury sample gave a mean peak absorption of 0.232 ± 0.004 absorption units. During the injection of the next 13 samples, the peak absorption gradually dropped to a mean level of 0.196 ± 0.007 for 17 samples. The remaining 48 replicate samples had absorptions of 0.201 ± 0.003. Then, although the damp magnesium perchlorate appeared to be still in good condition and was still removing water vapour, it was replaced and the absorption returned to the original level of 0.233 ± 0.004 units. However, unless all the damp desiccant was removed from the tube, mercury losses started to occur after as few as eight sample injections.

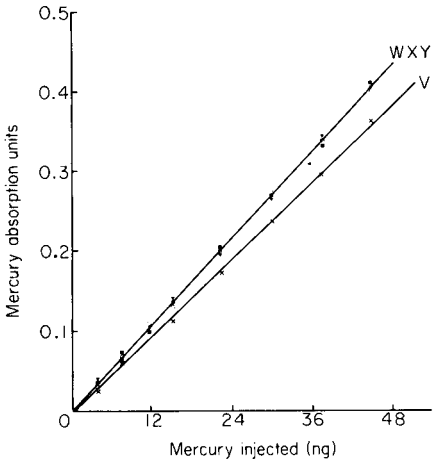

Fig. 1. Standard graphs of mercury absorption versus concentration for: (V) damp magnesium perchlorate; (W) fresh magnesium perchlorate; (X) with heat but no desiccant; (Y) without heat or desiccant.

Standard curves V and W in Fig. 1 show, for damp and fresh desiccant, respectively, how these mercury losses could affect calculated results if standardization is infrequent. For any sample, 15% of the mercury content is lost consistently once the desiccant becomes damp.

The memory effect with either fresh or damp magnesium perchlorate was negligible, as observed from the peak absorptions of samples injected after the highest standard (48 ng).

In order to determine whether mercury was being removed by fresh magnesium perchlorate, the above experiments were repeated after removal of the drying tube; the samples were injected into a cell that had previously been heated for 10 s with a hairdryer in order to eliminate possible condensation of water on the cell wall [3, 9, 10]. Standard curve X is the same as standard curve W, which shows that mercury is not removed by the magnesium perchlorate.

In further tests, no heat and no magnesium perchlorate were used. Standard curve Y shows these results. Again it is clear that mercury was not removed by fresh magnesium perchlorate and also that water was not condensing on the cell wall under the conditions used. However, under some laboratory conditions when samples are warmer than the cell, this would not be the case and the water vapour would have to be eliminated. Reproducibilities for replicate samples corresponding to standards V, W, X and Y are given in Table 1.

The mercury losses described here will not be obvious in techniques which require large samples and have large volumes of recycling vapour [11], as the equilibrium of magnesium perchlorate with water vapour and mercury would be set up almost immediately. Although the mechanism causing the mercury losses is unknown, mercury probably reacts with both physically and chemically bound water of hydration [12, 13].

TABLE 1

The effect of damp and fresh magnesium perchlorate, heat and no water vapour removal on the mean atomic absorption measurements of replicates from bulk samples.

Water vapour control	Sample	Standard graphs[a]	n	Mean absorption[b]
Used $Mg(ClO_4)_2$	A	V	27	0.201 ± 1.5
Fresh $Mg(ClO_4)_2$	A	W	22	0.232 ± 1.7
Heat cell, no $Mg(ClO_4)_2$	B	X	17	0.283 ± 0.95
No heat, no $Mg(ClO_4)_2$	C	Y	12	0.216 ± 0.69

[a]See Fig. 1. [b]Mean and relative standard deviation (%).

The final recommendation is that, if possible, neither a drying agent nor heat should be used to achieve best reproducibility. If water vapour must be removed, the cell should be heated. If this is not possible, magnesium perchlorate can be used under the following conditions: (i) a fresh tube of magnesium perchlorate should be inserted every 15—20 samples; or (ii) the magnesium perchlorate should be preconditioned by bubbling sample vapour through it until it reaches its damp state. The latter technique is preferable because it is less time-consuming, and allows over a hundred samples to be processed without fear of any change in the percentage of mercury being lost.

The author thanks G. Dal Pont for technical assistance.

REFERENCES

1 D. Gardner and G. Dal Pont, Anal. Chim. Acta, 108 (1979) 13.
2 S. Chilov, Talanta, 22 (1975) 205.
3 T. R. Gilbert and D. N. Hume, Anal. Chim. Acta, 65 (1973) 461.
4 J. F. Kopp, M. C. Longbottom and L. B. Bobring, J. Am. Water Works Assoc., 64 (1972) 20.
5 D. C. Stuart, Anal. Chim. Acta, 101 (1978) 429.
6 R. Stux and E. Rothery, Technical Topics; Varian Techtron January 1971.
7 D. Gardner, Lab. Pract., 28 (1979) 1071.
8 D. Gardner, Aust. CSIRO Div. Fish. Oceanogr. Rep. 107.
9 S. R. Koirtyohann and M. Khaill, Anal. Chem., 48 (1976) 136.
10 D. R. Christman and J. D. Ingle, Anal. Chim. Acta, 86 (1976) 53.
11 D. Gardner and J. P. Riley, J. Cons. Cons. Int. Explor. Mer, 35 (1974) 202.
12 J. H. Yoe, in R. C. Weast (Ed.), Handbook of Chemistry and Physics, 58th edn., CRC Press, Cleveland, OH, 1977—78, p. E41.
13 S. H. Ibrahim and N. R. Kuloor, Chem. Age India, 17 (1966) 871.

Analytica Chimica Acta, 119 (1980) 171—174

Short Communication

SPECTROPHOTOMETRIC DETERMINATION OF SELENIUM WITH DITHIZONE

A. D. CAMPBELL* and A. H. YAHAYA

Department of Chemistry, University of Otago, Dunedin (New Zealand)

(Received 14th February 1980)

Summary. Microgram amounts of selenium(IV) are determined by measuring the decrease in absorbance of dithizone in carbon tetrachloride solution at 620 nm. Relative standard deviations for samples containing 0.20 and 1.00 μg of selenium(IV) are 0.6% and 0.4%, respectively. Of several metals tested only copper (at the 10-μg level) and iron (at the 100-μg level) interfere but high concentrations of nitric or perchloric acid cause low results. A reinvestigation of the reaction of selenium(IV) with dithizone suggests a formula $Se(HDz)_4$ for the dithizonate.

The use of dithizone as an analytical reagent for the determination of a wide range of metals has been reviewed by Irving [1]. Two variations of the spectrophotometric method for the determination of selenium with dithizone have been described by Mabuchi and Nakahara [2]. They reacted selenium(IV) in 6 mol dm^{-3} hydrochloric acid with successive small portions of dithizone in carbon tetrachloride and determined the absorption of the carbon tetrachloride extract either directly at 410 nm or at 420 nm after treatment with dilute ammonia to remove unreacted dithizone. They reported some interferences from metals such as copper and mercury but these could be eliminated by appropriate treatment.

The nature of the product formed when selenium(IV) reacts with dithizone has been the subject of considerable debate. Starý and Růžička [3] suggested the formula $Se(HDz)_4$ for the selenium dithizonate complex based on the decomposition of the complex with diethyldithiocarbamic acid to release free dithizone which was determined spectrophotometrically. The composition of the complex appears to have been well established as $Se(HDz)_4$ in later studies by Starý et al. [4, 5] who used ^{75}Se-labelled selenium(IV); they separated and identified free dithizone, its oxidation product, elemental selenium and the complex by the use of thin-layer chromatography. In contrast, Irving and Ramakrishna [6—8] maintained that the yellow material formed is not selenium dithizonate but an oxidation product of dithizone. Bonig and Heigener [9] reported a method for the determination of selenium in biological materials in which selenium is extracted as the dithizonate in carbon tetrachloride from an acidic sample digest and then, after wet oxidation of the complex with nitric acid, selenium is determined with 3,3′-diaminobenzidine. In a more recent paper, Shcherbov et al. [10] described

the reaction of dithizone with selenium(IV) in 5.5 mol dm^{-3} sulphuric acid; they reported that the yellow carbon tetrachloride extract contains an unstable selenium(IV) complex, selenium(II) dithizonate and dithizone disulphide. After purification of the extract by ammonia washing, they reduced the complexes with tin(II) chloride in sulphuric acid and measured the absorbance of the liberated dithizone at 620 nm. They avoided the presence of nitric acid which has been reported [11] to give oxidation products of dithizone of similar spectrum to selenium dithizonate.

Preliminary investigations

In view of the controversy regarding the product formed when selenium(IV) reacts with dithizone, the extraction of selenium(IV) into carbon tetrachloride was followed by using atomic absorption spectrometry. Aqueous solutions were aspirated into an air—acetylene flame and absorbances were measured at 196.0 nm. In the absence of dithizone, carbon tetrachloride did not remove selenium(IV) from an aqueous solution containing 6 mol dm^{-3} hydrochloric acid.

A series of solutions containing 3.166 μmol selenium(IV) in 10 cm^3 of 6 mol dm^{-3} hydrochloric acid was extracted with carbon tetrachloride solutions containing 0.6 μmol cm^{-3} dithizone according to the following schedule: (a) one extraction (9 cm^3, 5.40 μmol dithizone); (b) two extractions (9 cm^3 and 6 cm^3, 9.00 μmol dithizone); (c) three extractions (9 cm^3, 6 cm^3 and 4 cm^3, 11.40 μmol dithizone). The amount of selenium(IV) reacting with dithizone (1.24, 2.29 and 2.76 μmol, respectively) was determined by measuring the residual selenium in the aqueous layer in each case. In all three cases, the ratio of selenium(IV) extracted to dithizone used was about 1:4 (1:4.35, 1:3.93 and 1:4.13) which shows a stoichiometry consistent with the formula $Se(HDz)_4$ suggested by Starý and Růžička [3].

Calibration graphs over the range 0—10 μg of selenium were prepared by following the general procedure of Mabuchi and Nakahara [2]. The monocolour method, in which excess of dithizone was removed by treatment with aqueous ammonia, gave a rectilinear relationship for measurements at 420 nm. The marked sensitivity of the method is obviously satisfactory for analytical purposes. In contrast, the mixed colour method gave a considerable absorbance for zero concentration of selenium, curvature in the calibration graph and poorer sensitivity.

Excess of dithizone is usually removed by ammonia washing of the carbon tetrachloride extract; it was found that although the absorbance at 420 nm decreased rapidly at first, it continued to decrease on prolonged treatment with ammonia. A carefully controlled washing procedure is therefore necessary. During these experiments, it became apparent that the selenium dithizonate was not very stable in carbon tetrachloride, particularly when exposed to artificial light. The absorbance did not decrease so rapidly when the extract received a final wash with dilute hydrochloric acid. The instability of selenium dithizonate in carbon tetrachloride could, in part, be due to the effect of residual ammonia dissolved in the carbon tetrachloride.

An alternative procedure is to measure the decrease in absorbance of dithizone in carbon tetrachloride at 620 nm rather than the increase in absorbance at 420 nm caused by selenium dithizonate. Dithizone exhibits strong absorbance at 620 nm, a region where there is minimum absorbance by the selenium complex. At 420 nm, the region which is normally used for concentration measurements, both dithizone and selenium dithizonate exhibit considerable absorbance.

Experimental

Reagents. All reagents used were of analytical-reagent grade. Deionized glass-distilled water was used throughout.

For the dithizone solution (ca. 0.03 mmol dm^{-3}), dissolve 0.769 mg of dithizone in about 50 cm^3 of carbon tetrachloride and extract the dithizone into 100 cm^3 of 2 mol dm^{-3} ammonia solution. Acidify the aqueous layer with hydrochloric acid, re-extract the dithizone into about 50 cm^3 of carbon tetrachloride and make the volume up to 100 cm^3. This solution should be used within 24 h.

For the selenium(IV) solution (2.0 g dm^{-3}), dissolve 1.000 g of selenium metal (microanalytical reagent grade) in the minimum quantity of hot concentrated nitric acid and dilute to 500 cm^3 with distilled water. Other concentrations are prepared by dilution.

Procedure. Measure 5.00-cm^3 aliquots of the selenium(IV) solutions into 100-cm^3 conical flasks. Add 5.0 cm^3 of concentrated hydrochloric acid and 10.00 cm^3 of the above dithizone solution. Shake the mixture for 3 min on a mechanical shaker and separate the carbon tetrachloride layer. Dry the extract by allowing it to pass over a piece of filter paper in the exit tube of the separating funnel. Measure the absorbance at 620 nm. A Pye Unicam SP 600 spectrophotometer is suitable.

Results

Calibration graphs are rectilinear. Graphs for 0—2 and 0—5 μg selenium may be represented by the expressions $y = 0.41 - 0.089\,x$ and $y = 0.60 - 0.11\,x$, respectively, where y is absorbance and x is mass of selenium (in μg) per sample. A calibration graph for 0—1.0 μg selenium per sample was prepared by reducing the volumes of sample and reagents to half those recommended above. A dithizone concentration of 0.06 mmol dm^{-3} is required for a 0—10 μg selenium range. Absorbance shows a linear decrease with increasing concentration of selenium and the amount of work involved in each analysis is reduced to a minimum. The precision is also good. Five determinations each of 0.2 μg and 1.0 μg of selenium gave relative standard deviations of 0.6 and 0.4%, respectively. The standard deviation (σ) for 1.0 μg selenium per sample was 0.002 absorbance units. This new procedure also gave remarkably stable selenium dithizonate solutions. The absorbance of a dithizone solution containing 1.0 μg of selenium(IV) was monitored for a period of 40 min. There was a small decrease in absorbance (less than 2σ) during the first 20 min, but

no significant change after that. This is a considerable improvement over methods involving measurements at 420 nm.

The effects of several heavy metals, which can form coloured dithizonates, on the determination were studied by adding 1.0, 10.0 and 100 μg of the element (as an appropriate salt) to a series of 1.00-μg samples of selenium(IV). Cadmium(II), cobalt(II), manganese(II), nickel(II) and zinc(II) showed no interference, probably because of the instability of their dithizonates in the strongly acidic solution. Iron(III) interfered only at the 100-μg level (about 19% suppression) but copper depressed the absorbance by 9% at the 10-μg level and 53% at the 100-μg level. Although the reaction is normally carried out in the presence of about 50% hydrochloric acid, it was found that both nitric and perchloric acids reduced the absorbance exhibited by a sample containing 1.00 μg of selenium.

Methods which distinguish between selenium(IV) and selenium(VI) are particularly useful. In this case, although recovery of selenium from selenium(VI) was only about 15%, the figure is rather too high to permit satisfactory quantitative distinction to be made between the two valency states.

The authors thank the Research Committee of the University Grants Committee for financial assistance. One of us (A.H.Y.) acknowledges the receipt of a Malaysian Federal Government Scholarship.

REFERENCES

1 H. M. N. H. Irving, Dithizone, The Chemical Society Analytical Sciences Monograph No. 5., 1977.
2 H. Mabuchi and N. Nakahara, Bull. Chem. Soc. Jpn., 36 (1963) 151.
3 J. Starý and J. Růžička, Talanta, 15 (1968) 505.
4 J. Starý and J. Marek, Chem. Comm., (1970) 519.
5 J. Starý, J. Marek, K. Kratzer and F. Sebesta, Anal. Chim. Acta, 57 (1971) 393.
6 R. S. Ramakrishna and H. M. N. H. Irving, Chem. Comm., (1969) 1356.
7 H. M. N. H. Irving, Chem. Comm., (1970) 519.
8 R. S. Ramakrishna and H. M. N. H. Irving, Anal. Chim. Acta, 49 (1970) 9.
9 G. Bonig and H. Heigener, Landwirtsch. Forsch., 23 (1970) 258.
10 D. P. Shcherbov, A. I. Ivankova and G. P. Gladysheva, Zh. Anal. Khim, 32 (1977) 105.
11 N. Iordanov and K. Daskalova, C. R. Acad. Bulg. Sci., 23 (1970) 969.

Analytica Chimica Acta, 119 (1980) 175—178

Short Communication

DETERMINATION OF ANTIMONY IN TIN BY RADIOCHEMICAL NEUTRON ACTIVATION ANALYSIS

T. BEREZNAI

Max-Planck-Institut für Metallforschung, Institut für Werkstoffwissenschaften, Laboratorium für Reinststoffe, Seestrasse 92, D-7000 Stuttgart 1 (F.R.G.)

(Received 19th March 1980)

Summary. New types of correction for chemical yield and counting geometry in conjunction with the comparator method provide significant improvements in reproducibility and sensitivity compared to direct neutron activation analysis.

In a number of papers, Maenhaut et al. [1, 2] have reported on the n.a.a. of high-purity tin. Because of the intense activation of this matrix, the possibilities of purely instrumental n.a.a. are rather limited, although determinations of indium and manganese [3], and a γ-γ coincidence method for copper [4] have been described. It has been shown here that meticulous optimization of the experimental conditions allows some other elements (e.g. Au, Sb and Co) to be determined non-destructively if their concentrations are above the ppm level.

Neutron activation has generally been regarded as an extremely sensitive but expensive trace analytical method. Because of its inherent merits (sensitivity, selectivity and freedom from blank) and some recent methodological developments with respect to instrumentation, automation and standardization, n.a.a. is today a routine multi-element analytical technique [5, 6] competitive with other routine procedures in many fields of application [7—9]. The comparator (or single-standard) technique allows economical use of n.a.a. even when it is combined with complex radiochemical separations [10]. In this communication, a particularly simple procedure for radiochemical yield and counting geometry correction is described.

Theory

For routine multi-element i.n.a.a. of samples of diverse origin, the use of the so-called single comparator method has been recommended [11—13]. The comparator method consists in determining the so-called k-factors [11], i.e. the ratios of the specific full energy peak counting rates (A_{sp}) of the elements to be determined and that of the comparator:

$$k = A_{sp}/A^*_{sp} = (N/SDCmt_m)/(N/SDCmt_m)^* \quad (1)$$

Present address: Institut für Radiochemie der Technischen Universität München, D-8046 Garching bei München, F.R.G.

where the asterisk refers to the comparator; N is the net peak area of the full energy peak, accumulated during the measurement period t_m, corrected for dead-time and other pulse losses; $S = 1 - \exp(-\lambda t_{irr})$, the saturation factor; λ is the decay constant; t_{irr} is the irradiation time; $D = \exp(-\lambda t_c)$, the decay factor; t_c is the cooling time; $C = [1 - \exp(-\lambda t_m)]/\lambda t_m$, the correction factor for decay during measurement; and m is the mass of the element in question.

Equation (1) should, in general, be modified if the analysis is based on the intensity measurement of a radioactive daughter isotope, such as the reaction $^{124}Sn\ (n, \gamma)\ ^{124m}Sn \xrightarrow{\beta^-} {}^{125}Sb$ (neglecting the formation of the ^{125}Sn nuclide under the given experimental conditions). Yet, considering that the branching ratio is unity for the above reaction, and that the half-life of ^{125}Sb (2.73 years) is much longer than that of ^{125m}Sn (9.6 min), it follows that eqn. (1) can be applied here without any modification. Because of the poor sensitivity, there is, in general, no sense in counting the activity of ^{125}Sb for the determination of tin. In our case, however, use is made of this reaction for the intended corrections. Moens et al. [13] have also indicated that if the matrix is used as a comparator, correction for changes in counting geometry is unnecessary.

For the separation of ^{122}Sb produced by the $^{121}Sb(n, \gamma)$ reaction, the rapid radiochemical deposition of the carrier-free antimony from a 6 M hydrochloric acid medium on iron powder (in a slightly modified form of the method described by Maenhaut et al. [1]) was used.

Experimental

The tin sample(s) (ca. 1 g) and the comparator (ruthenium powder) were irradiated in a thermal flux of about 2×10^{13} n cm^{-2} s^{-1} for 2 h. To allow the decay of all the short-lived activity, the sample was cooled for one day and then dissolved in 50 ml of concentrated hydrochloric acid in a refluxing apparatus. The solution was then diluted (1 + 1) with water and directly transferred to a beaker containing about 3 g of wet iron powder. (Maenhaut et al. [1] applied a prior halide distillation in the framework of a complex separation scheme.) The beaker covered with a watch-glass was allowed to stand for 1 h, being swirled carefully several times during this period. The iron powder was filtered off, washed with water and transferred to a polyethylene capsule. The γ-ray spectra of the deposited radioactive materials were observed with a Ge(Li) detector coupled to 4096-channel pulse-height analyser. The spectra were stored on punched-tape and the data reduced off-line. The peaks used for the calculation were the 564.1-keV line of ^{122}Sb ($t_{1/2}$ = 2.68 d) and the 600.8-keV line of ^{125}Sb. The spectral interference from the 602.7-keV line of ^{124}Sb is negligible in the concentration range 1—50 μg g^{-1}.

Discussion and results

The k-factors determined are valid for a well-defined counting geometry, generally for point sources and relative small solid angles. In the present case,

TABLE 1

Comparison of results obtained by different methods

Sample	Sb content ($\mu g\ g^{-1}$)	
	I.n.a.a.	Radiochemical n.a.a.
A	11 ± 2	11.9 ± 0.5
B	18 ± 2	16.0 ± 0.5
Detection limit	4	0.1

this necessitates not only determination of the chemical yield but also a correction for the changed counting geometry and γ-ray attenuation in the iron. Since it is not important in this investigation, the ratio of the attenuation correction factors can be approximated by the value 1. This simplification is justified because of the small energy difference of the above γ-lines.

For determining the mass of the antimony (m_{Sb}) present in the sample, the two correction factors discussed above should be introduced into eqn. (1). Thus for m_{Sb}:

$$m_{Sb} = N\ (564\ \text{keV})/SDCk(^{122}\text{Sb})A^{*}_{sp}t_m f_G f_Y \qquad (2)$$

where f_G and f_Y are the correction factors for the counting geometry and the chemical yield, respectively.

Fortunately, exactly the same corrections can be applied for calculation of the mass of the tin matrix. Therefore, in the determination of the m_{Sb}/m_{Sn} ratio, i.e. the concentration of antimony in the tin sample, the above correction factors cancel each other.

The sensitivity and reproducibility of this determination of antimony in tin are increased by means of the above simple and rapid separation procedure by a factor of 40 and 4, respectively (Table 1). However, a limiting factor in this method is still the ^{125}Sb activity present. The applicability of the "correction" used is illustrated by comparing results obtained by direct i.n.a.a. and by the described radiochemical n.a.a. (Table 1). The agreement between the two sets of data is good, although it should be admitted that results from a third, totally independent method are needed for full confirmation.

As a final note it may be added that this correction method can theoretically be applied to some other matrix/impurity element pairs, e.g. Ru/Rh, Pd/Ag, Cd/In, Pt/Au.

The author is deeply indebted to Professor G. Tölg for his interest in this work. Thanks are due to Dr. F. De Corte, University of Ghent, Belgium, for helpful criticism, and to Mrs. E.Sz. for technical assistance.

REFERENCES

1 W. Maenhaut, F. Adams and J. Hoste, J. Radioanal. Chem., 6 (1970) 83.
2 W. Maenhaut, F. Adams and J. Hoste, J. Radioanal. Chem., 14 (1973) 295, 351; 16 (1973) 39.
3 W. Maenhaut, F. Adams and J. Hoste, J. Radioanal. Chem., 9 (1971) 27.
4 R. Wölfle, U. Herpers and W. Herr, J. Radioanal. Chem., 2 (1969) 171.
5 J. Op de Beeck and J. Hoste, Analyst, 99 (1974) 973.
6 V. Krivan, Angew. Chem., 91 (1979) 132.
7 G. Tölg, Nachr. Chem. Tech. Lab., 27 (1979) 250.
8 G. H. Morrison, Crit. Rev. Anal. Chem., (Nov. 1979) 287.
9 R. Gijbels and J. Hertogen, Pure Appl. Chem., 49 (1977) 1555.
10 P. Schramel, Mikrochim. Acta, (1978) 287.
11 F. Girardi, G. Guzzi and J. Pauly, Anal. Chem., 37 (1965) 1085.
12 A. Simonits, F. De Corte and J. Hoste, J. Radioanal. Chem., 24 (1975) 31.
13 L. Moens, F. De Corte and J. Hoste, Anal. Chim. Acta, 88 (1977) 319.

Analytica Chimica Acta, 119 (1980) 179—185

Short Communication

ULTRAVIOLET PHOTOELECTRON SPECTROSCOPY AND OXIDATIVE ELECTROCHEMISTRY OF 8-HYDROXYQUINOLINE AND ITS DERIVATIVES

MICHAEL THOMPSON* and ELIZABETH A. STUBLEY

Department of Chemistry, University of Toronto, 80 St. George Street, Toronto, Ontario M5S 1A1 (Canada)

(Received 31st January 1980)

Summary. The gas-phase ionization potentials of 8-hydroxyquinoline and several of its alkyl derivatives in the region 8—12 eV are assigned. The energies of the highest occupied molecular orbitals and the half-wave oxidation potentials at a rotating platinum electrode are used to derive empirical values for differential solvation energies for the compounds in acetonitrile and dichloromethane solution.

Correlations between ionization potentials, obtained from either experimental or theoretical work, and electrochemical oxidation potentials are appropriate because the energy of the highest occupied molecular orbital primarily determines both values [1]. Several studies in the 1960's were concerned with the correlation of polarographic oxidative half-wave potentials, $E^{ox}_{1/2}$, with ionization potentials (*IP*) obtained by photoionization and/or electron impact methods [2—4]. (Positive $E^{ox}_{1/2}$ values really correspond to reduction potentials according to IUPAC convention, but the designation is retained in this paper for consistency with the literature in this field.)

Several workers have compared electrochemical parameters obtained from polarography and cyclic voltammetry with adiabatic or vertical ionization potentials measured by ultraviolet photoelectron spectroscopy (u.p.s.) or calculated by theoretical methods [5—9]. In 1976, Ballard [10] reviewed the work carried out by several groups concerning the relationship between *IP* and $E^{ox}_{1/2}$ and concluded that the correlation could be approximated to

$$IP = 1.1\, E^{ox}_{1/2} + 6.6 \qquad (1)$$

the 1.1 factor being related to neglected entropy terms. In contrast to these relationships, Nelsen et al. [11] found a slope of over ten for a plot of vertical *IP* (from u.p.s.) versus E^0 (from cyclic voltammetry) for acyclic, n-alkyl hydrazines. This result is attributed to the large effect on *IP* relative to E^0 of the magnitude of the lone pair—lone pair interactions of the two nitrogen atoms.

Recently, Loutfy et al. [12] carried out a correlation study of vertical ionization potentials of thiochromones and thiochromanones measured by u.p.s. with appropriate $E^{ox}_{1/2}$ values. Unlike the previous studies, the anodic

oxidation reactions of these molecules are irreversible. Although an irreversible reaction implies that expressions such as eqn. (1) are no longer valid, an $E^{ox}_{1/2}$—*IP* correlation was found. Furthermore, the solvation energy of the derivatives in dichloromethane was calculated by using the equation

$$E^{ox}_{1/2} = IP + \Delta E_{solv} - 4.38 \quad (2)$$

where ΔE_{solv} represents the difference in solvation energy between the neutral molecule and its oxidized product and the last term represents a constant which includes the free energy of the electron in the reference electrode versus an electron in vacuo at infinity.

Although various studies have been concerned with the reductive electrochemistry of 8-hydroxyquinoline, little oxidative work has been done. A comparison of ionization potentials of this molecule and several of its derivatives measured by u.p.s. with $E^{ox}_{1/2}$ values determined by voltammetry, is reported in the present communication.

Experimental

8-Hydroxyquinoline and its derivatives. Commercial samples of the parent compound and its 2-methyl derivative (Fisher Scientific) were purified by recrystallization from aqueous ethanol. The 3-methyl and 4-methyl derivatives were synthesized by known procedures [13, 14]. The 2-ethyl, 2-n-propyl and 2-n-butyl-8-hydroxyquinolines were prepared as described by Kaneko and Ueno [15], except that they were isolated as the neutral compounds by vacuum distillation, rather than as hydrochlorides. 2-t-Butyl-8-hydroxyquinoline was synthesized by the method of Thompson and Stubley [16] via condensation of 3-chloro-4,4-dimethylpent-2-enal with *o*-aminophenol. The 7-methyl and 7-t-butyl derivatives were donated.

Photoelectron spectroscopy. The ultraviolet photoelectron spectra of 8-hydroxyquinoline and its derivatives were recorded on either a modified PS-16 (Perkin-Elmer) or ESCA 36 (McPherson) spectrometer. The He I resonance line at 21.22 eV was used as the excitation source and spectra were calibrated internally against xenon lines at 12.13 and 13.44 eV and the argon signal at 15.76 eV.

Voltammetry. All electrochemical measurements were done with a model 174A polarographic analyzer (Princeton Applied Research) equipped with an electrochemical cell (PAR model 9301) and either a wax-impregnated graphite electrode for cyclic voltammetry or a rotating platinum disc electrode (Beckman Instruments) for oxidative voltammetry. A platinum wire was used as auxiliary electrode with a silver/silver chloride reference electrode. A simple correction factor was applied to the data to yield values relative to the standard calomel electrode. The solvent system consisted of a 0.1 M solution of tetrabutylammonium perchlorate (TBAP) in either acetonitrile or dichloromethane. D.c. voltammograms were obtained from 0.05 mM solutions of 8-hydroxyquinoline and its derivatives in these solvents. A cyclic voltammogram was recorded for 8-hydroxyquinoline in 0.1 M TBAP—acetonitrile solution.

Results and discussion

Photoelectron spectroscopy. The spectra of quinoline, 8-hydroxyquinoline and some of its derivatives are shown in Fig. 1. Ionization potentials obtained from the spectra in the 8—12-eV range are given in Table 1. The spectrum of the 2-ethyl derivative could not be obtained because of decomposition effects on the hot probe in the spectrometer. The spectra can be rationalized by consideration of previous analyses of the spectra of naphthalene, quinoline, and substituted phenols and pyridines. Substitution of the nitrogen atom into the naphthalene nucleus results in the expected shift of the first four spectral bands assigned to π-levels (naphthalene: π_1, $1a_{1u}$ 8.15 eV; π_2, $2b_{1u}$ 8.8 eV; π_3, $1b_{3g}$ 10.10 eV; and π_4, $1b_{2g}$ 10.68 eV) to higher ionization potentials (quinoline: π_1 8.62 eV; π_2 9.25 eV; π_3 10.58 eV; and π_4 11.40 eV) [17]. The peak at 9.25 eV in the spectrum of quinoline is also assigned to ionization of the nitrogen lone-pair (n) because its intensity is greater than that of the corresponding band in the spectrum of naphthalene.

The u.p. spectra of phenols exhibit three bands between 8 and 11.6 eV that correspond to ionization from the b_1 and a_2 π-orbitals and from the oxygen lone-pair [18]; the spectrum of pyridine in this region shows peaks due to ionization of the nitrogen lone-pair and two π-orbitals [19]. Methyl substitution in both systems results in a general shift to lower ionization potential.

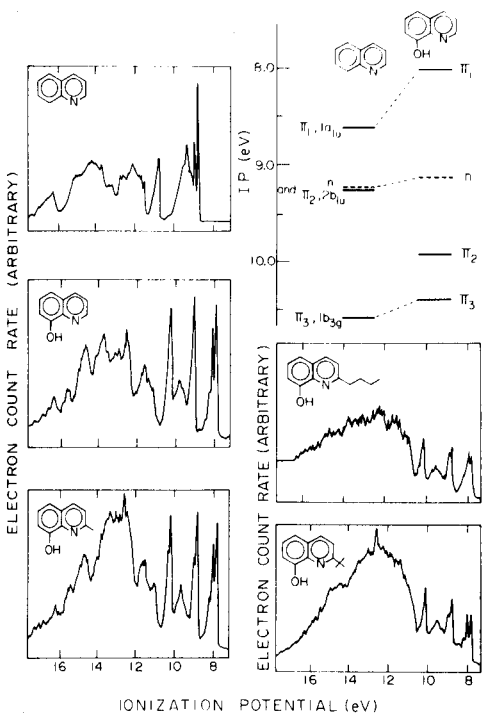

Fig. 1. Ultraviolet photoelectron spectra of quinoline and 8-hydroxyquinoline and a number of its derivatives.

TABLE 1

Ionization potentials of 8-hydroxyquinoline and its derivatives measured by u.p.s.

Molecule	Ionization potentials (± 0.05 eV)[a]				
	π_1	n	π_2	π_3	π_4
Quinoline	8.62	9.25	9.25	10.58	11.40
8-Hydroxyquinoline	8.02	9.14	9.93	10.40	11.41
2-Methyl-8-hydroxyquinoline	7.88	8.90	9.73	10.25	
3-Methyl-8-hydroxyquinoline	7.89	8.90	9.64	10.10	
4-Methyl-8-hydroxyquinoline	7.92	8.99	9.59	9.94	
7-Methyl-8-hydroxyquinoline	7.96	8.90	9.82	10.10	11.57
2-n-Propyl-8-hydroxyquinoline	7.88	8.88	9.67	10.21	
2-n-Butyl-8-hydroxyquinoline	7.94	8.85	9.56	10.13	
2-t-Butyl-8-hydroxyquinoline	7.79	8.83	9.35	10.13	
7-t-Butyl-8-hydroxyquinoline	7.72	8.90	9.77	10.14	

[a]Values for π_1 are adiabatic ionization potentials for the parent molecule and its derivatives. The remainder are vertical ionization potentials.

This background information helps to elucidate the u.p. spectrum of 8-hydroxyquinoline. The five bands in the 7—12-eV region can clearly be assigned to ionization from four π-levels and the nitrogen lone-pair. The oxygen non-bonding electrons are expected to have an ionization potential slightly greater than 12 eV; the appropriate peak is therefore merged with structure originating from the various σ-levels. The first band at 8.02 eV shows a similar structure to the π_1-band of quinoline, although it occurs at 0.6 eV lower IP than the parent molecule because of the expected mesomeric effect of the hydroxyl group. The overlap of the n- and π_2-bands in the quinoline spectrum is no longer apparent. The spectra of pyridine and its derivatives show

TABLE 2

Comparison of π_1 ionization potentials and half-wave oxidation potentials

Molecule	π_1[a]	$E^{ox}_{1/2}$ (CH_3CN)[b]	$E^{ox}_{1/2}$ (CH_2Cl_2)[b]	ΔE_{solv} (CH_3CN)[c]	ΔE_{solv} (CH_2Cl_2)[c]
8-Hydroxyquinoline	8.02	1.28	1.54	−2.36	−2.10
2-Methyl-8-hydroxyquinoline	7.88	1.27	1.49	−2.23	−2.01
3-Methyl-8-hydroxyquinoline	7.89	1.29	1.67	−2.22	−1.84
4-Methyl-8-hydroxyquinoline	7.92	1.27	1.51	−2.27	−2.03
7-Methyl-8-hydroxyquinoline	7.96	1.27	1.48	−2.31	−2.10
2-Ethyl-8-hydroxyquinoline	—	1.27	1.45	—	—
2-n-Propyl-8-hydroxyquinoline	7.88	1.19	1.48	−2.31	−2.03
2-n-Butyl-8-hydroxyquinoline	7.84	1.29	1.52	−2.17	−1.94
2-t-Butyl-8-hydroxyquinoline	7.79	1.44	1.70	−1.97	−1.70
7-t-Butyl-8-hydroxyquinoline	7.72	1.34	1.32	−2.00	−2.02

[a]±0.05 eV. [b]±0.08 V vs. SCE. [c]±0.13 eV.

that the hydroxyl group should have little effect on the IP of the nitrogen lone-pair. Thus, the second band at 9.14 eV is attributed to ionization from the nitrogen non-bonding level (compared with 9.25 eV for quinoline). The lack of vibrational structure in the peak supports this assignment. Unlike the other bands in the 8—12-eV region, the peak at 9.93 eV is broad with poorly resolved structure. It is noteworthy that this π_2-band is similar in structure to the π_2-band in the spectrum of heptafluoroquinoline [20]. The fourth and fifth peaks have similar structures and are shifted to lower *IP* compared with the π_3 and π_4-bands of quinoline. The correlation diagram included in Fig. 1 compares the assignments for quinoline and 8-hydroxyquinoline.

The u.p. spectra of the derivatives of 8-hydroxyquinoline are similar to that of the parent molecule. The ionization potentials for π_1 (Table 1) are adiabatic values. The π_4 band could not be distinguished in several of the spectra. The effects of methyl substitution in the 2-, 3-, 4- and 7-positions of 8-hydroxyquinoline resemble the phenol and pyridine systems. However, unlike the pyridine case, there is no rearrangement of the π_1 -and n-levels since they are well separated (ca. 1 eV) and the shifts created by introduction of the methyl group are generally smaller. For the 2-alkyl derivatives, the ionization potentials of the π_1, n, π_2 and π_3-bands exhibit the expected shift to lower values with increasing electron donation to the ring system, although the π_3-level seems somewhat more sensitive to substitution. The various trends outlined above are summarized in Fig. 2.

Extended Huckel molecular orbital calculations (SCF) were carried out for 8-hydroxyquinoline and several of its derivatives; the results are in complete agreement with the assignments discussed above.

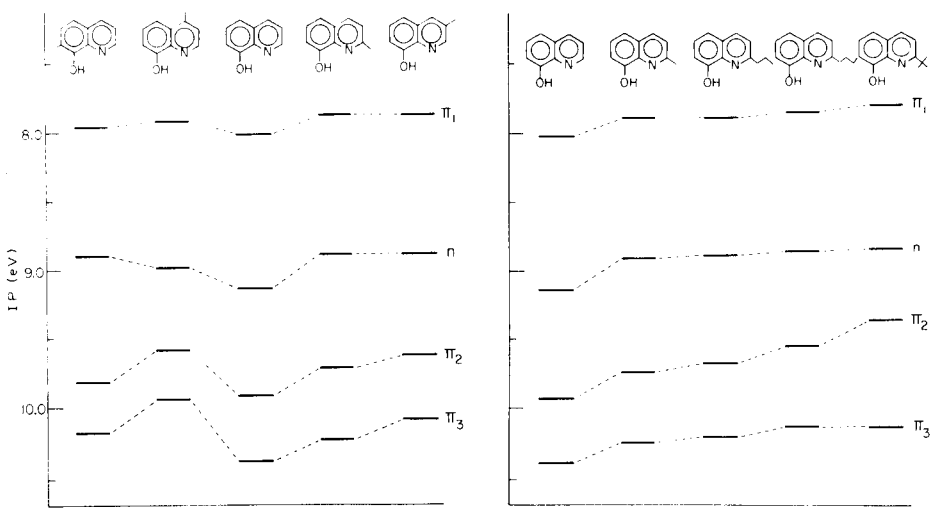

Fig. 2. Ionization potential correlation for alkyl-substituted 8-hydroxyquinolines.

Electrochemistry. Cyclic voltammetry in TBAP—acetonitrile solutions showed that oxidation of 8-hydroxyquinoline under these conditions is irreversible. Because of the irreversibility, the $E_{1/2}^{ox}$ values of 8-hydroxyquinoline and its derivatives in acetonitrile and dichloromethane were measured at the rotating platinum electrode. These values are given in Table 2 together with the adiabatic ionization potentials of the highest occupied orbital (π_1). The solution potentials were measured from the first of two peaks that were observed in most of the voltammograms. The second peak is believed to originate from an oxidative coupling reaction. Such processes are well known in phenol chemistry and there is strong evidence that 8-hydroxyquinoline exhibits similar reactions [21].

These results (Table 2) clearly show that differences in $E_{1/2}^{ox}$ for the derivatives in either solvent are not significant, except for the 2-t-butyl compound. The value for 3-methyl-8-hydroxyquinoline in dichloromethane is anomalously high at 1.67 V. Since the colour of this solution was bright yellow, it is proposed that the oxidation potential observed here can be ascribed to a photodecomposition product. An empirical value for the differential solvation energy between the radical cation and neutral species (ΔE_{solv}) was calculated for each of the derivatives in both solvents using the π_1 values for u.p.s. and the equation of Loutfy et al. (Table 2). (With the assumption that the solvation energy of the neutral molecule is small, ΔE_{solv} becomes the solvation energy of the radical cation produced in the electrochemical reaction.)

Two features of these results merit discussion. The solvation energy for the 2-t-butyl derivative in both solvents is less than those for the other compounds. This observation undoubtedly relates to steric hindrance to the cation—dipole (solvent) interaction which implies that significant charge resides on the ring nitrogen atom in view of the proximity of t-butyl group. In this respect it is of interest that Arnett and Chawla [22] observed a similar restricted access to a protonated nitrogen atom for solvation in a hydration study of 2,6-di-t-butylpyridine. Secondly, a significant difference in solvation energy between acetonitrile and dichloromethane is observed which obviously reflects the polarity of these solvent molecules; the dipole moments are 3.38 for acetonitrile and 1.55 for dichloromethane. This difference appears, for the most part, to be invariant at about 0.2 eV. Although the validity of the numerical values for solvation energy found here is open to question, not least because of the irreversibility of the oxidation and the empirical nature of eqn. 2, the method does provide a basis for the establishment of a relative scale of cation solvation energies.

We are indebted to the Natural Sciences and Engineering Research Council of Canada for support, and thank A. Corsini of McMaster University for samples of the 7-methyl and 7-t-butyl-8-hydroxyquinolines and A. D. Baker, Queens College of C.U.N.Y., for assistance in obtaining several photoelectron spectra.

REFERENCES

1 L. L. Miller, G. D. Nordblom and E. A. Majeda, J. Org. Chem., 37 (1972) 916.
2 J. W. Loveland and G. R. Dimeler, Anal. Chem., 33 (1961) 1196.
3 W. C. Neikam, G. R. Dimeler and M. M. Desmond, J. Electrochem. Soc., 111 (1964) 1190.
4 E. S. Pysh and N. C. Yang, J. Am. Chem. Soc., 85 (1963) 2124.
5 M. J. S. Dewar, J. A. Hashmall and N. Trinajstic, J. Am. Chem. Soc., 92 (1970) 5555.
6 N. Takeno, N. Takano, M. Sugano and M. Morita, Nippon Kagaku Kaishi, (1973) 1297.
7 S. C. Sharma and B. Krishna, Ind. J. Chem., 14A (1976) 436.
8 L. L. Miller, V. R. Koch, T. Koenig and M. Tuttle, J. Am. Chem. Soc., 95 (1973) 5075.
9 V. R. Koch and L. L. Miller, J. Am. Chem. Soc., 95 (1973) 8361.
10 R. E. Ballard, Chem. Phys. Lett., 42 (1976) 97.
11 S. F. Nelsen, V. Peacock and G. R. Weisman, J. Am. Chem. Soc., 98 (1976) 5269.
12 R. O. Loutfy, I. W. J. Still, M. Thompson and T. S. Leong, Can. J. Chem., 57 (1979) 638.
13 J. P. Phillips, J. Am. Chem. Soc., 74 (1952) 552.
14 J. P. Phillips, R. L. Elbinger and L. L. Merritt, J. Am. Chem. Soc., 71 (1949) 3986.
15 H. Kaneko and K. Ueno, Bull. Chem. Soc. Jpn., 39 (1966) 1910.
16 M. Thompson and E. A. Stubley, Talanta, 26 (1979) 601.
17 F. Brogli, E. Heilbronner and T. Kobayashi, Helv. Chim. Acta, 55 (1972) 274.
18 T. Kobayashi and S. Nagakura, Bull. Chem. Soc. Jpn., 47 (1974) 2563.
19 E. Heilbronner, V. Hornung, F. H. Pinterton and S. F. Thames, Helv. Chim. Acta, 55 (1972) 289.
20 D. M. W. Van der Ham and D. Van der Meer, Chem. Phys. Lett., 15 (1972) 549.
21 M. Thompson and M. A. Brook, unpublished work.
22 E. M. Arnett and B. Chawla, J. Am. Chem. Soc., 101 (1979) 7141.

Analytica Chimica Acta, 119 (1980) 187

Errata

P.-K. Hon and A. Townshend, An Improved Spectrophotometric Determination of Chloride via Chromyl Chloride Formation.
Anal. Chim. Acta, 115 (1980) 395—399.

p. 396. The sentence starting on line 11 of the text should read: Pipette a 3.60-ml portion of the organic phase (upper layer) into another glass vial containing 2.00 ml of the buffer solution. Immediately cap the vial and shake for 10 s to extract the chromyl chloride into the aqueous phase.

H. D. Fleming, Design and Performance of an On-Line Atomic Fluorescence Monitor for Magnesium.
Anal. Chim. Acta, 117 (1980) 241—246.

p. 244. The sentence starting on the third line of the text should read: The optical system was as previously described ... instead of the official system as in the text.

(continued from outside of cover)

A double quadrupole for mass spectrometry/mass spectrometry
D. Zakett, R. G. Cooks (West Lafayette, IN, U.S.A.) and W. J. Fies (Sunnyvale, CA, U.S.A.) . 129
Ion structure determinations and ion–molecule reactions by double quadrupole mass spectrometry
G. L. Glish, P. H. Hemberger and R. G. Cooks (West Lafayette, IN, U.S.A.) 137

Short Communications

Direct analysis of mixtures by double quadrupole mass spectrometry
G. L. Glish and R. G. Cooks (West Lafayette, IN, U.S.A.) 145
Functional group screening of complex mixtures with a double quadrupole mass spectrometer
D. Zakett, P. H. Hemberger and R. G. Cooks (West Lafayette, IN, U.S.A.) 149
Charge exchange using a double quadrupole mass spectrometer
K. L. Busch, T. L. Kruger and R. G. Cooks (West Lafayette, IN, U.S.A.) 153
Determination of traces of chromium(VI) as a thiosemicarbazide complex by solvent extraction and atomic absorption spectrometry
W.-J. Wang (Tamsui, Taiwan) 157
The determination of barium, lanthanum and magnesium in pancreatic islets by electrothermal atomic absorption spectrometry
P.-O. Berggren (Uppsala, Sweden) 161
The use of magnesium perchlorate as desiccant in the syringe injection technique for determination of mercury by cold-vapour atomic absorption spectrometry
D. Gardner (Cronulla, N.S.W., Australia) 167
Spectrophotometric determination of selenium with dithizone
A. D. Campbell and A. H. Yahaya (Dunedin, New Zealand) 171
Determination of antimony in tin by radiochemical neutron activation analysis
T. Bereznai (Stuttgart, W. Germany) 175
Ultraviolet photoelectron spectroscopy and oxidative electrochemistry of 8-hydroxyquinoline and its derivatives
M. Thompson and E. A. Stubley (Toronto, Ont., Canada) 179
Errata 187

CONTENTS

Review: Glassy carbon as electrode material in electroanalytical chemistry
W. E. van der Linden and J. W. Dieker (Amsterdam, The Netherlands) 1
A cesium-selective electrode prepared from a crystalline synthetic zeolite of the mordenite type
G. Johansson, L. Risinger and L. Fälth (Lund, Sweden) 25
Determination of L-thyroxine sodium and L-triiodothyronine sodium in tablets by differential pulse polarography
E. Jacobsen and W. Fonahn (Oslo, Norway) 33
Donnan dialysis matrix normalization for the voltammetric determination of metal ions
J. A. Cox and Z. Twardowski (Carbondale, IL, U.S.A.) 39
Determination of tellurium(IV) in perchloric acid by stripping voltammetry with collection
R. W. Andrews (Birmingham, AL, U.S.A.) 47
Stripping voltammetry of tellurium(IV) in 0.1 M perchloric acid at rotating gold disk electrodes
R. S. Posey and R. W. Andrews (Birmingham, AL, U.S.A.) 55
Direct determination of lead in polluted sea water by carbon-furnace atomic absorption spectrometry
M. C. Halliday, C. Houghton (Edinburgh, Gt. Britain) and J. M. Ottaway (Glasgow, Gt. Britain) 67
Investigations of reactions involved in electrothermal atomic absorption procedures. Part 8. A theoretical and experimental study of factors influencing the determination of phosphorus
J.-A. Persson (Umea, Sweden) 75
Kinetic determination of alcohols and their binary mixtures with a stopped-flow spectrophotometric technique
E. Mentasti and C. Baiocchi (Torino, Italy) 91
Effect of acidity and alkalinity on the distillation of phenol and interferences of aromatic amines and formaldehyde with the 4-aminoantipyrine spectrophotometric method for phenol
G. Norwitz and P. N. Keliher (Villanova, PA, U.S.A.) 99
Spectrophotometric determination of traces of cobalt in water after preconcentration on reagent-loaded polyurethane foams
T. Braun and M. N. Abbas (Budapest, Hungary) 113
The determination of sulphur in copper, nickel and aluminium alloys by proton activation analysis
C. Vandecasteele, J. Dewaele, M. Esprit and P. Goethals (Gent, Belgium) 121

(continued on inside page of cover)

Printed in The Netherlands.